



**Carina Rafaela
Faria Da Costa
Félix**

**Abordagem multi-ómica no estudo da resposta a
temperatura em *Lasiodiplodia theobromae*, um
fungo patogénico de plantas e humanos**

**Multi-omics approach to study responses to
temperature in *Lasiodiplodia theobromae*, a human
and plant fungal pathogen**



**Carina Rafaela
Faria Da Costa
Félix**

Abordagem multi-ómica no estudo da resposta a temperatura em *Lasiodiplodia theobromae*, um fungo patogénico de plantas e humanos

Multi-omics approach to study responses to temperature in *Lasiodiplodia theobromae*, a human and plant fungal pathogen

Tese apresentada à Universidade de Aveiro para cumprimento dos requisitos necessários à obtenção do grau de Doutor em Biologia, realizada sob a orientação científica do Doutor Artur Jorge da Costa Peixoto Alves, Investigador Principal do Departamento de Biologia da Universidade de Aveiro, da Doutora Ana Cristina de Fraga Esteves, Professora Auxiliar Convidada do Departamento de Biologia da Universidade de Aveiro e do Professor Jesús Jorrín-Novo, Professor Catedrático do Departamento de Bioquímica e Biologia Molecular da Universidade de Córdoba.

Apoio financeiro da FCT e do FEDER através do programa COMPETE no âmbito do projeto de investigação ALIEN.

Bolsas com referência:
PTDC/AGR-PRO/2183/2014
POCI-010145FEDER-016788

FCT

Fundação para a Ciência e a Tecnologia
MINISTÉRIO DA CIÊNCIA, INOVAÇÃO E DO ENSINO SUPERIOR

Cofinanciado por:

**COMPETE
2020**

**PORTUGAL
2020**

 UNIÃO EUROPEIA
Fundo Europeu
de Desenvolvimento Regional

Apoio financeiro da FCT e do FSE no âmbito do III Quadro Comunitário de Apoio.

Bolsa de Doutoramento:
SFRH/BD/97613/2013

**QR
EN** QUADRO
DE REFERÊNCIA
ESTRATÉGICO
NACIONAL
PORTUGAL 2007-2013



UNIÃO EUROPEIA
Fundo Social Europeu

o júri

presidente

Doutor Amadeu Mortágua Velho da Maia Soares
professor catedrático da Universidade de Aveiro

vogais

Doutora Cristina Maria da Costa Silva Pereira
professora associada da Universidade Nova de Lisboa

Doutora Raquel Monteiro Marques da Silva
professora auxiliar convidada da Universidade de Aveiro

Doutor Luis Valledor González
Investigador da Universidade de Oviedo

Doutor Artur Jorge da Costa Peixoto Alves
investigador principal da Universidade de Aveiro

agradecimentos

Nesta aventura tão intensa que foi o doutoramento, tenho que agradecer profundamente aos meus orientadores, Doutor Artur Alves, Doutora Ana Cristina Esteves e Professor Jesús Jorrín-Novo, que me fizeram acreditar desde o início que era capaz de concretizar mais esta etapa. Pela presença constante e dedicação, um muito obrigada!

Não apenas por toda a confiança e carinho, mas também pela amizade e compreensão para comigo ao longo de todos estes anos, um obrigado muito especial à “Chefe Cristina”.

À Sofia, que apesar de não fazer parte oficialmente da minha orientação, tanto me ensinou e ajudou ao longo deste percurso. Sempre paciente, sempre com um sorriso, sempre com uma palavra reconfortante.

A todos aqueles que contribuíram para a realização deste trabalho, em especial à Sofia Libório, pela forma incrível que abraçou o trabalho, pela alegria constante no laboratório e pela grande amizade.

Ao microlab, a minha segunda casa. É um orgulho fazer parte de um grupo que ultrapassa qualquer obstáculo sempre em equipa. Ao Professor António Correia, que apesar de já não estar presente continua a fazer parte desta equipa, fazendo valer os seus valiosos ensinamentos todos os dias.

Às “minhas meninas” do laboratório, Carla, Eliana, Forough, Anabela, Susana, Marta Alves e Cátia. Equipa incrível! Fazer um doutoramento ao lado de amigos assim torna tudo mais fácil.

À minha “companheira de tese”, Marta, obrigada por todo o apoio e ajuda ao longo dos últimos meses em alturas mais difíceis e por todas as risadas que me ajudaram a encarar esta fase de forma divertida.

Aos meus pais, que apesar de todas as adversidades sempre acreditaram em mim e me deram a possibilidade de hoje estar a terminar um doutoramento. E ao meu irmão, que me estimula sempre a querer fazer mais e melhor. Que me ajuda tantas vezes e de variadas formas. Espero em breve ver-te nesta fase também!

Ao Cláudio, por tudo o que representa na minha vida. Pelo apoio diário e constante, por toda a paciência e dedicação. Sem ti era tudo muito mais difícil. Espero conseguir ajudar-te tanto como me tens ajudado a mim.

palavras-chave

Fungo fitopatogénico, temperatura, proteómica, transcriptómica, genómica, metabolómica, citotoxicidade, mecanismo de infeção

resumo

Lasiodiplodia theobromae é um fungo fitopatogénico considerado agressivo, sobretudo para algumas culturas, que tem sido também associado a infeções oportunistas em humanos.

Pequenas alterações ambientais, como o aumento da temperatura global, podem ter grande impacto na dinâmica entre hospedeiros e agentes patogénicos, levando a alterações na virulência ou mesmo à colonização de novos hospedeiros.

Assim, o objetivo principal deste trabalho consistiu em caracterizar os mecanismos moleculares de patogenicidade de *L. theobromae* sob diferentes temperaturas.

Para atingir este objetivo utilizou-se uma abordagem multi-ómica – genómica, transcriptómica, proteómica e metabolómica. Esta abordagem holística foi ainda complementada com outras estratégias específicas (perfil enzimático e avaliação da citotoxicidade).

De uma forma geral, o fungo investe mais recursos energéticos na sua disseminação quando é cultivado a 25 °C, apresentando uma maior expressão de transcritos/proteínas associados ao metabolismo primário e de carboidratos, e também de patogénese. A 37 °C esta espécie parece concentrar-se mais na sua proteção, apresentando uma sobre-expressão de transcritos/proteínas relacionados com resposta ao stress.

Foram identificados vários transcritos/proteínas/metabolitos conhecidos por participar na penetração, colonização e disseminação do agente patogénico no hospedeiro, plantas e humanos. Entre eles, enzimas responsáveis pela degradação da parede celular vegetal e moléculas envolvidas em vias que contribuem para uma penetração do hospedeiro bem sucedida, como vias MAPKs. Foram também identificadas proteínas de choque térmico e efetores nudix, responsáveis por ajudar a ultrapassar o stress originado pelo hospedeiro e proteínas do complexo velvet, importantes no desenvolvimento do fungo e na regulação do metabolismo secundário.

Parece existir uma tendência para que a estirpe CBS339.90, isolada a partir de um humano, seja mais agressiva a 37 °C, expressando várias moléculas conhecidas por participar em infeções em humanos e sendo responsável por elevadas taxas de mortalidade de células de mamíferos. Contrariamente, as estirpes isoladas de plantas apresentaram mais transcritos/proteínas relacionados com patogénese a 25 °C e maior toxicidade em tomateiros também a esta temperatura.

Este trabalho atesta a utilidade da utilização de uma abordagem multi-ómica para dissecar o mecanismo molecular de patogénese de fungos, assim como as diferenças encontradas entre as estirpes e as suas respostas à temperatura ambiental, contribuindo para desvendar a capacidade desta espécie em colonizar uma vasta gama de ambientes assim como hospedeiros de diferentes reinos.

keywords

Phytopathogenic fungus, temperature, proteomics, transcriptomics, genomics, metabolomics, cytotoxicity, infection mechanism

abstract

Lasiodiplodia theobromae is a phytopathogenic fungus considered an aggressive pathogen, especially for some crops, and has also been associated to opportunistic human infections. Small environmental alterations, such as the increasing of the global temperature, can have a huge impact on the dynamic between hosts and their pathogens, leading to changes in virulence or even to the colonization of different hosts. Thus, the main goal of this work was to characterize the molecular mechanisms of pathogenicity of *L. theobromae* under increasing temperatures. To achieve this, a multi-omics approach – genomics, transcriptomics, proteomics and metabolomics – was used. This holistic approach was complemented with targeted strategies (enzymatic profiling and cytotoxicity evaluation).

In a general way, an investment of the fungus in dissemination was found when grown at 25 °C, with higher expression of transcripts/proteins associated to primary and carbohydrate metabolism and pathogenesis. At 37 °C, a self-protection state seems to be used by this species, with an over expression of transcripts/proteins related to stress response. However, temperature- and strain-specific virulence factors were identified.

Several transcripts/proteins/metabolites known to participate in the penetration, colonization and dissemination of the pathogen inside the plant and human hosts were identified. Between them, enzymes responsible to degrade the cell wall and molecules involved in pathways that contribute to a successful penetration inside the host, as MAPKs, were identified. Helping to overcome the stress originated by the host, heat shock proteins and nudix effectors were also identified. Proteins from velvet complex, important for fungal development and regulation of secondary metabolism, were also expressed. It seems that there is a tendency of the human isolated strain CBS339.90 to be more aggressive at 37 °C, expressing several molecules known to participate in human infections and being responsible for high rates of mammalian cell mortality. Contrarily, the strains isolated from plants, presented more transcripts/proteins related with pathogenesis at 25 °C and were more toxic for the tomato cuttings, at this temperature.

This work attests the usefulness of using a multi-omics strategy to dissect fungal molecular pathogenesis mechanisms as well as differences between strains and temperatures, contributing to unveil the ability of this species to colonize a wide range of environments and hosts from different kingdoms.

TABLE OF CONTENTS

FIGURES LIST	VI
TABLES LIST	X
THESIS OUTLINE	1
CHAPTER 1: GENERAL INTRODUCTION.....	3
Cross-kingdom host jumps in pathogenic fungi.....	5
The starting point of pathogenicity.....	5
Stages of a microbial infection.....	6
Requirements for cross-kingdom host jumps.....	8
How to overcome the host immune system	9
How to remain in the host.....	11
The family Botryosphaeriaceae and the case of <i>Lasiodiplodia theobromae</i>	12
Unraveling pathogenicity mechanisms using OMICS approaches.....	16
Aims.....	19
CHAPTER 2: TEMPERATURE MODULATES THE SECRETOME OF <i>L. THEOBROMAE</i>.....	21
Abstract	23
Introduction.....	23
Materials and Methods	25
Microorganisms	25
Radial Growth	25
Biomass.....	25
Extracellular Enzymes.....	25
Detection and Quantification of Enzymatic Activity	26
Characterization of Extracellular Enzymes by Zymography	26
Protein Quantification.....	28
Secretome Analysis	28
Tryptic Digestion, Mass Spectrometry Analysis, and Protein Identification	28
Cytotoxicity Assay	30
Results and Discussion	30
Radial Growth and Biomass.....	30
Extracellular Enzymatic Activity	31
Secretome Analysis	34
Cytotoxicity.....	40

Conclusion	41
Acknolegments	42
CHAPTER 3: <i>L. THEOBROMAE</i> AS A PRODUCER OF BIOTECHNOLOGICALLY RELEVANT ENZYMES	43
Abstract	45
Introduction	45
Materials and Methods	47
Microorganisms	47
Detection of Extracellular Enzymes.....	47
Quantification of Extracellular Activities.....	48
Cellulolytic Activity Quantification	48
Proteolytic Activity Quantification	49
Lipolytic Activity Quantification	49
Zymography	50
Statistical Analysis	51
Results	51
Extracellular Enzymatic Activity	51
Thermostability of Endoglucanases	56
Thermostability of Proteases	57
Thermostability of Lipases.....	57
Multi Factor Analysis of Extracellular Activity	58
Discussion	60
Extracellular Enzymatic Activity	60
Multi Factor Analysis of Extracellular Activity	61
Thermostability.....	62
Conclusions.....	63
Acknowledgments.....	63
CHAPTER 4: PRODUCTION OF TOXIC METABOLITES BY TWO STRAINS OF <i>L. THEOBROMAE</i>	65
Abstract	67
Introduction.....	67
Material and Methods	69
Fungal strains and growth conditions	69
Extraction and purification of fungal metabolites	69
Metabolite identification.....	71
Phytotoxicity assays	71

Cytotoxicity assays on mammalian cell cultures.....	72
Statistical analysis	72
Results	73
Metabolites isolation, purification and distribution	73
Analysis of GC/MS data acquired on LtCEs.....	74
Phytotoxicity Assays.....	76
Cytotoxicity of culture filtrates and pure metabolites	77
Discussion.....	78
Acknowledgments.....	81
CHAPTER 5: SECONDARY METABOLITES PRODUCED BY GRAPEVINE STRAINS OF <i>L. THEOBROMAE</i>.....	83
Abstract	85
Introduction.....	85
Materials and Methods	87
General Experimental Procedures	87
Fungal Strains and Culture Filtrates Production	87
Extraction and purification of fungal metabolites	87
Phytotoxicity Assays.....	88
Cytotoxicity Assay on Mammalian Cells Culture.....	89
Results.....	89
Discussion.....	95
Acknowledgements.....	98
CHAPTER 6: A MULTI-OMICS ANALYSIS OF THE GRAPEVINE PATHOGEN <i>L. THEOBROMAE</i>	99
Abstract	101
Introduction.....	101
Materials and Methods	103
Fungal strains and culture conditions	103
DNA extraction, Genome sequencing and assembly	103
Gene prediction and annotation.....	103
Genome function analysis	104
RNA extraction, library preparation and sequencing.....	105
Protein extraction and identification	106
Protein Quantification.....	107
Protein Separation	107
Results	109

Genome Analysis.....	109
Transcriptomic Analysis.....	114
Proteomic Analysis.....	114
Discussion.....	117
Conclusions.....	125
Acknowledgments.....	126
CHAPTER 7: MULTI-OMICS ANALYSES REVEAL THE MOLECULAR PATHOGENESIS TOOLKIT OF <i>L. HORMOZGANENSIS</i>	127
Abstract.....	129
Introduction.....	130
Material and Methods.....	131
Fungal strain and culture conditions.....	131
Genome Sequencing and Assembly.....	132
Gene prediction and annotation.....	132
Genome functional analyses.....	133
RNA extraction, library preparation and sequencing.....	134
Proteomics.....	135
Protein Quantification.....	135
Protein separation.....	135
Siderophores production.....	137
Results.....	137
Fungal strain identity.....	137
Genomic Analysis.....	138
Transcriptomic Analysis.....	144
Proteomic Analysis.....	144
Siderophores Production.....	146
Discussion.....	147
Conclusions.....	154
Acknowledgments.....	155
CHAPTER 8: PROTEOMIC STUDY OF TWO STRAINS OF <i>L. THEOBROMAE</i> AT DIFFERENT TEMPERATURES.....	157
Abstract.....	159
Introduction.....	160
Materials and Methods.....	161
Fungal strains and culture conditions.....	161
Radial Growth.....	161

RNA extraction and cDNA synthesis.....	162
Extracellular Protein Extraction	162
Cellular Protein Extraction.....	162
Protein Quantification.....	162
Protein separation by electrophoresis	162
Primer design for target genes used for qPCR.....	163
Protein validation by Quantitative PCR (qPCR).....	163
Results	164
Discussion.....	168
Conclusions.....	173
Acknowledgments.....	174
CHAPTER 9: GENERAL DISCUSSION	175
Final Considerations.....	177
Future Perspectives.....	182
REFERENCES	185
SUPPLEMENTARY MATERIAL	211
Chapter 4.....	211
Chapter 5.....	218
Metabolite purification of strain LA-SOL3 grown at 25 °C	218
Metabolite purification of strain LA-SOL3 grown at 37 °C	218
Metabolite purification of strain LA-SV1 grown at 25 °C	219
Metabolite purification of strain LA-SV1 grown at 37 °C	219
Acetylation of epibotryodiplodin	220
Acetylation of 4-Hydroxymethyl-3,5-dimethyldihydro-2-furanone.....	220
Acetylation of botryodiplodin	220
Chapter 6.....	221
Chapter 7.....	235
Chapter 8.....	237

FIGURES LIST

Figure 1.1 General stages of a microbial pathogen infection.....	6
Figure 1.2 Disease triangle showing that only when the interaction between host, pathogen and environment is suitable, the result will be a disease.....	9
Figure 1.3 Black spots indicate the location and each colored zones indicate different geographical distribution from where isolates of <i>L. theobromae</i> were obtained.....	15
Figure 1.4 A multi-omics approach describing different types of omics data.....	16
Figure 2.1 Effect of temperature and culture medium on the growth of <i>L. theobromae</i>	30
Figure 2.2 Effect of time and temperature on the biomass of <i>L. theobromae</i>	31
Figure 2.3 Extracellular enzymatic activity of <i>L. theobromae</i> strains CAA019 and CBS339.90.....	32
Figure 2.4 Extracellular gelatinolytic, xylanolytic, amylolytic and cellulolytic activities of <i>L. theobromae</i>	33
Figure 2.5 Secretome of <i>L. theobromae</i> strains CAA019 and CBS339.90 analyzed by SDS-PAGE.....	35
Figure 2.6 Evaluation of cytotoxicity of the extracellular fraction of <i>L. theobromae</i>	41
Figure 3.1 Images showing positive results of extracellular enzymatic activity.....	52
Figure 3.2 Extracellular enzymatic activity (%) of <i>L. theobromae</i> strains.....	53
Figure 3.3 Extracellular endoglucanolytic, proteolytic and lipolytic activities of 5 strains of <i>L. theobromae</i>	54
Figure 3.4 Extracellular gelatinolytic and endoglucanolytic activities of 5 strains of <i>L. theobromae</i> grown at 25 °C, 30 °C and 37 °C.....	55
Figure 3.5 Extracellular endoglucanolytic activity of strains CAA019, CBS339.90, LA-MA-1, LA-SV1 and LA-SOL3 grown at 25 °C, 30 °C and 37 °C and assayed at 7 temperatures.....	56

Figure 3.6 Extracellular proteolytic activity of strains CAA019, CBS339.90, LA-MA-1, LA-SV1 and LA-SOL3 grown at 25 °C, 30 °C and 37 °C and tested at 7 different temperatures.....	57
Figure 3.7 Extracellular lipolytic activity of CAA019, CBS339.90, LA-MA-1, LA-SV1 and LA-SOL3 grown at 25 °C, 30 °C and 37 °C and tested at 4 different temperatures.....	58
Figure 3.8 Multi factor analysis of detection, quantification and characterization of extracellular enzymatic activity data at 25 °C, 30 °C and 37 °C <i>L. theobromae</i> strains.....	59
Figure 4.1 Annotated total ion chromatograms (TIC) of samples from LtCE2 and LtCE4.....	75
Figure 4.2 Typical outcome of phytotoxic assays on tomato stems.....	76
Figure 4.3 Phytotoxicity of pure metabolites produced by two strains of <i>L. theobromae</i> on tomato leaves.....	77
Figure 4.4 Evaluation of cytotoxicity to Vero and 3T3 cells of the culture filtrates of strains CAA019 and CBS339.90.....	78
Figure 5.1 Lasiolactols A and B, (3S,4R,5R)-4-hydroxymethyl-3,5-dimethyldihydro-2-furanone, botryodiplodin, epi-botryodiplodin, (3R,4S)- and (3S,4S)-4-acetyl-3-methyl-2-dihydrofuranones, 3-indolecarboxylic acid, (-)-jasmonic acid, (-)-mellein, (3R,4R)-cis-4-hydroxymellein, tyrosol, (3S,4R,5R)-4-hydroxymethyl-3,5-dimethyldihydro-2-furanone acetylate, botryodiplodin acetylate and acetyl-epi-botryodiplodins.....	88
Figure 5.2 Phytotoxicity assay on tomato stems using the filtrates of strains LA-SOL3 and LA-SV1.....	90
Figure 5.3 Evaluation of cytotoxicity in Vero and 3T3 cells of culture filtrates and pure metabolites and derivatives from strains LA-SOL3 and LA-SV1 grown at 25 °C and 37 °C.....	91
Figure 5.4 Annotated total ion chromatograms (TIC) acquired by processing samples from LA-SOL3CE ₂₅ and LA-SOL3CE ₃₇	92
Figure 5.5 Results of leaf puncture assay of the pure metabolites.....	95
Figure 6.1 Predicted CAZymes and predicted secreted CAZymes in the genome of <i>L. theobromae</i> LA-SOL3.....	111

Figure 6.2 Gene Ontology classification of the transcripts identified in <i>L. theobromae</i> LA-SOL3.....	114
Figure 6.3 Differential expression of proteins by <i>L. theobromae</i> LA-SOL3.....	115
Figure 6.4 Gene Ontology classification of extracellular proteins identified in <i>L. theobromae</i> LA-SOL3.....	116
Figure 6.5 Gene Ontology classification of cellular proteins identified in <i>L. theobromae</i> LA-SOL3.....	116
Figure 6.6 Pathway map assigned for MAPKs signaling.....	122
Figure 7.1 Phylogenetic relationship of strain CBS339.90 and ex-type strains of several <i>Lasiodiplodia</i> species.....	138
Figure 7.2 Gene Ontology classification of the transcripts identified in strain CBS339.90.....	144
Figure 7.3 Proteins identified in <i>L. hormozganensis</i> CBS339.90.....	145
Figure 7.4 Gene Ontology classification of the extracellular proteins identified in <i>L. hormozganensis</i> CBS339.90.....	146
Figure 7.5 Gene Ontology classification of the cellular proteins identified in CBS339.90.....	146
Figure 7.6 Siderophores' production by strain CBS339.90 grown at 25 °C and 37 °C.....	147
Figure 7.7 Pathway of salicylic acid degradation.....	150
Figure 8.1 Radial growth of the strains CAA019 and LA-SV1 in PDA medium at 8 temperatures...164	
Figure 8.2 Proteins identified in the secretome and in the cellular proteome of strains CAA019 and LA-SV1.....	165
Figure 8.3 Gene Ontology classification of the extracellular and cellular proteins identified in <i>L. theobromae</i> strains CAA019 and LA-SV1.....	166
Figure 8.4 Venn diagrams showing the common and specific proteins between the strains of <i>L. theobromae</i> CAA019 and LA-SV1 grown at 25 °C and 37 °C - secretome and cellular proteome.....	167

Figure 8.5 Target genes encode: a virulence protein SSD1 (Q5AK62) and an endo-1,4- β -xylanase B (P48824) in strain CAA019 and a low-redox potential peroxidase (COIW58) and a peroxiredoxin TSA1-A (Q9Y7F0) in strain LA-SV1.....	168
Figure 9.1 Schematic representation main transcripts/proteins and pathways potentially involved in various stages of an infection process in plants and humans identified in <i>L. theobromae</i>	178
Supplementary Figure S4.1 Isolation paths of metabolites from <i>L. theobromae</i> crude extracts...	211
Supplementary Figure S6.1 Volcano plot and hierarchical cluster analysis of the expression profiles of differentially expressed genes between 25 °C and 37 °C.....	221
Supplementary Figure S6.2 One-DE gel of extracellular medium and mycelium of LA-SOL3 strain grown at 25 °C and 37 °C for 4 days.....	221
Supplementary Figure S7.1 Volcano plot and hierarchical cluster analysis of the expression profiles of differentially expressed genes between 25 °C and 37 °C.....	236
Supplementary Figure S7.2 One-DE gel of extracellular medium and mycelium of strain CBS339.90 grown at 25 °C and 37 °C for 4 days.....	236
Supplementary Figure S8.1 One-DE gel of extracellular medium and mycelium of strains CAA019 and LA-SV1 grown at 25 °C and 37 °C for 4 days.....	238

TABLES LIST

Table 1.1 Case reports of patients infected with <i>L. theobromae</i> described in literature.....	14
Table 2.1 Protein identification by LC-MS/MS of proteins secreted by <i>L. theobromae</i>	37
Table 2.2 Summary of the proteins identified in <i>L. theobromae</i> strains CAA019 and CBS339.90 at 25, 30, and 37 °C.....	39
Table 4.1 Structures and distribution of secondary metabolites produced by strains CAA019 and CBS339.90, according to strain and culture temperature.....	73
Table 4.2 Phytotoxicity (%) of culture filtrates of strains CAA019 and CBS339.90 grown at 25 °C and 37 °C.....	76
Table 5.1 Distribution of secondary metabolites produced by strains of <i>Lasiodiplodia theobromae</i> , according to strain (LA-SOL3 and LA-SV1) and culture temperatures.....	93
Table 5.2 Phytotoxicity of pure compounds in leaf puncture assay on tomato leaves.....	94
Table 6.1 General statistics of <i>L. theobromae</i> LA-SOL3 genome assembly, gene prediction and comparison with the available genome of <i>L. theobromae</i> CSS-01s	109
Table 6.2 Genes predicted to code for secreted enzymes by E2P2 in the genome of <i>L. theobromae</i> LA-SOL3.....	110
Table 6.3 Metabolic gene clusters identified in the genome of <i>L. theobromae</i> LA-SOL3.....	111
Table 6.4 Fungal cytochrome P450 families predicted to be encoded by <i>L. theobromae</i> LA-SOL3.....	112
Table 6.5 Genes predicted to code for transporters in the genome of <i>L. theobromae</i> LA-SOL3.....	113
Table 6.6 Predicted heat shock proteins involved in responses to heat stress in the genome of <i>L. theobromae</i> LA-SOL3.....	113

Table 6.7 Genes predicted to be involved in pathogen-plant interaction in the genome of <i>L. theobromae</i> LA-SOL3 and comparison with <i>L. theobromae</i> CSS-01s.....	117
Table 6.8 Functions identified in the transcriptome and proteome of strain LA-SOL3.....	119
Table 6.9 Proteins with direct roles in pathogenesis of fungi identified in the proteome of <i>L. theobromae</i> strain LA-SOL3.....	124
Table 7.1 General statistics of the <i>Lasiodiplodia hormozganensis</i> CBS339.90 genome assembly and gene prediction.....	139
Table 7.2 Metabolic gene clusters identified in the genome of <i>L. hormozganensis</i> CBS339.90....	139
Table 7.3 Genes predicted to code for secreted enzymes by E2P2 in the genome of <i>L. hormozganensis</i> CBS339.90.....	140
Table 7.4 Genes predicted to code for CAZymes in the genome of <i>L. hormozganensis</i> CBS339.90.....	141
Table 7.5 Genes predicted to code for fungal peroxidases in the genome of <i>L. hormozganensis</i> CBS339.90.....	141
Table 7.6 Genes predicted to code for transporters in the genome of <i>L. hormozganensis</i> CBS339.90.....	142
Table 7.7 Predicted heat shock proteins involved in responses to heat stress in the genome of <i>L. hormozganensis</i> CBS339.90.....	143
Table 7.8 Genes predicted to have a role in the interaction pathogen-host in the genome of <i>L. hormozganensis</i> CBS339.90.....	143
Table 8.1 Reference and target genes and respective primers.....	163
Supplementary Table S4.1 Mass spectra of identified metabolites.....	212
Supplementary Table S6.1 Genes predicted to code for fungal peroxidases in the genome of <i>L. theobromae</i> LA-SOL3.....	222
Supplementary Table S6.2 Proteins identified in the secretome of LA-SOL3 strain at 25 °C.....	222

Supplementary Table S6.3 Proteins identified in the cellular proteome of LA-SOL3 strain at 25 °C.....	222
Supplementary Table S6.4 Proteins identified in the secretome of LA-SOL3 strain at 37 °C.....	223
Supplementary Table S6.5 Proteins identified in the cellular proteome of LA-SOL3 strain at 37 °C.....	223
Supplementary Table S6.6 Up and down-regulated genes at 37 °C identified in LA-SOL3 strain and biological process.....	223
Supplementary Table S6.7 Up and down-regulated proteins identified in the secretome of LA-SOL3 strain and biological process.....	223
Supplementary Table S6.8 Up and down-regulated proteins identified in the cellular proteome of LA-SOL3 strain and biological process.....	223
Supplementary Table S6.9 Potentially relevant proteins identified in the secretome of strain LA-SOL3 grown at 25 °C and 37 °C.....	223
Supplementary Table S6.10 Potentially relevant proteins identified in the cellular proteome of strain LA-SOL3 grown at 25 °C and 37 °C.....	228
Supplementary Table S7.1 Proteins identified in the secretome of CBS339.90 strain at 25 °C.....	237
Supplementary Table S7.2 Proteins identified in the cellular proteome of CBS339.90 strain at 25 °C.....	237
Supplementary Table S7.3 Proteins identified in the secretome of CBS339.90 strain at 37 °C.....	237
Supplementary Table S7.4 Proteins identified in the cellular proteome of CBS339.90 strain at 37 °C.....	237
Supplementary Table S7.5 Up and down-regulated genes at 37 °C identified in CBS339.90 strain and biological process.....	237
Supplementary Table S7.6 Up and down-regulated proteins identified in the secretome of CBS339.90 strain and biological process.....	237

Supplementary Table S7.7 Up and down-regulated proteins identified in the cellular proteome of CBS339.90 strain and correspondent GO biological process.....	237
Supplementary Table S8.1 Proteins identified in the secretome of CAA019 strain at 25 °C.....	238
Supplementary Table S8.2 Proteins identified in the secretome of CAA019 strain at 37 °C.....	238
Supplementary Table S8.3 Proteins identified in the cellular proteome of CAA019 strain at 25 °C.....	238
Supplementary Table S8.4 Proteins identified in the cellular proteome of CAA019 strain at 37 °C.....	238
Supplementary Table S8.5 Proteins identified in the secretome of LA-SV1 strain at 25 °C.....	238
Supplementary Table S8.6 Proteins identified in the secretome of LA-SV1 strain at 37 °C.....	238
Supplementary Table S8.7 Proteins identified in the cellular proteome of LA-SV1 strain at 25 °C.....	238
Supplementary Table S8.8 Proteins identified in the cellular proteome of LA-SV1 strain at 37 °C.....	238
Supplementary Table S8.9 Up and down-regulated proteins identified in the secretome of CAA019 strain and biological process.....	238
Supplementary Table S8.10 Up and down-regulated proteins identified in the cellular proteome of CAA019 strain and biological process.....	238
Supplementary Table S8.11 Up and down-regulated proteins identified in the secretome of LA-SV1 strain and biological process.....	239
Supplementary Table S8.12 Up and down-regulated proteins identified in the cellular proteome of LA-SV1 strain and biological process.....	239

THESIS OUTLINE

The present work is focused on the problematic of determined fungi to adapt to different environments and infect a wide and distinct range of hosts, taking as the main goal improve the knowledge about pathogenicity mechanisms of the species *Lasiodiplodia theobromae*.

Different approaches were used to achieve that, being the thesis organized in 9 chapters.

Chapter 1 corresponds to a general introduction addressing the main topics of the work.

From the chapter 2 to 8, all the results obtained are described and discussed. The chapter 2 is a first approach using two strains of *L. theobromae* to understand if different hosts and temperatures affect or not the behavior of this fungus regarding its growth, protein profile, enzymatic profile and cytotoxicity. A more specific work regarding the enzymatic profiles of different strains of *L. theobromae* was performed in chapter 3, showing the importance of extracellular enzymes for this species, not only to pathogenesis but also potentially relevant for biotechnology. In the chapters 4 and 5, different strains were tested at different temperatures for the production of relevant secondary metabolites for pathogenicity, in order to understand the importance of the variables “host” and “temperature” on the metabolic profile of this species. The genome and the transcriptome at different temperatures of two strains from different hosts were also analyzed to assess the most detailed data about this organism. This information was complemented with the proteome of the same strains at different temperatures, giving rise to the chapters 6 and 7. Finally, the chapter 8 corresponds to the comparison of proteomes from grapevine isolated strains and grown at different temperatures.

In the chapter 9, the proposed goals and hypothesis are discussed, as well as relevant directions to follow in the future.

In the end of the dissertation, all the raw data used, especially in transcriptomics and proteomics, is discriminated, allowing the reader to search detailed and complementary information.

The thesis is presented in ‘article format’. Some of the chapters have been published, are accepted or are submitted for publication:

Chapter 2:

Félix, C., Duarte, A. S., Vitorino, R., Guerreiro, A. C. L., Domingues, P., Correia, A. C. M., Alves, A., and Esteves, A. C. (2016). Temperature modulates the secretome of the phytopathogenic fungus *Lasiodiplodia theobromae*. *Front Plant Sci.* 7, 1096. doi: 10.3389/fpls.2016.01096

Chapter 3:

Félix, C., Libório, S., Nunes, M., Félix, R., Duarte, A. S., Alves, A., and Esteves, A. C. (2018). *Lasiodiplodia theobromae* as a producer of biotechnologically relevant enzymes. *Int J Mol Sci.* 19, 2, pii-E29. doi: 10.3390/ijms19020029

Chapter 4:

Félix, C., Salvatore, M. M., DellaGreca, M., Meneses, R., Duarte, A. S., Salvatore, F., Naviglio, D., Gallo, M., Jorrín-Novo, J. V., Alves, A., Andolfi, A., and Esteves, A. C. (*in press*). Production of toxic metabolites by two strains of *Lasiodiplodia theobromae*, isolated from a coconut tree and a human patient. *Mycologia*. doi: 10.1080/00275514.2018.1478597

Chapter 5:

Submitted to *Mycologia*: **Félix, C.**, Salvatore, M. M., DellaGreca, M., Ferreira, V., Duarte, A. S., Salvatore, F., Naviglio, D., Gallo, M., Gallo, M., Alves, A., Esteves, A. C., and Andolfi, A. Secondary metabolites produced by grapevine strains of *Lasiodiplodia theobromae* grown at two different temperatures.

CHAPTER 1

General Introduction

Over the past decades fungal infections increased, due to multiple factors that range from alterations in hosts that are at risk and pathogens, to alterations on the environment. The improvements of the methods used for diagnostics (Nucci and Marr, 2005; Benedict et al., 2017) also contributed to the increasing number of fungal infections identified. The appearance of pathogenicity traits in traditionally non-pathogenic species, and a wider distribution of previously known pathogens, are reasons to endeavor a global effort to better understand fungal epidemiology (Nucci and Marr, 2005). Furthermore, alterations in host susceptibility to infection, the need to develop new diagnostic methods, and several other reasons, will continuously demand the study and comprehension of different pathogens to understand the alterations in the epidemiology (Nucci and Marr, 2005; Benedict et al., 2017).

CROSS-KINGDOM HOST JUMPS IN PATHOGENIC FUNGI

The starting point of pathogenicity

A host jump occurs when a microorganism, that normally colonizes a species, becomes able to infect repeatedly a species from a different kingdom (Baarlen et al., 2007). One well-established example of this condition is the pathogen *Agrobacterium tumefaciens*. This species is a globally soil-borne bacterium characterized by inducing crown gall or tumor formation in several plants (Hayward and Waterston, 1965, Hua et al., 2012). Tumor formation is achieved by plasmid DNA transmission to plant cells, making *A. tumefaciens* a good model to explore DNA transmission between organisms of different kingdoms (Baarlen et al., 2007). Indeed, this species is also known to transfer DNA into fungal and human genomes (de Groot et al., 1998; Kunik et al., 2001; Wood et al., 2001; Lacroix et al., 2006), leading to the question of how it can infect organisms so different, such as plants, fungi and humans.

The interaction between different organisms can be beneficial, neutral or detrimental. In addition, the damage-response concept (Casadevall and Pirofski, 2003) divides the pathogens in opportunistic, facultative and obligate. This division is made based on host damage induced by the microorganism, and the hosts immune responses (innate and acquire) or by the combination of both processes (Casadevall and Pirofski, 2003). While facultative pathogens usually infect a limited number of hosts, but have the ability to survive outside the host, opportunistic pathogens are usually capable to thrive on an extensive range of organic substrates and exhibit low virulence in a wide number of living hosts (Brown et al., 2006; Baarlen et al., 2007). However, in the presence of injured or immune compromised hosts, opportunistic pathogens may be aggressive (Baarlen et al.,

2007). In the interaction between hosts and pathogens, the genetic base of both organisms must allow the establishment of the molecular interactions (key-and-lock situations) that are responsible for the detrimental condition of the host, being the genetic variation and selection of best-fitting mutants and their retention, the crucial processes for successful interactions (Lynch and Conery, 2003).

Stages of a microbial infection

Among the different microbial pathogens and varied diseases caused on hosts of different kingdoms, some factors are common in the establishment of an infection (Figure 1.1).

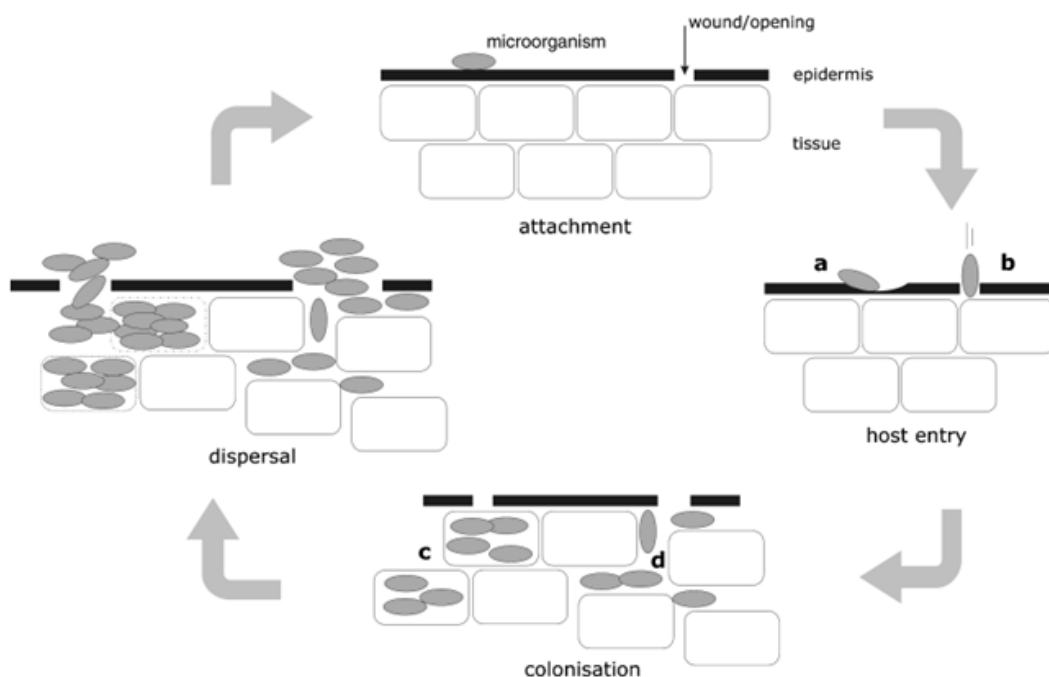


Figure 1.1 | General stages of a microbial pathogen infection. After the adhesion of the pathogen to the host, it actively penetrates the host tissues (a) or uses wounds or natural openings (b). The colonization of the host is the following step in the infection process: via intracellularly (c) or extracellularly (d). The dispersion of the pathogen is the last stage of a successful infection process (Baarlen et al.,2007).

The first step of an infection process includes the adhesion of the microorganism to host cells or tissues. Despite the major difference between plant and animal cells (the rigid and porous cell wall containing cellulose in plants), many similarities are found between both types of cells.

Adherence factors or adhesins are molecules produced by several pathogenic microorganisms to firmly attach to the host (Hahn, 1997), that in some cases could recognize more than one host, from different kingdoms. For instance, the bacteria *Erwinia chrysanthemi* is a plant pathogen that

expresses an adhesin that shares immunological identity with intimins (another adhesin), conserved in mammalian bacterial pathogens (Duarte et al., 2000). Thus, *E. chrysanthemi* has the ability to adhere not only to plant cells but also to human cells, promoting the death of both plant and human cells. After the adhesion to the host, the following step is the penetration inside the host. In the case of fungal mammalian pathogens, the penetration is mainly extracellular. However, there are cases of fungal pathogens that can invade the host cytoplasm, but the entire process is not well understood yet (Wasylnka and Moore, 2002). *Candida albicans* is a fungal pathogen known to switch phases. As unicellular, *C. albicans* induces phagocytosis of host cells (Filler et al., 1995), while the transformation into hyphae phase difficults the process of phagocytosis. But, *C. albicans* hyphae are able to enter into the host tissues by applying mechanical pressure (Kumamoto and Vices, 2005). Fungal plant pathogens usually have the ability to detect stomata and wounds and use these openings to invade plant tissues. However, several highly specialized fungal plant pathogens can force the entrance in the host by piercing the leaf through the appressorium formation, that facilitates the exertion of pressure (Ryder and Talbot, 2015). To establish an infection, the production of molecules that are secreted or injected into the host is common to any microbial pathogen. These components can act in the evasion of the host, suppression of its immune system or in the uptake of nutrients (Baarlen et al., 2007). Among these molecules, those targeting a specialized cell type will not facilitate cross-kingdom host jumps, while molecules that target a generally conserved host component will promote this capacity. Thus, microorganisms able to do cross-kingdom host jumps are usually associated with the expression of factors that act in a wide range of organisms (Ryder and Talbot, 2015).

Secondary metabolites are low-molecular-weight by-products of the regular metabolism that can have targets in hosts from distinct kingdoms. These compounds act in microbial defense and in antibiosis (Wicklow, 1988). Toxins that target cellular membranes (conserved cellular components) are among the most produced compounds of the secondary metabolism of microbes. The induction of necrosis is a common mode of action of toxins, which suggests that microbial pathogens that produce this kind of compounds will benefit from cellular lysis, taking up cellular components, such as nutrients.

After a successful penetration inside the host, colonization is crucial for nutrition and consequently allow the replication of the microorganism (Baarlen et al., 2007). For biotroph pathogens, feeding from living plant cells is achieved via specialized structures named haustoria. These structures emit signals that are believed to suppress host defense responses, promoting the interaction of the microorganism with the host (Vögele and Mendgen, 2003). For necrotrophs, contrary, the secretion

of toxins and lytic enzymes are the most common strategies, allowing the absorption of nutrients from the necrotic tissues. In this case, since there is not the suppression of the host defense responses, the action of toxins and lytic enzymes should be fast to kill the host cells before host activate their defense responses (Baarlen et al., 2007). Although different hosts offer different nutritional conditions, all of them can provide the essential cellular requirements: water, micronutrients and amino acids.

The role of siderophores

Iron is required for many cellular processes for almost all microorganisms (Johnson, 2008). Due to its two stable states (Fe^{2+} and Fe^{3+}), this element is an important cofactor for many proteins that mediate electron transfer and redox reactions. Microbial pathogens developed specialized mechanisms to acquire iron from the hosts. For those that multiply in extracellular spaces of the host, the production of siderophores is a solution to acquire iron (Johnson, 2008). These small iron-chelating molecules are responsible for chelating iron outside the cell and to transport the iron complex back into the microbial cell, where it is removed and used. Another possibility is the direct utilization of the host iron compounds (e.g. heme, hemoglobin or transferrin). But, for that, high-affinity outer membrane receptors are necessary (Byers and Arceneaux, 1998). As a host defense, vertebrates have developed iron-withholding defense mechanisms, which means that when the host recognizes the presence of the pathogen, the available iron is rapidly reduced. One example is the mechanism of iron complexing with ferritins, where a reduction of serum iron is verified as soon as the microbial invasion is sensed (Weinberg, 2000). Such mechanisms are not found only in vertebrates. In fact, a similar one involving ferritins is believed to be used by plants upon a microbial pathogen attack (Dellagi et al., 2005). Globally, the capacity to acquire iron from different environments seems to be correlated with cross-kingdom pathogenicity. Microorganisms as the bacteria *Pseudomonas aeruginosa* or the fungus *Rhizopus* are known to produce different types of siderophores that act in invasions of many distinct organisms, including organisms from different kingdoms (Ratledge and Dover, 2000).

Requirements for cross-kingdom host jumps

Multiple conditions are associated to a successful infection process: not only pathogen and host must be genetically compatible, but also environmental conditions need to favor the interaction between them (Scholthof, 2007). The disease triangle (Figure 1.2) illustrates the concept of disease,

showing that a specific interaction between host, pathogen and external environment are necessary for a disease to happen.

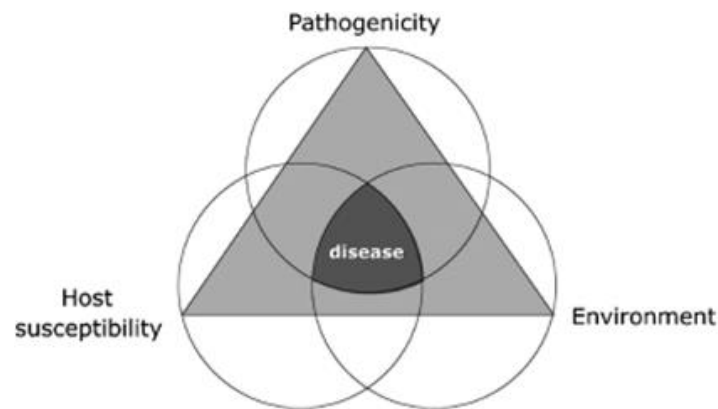


Figure 1.2 | Disease triangle showing that only when the interaction between host, pathogen and environment is suitable, the result will be a disease (Baarlen et al., 2007).

The host and the microbial pathogen should be in close proximity. Symbiosis is the closest relation between host and microorganism and can vary regarding the type of symbiosis (Baarlen et al., 2007). In a mutualistic symbiosis, both species benefit from each other, while in a commensalistic one, only one of the species benefits and the other part is not significantly affected. Parasitism is the symbiosis where the pathogen takes advantage from the host, promoting damages on it (Baarlen et al., 2007). In some cases, minor alterations in mutualistic and commensalistic relations can be responsible to turn these relations into pathogenic ones (Hube, 2004). A well-known example is the case of *C. albicans*, that is usually present in gastrointestinal and genital mucosa as a commensal yeast but can also become pathogenic if the host is immunocompromised, promoting infection in different body locations (Hube, 2004). Thus, endophytic bacteria and fungi may also develop the ability to cause disease in the presence of a stressed host.

How to overcome the host immune system

For a successfully stable pathogenicity, microbial pathogens need to avoid or suppress the immune responses of the host. In the case of invertebrates and plants, defense is exclusively achieved by their innate immunity (Da Cunha et al., 2006). For plants, a semi rigid vascular system is responsible to transport the dissolved compounds throughout the plant, but the distal part of the plant doesn't have circulation system, hampering the carry of host defense components to those areas (Baarlen et al., 2007). In vertebrates, a complex closed circulatory system is responsible for carrying the blood all over the body through blood vessels. Vertebrates have very efficient adaptive immune

systems, using T- and B-cells with a variety of antigen-specific receptors, capable to recognize and fight potential pathogens (Thomma et al., 2001). In addition, the quick production of antigen-specific receptors, gives to vertebrates an extensive capacity to prepare a large number of specific defense reactions (Baarlen et al., 2007). Nonetheless, not only the adaptive immune system is relevant for vertebrate's protection. The innate immune system still plays a crucial role in host defense, being the first line of defense against pathogens and contributing to the activation of the adaptive immune responses (Yang et al. 2000).

The immune system of plants, invertebrates and vertebrates, is very different: no adaptive capacity is found in plants or invertebrates. However, these organisms exhibit some specificity. In fact, the attack of certain types of pathogens is responsible to activate specialized defense mechanisms (Thomma et al., 2001). The host response usually requires kinase activity and further downstream mitogen-activated protein kinases cascades are activated. Then, calcium fluxes start and reactive oxygen species are produced. Transcriptional factors are also activated, participating on the expression of defense response effectors, as antimicrobial peptides and proteins (Baarlen et al., 2007).

Thus, it seems that the necessary molecular mechanisms required for host defense share high similarity and that the ability of a pathogen to overcome a specific host defense process could be important for the ability to overcome similar processes in other hosts (Baarlen et al., 2007).

In order to deal with host defenses, the first strategy of a pathogen is self-protection; the second one is the suppression of host defenses (Baarlen et al., 2007). Regarding self-protection, the production of pigments and its deposition in microbial cell walls (*e.g.* carotenoids or melanin) has been shown to play a role in microbial survival and pathogenicity. Melanins, brown to black pigments, are originated by the oxidative polymerization of phenolic/indolic compounds of different organisms, such as plants, animals and microorganisms (Nosanchuk and Casadevall, 2006). In microbial pathogens, these pigments influence their protection, especially propagative structures as spores and resting structures, preserving these specialized structures against adverse conditions and abiotic stresses (*e.g.* extreme temperature, UV radiation or detrimental compounds) (Rehnstrom and Free, 1996). In fungi, melanins are known to directly contribute to pathogenicity of several species. One well-known example is the case of *Magnaphorte grisea*, where the melanization of the appressorium is essential for tissue penetration (Howard and Valent, 1996). The melanized cells are more resistant to damages by oxygen species as well as to lysis, helping to prevent phagocytosis, when compared to unmelanized cells (Rosas and Casadevall, 2001).

In order to suppress host defenses, the production of toxins with immunosuppressive effects is a common strategy of microbial pathogens. Gliotoxin is a well characterized toxin that is involved in several animal mycoses. It is responsible to cause macrophage inhibition and induction of apoptosis in different cells by the inhibition of the assembly of the NADPH oxidase enzyme complex, involved in the respiratory burst (Tsunawaki et al., 2004) or the inhibition of the nuclear transcription factor NF- κ B, that regulates the inflammatory response (Pahl et al., 1996). This toxin is known to be produced by fungi phylogenetically separated, such as *Aspergillus fumigatus*, several *Penicillium* spp., *C. albicans* and *Trichoderma virens* (Gardiner et al., 2005). Apoptosis and programmed cell death processes have the function to modulate the basal defense responses. However, these processes may also be relevant in the modification of host defenses.

The role of oxylipins

Among plants, animals and fungi, oxylipins (oxygenated polyunsaturated fatty acids) (Fischer and Keller, 2016) are used as a common method of communication to elicit biological responses (Fischer and Keller, 2016). Oxylipins are related with basic fungal development, interfering in the ratio of sexual/asexual structures, spore shape, quorum sensing, germination rate and mycotoxin synthesis (Fischer and Keller, 2016). However, it has been demonstrated that fungi also produce oxylipins to modify plant and mammalian responses (Fischer and Keller, 2016). In plants, the expression of fungal oxylipins is crucial for the niche establishment. Tissue invasion is compromised when an oxylipin producing monooxygenase is deleted in *M. oryzae* (Patkar et al., 2016). In presence of mammalian cells, specific fungal oxylipins can be modified by the host cells, leading to a potent immune system-modulating oxylipins (Fischer and Keller, 2016). Therefore, oxylipins are crucial to several host-pathogen interactions (Fischer and Keller, 2016).

How to remain in the host

In most cases, microbial pathogens experience a free-living life style (Baarlen et al., 2007). The innate ability to quickly adapt the metabolic activity or take advantage of the host metabolism, allows the survival of the pathogen after entering a living organism (Baarlen et al., 2007). The life style of an organism is dependent of several factors that can influence growth, as humidity, pH, optimal temperature or nutrients, and that can be similar between pathogenic and nonpathogenic microorganisms (Heurlier et al., 2005).

However, there are features that are specific of pathogenic microorganisms - as the tolerance to higher temperatures (Araújo and Rodrigues, 2004) in the case of microbial pathogens of animals - that may allow them to persist inside the host. This ability to tolerate elevated temperatures may

have evolved due to the environment, that possibly favored the thermotolerance of microorganisms. A shift from a plant infection to a human infection requires an adaptation, or tolerance, to the new environment and not all microorganisms are prepared to survive in such different conditions. Thus, the biotic and abiotic environment is responsible to influence the success of host-pathogen interactions (Parker and Gilber, 2004).

The specialization process, where an adaptation to a specific environment or host is achieved, may lead to a decrease of the capacity to thrive in different environments or hosts. To confirm this hypothesis, Scully and Bidochka grew several strains of *Aspergillus flavus* in culture media and on living insects. The results showed that the radial growth of the fungi was constant when it was repeatedly subcultured on culture media. But after the repeated passage through the insect host, a decrease of the radial growth was found when fungi were again cultivated in artificial medium. Simultaneously, an increase on conidia number was observed in the presence of the host, suggesting that continued pathogenicity promoted the decrease of living as a saprobe (Scully and Bidochka, 2005).

For some species, especially nonpathogenic and opportunistic species, the production of fitness factors are also relevant for pathogenicity (Nierman et al., 2005). These fitness factors are associated to microbial survival, for example, through the protection of the fungus against the hostile conditions inside the host or even in the external environment. However, some fitness factors may predispose to true pathogenicity and may circulate between members of microbial communities (Baarlen et al., 2007).

THE FAMILY BOTRYOSPHAERIACEAE AND THE CASE OF *LASIODIPLODIA THEOBROMAE*

The family Botryosphaeriaceae comprises a wide range of pathogens, endophytes and saprobes. It counts with 23 genera and 187 species (Dissanayake et al., 2016) and is widely distributed, being absent only in polar regions (Phillips et al., 2013). This distribution of species is related with the wide geographic location, climatic conditions, and available hosts that these species tolerate (Baskarathevan et al. 2012). Thus, the interaction with an extensive range of plants allows those species to contact with new hosts that have not coevolved resistance to them, being usually very aggressive pathogens (Parker & Gilbert 2004; Slippers et al. 2005).

As endophytes, the species of this family can spread and be introduced in different regions, including cultivated and native plants (Burgess & Wingfield 2002; Slippers & Wingfield 2007; Slippers et al. 2009). When the plant is exposed to stressful environmental conditions such as

drought, or extreme temperature fluctuations, nutrient deficiencies and damage caused by other pathogens, these species may switch from a latent stage to a pathogenic one (Slippers & Wingfield 2007). The family Botryosphaeriaceae includes relevant pathogens to a wide diversity of woody and horticultural plant hosts economically important, arousing the interest of studying this family (Punithalingam 1980; Slippers and Wingfield 2007; Slippers et al. 2014; Li et al., 2015). They can enter the plant host through natural openings (*e.g.* stomata), reproductive structures (*e.g.* seeds) or wounds (Slippers & Wingfield 2007). Among the symptoms caused by Botryosphaeriaceae, the perennial cankers in the vascular system are one of the most important, since they can damage large parts of the plant, which often results in death of the plant host (Úrbez-Torres et al., 2016). The genus *Lasiodiplodia* Ellis & Everh. is typically found in tropical and subtropical regions. It is known to cause symptoms as branch dieback, stem cankers, seed and fruit decay, gum exudation, neck rot and foliage yellowing, leading to the plant death in several cases (Lima et al., 2013; Netto et al., 2014; Coutinho et al., 2017). It can also survive as saprophyte or endophyte within seeds and other living tissues (Punithalingam, 1980; Crous et al., 2006; Sakalidis et al., 2011; Phillips et al., 2013; Coutinho et al., 2017). In addition, some species are also known to cause opportunistic infections in humans (de Hoog et al. 2000).

For a long period, the identification of *Lasiodiplodia* species was based on morphological characteristics of asexual reproductive structures, plant symptoms and host pathogenicity (Coutinho et al., 2017). However, these characteristics can be altered by environmental factors, resulting in inaccurate identification. For an accurate one, phylogenetic data has been analyzed, revealing that these species are complex (Crous et al., 2006; Phillips et al., 2013; Slippers et al., 2013). DNA sequencing is an alternative method to overcome this problem on *Lasiodiplodia* species (Crous et al., 2006; Phillips et al., 2013; Slippers et al., 2013).

Lasiodiplodia theobromae (Pat.) Griffon & Maubl. is the most common species of *Lasiodiplodia* in tropical regions and it is the type species of the genus (Prasher et al., 2017). It was considered a weak phytopathogen in the past, but it is now known as one of the major pathogens of several plants (Lima et al., 2013; Netto et al., 2014; Rodríguez-Galvéz et al., 2015; Coutinho et al., 2017). Over the past decades, it has also been reported as human opportunist pathogen causing, generally, ocular and skin infections with different levels of severity (Saha et al., 2012a, b). Nevertheless, more unusual diagnosis has been found, as pneumonia (Woo et al., 2008), osteomyelitis (Mohan et al., 2016) or invasive sinusitis and neck lymph node (Gu et al., 2016), showing the clinical relevance of *L. theobromae* (Table 1.1).

Table 1.1 | Case reports of patients infected with *L. theobromae* described in literature. M- male, F- female.

YEAR	GEOGRAPHICAL AREA	GENDER	AGE (YEARS)	DIAGNOSIS	REFERENCE
1960-1964	India	M	31	Corneal ulcer	Puttana, 1967
1960-1964	India	F	30	Corneal ulcer	Puttana, 1967
1968	USA	M	58	Keratitis	Rebell and Forster, 1976
1971	-	M	48	Keratitis	Laverde et al., 1973
1971	USA	M	14	Keratitis	Rebell and Forster, 1976
1974	USA	M	19	Keratitis	Rebell and Forster, 1976
1974	USA	F	69	Keratitis	Rebell and Forster, 1976
1974	Colombia	F	32	Onychomycosis	Restrepo et al., 1976
1975	Philippines	M	32	Keratitis and corneal abscess	Valenton et al., 1975
1976-1977/ 1980-1981	Sri Lanka	-	-	Keratitis	Gonawardena et al., 1994
1984	Japan	M	54	Corneal ulcer	Ishibashi and Matsumoto, 1984
1985	USA	M	62	Keratitis and endophthalmitis	Pflufelder et al., 1988
1988-1989	India	M	55	Keratitis	Thomas et al., 1991
1996	Cambodia	F	40	Subcutaneous abscess	Maslen et al., 1996
1996	Guyana	M	57	Keratitis and endophthalmitis	Borderie et al., 1997
1998-2008	Australia	-	-	Keratitis	Thew and Todd, 2008
2004	Jamaica	F	50	Subcutaneous phaeohyphomycosis	Summerbell et al., 2004
2006	France	M	68	Endophthalmitis	Donnio et al., 2006
2006	China	M	45	Pneumonia	Woo et al., 2008
2009	India	F	30	Noninvasive sinusitis	Kindo et al., 2010
2011	India	F	32	Keratitis	Saha et al., 2012
2014	Paraguay	M	60	Keratitis	Samudio et al., 2014
2014	Thailand	M	85	Keratitis	Lekhanont et al., 2015

2014	Cambodia	F	53	Keratitis	Lekhanont et al., 2015
2015	Kenia	M	59	Subcutaneous phaeohyphomycosis	Papacostas et al. 2015
2005-2014	France	F	47	Cutaneous Infection	Guégan et al., 2016
2015	USA	M	69	Osteomyelitis	Mohan et al., 2016
2016	Korea	M	66	Invasive sinusitis with neck lymph node involvement	Gu et al., 2016
2016	China	M	43	Keratitis	Li et al., 2016

A recent study analyzed a collection of 255 isolates of *L. theobromae* from 52 different plant hosts and locations (Figure 1.3) using sequence data from 4 nuclear *loci*, in order to understand the global genetic structure and the possible origin of *L. theobromae* (Mehl et al., 2017). The results showed that none of the dominant haplotypes could be associated to the geographic location or to the host (Mehl et al., 2017).

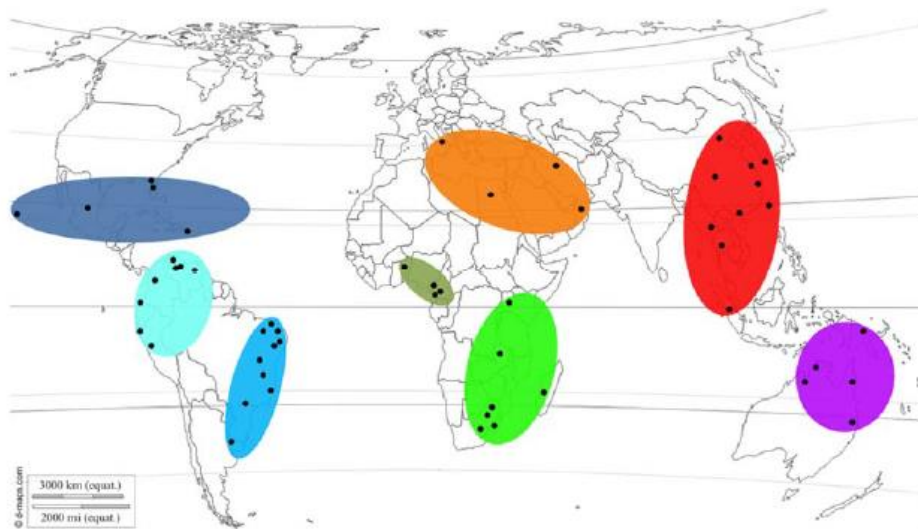


Figure 1.3 | Black spots indicate the location and each colored zones indicate different geographical distribution from where isolates of *L. theobromae* were obtained (Mehl et al., 2017).

The recent information about the diversity of the species have highlighted the importance of the global movement of infected plant material, since it can promote also the movement of the pathogen around the world (Mehl et al., 2017). This spread, accompanied by more regular extreme weather events caused by global alterations, may turn plants more susceptible to diseases by pathogens as *L. theobromae* (Mehl et al., 2017). Additionally, pathogens such as *L. theobromae* will

tend to become increasingly prominent, being very important the development of different strategies that could control its movement (Mehl et al., 2017).

UNRAVELING PATHOGENICITY MECHANISMS USING OMICS APPROACHES

The interactions associated to a host and a fungal pathogen are tremendously complex. To unveil this complexity, the use of different omics approaches allows to capture not only the drastic but also the subtle alterations within the host and the pathogen. Major approaches as genomics, transcriptomics, proteomics and metabolomics are usually applied (Culibrk et al., 2016). Depending on the goal of the work, different omics approaches may be applied (Figure 1.4). A “genome first”, that pursues the determination of mechanisms influenced by genome-wide associations *loci*; a “phenotype first” that seeks to understand the pathways that are involved in a determined situation, or an “environmental first” approach, where the primary variable to be investigated is the environment and how its alterations can influence the biology of an organism (Hasin et al., 2017).

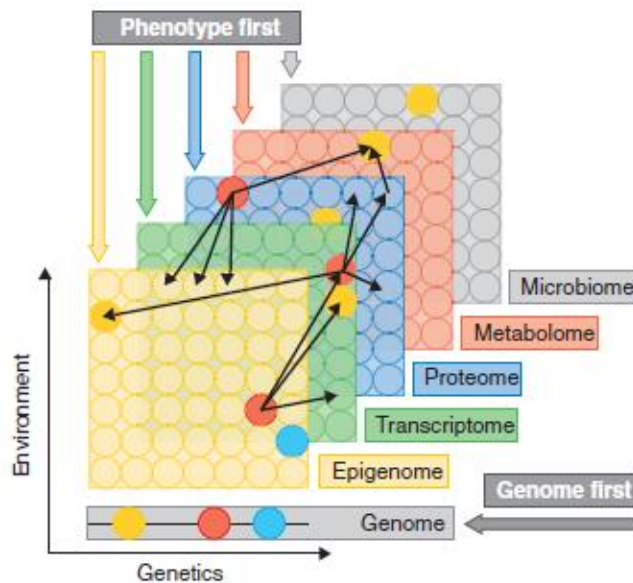


Figure 1.4 | A multi-omics approach describing different types of omics data. With the exception of the genome, all layers reproduce the genetic regulation and environment, which can influence the expression pattern and potential interactions between different types of molecules (Hasin et al., 2017).

An ideal analysis would involve the analysis of the complete and unbiased dataset of the biomolecules of interest (Culibrk et al., 2016). This is being improved by the increasing number and quality of data repositories, allowing the generation of a multi-scale host-fungus interaction models (Dix et al., 2016). Using a combination of different omics approaches with *in vitro* and *in vivo* assays

of infection, it is possible to provide a comprehensive view of the complex dynamic between a host and fungal pathogen (Carvalho and Goldman, 2017).

Currently, the large and increasing number of fully sequenced genomes, at least partially annotated, allow a forward genetic approach by searching for protein-coding genes based on predicted open reading frames (Culibrk et al., 2016). Today, a number of genomes from pathogenic fungi has been sequenced, helping the study of host-fungal interactions (Culibrk et al., 2016). As a positive complement, transcriptomics and proteomics are able to discriminate differences in gene expression under varying environmental conditions. Due to the high rates of false network discovery, the utilization of methods that overcome these problems is crucial, and the information obtained by proteomics provides a less biased view of gene expression than mRNA (Culibrk et al., 2016). Thus, the integration of transcriptomics and proteomics data improves the correlation and correction of inferred models. Also, other types of data can contribute to this improvement, as metabolomics data do (Culibrk et al., 2016). The analysis of the metabolome allows understanding how fungi interact with their host, since metabolites are the final downstream effector molecules of the transcriptome and proteome (Culibrk et al., 2016).

Although little is known regarding species of the family Botryosphaeriaceae, as *L. theobromae*, recent studies have improved the knowledge on the behavior of this species, and how it interacts with hosts in different environmental conditions. In a study conducted by Yan and colleagues (Yan et al., 2017) the whole genome of 6 species of Botryosphaeriaceae, including the first genome of *L. theobromae*, were sequenced. The genomes revealed important information regarding gene families associated to wood degradation, as cell wall degradation, membrane transport, nutrient uptake and secondary metabolism. The transcriptome of *L. theobromae* was also analyzed at two different temperatures (25 °C and 35 °C) in the presence of grapevine (host), revealing several groups of genes and pathways that seem to be induced during the infection process, such carbohydrate and pectin metabolism and pentose and glucuronate interconversion pathways.

Another study (Uranga et al., 2017) tested an adapted method of Folch lipid extraction and analyzed the proteins expressed by *L. theobromae* in the presence of triglycerides and glucose. Several proteins with biotechnological potential (*e.g.* allergenic enolases and proteases) and also pathogenesis-related proteins were identified. Novel peptide sequences were found, contributing to genomic annotations and consequently to improve fungal bioinformatics databases (Uranga et al., 2017). Another study including the transcriptome of *L. theobromae* under heat stress and in the presence of grapevine wood was carried out (Paolinelli et al., 2016). These authors identified several genes expressed during the infection process, that supported the hypothesis that heat

CHAPTER 1 – General Introduction

stress facilitates fungal colonization due to the ability of the fungus to use phenylpropanoid precursors and salicylic acid, compounds known to participate in host defense control (Paolinelli et al., 2016).

AIMS

Lasiodiplodia theobromae is a phytopathogenic fungus from the family Botryosphaeriaceae with more than 500 plant hosts and a wide geographic distribution. It is responsible to cause significant losses in several crops, and also known to cause human infections.

Thus, the main goal of this work was to characterize and improve the knowledge on the behavior, with focus on the molecular pathways of pathogenicity of *L. theobromae* under increasing temperatures.

The hypothesis of the work are:

- The pathogenicity of *L. theobromae* is modulated/affected by its original host.
- The pathogenicity of *L. theobromae* is modulated/affected by the growth temperature.
- Different temperatures favor the infection of different hosts by *L. theobromae*.

To validate these hypothesis, several specific goals were proposed:

- Compare strains of *L. theobromae* isolated from different hosts (plants and human) and with different geographical distribution: phenotype, extracellular enzymes and metabolites.
- Sequence the genome of strains of *L. theobromae* isolated from different hosts.
- Multi-omics approach - including genomics, transcriptomics and proteomics - to improve the knowledge about pathogenicity mechanisms of *L. theobromae* grown at different temperatures, 25 °C and 37 °C.

CHAPTER 2

Temperature modulates the secretome of the phytopathogenic
fungus *Lasiodiplodia theobromae*

ABSTRACT

Environmental alterations modulate host–microorganism interactions. Little is known about how climate changes can trigger pathogenic features on symbiont or mutualistic microorganisms. Current climate models predict increased environmental temperatures. The exposing of phytopathogens to these changing conditions can have particularly relevant consequences for economically important species and for humans. The impact on pathogen/host interaction and the shift on their biogeographical range can induce different levels of virulence in new hosts, allowing massive losses in agricultural and health fields. *Lasiodiplodia theobromae* is a phytopathogenic fungus responsible for a number of diseases in various plants. It has also been described as an opportunist pathogen in humans, causing infections with different levels of severity. *L. theobromae* has a high capacity of adaptation to different environments, such as woody plants, moist argillaceous soils, or even humans, being able to grow and infect hosts in a wide range of temperatures (9–39 °C). Nonetheless, the effect of an increase of temperature, as predicted in climate change models, on *L. theobromae* is unknown. Here we explore the effect of temperature on two strains of *L. theobromae* – an environmental strain, CAA019, and a clinical strain, CBS339.90. We show that both strains are cytotoxic to mammalian cells but while the environmental strain is cytotoxic mainly at 25 °C, the clinical strain is cytotoxic mainly at 30 and 37 °C. Extracellular gelatinolytic, xylanolytic, amylolytic, and cellulolytic activities at 25 and 37 °C were characterized by zymography and the secretome of both strains grown at 25, 30, and 37 °C was characterized by electrophoresis and by Orbitrap LC-MS/MS. More than 75 % of the proteins were identified, mostly enzymes (glycosyl hydrolases and proteases). The strains showed different protein profiles, which were affected by growth temperature. Also, strain specific proteins were identified, such as a putative f5/8 type c domain protein – known for being involved in pathogenesis – by strain CAA019 and a putative tripeptidyl- peptidase 1 protein, by strain CBS339.90. We showed that temperature modulates the secretome of *L. theobromae*. This modulation may be associated with host-specificity requirements. We show that the study of abiotic factors, such as temperature, is crucial to understand host/pathogen interactions and its impact on disease.

KEYWORDS: phytopathogenic fungi, extracellular enzymes, secretome, cytotoxicity, global changes

INTRODUCTION

It is widely accepted that the climate is changing at a global level. We will witness increased temperature and climatic extremes such as drought, floods, and storms (Piñeiro et al., 2010; Galant

et al., 2012). Nonetheless, little effort has been directed to the identification of the impact that these forecasted conditions, specifically increased temperature, will have on microbial pathogen (MP)/host interactions (Eastburn et al., 2011; Gallana et al., 2013). Stress induced by increased temperature experienced by MPs will certainly impact the dynamics of host/pathogen interactions and ultimately result in changes in virulence (Lindner et al., 2010). Altered environmental conditions are causing many organisms to shift their biogeographic distribution ranges (MacDonald et al., 2008), and the same may be occurring with microorganisms (Azevedo et al., 2012; Bebber et al., 2013). The study of increased environmental temperature on the behavior of phytopathogens is therefore of extreme relevance.

Fungi can establish commensal and pathogenic relationships with their hosts that can be altered by discrete environmental changes, inducing a commensal relationship to evolve into a pathogenic one (Bliska and Casadevall, 2009). Furthermore, endophytes and plant pathogens have extraordinarily similar methods of invasion, suggesting a similarity of attributes related to the adaptation of a fungus to its host (van der Does and Rep, 2007; Hube, 2009; Blauth de Lima et al., 2016). A number of fungal molecules, like cell wall degrading enzymes (CWDEs), inhibitory proteins and enzymes involved in toxin synthesis, are known to contribute to fungal pathogenicity and virulence (King et al., 2011; Gonzalez-Fernandez and Jorrín-Novo, 2012). Proteomics is a powerful tool to identify unknown mechanisms underlying environmental alterations (Lemos et al., 2010; Alves et al., 2015). In this context, the analysis of the extracellular proteome, the secretome, allows identifying which proteins are involved in the interaction with the host and attempt to relate them with fitness and/or pathogenicity mechanisms (Bregar et al., 2012; Gonzalez-Fernandez and Jorrín-Novo, 2012; Gonzalez-Fernandez et al., 2015). The analysis of the secretome has been successfully made for phytopathogenic fungi, such as *Botrytis cinerea* (Zhang et al., 2014), *Diplodia corticola* (Fernandes et al., 2014) or *Verticillium albo-atrum* (Mandelc and Javornik, 2015).

Lasiodiplodia theobromae (Pat.) Griff. & Maubl. is a phytopathogenic fungus typical of the tropics and subtropics (Alves et al., 2008; Phillips et al., 2013). Despite being able to grow between 9 and 39 °C, its optimal growth temperature is 27–33 °C (D'souza and Ramesh, 2002). Widely distributed, it is mostly confined to 40° North and 40° South of the equator. Although *L. theobromae* has the ability to colonize healthy tissues without causing any harm (Jami et al., 2013), disease may appear if the plant is under stress. Therefore, it has been considered as a latent pathogen, capable of inducing endophytic infections (Jami et al., 2013). It has been associated to approximately 500 hosts, mostly woody plants, such as *Eucalyptus spp.* and to different fruit trees, like grapevines (Phillips et al., 2013; Rodríguez-Gálvez et al., 2015). *Lasiodiplodia theobromae* has also been

associated to a number of cases of human infections, behaving as an opportunist (Summerbell et al., 2004; Kindo et al., 2010; Saha et al., 2012a, b). The most common cases are ocular infections, but human death has been reported (Woo et al., 2008).

In this study the effect of temperature on two strains of *L. theobromae* was investigated; an environmental (CAA019) and a clinical strain (CBS339.90). *Lasiodiplodia theobromae* metabolome has been widely studied, but the enzymes, and other proteins, expressed by this organism have never been investigated. Therefore, the effect of temperature on the production of extracellular enzymes, on the secretome and on cytotoxicity of the secretome was evaluated.

MATERIALS AND METHODS

Microorganisms

The strains used in this study were: CAA019, isolated from *Cocos nucifera* L. in Brazil, and CBS339.90, isolated from a phaeohyphomycotic cyst of patient from Jamaica (Alves et al., 2008). CBS339.90 was obtained from the Centraalbureau voor Schimmelcultures (CBS) Fungal Biodiversity Centre. Cultures were maintained on PDA (19.5 g.L⁻¹; Potato Dextrose Agar; Difco).

Radial Growth

Fungal growth was evaluated based on the development of the mycelium in solid media (PDA, Czapek, Oat Meal Agar and Corn Meal Agar). The plates were inoculated with a 7 mm-diameter agar plug from an actively growing fungal culture in PDA at 1 cm from the border of the plate and incubated at 25, 30, and 37 °C. After 48 h, the colony radius was measured. Assays were carried out in triplicate and data is presented as average ± standard error.

Biomass

Two plugs of 7 mm-diameter from an actively growing culture on PDA were inoculated on 50 mL of Potato Dextrose Broth (PDB) medium and incubated at 25, 30, or 37 °C. After 24, 48, 72, 96, 120, 168, and 360 h (1–15 days), the mycelium was separated from the culture medium by filtration (filter paper). The mycelium was dried at 50 °C for 48 h and the dry weight determined.

Extracellular Enzymes

The different agar media plates were inoculated with a 7 mm- diameter agar plug from an actively growing culture and incubated at 25, 30, and 37 °C for 48 h, unless otherwise stated. All assays were carried out in triplicate and data is presented as average ± standard error.

Detection and Quantification of Enzymatic Activity

The presence of caseinases, cellulases, amylases, xylanases, pectinases, ureases, and laccases was detected as described earlier (Esteves et al., 2014). Briefly, the various substrates [1 % (w/v) skimmed milk, 0.5 % (w/v) carboxymethylcellulose, 0.2 % (w/v) starch, 0.5 % (w/v) xylan, 0.5 % (w/v) pectin, 2 % (w/v) urea, and 1 % (w/v) tannic acid, respectively] were independently added to a solution of 0.5 % (w/v) malt extract and 1.5 % (w/v) agar. The activities were detected by the formation of a halo around the mycelium (caseinases, ureases, and laccases) or after the addition of lugol solution (amylases), congo red (cellulases and xylanases) or cetyltrimethyl ammonium bromide (pectinases).

Gelatinases were detected using a gelatin medium [1 % (w/v) gelatin, 0.5 % (w/v) malt extract, 1.5 % (w/v) agar]. The plates were inoculated and the degradation of gelatin was detected as a clear halo around colonies, against an opaque background.

The activity was determined as a percentage of the maximum halo (cm) measured for each activity assayed.

Characterization of Extracellular Enzymes by Zymography

Strains were grown as follows: two plugs of 7 mm-diameter from an actively growing culture on Potato Dextrose Agar (PDA) were inoculated on 50 mL of Potato Dextrose Broth (PDB) medium and incubated at the appropriate temperature for 28 days. Aliquots were taken every 48 or 72 h and stored at -80°C until analysis. The mycelium was separated from the culture medium by filtration (filter paper).

The characterization of extracellular enzymes was accessed by zymography (Esteves et al., 2014). Extracellular media were diluted in sample buffer [2:1 (v/v); 62.5 mM Tris, pH 6.8, 10 % SDS (w/v) and 20 % glycerol (v/v)] and incubated at room temperature during 10 min. Proteins were then separated in lab- cast gels (10 % polyacrylamide with the appropriated substrate) in a Mini-PROTEAN 3 (Bio-Rad) according to (Laemmli, 1970). Electrophoresis proceeded at 120 volts for 120 min at 4°C . After electrophoresis, the gel was washed twice with 0.25 % Triton X-100 (v/v) for 60 min to remove SDS.

Gel analysis was performed after staining the proteins and scanned on a GS-800 Calibrated Densitometer (Bio-Rad). Quantity One v. 4.6.9 (Bio-Rad) was used to estimate the molecular mass of proteins and their optical densities. The apparent molecular weight (MW) of the proteins was determined using a MW calibration kit as marker, consisting of a mixture of proteins with 250, 150, 100, 75, 50, 37, 25, 20, 15, and 10 kDa (Precision Plus Protein Standard, Bio-Rad). Only gels where activity was detected are shown.

Xylanases

Xylanolytic activity was characterized by zymography, as described previously (Peterson et al., 2011) with slight modifications. One percent xylan was incorporated in the gel. After electrophoresis, the gel was incubated overnight at 25 °C in 0.05 M Tris-HCl, pH 5.0, stained with congo red solution (1 %) for 10 min. The gel was rinsed with a solution of 1 M NaCl. Enzymes with xylanolytic activity were detected as clear bands against a red background of non-degraded substrate.

Cellulases

Cellulolytic activity was assessed by zymography, as described previously (Peterson et al., 2011) with slight modifications. Carboxymethylcellulose (1 %) was incorporated in the gel. After electrophoresis, the gel was incubated overnight at 25 °C in 0.05 M Tris-HCl, pH 5, stained with Congo Red solution (1 %) for 10 min. The gel was rinsed with 1 M NaCl. Enzymes with cellulolytic activity were detected as clear bands against a red background of non-degraded substrate.

Amylases

Amylolytic activity was assessed by zymography using 1 % (w/v) starch, as described previously (Peterson et al., 2011) with slight modifications. After electrophoresis, the gel was incubated 3 h at 40 °C in 0.05 M Tris-HCl, pH 5, stained with 1 mL Iugol's iodine stock solution [(0.05 g I₂, 0.1 g.mL⁻¹ KI (Potassium Iodide)] in 50 mL distilled water. The gel was rinsed with distilled water. Enzymes with amylolytic activity were detected as clear bands against a dark background of non-degraded substrate.

Proteases

Gelatinolytic and caseinolytic activity was assessed by zymography, using 1 % (w/v) gelatine or 1 % (w/v) casein, as described previously (Duarte et al., 2009; Esteves et al., 2014), with slight modifications. After electrophoresis, the gel was incubated overnight, at room temperature, in 1.5 mM Tris, pH 8.8, 1 M NaCl, 1 M CaCl₂, 2 mM ZnCl₂, pH 7.4, stained with Coomassie Brilliant Blue R-250 [(in 50 % ethanol (v/v), 10 % acetic acid (v/v))] and destained with 25 % ethanol (v/v), 5 % acetic acid (v/v). Enzymes with gelatinolytic/caseinolytic activity were detected as clear bands against a blue background of non-degraded substrate.

Protein Quantification

Protein quantification was made using BCA Protein Assay Kit (Pierce™, Rockford, IL, USA), according to the manufacturer's instructions. All the samples were quantified in triplicate.

Secretome Analysis

Two mycelial plugs with 7 mm were used to inoculate the fungi into 50 mL of PDB medium. Cultures were grown for 72 h at 25, 30, and 37 °C, in 250 mL Erlenmeyers flasks.

Extracellular medium of each strain was diluted (1:1) in loading buffer [2 % (v/v) 2-mercaptoethanol, 2 % (w/v) SDS, 8 M Urea, 100 mM Tris, 100 mM Bicine and traces of Bromophenol blue] and analyzed by electrophoresis (Laemmli, 1970). Lab-cast SDS-PAGE gels ran at 120 V for 2 h on 15 % (w/v) acrylamide running gels. The running buffer contained 100 mM Tris, 100 mM Bicine and 0.1 % (w/v) SDS. The samples were denatured at 100 °C for 5 min prior to electrophoresis. Gel staining and image acquisition and analysis was as described before (Santos et al., 2013; Costa et al., 2014; Alves et al., 2015). All visible bands were manually excised and proteins were identified by Orbitrap LC mass spectrometry.

A Permutational Multivariate Analysis of Variance (RStudio) was employed using R package 'vegan' and the RStudio v 0.98.1103 interface (Oksanen et al., 2015; R Core Team, 2015) to understand which factor (strain or temperature) – if any – has the main effect on the protein profile of *L. theobromae*.

Tryptic Digestion, Mass Spectrometry Analysis, and Protein Identification

Tryptic digestion was performed according to (Carvalhais et al., 2015), with a few modifications. Protein bands were manually excised from the gel and transferred to eppendorf tubes. Replicate bands were excised and also identified. The gel pieces were washed three times with 25 mM ammonium bicarbonate/50 % acetonitrile (ACN, VWR Chemicals) and one time with ACN. The protein's cysteine residues were reduced with 6.5 mM DTT and alkylated with 54 mM iodoacetamide. Gel pieces were dried in a SpeedVac (Thermo Savant) and rehydrated in digestion buffer containing 12.5 µg.mL⁻¹ sequence grade modified porcine trypsin (Promega) in 25 mM ammonium bicarbonate. After 90 min, the supernatant was removed and discarded, 100 µL of 25 mM ammonium bicarbonate were added and the samples were incubated overnight at 37 °C. Extraction of tryptic peptides was performed by the addition of 10% formic acid (FA, Fluka)/50% ACN three times and finally with ACN. Tryptic peptides were lyophilized in a SpeedVac (Thermo Savant) and resuspended in 5% ACN/0.1% FA solution. The samples were analyzed with a QExactive Orbitrap (Thermo Fisher Scientific, Bremen) that was coupled to an Ultimate 3000 (Dionex, Sunnyvale, CA,

USA) HPLC (high-pressure liquid chromatography) system. Prior to sample analysis, a complex mixture of peptides was obtained from the reduction, alkylation and tryptic digestion of six proteins (Sciex iTRAQ standard mixture), namely bovine serum albumin (P02769), *Escherichia coli* β -galactosidase (P00722), bovine α -lactalbumin (P00711), bovine β -lactoglobulin (P02754), chicken lysozyme C (P00698) and human serotransferrin (P02787). This peptide mixture was routinely used to test the nanoLC-MS/MS system performance, showing a protein identification coverage between 70 and 80 % for a 100 ng injection. The trap (5 mm \times 300 μ m I.D.) and analytical (150 mm \times 75 μ m I.D.) columns used were C18 Pepmap100 (Dionex, LC Packings), the latter having a particle size of 3 μ m. Peptides were trapped at 30 μ L.min⁻¹ in 95 % solvent A (0.1 % FA/5 % ACN v/v). Elution was achieved with the solvent B (0.1 % formic acid/100 % acetonitrile v/v) at 300 nL.min⁻¹. The 50 min gradient used was as follows: 0–3 min, 95 % solvent A; 3–35 min, 5–45 % solvent B; 35–38 min, 45–80 % solvent B; 38–39 min, 80 % solvent B; 39–40 min, 20–95 % solvent A; 40–50 min, 95 % solvent A. Nanospray was achieved using an uncoated fused silica emitter (New Objective, Cambridge, MA, USA; o.d. 360 μ m; i.d. 50 μ m, tip i.d. 15 μ m) biased to 1.8 kV. The mass spectrometer was operated in the data dependent acquisition mode. A MS2 method was used with a FT survey scan from 375 to 1600 m/z (resolution 35,000; AGC target 3E6). The 10 most intense peaks were subjected to HCD fragmentation (resolution 17,500; AGC target 5E4, NCE 25 %, max. injection time 120 ms, dynamic exclusion 35 s). Spectra were processed and analyzed using Proteome Discoverer (version 2.0, Thermo), with the MS Amanda search engine (version 2.1.4.3751, University of Applied Sciences Upper Austria, Research Institute of Molecular Pathology). Uniprot (TrEMBL and Swiss-Prot) protein sequence database (version of May 2016) was used for all searches under *Macrophomina phaseolina*, *Neofusicoccum parvum*, *Botryosphaeria dothidea*, and *L. theobromae*. Database search parameters were as follows: carbamidomethylation and carboxymethyl of cysteine as a variable modification as well as oxidation of methionine, and the allowance for up to two missed tryptic cleavages. The peptide mass tolerance was 10 ppm and fragment ion mass tolerance was 0.05 Da. To achieve a 1 % false discovery rate, the Percolator (version 2.0, Thermo) node was implemented for a decoy database search strategy and peptides were filtered for high confidence and a minimum length of six amino acids, and proteins were filtered for a minimum number of peptide sequences of 2 and only rank 1 peptides.

The subcellular localization of the identified proteins was deduced using Bacello (Pierleoni et al., 2006), as described before for Botryosphaeriaceae fungi (Fernandes et al., 2014) and function was obtained from Uniprot records.

Cytotoxicity Assay

In vitro cytotoxicity evaluation was performed as described earlier (Cruz et al., 2013; Duarte et al., 2015) with slight modifications. Each strain was grown in PDB medium at 25, 30, and 37 °C for 72, 96, and 120 h. The supernatants were filtered (0.20 µm pore size filter, Orange Scientific) and used to assess cytotoxicity. A Vero cell line (ECACC 88020401, African Green Monkey Kidney cells, GMK clone) was grown and maintained according to Ammerman et al. (2009). The microtiter plates were incubated at 37 °C in 5 % CO₂ for 24 h. After cell treatment, the medium was removed by aspiration and 50 µL of DMEM with 10 % resazurin (0.1 mg.mL⁻¹ in PBS) was directly added to each well. The microtiter plates were incubated at 37 °C in 5 % CO₂ until reduction of resazurin (Al- Nasiry et al., 2007). The absorbance was read at 570 and 600 nm wavelength in a microtiter plate spectrophotometer (Thermo scientific, Multiskan Spectrum).

RESULTS AND DISCUSSION

Radial Growth and Biomass

Both strains were unable to grow at 5 and at 40 °C and showed maximum radial growth at 30 °C on PDA (considered the best growth conditions for these strains from this point forward). Czapek medium was the least adequate to the growth of *L. theobromae* (Figure 2.1).

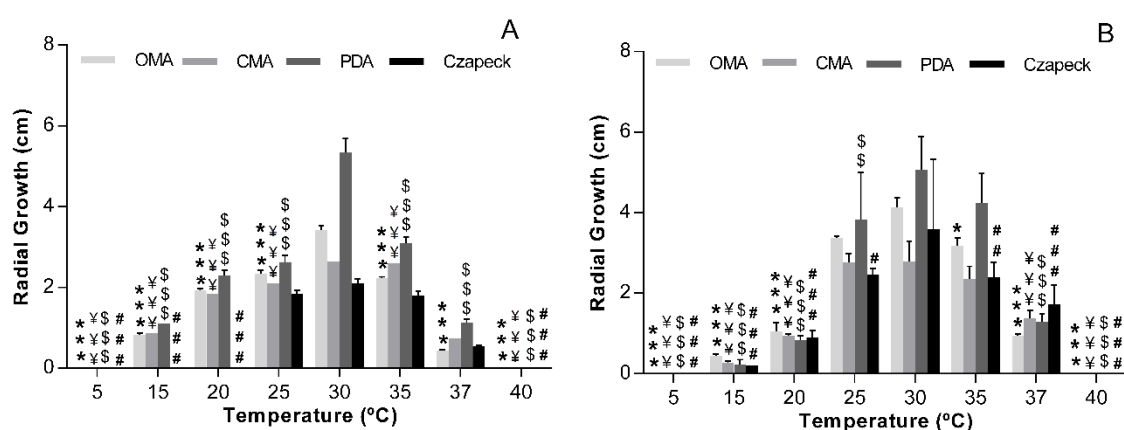


Figure 2.1 | Effect of temperature and culture medium on the growth of *L. theobromae*. Radial growth of *L. theobromae*, CAA019 (A) and CBS339.90 (B), grown at different temperatures (between 5 °C and 40 °C) and in different culture media was determined after 48 h of incubation. Data is presented as average ± standard error. Two-way ANOVA, Bonferroni test, was used to determine the statistical significance compared to 30 °C (*p < 0.05 and **p < 0.001, for OMA; ¥p < 0.05 and ¥¥¥p < 0.001, for CMA; \$p < 0.05 and \$\$\$p < 0.001, for PDA; #p < 0.05 and ###p < 0.001, for Czapek).

Lasiodiplodia theobromae biomass was determined (growth in liquid media; Figure 2.2). Both strains exhibit a biomass increase until 4 or 5 days of incubation; after this period, both strains start to degenerate with the consequent loss of biomass. The maximum biomass was obtained at 25 °C. The biomass growth profile at 25, 30, and 37 °C was significantly different (Figure 2.2, two-way Anova, $p < 0.001$). Strain CBS339.90 exhibited a similar growth pattern when compared with CAA019, with higher growth rates at 25 and 30 °C although its biomass values were significantly higher (two-way Anova, $p < 0.001$) than those of the CAA019.

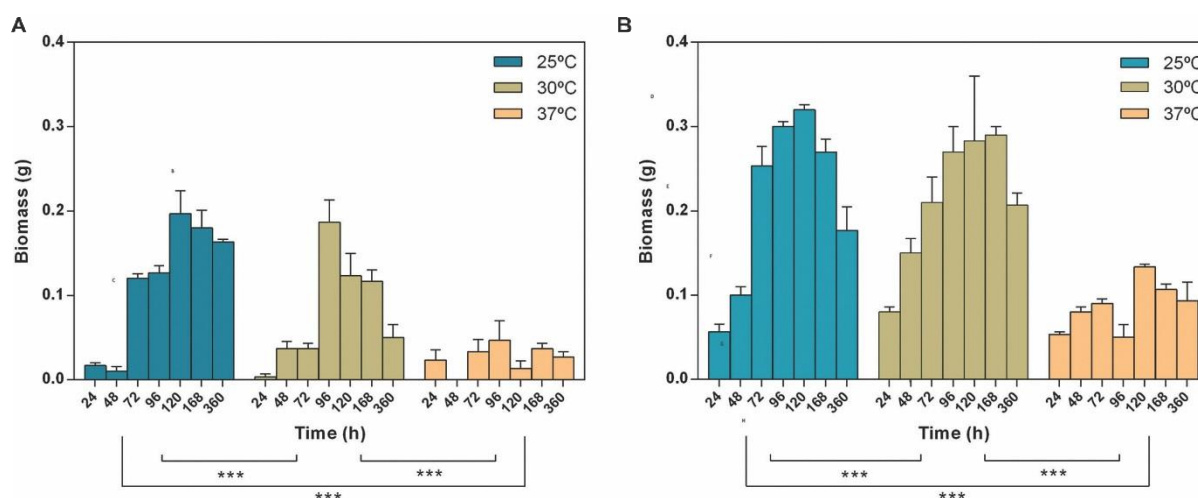


Figure 2.2 | Effect of time and temperature on the biomass of *Lasiodiplodia theobromae* [CAA019 (A) and CBS339.90 (B)]. Data is presented as average \pm standard error. Two-way ANOVA (* $p < 0.05$, ** $p < 0.01$, *** $p < 0.001$) was used to determine the statistical significance between the strains.

Extracellular Enzymatic Activity

The extracellular enzymatic activity of *L. theobromae* was detected and quantified by plate assay and by zymography. Several extracellular enzymatic activities were tested at 25, 30, and 37 °C by plate assay. The activities assayed are involved in the degradation of plant cell walls (as is the case of cellulases, xylanases, laccases, and pectinases), in the degradation of plant defenses (proteases) and in animal pathogenesis (gelatinases and ureases). Positive activities were evaluated by zymography.

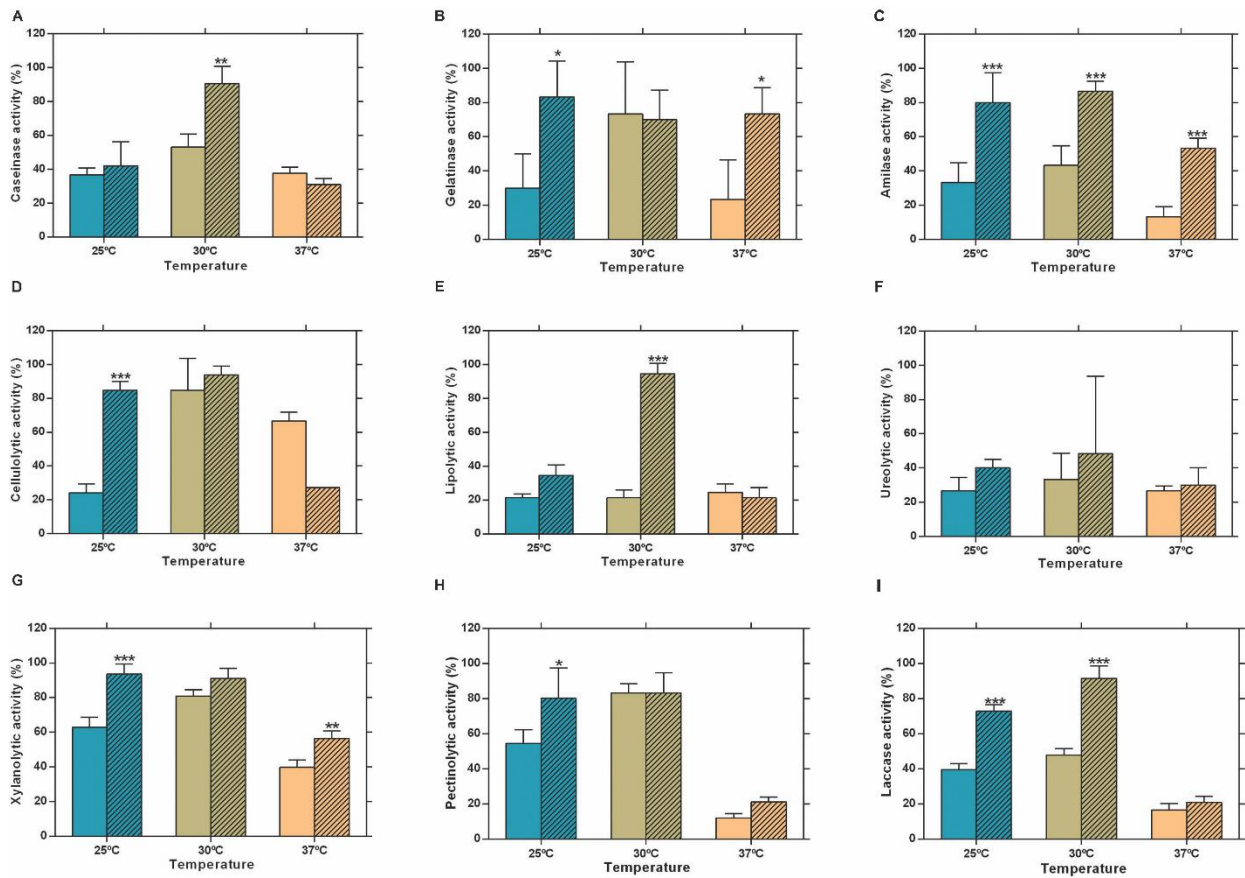


Figure 2.3 | Extracellular enzymatic activity of *L. theobromae* strains CAA019 (solid bars) and CBS339.90 (pattern bars) after a 48 h incubation period. (A) caseinolytic, (B) gelatinolytic, (C) amylolytic, (D) cellulolytic, (E) lipolytic, (F) ureolytic, (G) xylanolytic, (H) pectinolytic, and (I) laccase activities. Data is presented as average \pm standard error. Two-way ANOVA, followed by a Bonferroni multiple comparison test, was used to determine the statistical significance of extracellular enzymatic activity within the same temperature (* $p < 0.05$, ** $p < 0.01$, *** $p < 0.001$).

Due to the nature of the hosts – *C. nucifera* for CAA019 and a human patient for CBS339.90 – the zymographies were performed at 25 and 37 °C, to investigate the effect that human body temperature could have on the strains. Both strains were able to secrete all enzymes assayed (Figure 2.3). Nonetheless, CBS339.90 displayed higher enzymatic activity than strain CAA019 in most conditions tested (Figure 2.3). Only one exception was detected; at 37 °C CAA019 had a higher cellulolytic activity than CBS339.90 grown at the same temperature ($p < 0.001$; Figure 2.3D). Zymography analysis confirms the data obtained by plate assay. One exception was the cellulolytic activity of *L. theobromae*, which was higher at 25 °C when analyzed by zymography, but not by plate assay. The difference observed could be related to the short culture time of *L. theobromae* in the plate assays.

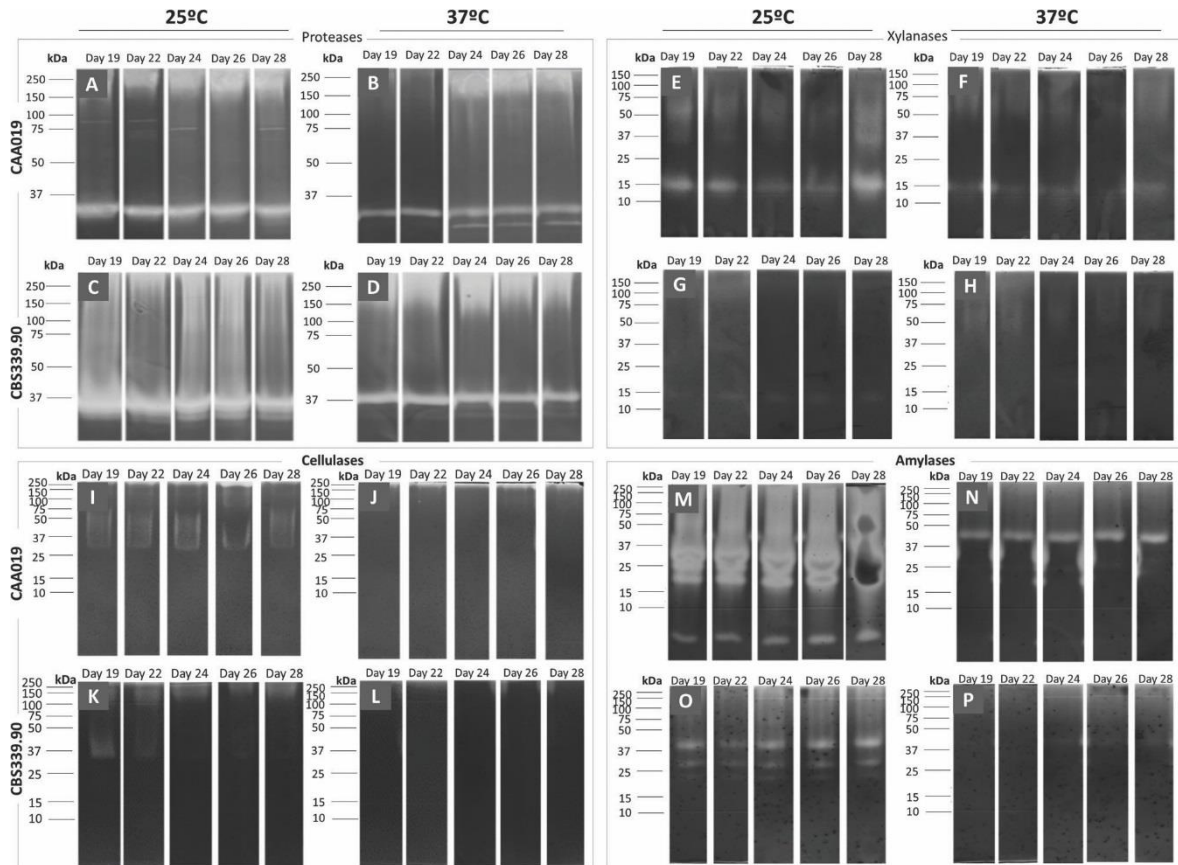


Figure 2.4 | Extracellular gelatinolytic (A–D), xylanolytic (E–H), amylolytic (I–L) and cellulolytic (M–P) activities of *L. theobromae*. Strain CAA019 (A/B, E/F, I/J, M/N) and strain CBS339.90 (C/D, G/H, K/L, O/P) were grown for 28 days at 25 °C (A/C, E/G, I/K, M/O) or 37° C (B/D, F/H, J/L, N/P). Each gel is representative of three independent runs.

As seen in figures 2.3 and 2.4, CAA019 and CBS339.90 express extracellular proteolytic, amylolytic, cellulolytic and xylanolytic enzymes. Most enzymes have very high (≈ 200 kDa) or very low (≈ 4.2 kDa) apparent MWs. These MWs could correspond to aggregation or multimeric forms of these enzymes or to degraded peptides with enzyme activity, rather than the MW of the discrete enzymes. In fact, the MWs of the enzymes identified by mass spectrometry (Table 2.2) are in the range of 26.9–58.7 kDa. We have observed a strain-, temperature-, and time-dependent expression pattern of many of these enzymes, particularly cellulases (Figure 2.4-M/N and O/P).

Fungal pathogens have a detrimental impact on plant production and the strategies they use to infect their hosts should be investigated to predict their behavior and protect the plants from fungal infections (Gonzalez-Fernandez and Jorrín-Novo, 2012; Fernandes et al., 2014). Fungal pathogenicity results in the synthesis of molecules, such as CWDEs, inhibitory proteins and toxins, that have been described as being involved in the infection mechanisms of fungi (Kikot et al., 2009). We expect that a plant adapted pathogen will secrete enzymes able to degrade plant specific

substrates (as is the case of CWDEs) while an animal adapted strain will secrete a lower number (or exhibit a lower activity) of these enzymes. On the other hand, we expect that a strain adapted to animal environment will express a higher number of enzymes able to interact with mammalian specific substrates.

Cellulose, hemicellulose, and lignin are the major components of the plant cell wall, cellulose being the most abundant (Gibson et al., 2011). The ability of fungi to produce CWDEs facilitate fungal penetration (Gibson et al., 2011). There are some evidences that plant pathogens may produce different amounts of specific CWDEs depending on the plant host (van der Does and Rep, 2007; King et al., 2011). In this context it is curious that both strains have such distinct cellulolytic activity profiles. It is plausible that strain CBS339.90 may have developed some type of adaptation to colonize human hosts. For example, the high protein-content matrix (without complex carbohydrates like cellulose) may have contributed to the high secretion of proteases by CBS339.90.

Secretome Analysis

The secretome of both strains of *L. theobromae* grown at 25, 30, and 37 °C (Figure 2.5) was analyzed by SDS-PAGE/LC/MS/MS. Approximately 77 % of the selected proteins were identified (10 proteins were identified for CAA019 strain and 11 for CBS339.90 strain); most of proteins are extracellular enzymes (87.5 %) and only 12.5 % are extracellular proteins with non-enzymatic functions (Table 1.1).

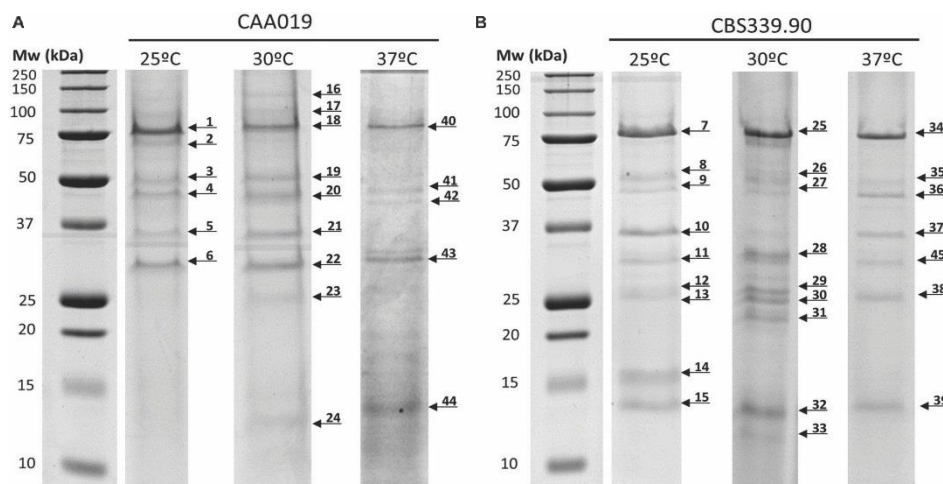


Figure 2.5 | Secretome of *L. theobromae* strains CAA019 (A) and CBS339.90 (B) analyzed by SDS-PAGE. Cultures were grown for 72 h, at 25 and 37 °C. Each gel is representative of three independent analyses. Arrows represent the different proteins found in these conditions.

Due to the lack of genome sequence, all proteins were identified based on their homology with the proteins of *M. phaseolina MS6* and *N. parvum UCRNP2*, two pathogenic members of the family Botryosphaeriaceae, whose genome is sequenced and integrated into UniProtKB (Islam et al., 2012).

The strains showed different protein profiles, which were affected by growth temperature, suggesting different interactions with the environment. For each strain some unique proteins were found. For CAA019 we identified four strain-specific proteins – a glucose-methanol-choline oxidoreductase (K2RRJ6), a putative choline dehydrogenase protein (R1E7Q5), a β -galactosidase (K2SSA3) and a putative f5/8 type c domain protein (R1GH64). From these, the three enzymes are known to be involved in cellulose degradation (Yoshida et al., 2002; Van den Brink and de Vries, 2011), which is expected, since this is a phytopathogenic strain. However, the putative f5/8 type c domain protein, found only at 30 °C, is a coagulation factor. The coagulation factor expressed by CAA019 possesses a functional domain that promotes binding to anionic phospholipids (Hunter et al., 2012), known to be involved in pathogenesis for some species of fungi (Chaffin et al., 1998).

For CBS339.90, also four strain-specific proteins were identified – a putative tripeptidyl-peptidase 1 protein (R1GTC8), a phosphoesterase (K2RUW5), a putative glucan endo- α -glucosidase agn1 protein (R1GU94) and a glycoside hydrolase family 71 (K2R498). It is important to highlight that the putative tripeptidyl-peptidase 1 protein was found only at 25 °C. This protease has a serine-type endopeptidase activity (Hunter et al., 2012). In *Aspergillus fumigatus*, it is part of a set of proteases (sedolisins) that have the ability to degrade proteins at acidic pH values. This allows the generation of assimilable nitrogen in decomposing organic matter and composts (Reichard et al., 2006). Also, it is responsible to acidify the culture supernatant of this species *in vitro*, which can be related with the acidification of its microenvironment in the living host to facilitate nutrition and proliferation of the hyphae during the infection process (Reichard et al., 2006). The glycoside hydrolases are typically produced by phytopathogenic fungi to degrade cellulose and xylans of the plant cell wall and penetrate into the host tissue (Murphy et al., 2011). These enzymes act hydrolyzing the glycosidic bonds between two or more carbohydrates or between a carbohydrate and a non-carbohydrate moiety. The GH family 71 was expressed only by CBS339.90 and comprises the α -1,3-glucanases (Hunter et al., 2012).

Other families of GH were found in both strains, as the GH family 10, that includes xylanases and cellobiohydrolases and GH family 17, that comprises enzymes as endo-1,3- β -glucosidases, lichenases and exo-1,3-glucanases (Hunter et al., 2012). Glucoamylases whose function is also

related with the degradation of plant cell wall, by hydrolyzing 1,4- α -glucose (Hunter et al., 2012; Kubicek et al., 2014) are also expressed by both strains.

Several aspartic proteases are expressed by *L. theobromae*. Aspartic proteases from the family A1 and a putative a chain endothiapepsin are expressed by both strains. Besides its involvement in physiologic cellular functions, aspartic proteases play a crucial role as virulence factors, dissemination, and host evasion (Rawlings and Bateman, 2009). These enzymes have been related to human pathogenesis (Monod et al., 2002; Yike, 2011), which is concordant with the fact that we identified these enzymes at 37 °C. In these cases, aspartic proteases are probably involved in several processes such as the degradation of the extracellular matrix (mainly composed by collagens and other proteins; Duarte et al., 2007, 2016) leading to the progression of the pathogen.

Thus, some of the proteins seem to be involved in plant pathogenesis processes, as is the case of glycoside hydrolases (Murphy et al., 2011), but also in animal pathogenesis processes, as is the case of proteases or aspartic proteases. The plate assay confirmed the presence of these enzymes for both isolates and the zymography analysis, the presence of multiple endoglucanases, xylanases, and proteases (Figure 2.4).

Table 2.1 | Protein identification by LC-MS/MS of proteins secreted by *L. theobromae* strains CAA019 and CBS339.90.

Bands ⁽¹⁾	Accession Number	Proteins	Theoretical Mw (kDa)	Organism	Function ⁽²⁾	Biological process ⁽²⁾	Number of peptides ⁽³⁾	Score MS AMANDA
1, 40	K2RRJ6	Glucose-methanol-choline oxidoreductase	72	<i>Macrophomina phaseolina</i>	oxidoreductase activity, acting on the CH-OH group of donors, other acceptors	catalysis of an oxidation-reduction reaction	2	679.27
1, 40	R1E7Q5	Putative choline dehydrogenase protein	71.3	<i>Neofusicoccum parvum</i>	oxidoreductase activity, acting on the CH-OH group of donors, other acceptors	catalysis of an oxidation-reduction reaction	2	679.27
7	R1GTC8	Putative tripeptidyl-peptidase 1 protein	64.8	<i>Neofusicoccum parvum</i>	serine-type endopeptidase activity	proteolysis	2	426.40
8	K2RUW5	Phosphoesterase	43.9	<i>Macrophomina phaseolina</i>	hydrolase activity, acting on ester bonds	hydrolase	2	663.55
9	R1GU94	Putative glucan endo--alpha-glucosidase agn1 protein	49.3	<i>Neofusicoccum parvum</i>	hydrolase activity	hydrolase	2	579.98
10	K2RGL3	Peptidase A1	26.9	<i>Macrophomina phaseolina</i>	aspartic-type endopeptidase activity	proteolysis	2	4710.33
6, 11	K2SBN0	Beta-xylanase	34.2	<i>Macrophomina phaseolina</i>	hydrolase activity	carbohydrate metabolic process, metabolic process	2	1020.33
6, 11	R1FWZ0	Beta-xylanase	34.8	<i>Neofusicoccum parvum</i>	hydrolase activity	carbohydrate metabolic process, metabolic process	2	1020.33

CHAPTER 2 – Temperature modulates the secretome of *L. theobromae*

16	K2SSA3	Beta-galactosidase	107.8	<i>Macrophomina phaseolina</i>	beta-galactosidase activity	carbohydrate metabolic process	2	382.31
18	R1GH64	Putative f5 8 type c domain protein	59.2	<i>Neofusicoccum parvum</i>	hydrolase activity, hydrolyzing O-glycosyl compounds	carbohydrate metabolic process, cell adhesion	2	2398.24
19, 20, 41	K2RQR5	Peptidase A1 (Fragment)	39.9	<i>Macrophomina phaseolina</i>	aspartic-type endopeptidase activity	proteolysis	2	781.41
5, 10, 13, 15, 21, 24, 30, 31, 32, 33, 37, 42, 44	R1ESA5	Putative a chain endothiapepsin	42.5	<i>Neofusicoccum parvum</i>	Aspartic-type endopeptidase activity	proteolysis	2	5116.87
7, 25	K2S7L9	Glucoamylase	67.8	<i>Macrophomina phaseolina</i>	glucan 1,4-alpha-glucosidase activity; starch binding	polysaccharide catabolic process	2	5006.77
9, 28, 36	K2R498	Glycoside hydrolase family 71	49.2	<i>Macrophomina phaseolina</i>	Hydrolase activity	hydrolase	2	2124.51
6, 12, 22, 29, 43	K2STT8	Glycoside hydrolase family 17	32	<i>Macrophomina phaseolina</i>	carbohydrate metabolic processes	hydrolase activity	2	5379.70
1, 7, 25, 26, 27, 34, 40	R1GLG1	Glucoamylase	68.5	<i>Neofusicoccum parvum</i>	glucan 1,4-alpha-glucosidase activity; starch binding	polysaccharide catabolic process	4	9860.40

Band number corresponds to the numbering indicated in Figure 2.5 ⁽¹⁾. The GO terms correspondent to the function and the biological processes ⁽²⁾ of the proteins were searched with InterPro (Hunter et al., 2012). The subcellular localization was deduced with Bacello (Pierleoni et al., 2006): all proteins were inferred to be extracellular. Only proteins with two unique peptides identified were included in the table. The number of peptides ⁽³⁾ is the number of peptides identified per band.

Globally, both strains showed a similar tendency regarding the number of detected bands, with a decrease of the number with increasing temperature. However, CBS339.90 strain presented more detected bands when compared with CAA019 strain (Figure 2.5; Table 2.2).

A Permutational Multivariate Analysis of Variance was employed using R package ‘vegan’ and the RStudio v 0.98.1103 interface (Oksanen et al., 2015; R Core Team, 2015). It was shown that for the identified proteins (computed through a presence-or-absence matrix), 44 % of the variance is explained by the strain factor ($R^2 = 0.4467$). Contrary, the differences found for fungi growth temperature were not statistically significant, suggesting that the strain has a large relevance on the protein profile in this study (p -value < 0.01), which could be related to a host-adaptation of these strains.

Table 2.2 | Summary of the proteins identified in *L. theobromae* strains CAA019 and CBS339.90 at 25, 30, and 37 °C.

Accession Number	Proteins	CAA019			CBS339.90		
		25 °C	30 °C	37 °C	25 °C	30 °C	37 °C
K2RRJ6	Glucose-methanol-choline oxidoreductase	+	-	+	-	-	-
R1E7Q5	Putative choline dehydrogenase protein	+	-	+	-	-	-
R1GTC8	Putative tripeptidyl-peptidase 1 protein	-	-	-	+	-	-
K2RUW5	Phosphoesterase	-	-	-	+	-	-
R1GU94	Putative glucan endo- α -glucosidase agn1 protein	-	-	-	+	-	-
K2RGL3	Peptidase A1	-	-	-	+	-	-
K2SBNO	Beta-xylanase	+	-	-	+	-	-
R1FWZ0	Beta-xylanase	+	-	-	+	-	-
K2SSA3	Beta-galactosidase	-	+	-	-	-	-

R1GH64	Putative f5 8 type c domain protein		+					
K2RQR5	Peptidase A1 (Fragment)		+	-				
R1ESA5	Putative a chain endothiapepsin	+	+	+	+	+	+	
K2S7L9	Glucoamylase				+	+		
K2R498	Glycoside hydrolase family 71				+	+	+	
K2STT8	Glycoside hydrolase family 17	+	+	+	+	+		
R1GLG1	Glucoamylase	+		+	+	+	+	

The symbols represent the presence (+) or the absence (-) of the proteins.

Cytotoxicity

We investigated the influence of temperature on the cytotoxic potential of *L. theobromae*, strains CAA019 and CBS339.90, to Vero cell line. Both strains were cytotoxic under all conditions tested, with the exception of the environmental strain (CAA019) grown at 37 °C (Figure 2.6). Interestingly, temperature had opposite effect on both strains; the cytotoxic effect of CAA019 was detected mostly when cultured at 25 °C, decreasing at 30 °C and being absent at 37 °C (Figure 2.6A). The cytotoxic effect of CBS339.90 (Figure 2.6B) increased with temperature ($p < 0.001$), reaching 90 % of cell mortality when grown at 37 °C. Interestingly, CBS339.90 also showed higher growth rates (Figure 2.2) and extracellular enzymatic activity (Figure 2.3) at 37 °C when compared with CAA019. Proteins typically related with infection mechanisms were found in the secretome of CBS339.90 (aspartic proteases), suggesting that they can be involved in the high level of cell mortality found for this strain.

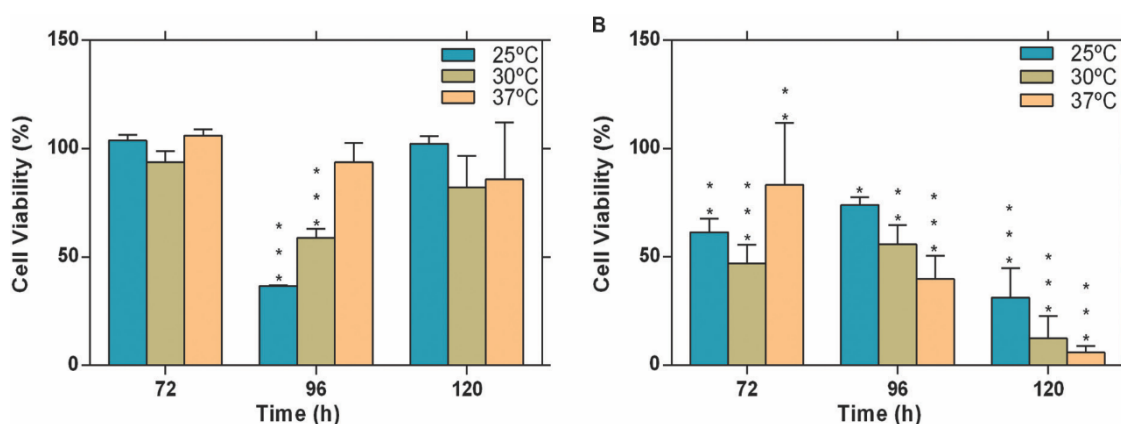


Figure 2.6 | Evaluation of cytotoxicity of the extracellular fraction of *L. theobromae*. (A) strain CAA019 incubated at 25, 30, and 37 °C and (B) strain CBS339.90, incubated at 25, 30, and 37 °C. Data is presented as average \pm standard error of two independent experiments performed in triplicate. Two-way ANOVA, followed by a Bonferroni multiple comparison test, was used to determine the statistical significance of cytotoxicity within the same temperature (* $p < 0.05$, ** $p < 0.01$, *** $p < 0.001$).

Host specificity in plant-pathogenic fungi impact their host range. Although it has been suggested that for most Botryosphaeriaceae species there is no host specificity (Esteves et al., 2014), the differences between the secretome profiles of both strains at 25 and 37 °C can be related to adaptation to specific host conditions. While strain CAA019 was isolated from a coconut tree, CBS339.90 was isolated from a human, at approximately 37 °C. Since the optimal growth of this species is between 27 and 33 °C, we can argue that the ability to infect humans may be the result of an adaptation to an increased temperature. This agrees with the fact that only strain CBS339.90 was cytotoxic to Vero cells at 37 °C and that it produces more biomass and extracellular enzymes at this temperature than CAA019.

CONCLUSION

We showed that temperature modulates the extracellular protein production of strains of *L. theobromae* found in different ecological niches: a tropical fruit tree and a hospitalized patient. The temperature growth range was wide, between 15 and 37 °C, a feature common for species in the family Botryosphaeriaceae. The extracellular enzymatic activity also varied with fungal growth temperature. Both strains were able to induce cytotoxic effects in mammalian cells. However, CBS339.90 is more cytotoxic than CAA019, especially at 37 °C, where cell mortality reached 90 %. The ability to grow at 37 °C and the secretion of hydrolytic enzymes, namely of aspartic proteases,

at this temperature are typical characteristics of human pathogenic fungi that may be related to virulence (Karkowska-Kuleta et al., 2009). Our data suggests that the colonization of different hosts may lead to strain specificity.

ACKNOWLEDGMENTS

Thanks are due, to FCT/MEC through national funds, for the financial support of CESAM (UID/AMB/50017 – POCI-01-0145-FEDER-007638), of QOPNA research Unit (UID/QUI/00062/2013), of iBiMED (UID/BIM/04501/2013), of UIDC (UID/IC/00051/2013) and RNEM (REDE/1504/REM/2005 that concerns the Portuguese Mass Spectrometry Network), and the co-funding by the FEDER, within the PT2020 Partnership Agreement and Compete 2020. This study was partially supported by FEDER funding through COMPETE program and by national funding through FCT within the research project ALIEN (PTDC/AGR-PRO/2183/2014 – POCI-01-0145-FEDER-016788). The authors acknowledge FCT financial support to AA (IF/00835/2013), to AE and to AD (BPD/102572/2014 and BPD/46290/2008) and to CF (BD/97613/2013).

CHAPTER 3

Lasiodiplodia theobromae as a producer of biotechnologically
relevant enzymes

ABSTRACT

Phytopathogenic fungi are known to produce several types of enzymes usually involved in plant cell wall degradation and pathogenesis. The increasing of the global temperature may induce fungi, such as *Lasiodiplodia theobromae*, to alter its behavior. Nonetheless, there is only limited information regarding the effect of temperature on the production of enzymes in *L. theobromae*. The need for new, thermostable enzymes, that are biotechnologically relevant, led us to investigate the effect of temperature on the production of several extracellular enzymatic activities by different *L. theobromae* strains. Fungi were grown at 25 °C, 30 °C and 37 °C and the enzymatic activities were detected by plate assays, quantified by spectrophotometric methods and characterized by zymography. The thermostability (25–80 °C) of the enzymes produced was also tested. Strains CAA019, CBS339.90, LA-SOL3, LA-SV1 and LA-MA-1 produced amylases, gelatinases, caseinases, cellulases, lipases, laccases, xylanases, pectinases and pectin liases. Temperature modulated the expression of the enzymes, and this effect was more visible when fungi were grown at 37 °C than at lower temperatures. Contrary to proteolytic and endoglucanolytic activities, whose highest activities were detected when fungi were grown at 30 °C, lipolytic activity was not detected at this growth temperature. Profiles of proteases and endoglucanases of fungi grown at different temperatures were characterized by zymography. Enzymes were shown to be more thermostable when fungi were grown at 30 °C. Proteases were active up to 50 °C and endoglucanases up to 70 °C. Lipases were the least stable, with activities detected up to 45 °C. The enzymatic profiles detected for *L. theobromae* strains tested showed to be temperature and strain-dependent, making this species a good target for biotechnological applications.

KEYWORDS: extracellular enzymatic activity, temperature, proteases, endoglucanases, lipases, thermostability

INTRODUCTION

Fungal plant pathogens are known to express high amounts of hydrolytic and oxidative enzymes (Yike, 2011; Do Vale et al. 2012; Suryanarayanan et al., 2012; Esteves et al., 2014). The lack of specialized host penetration structures makes hydrolytic and oxidative enzymes crucial to degrade plant cell wall and extracellular matrices, which are plants' major barriers (Gibson et al., 2011; Kubicek et al., 2014). Although the composition and structure of plant cell walls differ among plant lineages, they share basic constituents, as cellulose microfibrils embedded in a matrix of pectin,

hemicellulose, lignin, and structural proteins (Kubicek et al., 2014). Also, fungal nutrition is achieved via the absorption of small constituents obtained by the enzymatic catabolism of environmental complex organic polymers, such as cellulose or proteins (Suryanarayanan et al., 2012; Esteves et al., 2014). Thus, the most highly recognized extracellular hydrolytic enzymes involved in plant invasion include cellulases, proteases, and lipases. Cellulases are responsible for catalyzing the hydrolysis of cellulose into simple sugars, weakening the plant cell wall (Sajith et al., 2016). Proteases are known to degrade proteins of the cell wall, facilitating hyphal penetration through it, and to modify chemical signals involved in the plant defense mechanisms (Esteves et al., 2014). In contrast, lipases also contribute to the degradation of the plant cell wall, but the exact mechanism remains widely unknown (Park et al., 2013; Esteves et al., 2014).

Lasiodiplodia theobromae (Pat.) Griff. and Maubl. is a phytopathogenic fungus from the family Botryosphaeriaceae, typically found in tropical and subtropical regions (Alves et al., 2008; Phillips et al., 2013). It is widely distributed, but mostly confined to 40° North and 40° South of the equator, presenting its optimal growth temperature between 27 °C to 33 °C (D'souza and Ramesh, 2002). It has been considered a latent pathogen but *L. theobromae* is also able to establish endophytic relations (Jami et al., 2013) and was associated to approximately 500 hosts, mostly woody plants (Phillips et al., 2013; Rodríguez-Gálvez et al., 2015). It has also been associated with human infections, behaving as an opportunist pathogen (Summerbell et al., 2004; Kindo et al., 2010; Saha et al., 2012a,b). Filamentous fungi are the preferred source of industrial enzymes due to their easy cultivation and high production of extracellular enzymes (Bennet, 1998; Dekker, 2003; Corrêa et al., 2014). Several types of enzymes produced by filamentous fungi are found available in the market: glucoamylases, cellulases, lipases, pectinases, laccases, catalases, proteases, and others (Bennet, 1998; Dekker, 2003; Corrêa et al., 2014). Among them, *Aspergillus* species dominate the production of many enzymes (Banerjee et al., 2003; Blackwell, 2011; Braaksma and Punt, 2008). These enzymes are currently applied in the production of detergents, starch, drinks, food, textile, animal feed, chemicals, and biomedical products (Bennet, 1998; Dekker, 2003; Corrêa et al., 2014). Phytopathogenic fungi, known to produce a huge arsenal of extracellular enzymes to penetrate the plant host, can be a good source of enzymes with biotechnological potential (Barros et al., 2010). The great ability of adaptation to different environments, the capacity to infect a vast number of hosts and the expression of high amounts of extracellular enzymes makes *L. theobromae* a potential producer of biotechnologically relevant enzymes (Dekker, 2003; Esteves et al., 2014).

The goal of this work was to characterize the extracellular enzymatic activities of different strains of *L. theobromae* and evaluate the impact that temperature has on their production and activity.

MATERIALS AND METHODS

Microorganisms

The strains used in this study were: *L. theobromae* strains LA-SOL3 and LA-SV1, isolated from *Vitis vinifera* in Peru (Rodríguez-Gálvez et al., 2015), strain CAA019, isolated from *Cocos nucifera L.* in Brazil, strain LA-MA-1, isolated from *Mangifera indica*, in Peru and strain CBS339.90, isolated from a phaeohyphomycotic cyst of a patient from Jamaica. Strain CBS339.90 was obtained from the Westerdijk Fungal Biodiversity Institute. Cultures were maintained on Potato Dextrose Agar medium (PDA, Merck, Darmstadt, Germany). For liquid growth, two plugs (5 mm diameter) from a culture with 4 days were inoculated into a 250 mL flask containing 50 mL of the desired medium and incubated at 25 °C, 30 °C or 37 °C. All assays were performed in triplicate. Culture supernatants were collected by gravitational filtration through filter paper and stored at –80 °C until use. Mycelia were dried at 50 °C for 48 h, to determine the dry weight.

Detection of Extracellular Enzymes

Different solid media were inoculated with a 5 mm-diameter agar plug from an actively growing culture and incubated at 25 °C, 30 °C and 37 °C, for 48 h. Data is presented as enzymatic index: the ratio between the halo of enzymatic degradation and the radial growth of the mycelium. The obtained ratio was then transformed into percentage, being the highest value of enzymatic index found used as 100 %.

Proteases

A supplement of 1 % of skim milk (w/v) or gelatin (w/v) was added to the malt extract agar medium (MEA) (Esteves et al., 2014). After 48 h, the activity was detected as a clear halo around the mycelium.

Xylanases and Cellulases

Cellulolytic and xylanolytic activity were detected by adding 1.5 % agar (w/v) and 0.5 % carboxymethylcellulose (w/v) (CMC) for cellulases' detection, or 0.5 % xylan (w/v) and 0.1 % yeast extract (w/v) for xylanase's detection (St Leger et al., 1997) to a minimal medium (MM) [0.3 % NaNO₃ (w/v), 0.1 % KH₂PO₄ (w/v), 0.05 % MgSO₄ (w/v)]. After 48 h, plates were covered with Congo Red (Sigma, St. Louis, MO, USA) (1 mg.mL⁻¹) during 15 min and destained with 1 M NaCl. Activity was detected as a yellow halo around the mycelium in a red background.

Lipases

Lipolytic activity was detected using a solid medium consisting in 1.5 % agar (w/v), 1 % peptone (w/v), 0.5 % NaCl (w/v), 0.01 % CaCl₂ (w/v) and 1 % Tween 20 (v/v) (Hankin and Anagnostakis, 1975). After 48 h, activity was detected as a precipitate around and under the mycelium.

Amylases

Amylolytic activity was detected using starch agar [1 % peptone (w/v), 0.5 % yeast extract (w/v), 0.5 % NaCl (w/v) and 0.2 % starch (w/v)]. After 48 h, the plates were covered with lugol solution during 10 min and the activity was detected as a clear halo in a dark background (Hankin and Anagnostakis, 1975).

Pectinases and Pectin Lyases

A minimal medium supplemented with 0.1 % yeast extract (w/v), 0.5 % pectin (w/v) and 1.5 % agar (w/v), at pH 5.0 was used to detect pectinases and the same medium at pH 7.0 for pectin lyases. After 48 h, plates were covered with 1 % of cetyltrimethyl ammonium bromide. Activity was detected as a transparent halo around the mycelium (Hankin and Anagnostakis 1975; St Leger et al., 1997).

Laccases

For detection of laccase activity, a solid medium containing a solution of 1 % of tannic acid previously sterilized was added to 1.5 % (w/v) malt extract and 2 % agar (w/v) (Rigling, 1995). After 48 h, activity was detected as an alteration of the medium color to brown around the mycelium.

QUANTIFICATION OF EXTRACELLULAR ACTIVITIES

Cellulolytic Activity Quantification

A crude enzymatic extract was obtained after inoculation of two plugs with 5 mm of diameter in 50 mL of MM supplemented with 0.5 % (w/v) CMC and 0.1 % yeast extract (w/v). Endoglucanase activity was measured by CMC degradation, using 3,5-dinitrosalicylic acid (DNS) method to the reduction of sugars (Miller, 1959). Briefly, 225 µL of enzymatic extract was added to the mixture of 75 µL of 0.1 M sodium acetate buffer, pH 5, and 1200 µL of 5 % CMC, previously incubated at the desired temperature. An aliquot of 125 µL was taken at 0 min, 20 min, 60 min and 120 min of incubation and added to 500 µL of DNS, at 100 °C, during 5 min. After cooling, 750 µL of ultrapure

water was added to all the tubes and the absorbance was measured at 540 nm. The blank sample was treated as all the samples, replacing the enzymatic crude by ultrapure water. As standard curve, several concentrations of glucose were prepared. The quantification of the cellulolytic activity was made for 7 different temperatures: 25 °C, 30 °C, 37 °C, 45 °C, 50 °C, 70 °C and 80 °C. Data is presented as mean of three replicates, normalized for mycelium dry weight.

Proteolytic Activity Quantification

Proteolytic activity was determined as described by Macchione et al. 2008, with slight modifications. A crude enzymatic extract was obtained after inoculation of two plugs (5 mm of diameter) in 50 mL of Potato Dextrose Broth (PDB) medium. An aliquot of 300 µL of crude extract was added to 1.7 mL of casein [2 % (w/v), in 100 mM sodium phosphate buffer, pH 6.5] at the desired temperature and 400 µL of this mixture was added to 900 µL of 6 % trichloroacetic acid TCA (w/v) after 0 min, 5 min, 10 min and 20 min of incubation. All the samples were maintained in ice and centrifuged at 13000 rpm for 10 min. The blank sample was prepared by replacing the enzymatic crude extract by ultrapure water and treated as all the samples. The supernatant was used to measure the absorbance at 280 nm. The quantification of the proteolytic activity was made at: 25 °C, 30 °C, 37 °C, 45 °C, 50 °C, 70 °C and 80 °C. Data is presented as mean of three replicates, normalized for mycelium dry weight.

Lipolytic Activity Quantification

Lipolytic activity was determined according to Kotogán et al. 2014, with slight modifications. A crude enzymatic extract was obtained after inoculation of two plugs (5 mm of diameter) in 50 mL of PDB medium. p-nitrophenyl palmitate (pNPP; Sigma-Aldrich, Lisbon, Portugal) was used as substrate. A stock solution (3 mM) was prepared in 25 % dimethyl sulfoxide and 0.5 % of Triton X-100 and completed with potassium phosphate buffer (pH 6.8). A volume of 50 µL of buffered pNPP solution was added to 150 µL of crude extract, and incubated at the test temperature for 0 min, 45 min and 90 min. The reaction was stopped by adding 50 µL of 0.1 M sodium carbonate. The released p-nitrophenol (pNP) was measured at 405 nm in 96-well plates using a microplate reader (Biotek, Synergy HT, Winooski, VE, USA). The blank sample was treated as all the samples, replacing the enzymatic crude extract by ultrapure water. The molar absorption coefficient of pNP ($\epsilon = 1.2475 \times 10^4 \text{ M}^{-1} \cdot \text{cm}^{-1}$) was estimated from the absorbance of pNP standard solutions measured at 405 nm. One enzymatic unit was defined as the amount of the enzyme that releases 1 mmol of pNP per minute.

The quantification of the lipolytic activity was made at 25 °C, 30 °C, 37 °C and 45 °C since higher temperatures lead to spontaneous substrate degradation. Data is presented as mean of three replicates, normalized for mycelium dry weight.

Zymography

For each strain, two 5 mm-diameter plugs from an actively growing culture were inoculated on 50 mL PDB for 4 days. The enzymatic crude extract was obtained by filtration as described earlier (Félix et al., 2016). The characterization of the extracellular enzymes was carried out by zymography (Esteves et al., 2014). Enzymatic crude extracts were diluted in sample buffer [2:1 (v/v); 62.5 mM Tris (w/v), pH 6.8, 10 % SDS (w/v) and 20 % glycerol (v/v)] and incubated at room temperature for 10 min. The separation of the proteins was carried out in lab casted gels (10 % polyacrylamide with the correspondent substrate) in a Mini-PROTEAN 3 (Bio-Rad, Hercules, CA, USA) (Laemmli, 1970). Electrophoresis proceeded at 100 volts for 100 min. Gels were then washed twice with 0.25 % Triton X-100 (v/v) for 30 min. Gel analysis was performed after adequate staining of the gels (described below). Images were acquired on a GS-800 Calibrated Densitometer (Bio-Rad). Quantity One v. 4.6.9 (Bio-Rad) was used to estimate the apparent molecular weight (MW) of the proteins using a MW calibration kit as marker (Precision Plus Protein Standard, Bio-Rad).

Cellulases

Cellulolytic activity was assessed by zymography, as described previously (Peterson et al., 2011) with slight modifications. The substrate CMC, 1 % (w/v), was included on the preparation of the gel. After electrophoresis, the gel was incubated overnight at 25 °C in 0.05 M Tris-HCl, pH 5.0. After this period, gels were stained in Congo Red (1 %), 10 min, and destained with 1 M NaCl. Enzymes with cellulolytic activity were detected as clear bands against a red background of non-degraded substrate.

Proteases

Gelatinolytic activity was assessed by zymography, as described previously (Duarte et al., 2009), with slight modifications. Gelatin [1 % (w/v)] was used. After electrophoresis, the gel was incubated for 1 h at 37 °C, in 1.5 mM Tris, pH 8.8, 1 M NaCl, 1 M CaCl₂, 2 mM ZnCl₂, pH 7.4. Gels were stained with Coomassie Brilliant Blue R-250 [(in 50 % ethanol (v/v), 10 % acetic acid (v/v))] and destained with 25 % ethanol (v/v) and 5 % acetic acid (v/v). Enzymes with gelatinolytic activity were detected as clear bands against a blue background of non-degraded substrate.

Lipases

Lipolytic activity was accessed by zymography as described before, (Castro-Ochoa et al., 2005; Peterson et al., 2011) with slight modifications. A solid medium containing 0.001 % of rhodamine B (w/v), 3 % of olive oil (v/v) and 2.5 % agar (w/v) was prepared in Tris-HCl buffer, pH 8.0 and heated with agitation until dissolution of the agar. After electrophoresis, the gel was overlaid onto the solid medium of rhodamine B/olive oil for 3 h at 37 °C. Lipolytic activity was detected exposing the plate with the gel to 365 nm, where the enzymes with activity appeared as fluorescent bands.

Statistical Analysis

Two-way analysis of variance (ANOVA) was used to examine the extracellular enzymatic activity profiles at different temperatures for each strain ($p < 0.05$). A Tukey's multiple comparison test was employed to identify significant differences on the enzymatic profiles of a strain grown at different temperatures. All the analyses were performed with GraphPad Prism v.7 (GraphPad Software, Inc., La Jolla, CA, USA).

A Multi Factor Analysis (MFA) was carried out to infer which factors, temperature or strain, is the most relevant on the modulation of the extracellular enzymatic profiles: detection and quantification of enzymatic activity data and zymography data (molecular weight of the bands detected). Due to the different type of data (quantitative—detection and quantification of enzymatic activity—and qualitative—presence/absence of bands in zymography and their molecular weights), MFA was considered the most suitable dimension-reducing method. The MFA was conducted with R Statistical Software (R Core Team, 2015), using the function MFAmix of the package PCAmixdata (Chavent et al., 2017). The significance of the samples groups along MFA's first three dimensions was assessed by Kruskal-Wallis non-parametric analysis of variance of the samples' scores by factor. The significance of pairwise differences was computed by Tukey–Kramer (Nemenyi) post-hoc test, both functions of the PMCMR package (Pohlert et al., 2014).

RESULTS

Extracellular Enzymatic Activity

Three temperatures were selected for testing: 25 °C, 30 °C and 37 °C. Those include the average temperature of tropical and subtropical regions infected by this species (25 °C), the optimal growth temperature of the fungus (30 °C) (Félix et al., 2016) and the human body temperature (37 °C). This allows us to compare the effect that optimal and stress temperatures have on the enzymatic profile

of these strains. All strains secreted amylases, cellulases, xylanases, pectinases, pectin lyases, gelatinases, caseinases, lipases and laccases when grown at 25 °C, 30 °C and 37 °C (Figure 3.1).

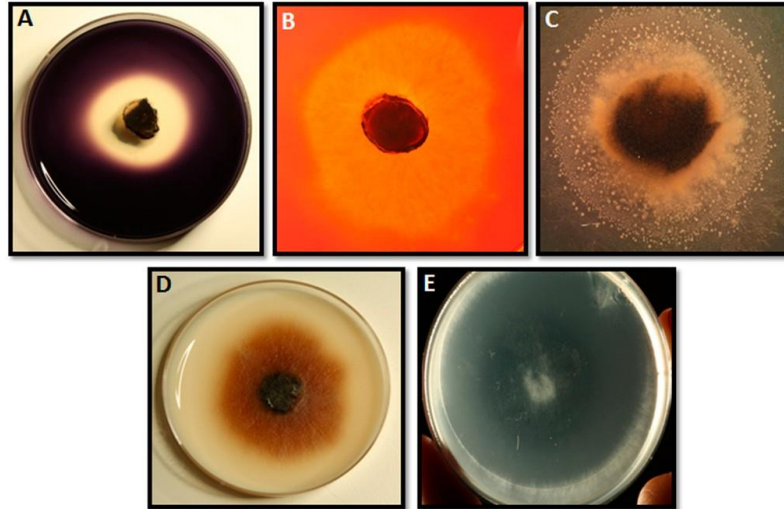


Figure 3.1 | Images showing positive results of extracellular enzymatic activity of some types of enzymes tested. (A) amylases; (B) cellulases/xylanases; (C) lipases; (D) laccases; (E) proteases.

Figure 3.2 shows the enzymatic index (%) of all tested enzymes for all the strains grown at 25 °C, 30 °C and 37 °C.

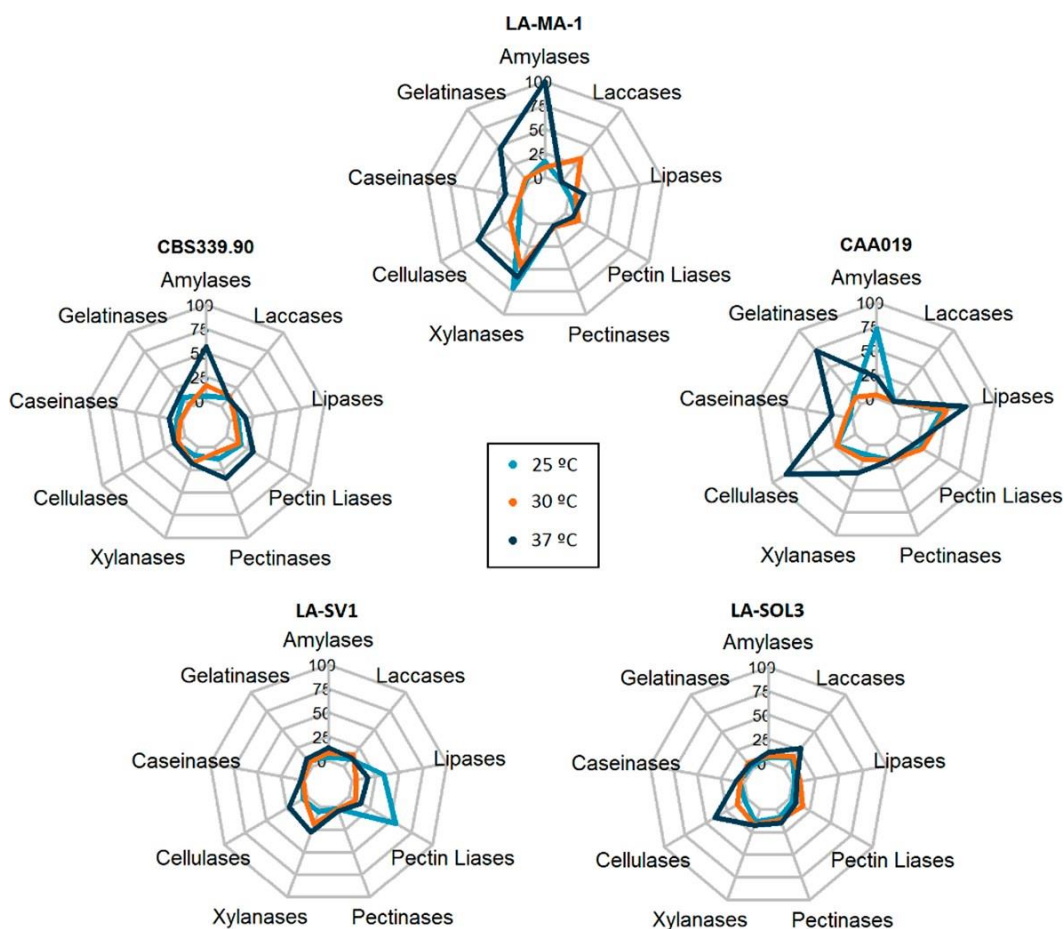


Figure 3.2 | Extracellular enzymatic activity (%) of *L. theobromae* strains after a 48-h incubation period. The percentages were calculated using the higher enzymatic index determined as 100 %.

It is possible to verify that, globally, the enzymatic indexes at 37 °C for all the enzymes tested were more variable than those obtained at 25 °C and 30 °C. It is important to highlight that the expression of gelatinases, cellulases and lipases, by strain CAA019 grown at 37 °C (Figure 3.2-CAA019) and of amylases by strain LA-MA-1 (Figure 3.2-LA-MA-1) was significantly higher ($p < 0.0001$) than when the strain was grown at 25 °C or 30 °C. For the clinical strain, CBS339.90 (Figure 3.2-CBS339.90), the profiles obtained after growth at 25 °C and 30 °C were similar, being the extracellular activity significantly higher at 37 °C ($p < 0.0001$) for most enzymes (amylases, gelatinases, caseinases, pectinases and pectin liases). For the strains isolated from grapevines, LA-SV1 and LA-SOL3, the activities were low at all growth temperatures (Figure 3.2).

Although the plate assay is very useful to evaluate the presence/absence of a specific enzyme, only a semi-quantification of the activity can be carried out. Thus, some enzymes were selected to be

quantified due to their relevance for fungal pathogenicity processes as well due to their biotechnological potential: endoglucanases, proteases and lipases (Figure 3.3).

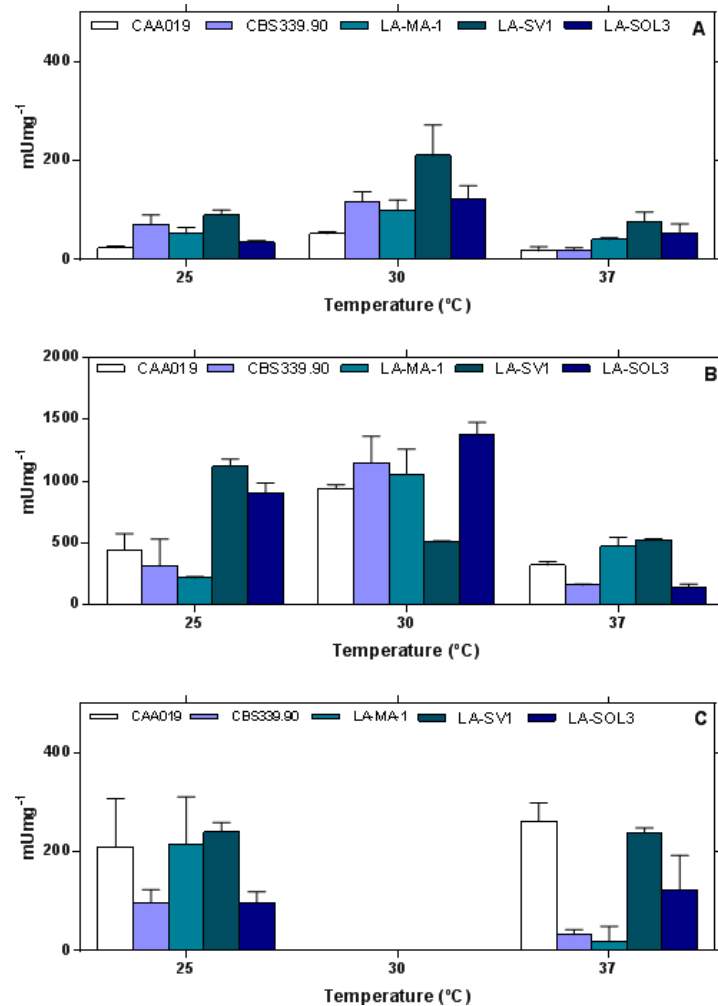


Figure 3.3 | Extracellular endoglucanolytic (A); proteolytic (B) and lipolytic (C) activities of the 5 strains of *L. theobromae* grown at 25 °C, 30 °C and 37 °C and tested at the same temperature of growth. Data is presented as average ± standard deviation, normalized for mycelium dry weight.

Globally, strains grown at 30 °C presented higher enzymatic activities than when grown at 25 °C and 37 °C. Lipolytic activity was not detected when the strains were grown at 30 °C. The expression of proteases by *L. theobromae* strains was higher than the expression of lipases and endoglucanases, especially when fungi were grown at 30 °C. Endoglucanolytic activities of strains LA-MA-1, LA-SV1 and LA-SOL3 grown at 30 °C were significantly higher than when the fungi were grown at 25 °C or 37 °C ($p < 0.0001$). Endoglucanolytic activity of strain CAA019 was independent of growth temperature.

Proteolytic activity (Figure 3.3B) was significantly higher when strains were grown at 30 °C ($p < 0.001$). The lipolytic activity detected when fungi were grown at 25 °C and 37 °C was similar for all strains (Figure 3.3C), except for strains CBS339.90 and LA-MA-1, where a significant lower activity was detected at 37 °C ($p < 0.05$ and $p < 0.0001$, respectively).

The crude extracts were also characterized by sodium dodecyl sulfate (SDS)-zymography analysis. Figure 3.4 shows the proteolytic and endoglucanolytic profiles for all strains grown at 25 °C, 30 °C and 37 °C. Lipolytic activities were not detected by zymography, either because activity is below the limits of detection of the technique, or because these enzymes were not able to digest olive oil.

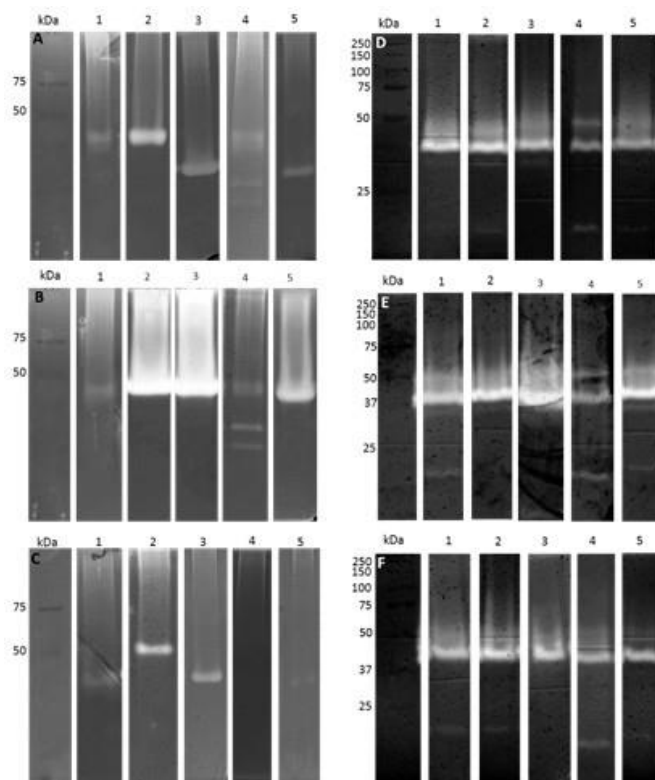


Figure 3.4 | Extracellular gelatinolytic (A–C) and endoglucanolytic (D–F) activities of 5 strains of *L. theobromae* grown at 25 °C (A/D), 30 °C (B/E) and 37 °C (C/F). 1- LAMA-1, 2- CBS339.90, 3- LA-SV1, 4- CAA019, 5- LA-SOL3. Each gel is representative of three independent runs.

Proteolytic profiles varied depending on the temperature of growth and on the strain. Enzymes with apparent molecular weights between 45.5 and 20.9 kDa (Figure 3.4A–C) were detected. The most intense bands were detected for strains CBS339.90, LA-SV1 and LA-SOL3, grown at 30 °C.

Cellulolytic profiles were similar between strains and growth temperatures: it was possible to detect bands with apparent molecular weights between 51.3 and 11.5 kDa (Figure 3.4D–F). However, at 30 °C, the bands are more intense when compared with the profiles obtained for 25 °C and 37 °C. This agrees with activity quantification, where the growth temperature that led to higher activities was 30 °C. At 25 °C, the clinical strain secreted less proteases than some environmental strains (CAA019, LA-MA-1 and LA-SV1). However, at 37 °C, strain CBS339.90 exhibited a different and more intense profile than the other strains.

Thermostability of Endoglucanases

Endoglucanolytic activity was quantified for all strains grown at 25 °C, 30 °C and 37 °C (Figure 3.5) at increasing reaction temperatures (25–80 °C). There is a general increase of activity from 25 °C to 70 °C, and a strong decrease at 80 °C.

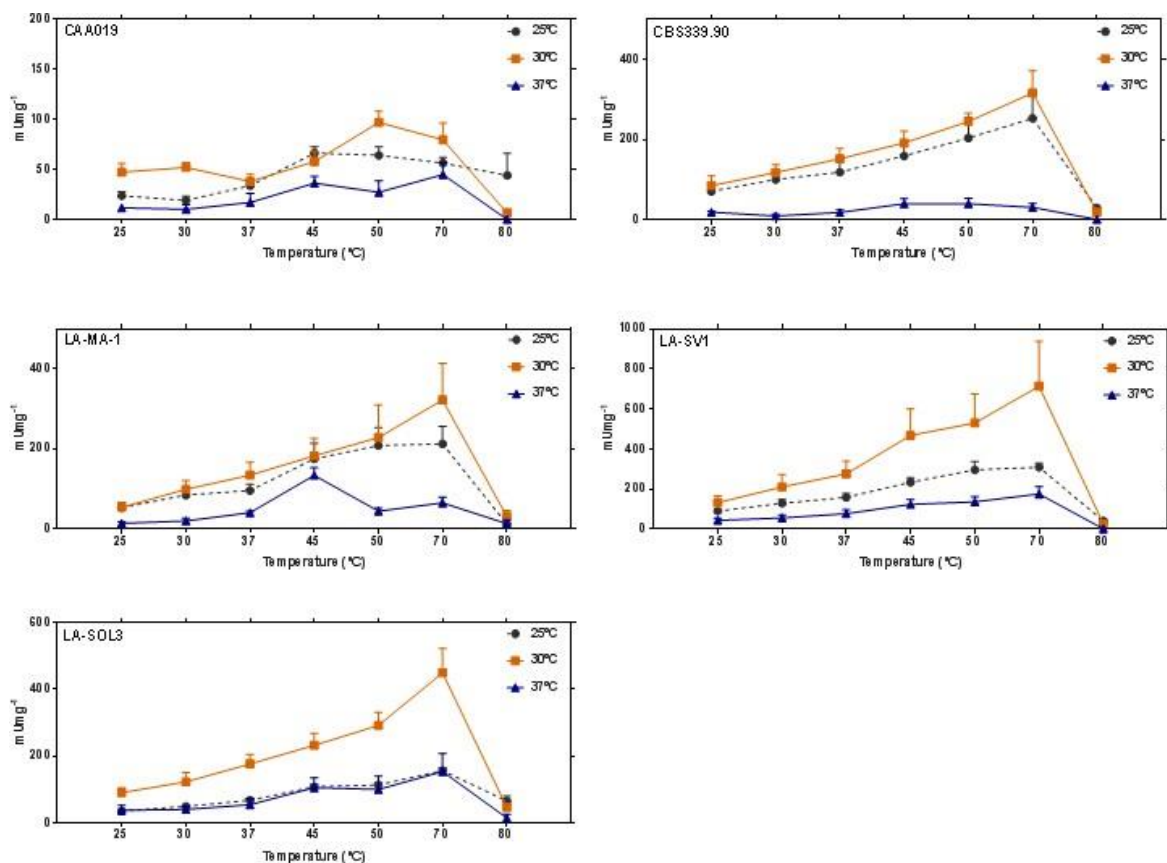


Figure 3.5 | Extracellular endoglucanolytic activity of strains CAA019, CBS339.90, LA-MA-1, LA-SV1 and LA-SOL3 grown at 25 °C, 30 °C and 37 °C and assayed at 7 temperatures. Data is presented as average ± standard deviation.

Thermostability of Proteases

At 30 °C growth temperature, there is a general increase of activity until 50 °C and a decrease at 70 °C and 80 °C. At growth temperatures of 25 °C and 37 °C the pattern of proteolytic activity is consistent with the presence of several enzymes, with different optimal temperatures (Figure 3.6).

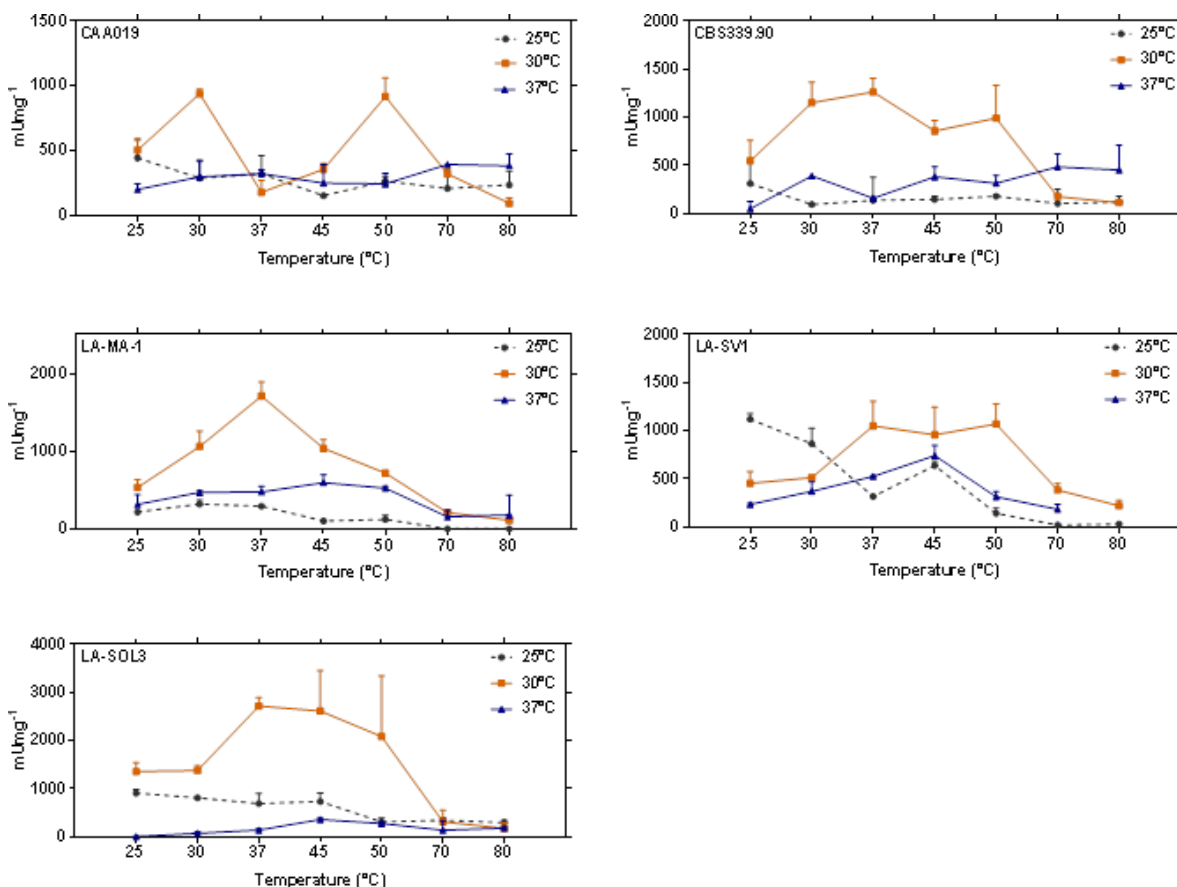


Figure 3.6 | Extracellular proteolytic activity of strains CAA019, CBS339.90, LA-MA-1, LA-SV1 and LA-SOL3 grown at 25 °C, 30 °C and 37 °C and tested at 7 different temperatures. Data is presented as average \pm standard deviation.

Thermostability of Lipases

Lipolytic activity was tested for all strains grown at 25 °C, 30 °C and 37 °C. However, due to the spontaneous degradation of the substrate at high temperatures, only 4 different temperatures of incubation were tested (25 °C, 30 °C, 37 °C and 45 °C), (Figure 3.7). For strains grown at 25 °C and 37 °C, extracellular lipolytic activity was detected for all temperatures tested. However, when strains were grown at 30 °C it was detected only at 25 °C, being absent at 30 °C, 37 °C and 45 °C

incubation. For extracellular lipases, the global average remained below 500 mU.mg⁻¹, with no significant trend with increasing temperature.

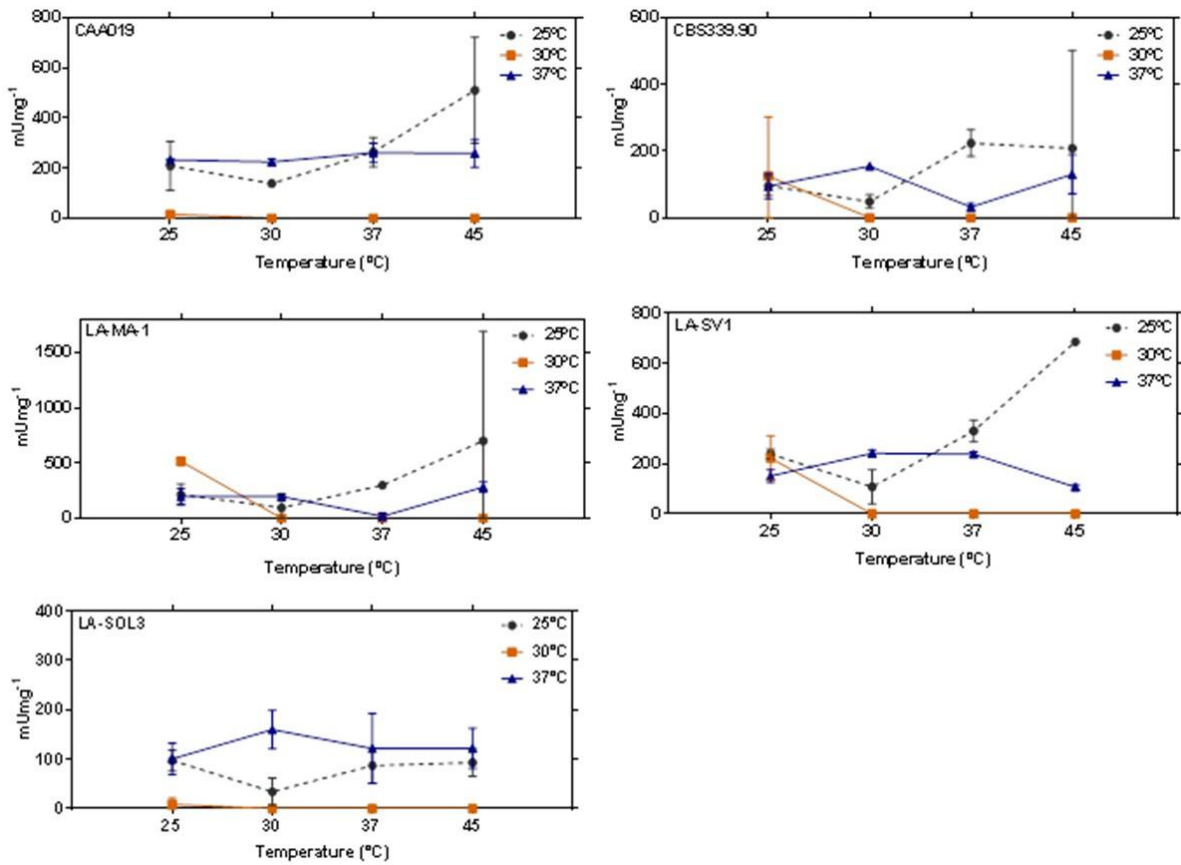


Figure 3.7 | Extracellular lipolytic activity of CAA019, CBS339.90, LA-MA-1, LA-SV1 and LA-SOL3 grown at 25 °C, 30 °C and 37 °C and tested at 4 different temperatures. Data is presented as average ± standard deviation.

Multi Factor Analysis of Extracellular Activity

A multifactor analysis (MFA) was conducted in order to be able to infer which of the factors—temperature or strain—had the major influence in the expression of the enzymes in study (Figure 3.8).

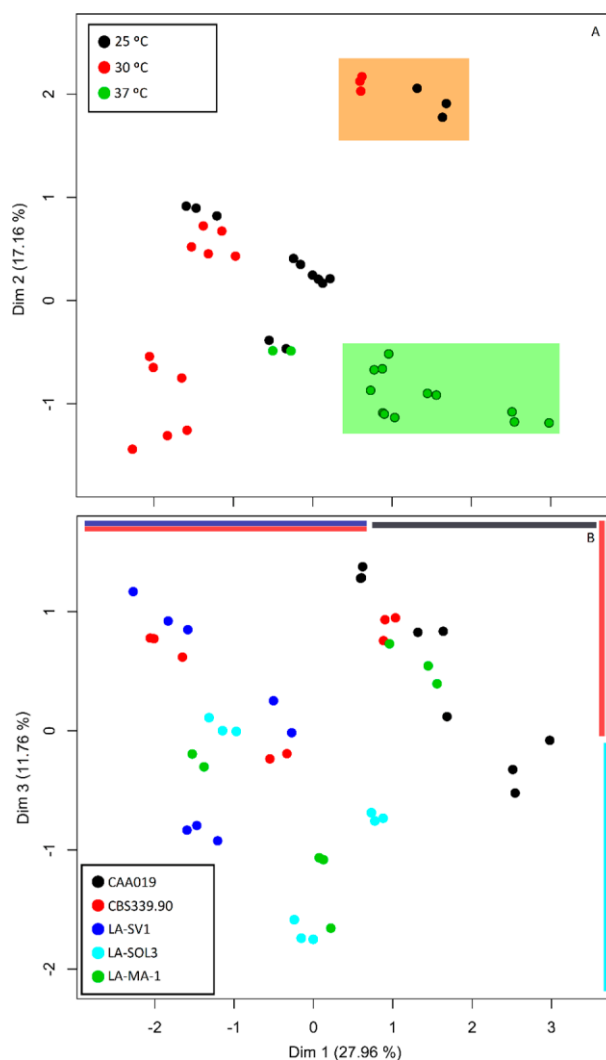


Figure 3.8 | Multi factor analysis of detection, quantification and characterization of extracellular enzymatic activity data at 25 °C, 30 °C and 37 °C of *L. theobromae* strains using the growth temperature (A) and the strains (B) as factors. Post-hoc analysis of the scores of both dimensions 1 and 3 revealed the one-dimensional separations (colored bars: top–horizontal, right–vertical).

Dimensions 1 and 2 (Figure 3.8) account to 43.9 % of the variance of the data, providing a good reduction of dimensions in our data. Dimension 1 summarizes a total of 27.3 % of the variance, of which 77.2 % comes from enzymatic detection and quantification data. Dimension 2 accounts for 17.16 % of the variance, mainly explained by zymography data (70.9 %) and dimension 3 provides a scoring that despite its lower variance (11.8 %) has the advantage of resolving quantity and identity information of enzymes in equal proportions.

Using the growth temperature as a factor (Figure 3.8A), dimensions 1 and 2 were shown to effectively produce different scores for our samples ($p < 0.001$ for Kruskal–Wallis test). It is possible to verify that one cluster is formed by data from fungi grown at 37 °C (green-shaded box in Figure 3.8A), validated by a post hoc Nemenyi analysis. At dimension 1, *L. theobromae* strains grown at 37 °C have significantly higher scores than those grown at 30 °C ($p < 0.001$). At dimension 2, scores were significantly lower for data from fungi grown at 37 °C than at 30 °C or 25 °C ($p < 0.05$ and $p < 0.001$, respectively). Strain was also analyzed as a factor in the MFA (Figure 3.8B). Dimension 2 did not significantly separate strains ($p > 0.05$). Thus, dimension 3 ($p < 0.01$) was plotted and analyzed with dimension 1 ($p < 0.001$) as a function of strains. Grouping by strains is not clear upon visual inspection of the MFA. However, post-hoc analysis of the scores of both dimensions 1 and 3 revealed the one-dimensional separations depicted in Figure 3.8B (colored bars: top–horizontal, right–vertical). In dimension 1, a significant difference between strain CAA019 and both strains CBS339.90 ($p < 0.05$) and LA-SV1 ($p < 0.001$) was found, suggesting the peculiarity of strain CAA019 concerning extracellular enzymatic activity. In dimension 3, which has equal contributions of enzymatic activities and molecular weight-based identities of enzymes, strain LA-SOL3 was distinguished from strains CAA019 ($p < 0.05$) and CBS339.90 ($p < 0.05$).

DISCUSSION

Extracellular Enzymatic Activity

There are indications that plant pathogens may secrete different quantities of host-specific cell wall degrading enzymes (CWDEs) (van der Does and Rep, 2007; King et al., 2011). Thus, if a pathogen infects plants, it is expected that the enzymes secreted will be related to specific substrates such as, cellulose, hemicellulose and lignin (Gibson et al., 2011). The same happens with other hosts: if a pathogen infects animals, a secretion of enzymes able to degrade mammalian-specific substrates is expected. Therefore, it was surprising to verify that the cellulolytic activity, among the strains of *L. theobromae* studied was low. However, only endoglucanases were evaluated, and the hydrolysis of insoluble cellulose requires multiple cellulases (endoglucanases, exoglucanases and β -glucosidases) acting simultaneously to convert the complex matrix into simple sugars (Sajith et al., 2016).

Esteves and colleagues (Esteves et al., 2014) found that several species of *Lasiodiplodia* express active endoglucanases at high temperatures (50 °C). Our data agrees with that previous report,

since we showed an increase of the endoglucanolytic activity up to 70 °C and a marked decrease only at 80 °C (Esteves et al., 2014).

The absence of lipolytic activity at the optimal fungal growth temperature, 30 °C, was not expected (Figure 3.3), suggesting that this class of hydrolytic enzymes is associated with adaptive responses to temperature. The expression of lipases only at 25 °C and 37 °C, at which pathogenesis has been reported [see (Rodríguez-Gálvez et al., 2017; Félix et al., 2016)], might implicate a role of lipases in the virulence of *L. theobromae*. The importance of lipolytic activity in opportunistic fungal human infections has long been discussed (Khan et al., 2010; Park et al., 2013). While a role of hydrolytic enzymes in host penetration has been generally recognized, a more intricate mechanism of lipase-induced immune modulation was characterized in *Candida parapsilosis* (Tóth et al., 2014), providing a stronger link of these enzymes to this organism's pathogenicity. Also, the existence of a waxy cuticle in the leaves, young shoots and other aerial plants has been similarly proposed to be the reason for the lipase-associated virulence (Nguyen, 2008), through tissue invasion. Although some examples of lipase knock-outs with retained virulence have been published (Reis et al., 2005), definite evidence for a lipase-mediated pathogenicity mechanism was obtained by Voigt et al. 2005, which managed to drastically reduce symptoms in *Fusarium graminearum* infected plants using a potent lipase inhibitor, Ebelactone B (Voigt et al., 2005). Alternatively, it may reveal that these fungi do not rely on fatty acids and glycerol (the products of triacylglycerols' digestion) for nutrition at their optimal growth temperature.

Multi Factor Analysis of Extracellular Activity

In MFA, a principal component analysis (PCA) is performed on each quantitative data set and a multi correspondence analysis (MCA) on each qualitative data set, and the first eigenvalue of each eigenvector is used to standardize the data, which can then be merged to form a matrix on which a PCA is performed (Abdi, 2003).

Considering the relative contributions of the different data (Figure 3.8A) the differences suggest that the enzymatic activity and the zymographic profiles of the strains tend to be more severely altered and more strain-independent at 37 °C. At 25 °C and 30 °C there is not a clear distinction of groups by temperature. This does not mean that those temperatures do not induce changes, but rather suggests that the changes induced are differentially determined by other factors, such as the strain. For instance, a discrete group (orange-shaded box in Figure 3.8A) of 25 °C and 30 °C-grown CAA019 is formed by the first two dimensions. This may mean that enzymes produced by this strain, grown at those temperatures, still constitute much more similar profiles than when compared with other strains. When analyzing strain as a factor, the variance in data accounts for circa 39 %, may

indicate that different strains may have evolved by producing different enzymes, which could be an adaptation to environment (i.e., their host).

Thermostability

The enzymatic hydrolysis of cellulosic biomass is an alternative for the generation of sugars, that are the base materials to produce products that are commercially important, such as organic acids, bioethanol, free sugars, animal feeds and antibiotics. Since enzymes are non-polluting, specific, recoverable and do not require high levels of energy to work, they are more efficient and eco-friendly than acid or alkali hydrolysis (Sajith et al., 2016). Our data shows that *L. theobromae* strains express thermostable endoglucanases (active up to 70 °C), especially when the fungi are grown at 30 °C (Figure 3.5).

Proteases are known to have distinct functions in fungal biology, such as in nutrition and in virulence mechanisms. In industry, these proteases also have a high number of applications, such as in detergents, food industry and pharmaceutical industry or in bioremediation processes (Duarte et al., 2016). The higher levels of proteolytic activity found for some of the strains under study, especially when grown at 30 °C, as well as their thermostability up to 80 °C (Figure 3.6), and the different profiles found by SDS-Zymography (Figure 3.4), demonstrates the biotechnological potential of this species.

Lipases catalyze the hydrolysis of triacylglycerols with long fatty acid chains in free fatty acids and glycerol, which makes these enzymes essential to several biotechnology industries, such as the pharmaceutical industry, detergent and soap industries and cosmetics industry, among others (Facchini et al., 2015; Sadati et al., 2015). These enzymes are considered as one of the leader biocatalysts, contributing to a capital underexploited of bioindustry (Facchini et al., 2015).

Amongst microorganisms, filamentous fungi are important producers of lipases, mostly by submerged fermentation processes (Corrêa et al., 2014). This kind of process to produce lipases contributes to high levels of activity with low cost and residue formation for the industry (Facchini et al., 2015). Our results showed that all strains tested presented lipolytic activity up to 45 °C (Figure 3.7), showing a good potential for a future application in several industries that deal with high-temperature processes (Salihu and Alam, 2014). The major advantages of catalysis at higher temperatures include the high rate of product formation, high dissolution of hydrophobic substrates, high conversion efficiency and a low chance of contamination (Salihu and Alam, 2014).

CONCLUSIONS

We showed that temperature modulates the extracellular enzymatic profile of the strains of *L. theobromae*. All strains produce an arsenal of enzymes typically involved in the degradation of plant cell walls (amylases, cellulases, xylanases, laccases, gelatinases, caseinases, lipases, pectinases and pectin liases), whose expression was influenced by the temperature of growth. These alterations show the capacity of adaption of these strains to different environments, which could also result in changes in pathogenicity. The analysis of the enzymatic profile of *L. theobromae* showed that different strains produce significantly different enzymatic profiles, indicating a strain-dependency. The wide range of temperatures tested (from 25 °C to 80 °C) showed that these strains express thermostable enzymes (proteases, endoglucanases and lipases), which could be very interesting to several types of industries using these kinds of enzymes, such as detergents, starch, food or biomedical industries.

ACKNOWLEDGMENTS

Thanks are due, for the financial support to CESAM (UID/AMB/50017-POCI-01-0145-FEDER-007638) and the research project ALIEN (PTDC/AGR-PRO/2183/2014-POCI-01-0145-FEDER-016788), to FCT/MEC through national funds, within the PT2020 Partnership Agreement and Compete 2020. The authors acknowledge FCT financial support to Artur Alves (IF/00835/2013), Ana Cristina Esteves (BPD/102572/2014) and Carina Félix (BD/97613/2013).

CHAPTER 4

Production of toxic metabolites by two strains of *Lasiodiplodia theobromae*, isolated from a coconut tree and a human patient

ABSTRACT

Lasiodiplodia theobromae is a phytopathogenic fungus that causes diseases not only in a broad number of plant hosts, but also occasionally in humans. The capacity to produce bioactive metabolites at 25 °C (environmental mean temperature) and at 37 °C (body mean temperature) of *L. theobromae* was investigated. Two strains, CAA019 and CBS339.90 isolated, respectively, from a coconut tree and a human patient were characterized. The phytotoxicity and cytotoxicity (on mammalian cells) of the secretomes of both strains of *L. theobromae* were investigated. Also, phytotoxicity and cytotoxicity of pure compounds were evaluated. The phytotoxicity of the secretome of strain CAA019 is higher than the phytotoxicity of the secretome of strain CBS339.90 at 25 °C. However, the phytotoxicity for both strains decreased when they were grown at 37 °C. Only the secretome of strain CBS339.90 grown at 37 °C induced up to 90 % Vero and 3T3 cell mortality. This supports the presence of different metabolites in the secretome of strains CAA019 and CBS339.90. Metabolites typical of *L. theobromae* were isolated and identified from organic extracts of the secretome of both strains [e.g., 3-indolecarboxylic acid, jasmonic acid, lasiodiplodin, four substituted 2-dihydrofuranones, two melleins, and cyclo-(Trp-Ala)]. Also, metabolites such as scytalone, not previously reported for this species, were isolated and identified. Metabolite production is affected by strain and temperature. In fact, some metabolites are strain specific (e.g., lasiodiplodin) and some metabolites are temperature specific (e.g., jasmonic acid). Although more strains should be characterized, it may be anticipated that temperature tuning of secondary metabolites production emerges as a putative contributing factor in the modulation of *L. theobromae* pathogenicity towards plants, and also towards mammalian cells.

KEYWORDS: cytotoxicity, global changes, phytopathogenic fungi, phytotoxicity, secondary metabolites, temperature

INTRODUCTION

Lasiodiplodia theobromae is a phytopathogenic fungus from the family *Botryosphaeriaceae*, which is found typically in tropical and subtropical regions and has an optimal growth temperature of 27 °C – 33 °C (Phillips et al., 2013). It has been associated with many hosts causing diverse diseases, being responsible for serious damages on crops, such as mango and grapevines (Cimmino et al., 2017; Phillips et al., 2013; Rodríguez-Gálvez et al., 2015). This fungus has also been associated with infections in humans, acting as an opportunist and causing diseases with various levels of severity,

from simple ocular infections to death (Kindo et al., 2010; Saha et al., 2012; Saha et al., 2013; Summerbell et al., 2004; Woo et al., 2008).

There are a number of fungal compounds, such as cell wall degrading enzymes and inhibitory proteins (Esteves et al., 2014) that contribute to fungal pathogenicity (Fernandes et al., 2014; González-Fernández et al., 2015; King et al., 2011) and that can be modulated by abiotic factors (Felix et al., 2018). Temperature was shown to modulate the extracellular protein production, enzymatic activity and cytotoxicity of two strains of *L. theobromae* collected from different hosts, suggesting an adaptation to different ecological niches (Félix et al., 2016).

The host-adaptability of *L. theobromae* is a result of the capacity to produce different metabolites at different environmental conditions. This host-adaptability may also be related to the ability to produce secondary metabolites directly involved in host-pathogen interactions. To be more detailed, these metabolites, mostly bioactive, belong to different classes of compounds: jasmonates, melleins, lasiodiplodins, furanones, diketopiperazines, polysaccharides (Aldridge et al., 1971; Alves da Cunha et al., 2012; Andolfi et al., 2014; Pandi et al., 2010; Qian et al., 2014; Yang et al., 2000).

In vitro production of secondary metabolites is closely related to cultural conditions as well as to the strain. For instance, *L. theobromae* is a good source of jasmonic acid and analogues used in cosmetics and pharmaceutical industries. In order to optimize cultural conditions, many studies were conducted (Eng et al., 2016) and among other factors, the effect of temperature on growth was evaluated (Dhandhukia et al., 2007). Despite all the available information concerning *L. theobromae* secondary metabolites, there are no comparative studies that evaluate how metabolites' production, specifically toxic metabolites, is affected by temperature.

From the evidences that climate is changing, increasing temperature is one of the alterations reported (Galant et al., 2012; Piñeiro et al., 2010). This increase of the average global temperature will modify microbial pathogen/host interactions, changing the dynamics of relationships between hosts and pathogens, and possibly resulting in alterations in virulence (Eastburn et al., 2011; Gallana et al., 2013; Lindner et al., 2010). The adaptation of microbial pathogens to new environmental temperatures results from complex processes that involve a number of physiological and biochemical alterations, such as altered gene, protein and primary and secondary metabolite expression (Kaplan et al., 2004).

The aim of this study was to investigate *in vitro* secondary metabolites production of two strains of *L. theobromae*: CAA019 and CBS339.90, isolated from a coconut tree and a human patient. Both strains were grown at 25 °C and 37 °C, respectively, environmental and body mean temperature.

Metabolic profiles were compared and phytotoxicity and cytotoxicity of the culture filtrates (the secretome) and of pure compounds were evaluated.

MATERIAL AND METHODS

Fungal strains and growth conditions

Strain CAA019 was originally isolated from a coconut tree in Brazil and strain CBS339.90 (obtained from the Westerdijk Fungal Biodiversity Institute) was isolated from a human patient from Jamaica. Cultures were maintained on Potato Dextrose Agar (PDA) medium (Merck, Germany) at 25 °C in the dark (Fernandes et al., 2014). Before each experiment, strains were recovered by plating a mycelial plug on PDA and incubating at 25 °C for 4 days until mycelium filled a 45-mm diameter plate.

For metabolite production, both strains were grown in 1 L Erlenmeyer flasks, containing 250 mL of Czapek medium amended with 2 % cornmeal (pH 5.7). The mycelium of a filled plate (45 mm) was scraped from PDA and suspended in 5 mL of sterilized ultra-pure water. This mycelial suspension was added to Czapek medium and incubated for 21 days in darkness at 25 °C or 37 °C without agitation. Culture filtrates were obtained by filtering the culture through sterile 0.45 µm cellulose membranes (Lifesciences) in a vacuum system.

Extraction and purification of fungal metabolites

Metabolites were isolated from culture filtrates as described below and in supplementary material – chapter 4. The most adequate methods to obtain pure compounds were optimized considering the nature of the compounds present in the culture filtrate. See Supplemental Scheme S4.1, and the correspondent text for a visual description of separation procedures and more information regarding metabolite purification.

Metabolite purification of strain CAA019 grown at 25 °C

The culture filtrate (1.6 L) was obtained as described above, acidified to pH 2 with 1 M of formic acid and extracted exhaustively with ethyl acetate. After solvent evaporation, 128.4 mg of crude extract LtCE1 (*L. theobromae* crude extract 1, Supplemental Figure S4.1), which had the appearance of brown oil was obtained. LtCE1 (Supplemental Figure S4.1) was submitted to fractionation by column chromatography (CC, Merck, Kieselgel 60, 0.063–0.200 mm, eluted with 95:5 chloroform/isopropanol), originating ten homogeneous fractions of which the last fraction was eluted with methanol (Scheme 4.1: fractions aA 4.8 mg, aB 4.3 mg, aC 5.3 mg, aD 4.9 mg, aE 24.2

mg, aF 14.5 mg, aG 10.5 mg, aH 3.3 mg, aI 0.9 mg, aL 51.8 mg). TLC spots were visualized by exposure to UV radiation (253 nm), or by spraying first with 10 % of sulfuric acid in methanol followed by heating at 110 °C for 10 min.

Metabolite purification of strain CBS339.90 grown at 25 °C

The culture filtrate from strain CBS339.90 (3 L) grown at 25 °C, was obtained as described above. The crude extract [LtCE2 (*L. theobromae* crude extract 2, Supplemental Figure S4.1), 147.8 mg, brown oil] was submitted to a bioassay-guided fractionation through CC on silica gel, eluted with chloroform/isopropanol (95:5) originating six homogeneous fractions, the last was eluted with methanol (Supplemental Figure S4.1).

Metabolite purification of strain CAA019 grown at 37 °C

The culture filtrate of strain CAA019 (0.4 L) grown at 37 °C was obtained as described above. The crude extract LtCE3 (*Lasiodiplodia theobromae* crude extract 3, Supplemental Scheme S4.1, brownish oil) was obtained as described in Scheme 4.1. LtCE3 (160.6 mg) was dissolved in ethyl acetate and extracted with a saturated solution of sodium bicarbonate (pH 8.5) (see Supplemental Figure 4.1). The aqueous phase and the ethyl acetate organic phase (*primary organic phase* in Supplemental Figure S4.1) were further processed. The aqueous phase was acidified with concentrated hydrochloric acid and re-extracted with ethyl acetate.

Metabolite purification of strain CBS339.90 grown at 37 °C

The culture filtrate of strain CBS339.90 (1.6 L) grown at 37 °C was obtained as described above. The crude extract LtCE4 (*L. theobromae* crude extract 4, Supplemental Scheme S4.1, brownish oil) was obtained as described in Scheme S4.1. 252.2 mg of LtCE4 were dissolved in ethyl acetate and extracted with a saturated solution of sodium bicarbonate (pH 8.5). The aqueous phase and the ethyl acetate organic phase (*primary organic phase*) were further processed. The aqueous phase was acidified with concentrated HCl and re-extracted with ethyl acetate. The organic phase from this liquid-liquid extraction (*secondary organic phase*) was recovered, dried with hydrochloric acid anhydrous and filtered.

Metabolite identification

All metabolites were identified by physical and spectroscopic techniques and by comparison of the obtained data to those reported in the literature for indole-3-carboxylic acid (Qian et al., 2014), (-)-jasmonic acid (JA) (Husain et al., 1993), lasiodiplodin (Aldridge et al., 1971), botryosphaerilactone A (Rukachaisirikul et al., 2009), (3*S*,4*R*,5*R*)-hydroxymethyl-3,5-dimethylidihydro-2-furanone (Andolfi et al., 2014), (3*S*,4*S*)- and (3*R*,4*S*)-4-acetyl-3-methyl-2-dihydrofuranones (Forzato et al., 2005), *cis*-(3*R*,4*R*)- and *trans*-(3*R*,4*S*)-4-hydroxymelleins (Cabras et al., 2006), scytalone (Mazzeo et al., 2014), cyclo-(Trp-Ala) (Hamasaki et al., 1976).

Optical rotations of pure metabolites were measured either in chloroform or in methanol (Sigma-Aldrich), on a Jasco polarimeter. ¹H and ¹³C NMR spectra were recorded at 400 and at 100 MHz, respectively, in deuterated chloroform (CDCl₃) or in deuterated methanol (CD₃OD), on Bruker spectrometers, and the same solvent was used as internal standard. ESI-MS analyses were performed with the LC/MS TOF system (AGILENT 6230B, HPLC 1260 Infinity).

GC/MS measurements were performed with an Agilent 6850 GC equipped with an HP-5MS capillary column (5 % phenyl methyl polysiloxane stationary phase) and the Agilent 5973 Inert MS detector (used in the scan mode). GC/MS data were acquired on crude or purified metabolites after trimethylsilylation with BSTFA (N,O-Bis(trimethylsilyl)trifluoroacetamide). Samples were derivatized and analyzed according the method previously reported (Guida et al., 2015).

Several of the eleven metabolites reported were identified (or their identity confirmed) by comparing their mass spectra with spectra of pure compounds retrieved from an assortment of databases by employing the NIST Mass Spectral Search Program v.2.0g which, among others, could explore the NIST 14 mass spectral library (Stein 2017) and the Golm Metabolome Database (Hummel et al., 2010).

High-quality mass spectra for co-eluting compounds were obtained employing the NIST deconvolution software AMDIS (*Automatic Mass Spectral Deconvolution & Identification System*) (Kind 2014; Stein 1999), which used, as target MS library, the custom MS target library of metabolites (Table S4.1).

Phytotoxicity assays

Phytotoxicity was assayed both on tomato cuttings and by a leaf puncture assay (Andolfi et al., 2014). Testing with tomato cuttings was performed with the culture filtrates of strains CAA019 and CBS339.90, and pure compounds were assayed by the leaf puncture assay.

Two weeks old stems were first dipped for 24 h in a vial containing 2 mL of pure or diluted culture filtrate and then transferred to a vial containing 2 mL of sterile distilled water and kept for 48 h. Afterwards, stems were examined for wilting and dry leaves. Toxic effects were scored on a scale from 0 to 4 (0: no symptoms; 1: slight wilting and/or dry leaves; 2: intermediate wilting and/or dry leaves; 3: severe wilting and/or dry leaves; 4: full wilting and/or dry leaves). For each culture filtrate, five concentrations (ranging from the pure filtrate to 1 % (v/v) filtrate solution in sterile water) were tested. Finally, to each filtrate and at each dilution level a toxicity index (\bar{x}) was determined, consisting of the average of toxicity scores, x , of individual assays corrected for the score of the control, x_{control} . The control consisted of a tomato stem kept in sterile distilled water. The mean score \bar{x} was converted to a percentage toxicity index, % mean(x), through the formula: % mean(x) = $100((\bar{x} - \bar{x}_{\text{control}})/x_{\text{max}})$ (in which $x_{\text{max}} = 4$ represents the maximum score). For the leaf puncture assay, young tomato plant leaves were used. Pure compounds were dissolved in methanol and afterwards a stock solution (4 % methanol) was made with distilled water. A droplet (20 μL ; 1 mg mL⁻¹) of the compound solution was applied on the adaxial side of leaves. The leaves were previously punctured using a sterilized needle. As control, a droplet (20 μL) of 4 % methanol was applied on the leaves. Leaves were kept in a moist chamber for 10 days to prevent the droplets from drying and were observed daily and scored for symptoms after 10 days. The lesion diameter was expressed in mm. All assays were carried out in triplicate.

Cytotoxicity assays on mammalian cell cultures

In vitro cytotoxicity evaluation was performed as described previously (Duarte et al., 2015) with slight modifications. A Vero cell line (ECACC 88020401, African Green Monkey Kidney cells, GMK clone) and a 3T3 cell line (ECACC 86110401, mouse embryonic fibroblasts, A31 clone) were grown and maintained as described (Ammerman et al., 2008). The microtiter plates were incubated at 37 °C in 5 % CO₂ for 24 h. Vero and 3T3 cells were treated for 20 h with culture filtrates or pure metabolites [1:1 in Dulbecco's Modified Eagle Medium, DMEM (Dulbecco et al., 1959)]. Two different concentrations of each pure metabolite were assayed (25 μL , at 1 mg mL⁻¹ and 0.5 mg mL⁻¹ in PBS). After exposure, the medium was removed by aspiration and 50 μL of DMEM with 10 % resazurin (0.1 mg mL⁻¹ in PBS) were directly added to each well. The microtiter plates were incubated at 37 °C in 5 % CO₂ during 3 h. The absorbance was read at 570 and 600 nm wavelength in a microtiter plate spectrophotometer (Biotek Synergy, Bad Friedrichshall, Germany) and cell viability was assessed as described previously (Duarte et al., 2015).

Statistical analysis

Two-way ANOVA, followed by a Bonferroni multiple comparison test was used to determine the statistical significance of cytotoxicity of each strain within the same temperature against the control or between pure metabolites and control (* $p < 0.05$, ** $p < 0.01$, *** $p < 0.001$, **** $p < 0.0001$). All the analyses were performed with GRAPHPAD PRISM 6 (GraphPad Software, Inc.). Data are shown as the average of three independent replicates of each condition.

RESULTS

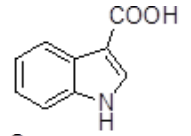
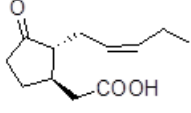
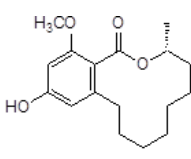
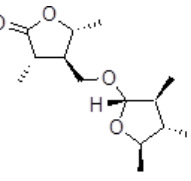
Metabolites isolation, purification and distribution

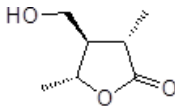
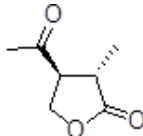
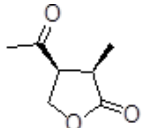
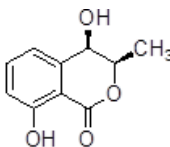
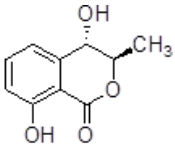
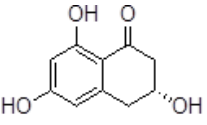
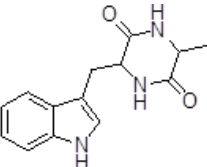
The crude extracts (LtCEs) were obtained from culture filtrates of two strains of *L. theobromae* grown at two different temperatures and extracted with ethyl acetate as described in Materials and Methods: CAA019 at 25 °C (LtCE1), CBS339.90 at 25 °C (LtCE2), CAA019 at 37 °C (LtCE3) and CBS339.90 at 37 °C (LtCE4).

In the text, reference shall be made to these abbreviations: LtCE1: strain CAA019 grown at 25 °C, LtCE2: strain CBS339.90 grown at 37 °C, LtCE3: strain CAA019 grown at 25 °C, LtCE4: strain CBS339.90 grown at 37 °C. The extracts were subjected to purification processes by combined column and TLC chromatography yielding eleven metabolites (Table 4.1).

The diversity in metabolites is lower when fungi were grown at 25 °C especially for the strain CAA019, while the largest number of metabolites were isolated for the strain CBS339.90 grown at 37 °C.

Table 4.1 | Structures and distribution of secondary metabolites produced by strains CAA019 and CBS339.90, according to strain and culture temperature.

Name	Structure	Shortcut	CAA019		CBS339.90	
			25 °C	37 °C	25 °C	37 °C
3-Indolecarboxylic acid (3-ICA)		Metb1	+	+	+	+
(-) Jasmonic acid		Metb2	+		+	
Lasiodiplodin		Metb3	+	+		
Botryosphaerilactone A		Metb4		+		+

(3 <i>S</i> ,4 <i>R</i> ,5 <i>R</i>)-4-hydroxymethyl-3,5-dimethyldihydro-2-furanone		Metb5	+	+
(3 <i>S</i> ,4 <i>S</i>)-4-Acetyl-3-methyl-2-dihydrofuranone		Metb6	+	+
(3 <i>R</i> ,4 <i>S</i>)-4-Acetyl-3-methyl-2-dihydrofuranone		Metb7	+	+
<i>cis</i> -(3 <i>R</i> ,4 <i>R</i>)-4-Hydroxymellein		Metb8		+
<i>trans</i> -(3 <i>R</i> ,4 <i>S</i>)-4-Hydroxymellein		Metb9		+
Scytalone		Metb10		+
Cyclo-(Trp-Ala)		Metb11	+	+

Analysis of GC/MS data acquired on LtCEs

Most metabolites, which are polar functionalized compounds, do not have suitable gas chromatographic properties. This difficulty was overcome by silylating the crude extracts. By way of example, figure 4.1(a) and (b) show the total ion chromatograms (TICs) of crude extracts of the strain CBS339.90 grown at 25 °C and 37 °C (LtCE2 and LtCE4). But apart from metabolites previously reported, we were able to identify some compounds present in the culture medium (A-I), due to

the high sensitivity of GC/MS. Retention indices and mass spectra of studied compounds are reported in Supporting Information (Table S4.1).

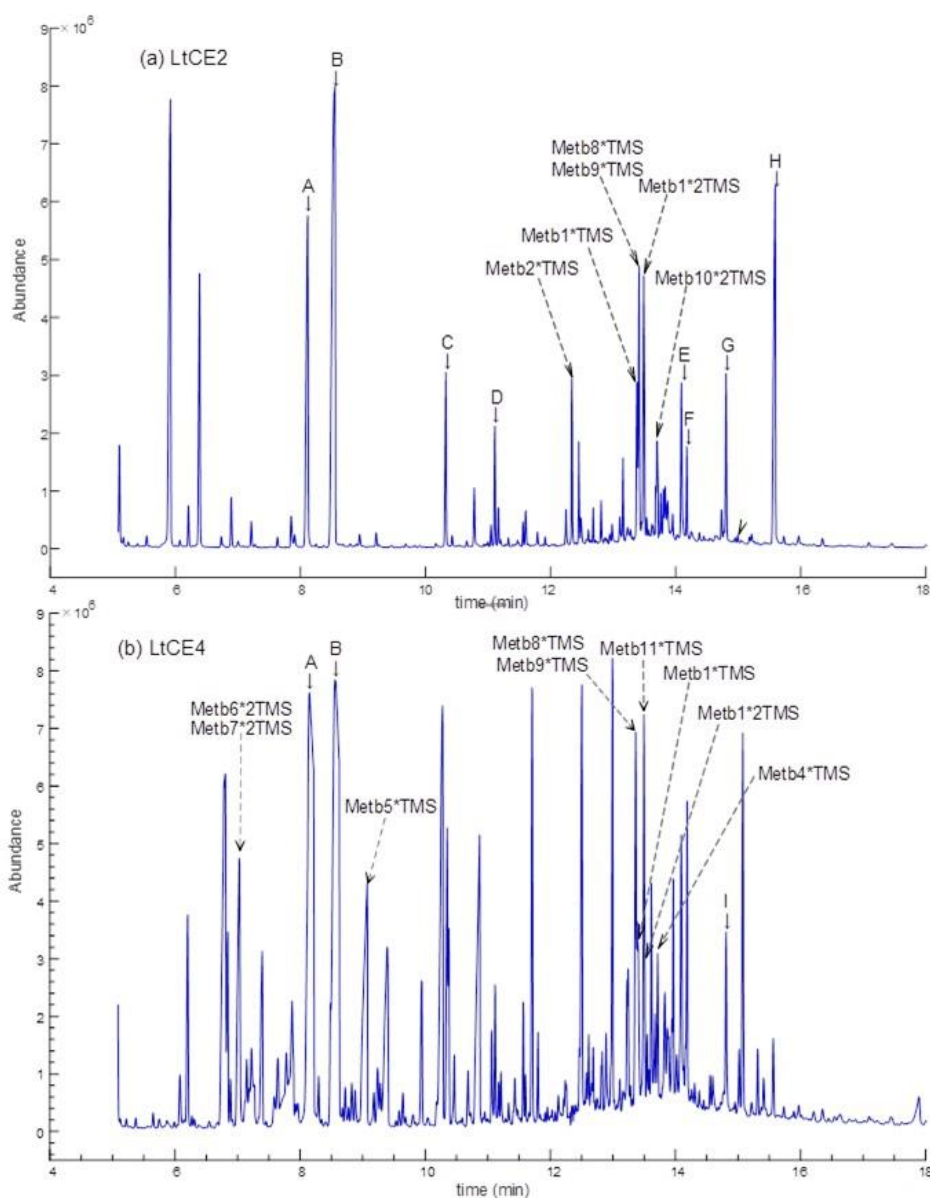


Figure 4.1 | Annotated total ion chromatograms (TIC) acquired by processing samples from LtCE2 (a) and LtCE4 (b): A = succinic acid ·2TMS; B = fumaric acid ·2TMS; C = malic acid ·3TMS; D = hydroxyglutaric acid ·3TMS; E = linoleic acid ·TMS; F = stearic acid ·TMS; G = bis(2-ethylhexyl) adipate; H = phthalic acid, mono-(2-ethylhexyl) ester; I = bis(2-ethylhexyl) adipate.

Phytotoxicity Assays

Phytotoxicity of the culture filtrates from the two strains of *L. theobromae*, CAA019 and CBS339.90, grown at 25 °C and 37 °C, was evaluated by an assay on tomato stems of rootless plants. Both strains, grown at both temperatures, induced phytotoxicity symptoms, such as wilting and dry leaves (Figure 4.2).

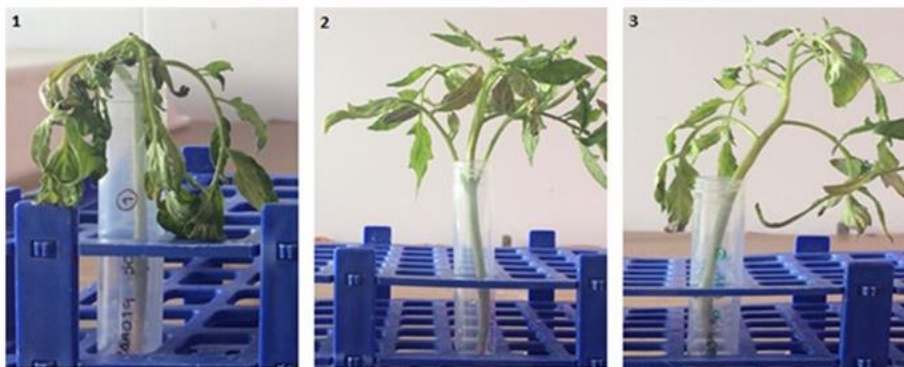


Figure 4.2 | Typical outcome of phytotoxic assays on tomato stems: (1) and (3) wilting symptoms of culture filtrates from strains CAA019 and CBS339.90 respectively; (2) distilled water control.

The culture filtrates more toxic to tomato stems were those from fungi grown at 25 °C, and the strain that induced more severe symptoms was strain CAA019 (Table 4.2). This supports the presence of one or more toxic metabolites in the culture filtrates of fungi grown at 25 °C, which are not produced, (or produced in lower amounts) at 37 °C. Also, it suggests the presence of different metabolites in culture filtrates from strains CAA019 and CBS339.90.

Table 4.2 | Phytotoxicity (%) of culture filtrates of strains CAA019 and CBS339.90 grown at 25 °C and 37 °C. All assays were carried out in triplicates.

Culture filtrate	Symptoms level (mean ± SD)	Phytotoxic activity (%)
Control (Czapek medium)	0.60 ± 0.75	20.8
Control (dH ₂ O)	0.17 ± 0.41	4.20
CAA019 – 25 °C	4.00 ± 0.00	100.0
CAA019 – 37 °C	3.00 ± 0.00	75.0
CBS339.90 – 25 °C	3.00 ± 0.00	75.0
CBS339.90 – 37 °C	1.67 ± 0.58	41.7

Phytotoxicity of the pure metabolites was evaluated by a leaf puncture assay on tomato leaves and results are presented in figure 4.3. Only four metabolites were phytotoxic for tomato leaves: lasiodiplodin (metb 3), produced by strain CAA019, 3-ICA (metb 1), produced by both strains, (3*S*,4*S*)- and (3*R*,4*S*)-4-acetyl-3-methyl-2-dihydrofuranone ratio 1:1 (metbs 6 and 7, respectively) and JA (metb 2), produced by both strains. JA (metb 2) and lasiodiplodin (metb 3) caused the largest lesions (Figure 4.3).

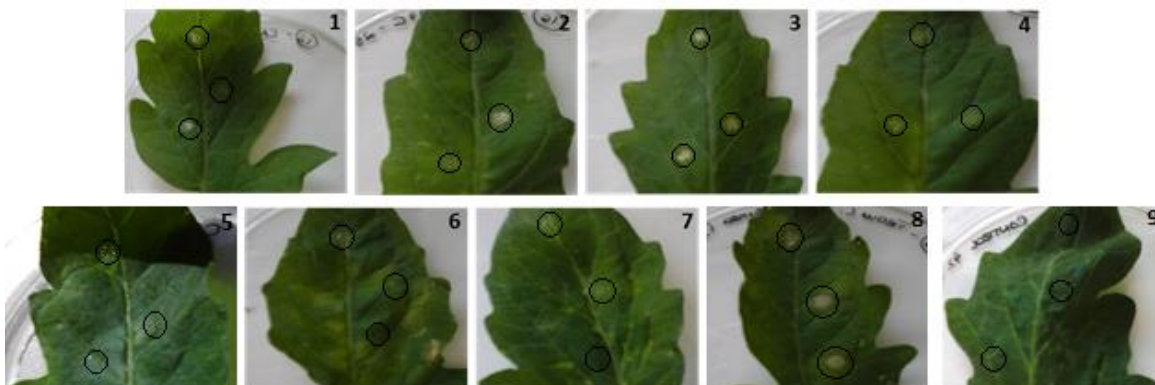


Figure 4.3 | Phytotoxicity of pure metabolites produced by two strains of *L. theobromae* on tomato leaves. Results are reported as lesion's size in mm after 10 days: **1**-Metb3=3.3 mm; **2**-Metb1=2.3; **3**-Metb6 + Metb7, ratio (1:1)=2.0; **4**-Metb6 + Metb 7, ratio (3:1)=0; **5**-Metb5=0; **6**-Metb4=0; **7**-Metb11=0; **8**-Metb2=4.7, and **9**-control=0. Leaf puncture assays on tomato leaves were carried in triplicates (inoculation sites are indicated by circles).

Cytotoxicity of culture filtrates and pure metabolites

In addition to phytotoxicity, we evaluated the cytotoxicity of the culture filtrates and of the pure metabolites from strains CAA019 and CBS339.90, grown at 25 °C and 37 °C, to mammalian cell cultures (Figure 4.4).

The culture filtrate of strain CAA019 (grown either at 25 °C or 37 °C) induced only a slight decrease in viability of Vero cells. However, the culture filtrate of strain CBS339.90 grown at 37 °C caused significant cytotoxicity ($P < 0.0001$), leading to the loss of about 80 % of cell viability. When the strain was grown at 25 °C no cytotoxicity was detected (Figure 4.4A). The same trend was observed for 3T3 cell line (Figure 4.4B): strain CAA019 grown either at 25 °C or at 37 °C showed low toxic effect, while strain CBS339.90 grown at 37 °C induced a significant severe mortality (10 % viability, $P < 0.0001$) of 3T3 cells.

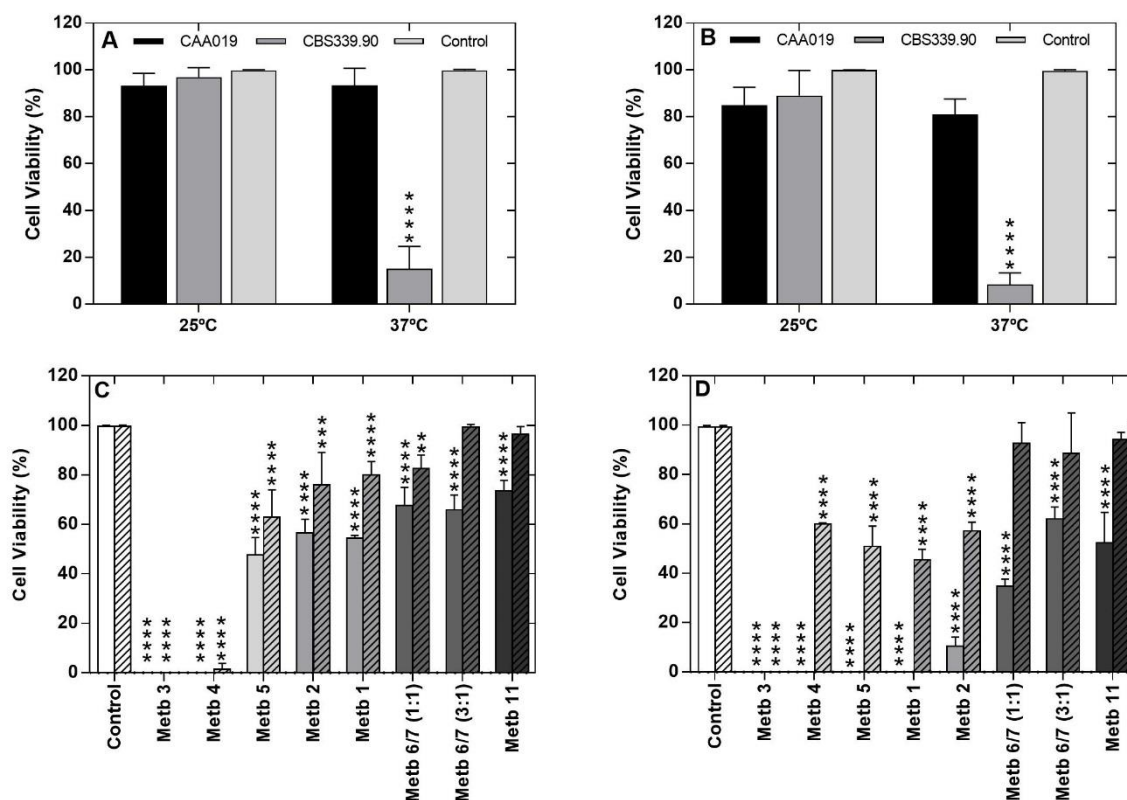


Figure 4.4 | Evaluation of cytotoxicity to Vero (A) and 3T3 (B) cells of the culture filtrates of strains CAA019 and CBS339.90 grown in Czapek medium amended with corn meal, during 21 days at 25 °C and 37 °C. Pure metabolites from strains CAA019 and CBS339.90 grown at 25 °C and 37 °C were also evaluated in Vero (C) and 3T3 (D) cells. Open and striped bars correspond to metabolite concentrations of 1 mg.mL⁻¹ and 0.5 mg.mL⁻¹, respectively. Data is presented as average ± standard error. Two-way ANOVA, followed by a Bonferroni multiple comparison test was used to determine the statistical significance of cytotoxicity of each strain within the same temperature against the control (A/B) or between pure metabolites and control (* $p < 0.05$, ** $p < 0.01$, *** $p < 0.001$, **** $p < 0.0001$).

Pure metabolites (Figures 4.4C and 4.4D) were also cytotoxic for both cell lines. In fact, lasiodiplodin (Metb3) and botryosphaerialactone A (Metb 4) caused 100 % mortality of Vero and 3T3 cells. The metabolites (3*S*,4*R*,5*R*)-4-hydroxymethyl-3,5-dimethyl-dihydro-2-furanone (Metb5) and ICA (Metb1) caused 100 % of 3T3 cell death. Until now, none of these metabolites was known to induce damages to non-tumoral mammalian cells.

DISCUSSION

Some phytopathogenic fungi cause not only disease in plants, but also in humans. For instance, several fungal species of *Aspergillus*, *Bipolaris*, *Curvularia*, *Fusarium* and *Lasiodiplodia* represent

“emerging pathogens” in humans. They are the causative agents of fatal opportunistic infections in immunocompromised patients (Badenoch et al., 2008; De Lucca 2007; Gauthier et al., 2013). Many species, associated to opportunistic infections, produce secondary metabolites that play important roles in the disease (Gauthier and Keller 2013).

In this regard, until now there were no studies on the production of secondary metabolites by *Lasiodiplodia* strains causing human infections. On the other hand, the characterization of the secondary metabolite production of plant isolated *L. theobromae* strains is scarce, and none describe the effect of temperature (Aldridge et al., 1971; Alves da Cunha et al., 2012; Andolfi et al., 2011; Chen et al., 2016; Matsumoto et al., 1994; Yang et al., 2000).

In this work, eleven different metabolites were isolated from two strains of *L. theobromae*. The metabolic profiles of each strain of *L. theobromae* were distinct, and both strains behaved differently from the increase on fungal growth temperature (Table 4.1). In fact, only one metabolite (ICA) (metb 1) was produced by both strains at both growth temperatures. Lasiodiplodin (metb 3) was produced only by strain CAA019, while *cis*-(3*R*,4*R*)- and *trans*-(3*R*,4*S*)-4-hydroxymelleins (metb 8 and 9, respectively) and scytalone (metb 10) were produced only by strain CBS339.90.

Scytalone (metb 10), jasmonic acid (metb 2), *cis*-(3*R*,4*R*)- and *trans*-(3*R*,4*S*)-4-hydroxymellein (metbs 8 and 9, respectively) are known to contribute to fungal pathogenicity to plants. Scytalone is produced by several fungi and is thought to be a precursor in the synthesis of dihydronaphthalene (DHN)-melanin that is involved in the melanin pathway (Andolfi et al., 2011). Due to the potential toxicity of the oxidative products of melanin precursors, certain melanotic fungi seem to secrete those products to induce injuries in their hosts. Indeed, several phytotoxins derived from DHN-melanin have been described (Jacobson 2000). Furthermore, absolute configuration of scytalone has also been determined recently (Evidente et al., 2011).

In 1993, Husain and co-workers described (-)-jasmonic acid as a phytotoxin, capable of inducing dieback symptoms caused by *Botryodiplodia theobromae* (= *L. theobromae*) in infected rose plants (Husain et al., 1993). Recent studies also demonstrated that the production of JA by pathogenic fungi, such as *L. theobromae*, leads to the inhibition of the defense pathway of the plant host, facilitating the infection process (Chanclud et al., 2016; Tsukada et al., 2010). Our results agree these observations: JA was extremely phytotoxic for tomato plants. Moreover, about the temperature role in the JA production, a maximum was reported at about 33 °C, and this is in line with our data (Dhandhukia and Thakkar 2007). We also showed that JA is cytotoxic for mammalian 3T3 cells, which may have implications in the ability of *L. theobromae* to infect animal hosts.

The metabolites *cis*-(3*R*,4*R*)- and *trans*-(3*R*,4*S*)-4-hydroxymelleins (Metb8 and Metb9), 3,4-dihydroisocoumarins from the family of pentaketides, are toxins known to be typically found in *Botryosphaeriaceae* culture filtrates contributing, in synergy with other extracellular metabolites, to several diseases in grapevines (Ramirez-Suero et al., 2014) and other plants (e.g. tomato plants) (Abou-Mansour et al., 2015; Cimmino et al., 2013; Ramirez-Suero et al., 2014). In fact, Andolfi et al., (2011) proposed mellein as a diagnostic marker of diseased plants.

From cultures grown at 37 °C, two mixtures of the two stereoisomers (3*S*,4*S*)- and (3*R*,4*S*)-4-acetyl-3-methyl-2-dihydrofuranones (Metb6 + Metb7) were isolated. From the ¹H NMR spectrum the ratio of the two stereoisomers (Metb6 : Metb7) was determined to be about 1:1 and 3:1. Since the 3:1 mixture of the two epimers is much less toxic than the 1:1 mixture, we hypothesize that phytotoxicity is caused mainly by isomer (3*R*,4*S*) which was applied in higher amounts when testing the 1:1 mixture. Therefore, it is expected that all metabolites may contribute to the phytotoxicity and cytotoxicity of the culture filtrates in study.

Strain CAA019 showed to be more aggressive to tomato stems at 25 °C than strain CBS339.90. The same trend was followed by pure metabolites tested: lasiodiplodin, detected only on strain CAA019 was the second most phytotoxic metabolite tested.

Vero (African green monkey kidney epithelial cells) and 3T3 (mouse fibroblasts cells) were selected to assess the effect of pure metabolites. Vero and 3T3 cells may display different sensitivity to test materials/compounds, and for that reason are broadly used to assess general toxicity, mainly for detection of the biological activity of test natural or synthetic substances. Epithelial cells and fibroblasts are the two cell types mainly involved in tissue repair after injury/infection. Monkey kidney cells (Vero) showed to be more robust, and fibroblasts (3T3), more sensitive, to strain CBS339.90 that was responsible to cause higher mammalian cell mortality, especially when grown at 37 °C. Earlier, Félix et al., (2016) showed a similar result for the same strains using Vero cells. Despite the fact that specific conditions (medium and incubation period) were used in the present work to stimulate metabolites production, Félix et al., found that several aspartic proteases are expressed by strain CBS339.90. These enzymes contribute to pathogenicity in mammals and humans, due to the rich protein extracellular matrix present in these organisms. For the pure metabolites, it was possible to verify that metabolites that were responsible to cause phytotoxicity in tomato leaves were also toxic to mammalian cells. Lasiodiplodin (metb 3) and ICA (metb 1) induced 100 % of cell mortality in 3T3 cells, suggesting that similar pathways may be used in plants and mammals.

In addition to several known secondary metabolites, such as jasmonic acid and 3-ICA, this is the first time that the phytotoxin scytalone was identified in a *Lasiodiplodia* species.

Some metabolites identified are known phytotoxins, but this is the first report of cytotoxicity to mammalian cells of 3-ICA, lasiodiplodin and of the 1:1 mixture of the stereoisomers (3*S*,4*S*)- and (3*R*,4*S*)-4-acetyl-3-methyl-2-dihydrofuranones.

We also produced evidence that temperature affects the phytotoxicity and cytotoxicity of strains CAA019 and CBS339.90 of *L. theobromae* grown, apparently due to the different production of secondary metabolites. Jasmonic acid, which was isolated only from cultures grown at 25 °C, owing to its high phytotoxicity, elegantly explains the high phytotoxicity of filtrates from cultures at this temperature.

The metabolite profile of both strains was revealed to be significantly affected by temperature, leading to relevant implications for plant pathogenicity. Although more strains would be important to use to guarantee the robustness of the study the results strongly suggest that temperature may be highly relevant to the pathogenicity of this species towards mammalian cells.

ACKNOWLEDGMENTS

This study was supported by FEDER funding through COMPETE program and by national funding through FCT within the research project ALIEN (PTDC/AGR-PRO/2183/2014 - POCI-01-0145-FEDER-016788) and the research unit CESAM (UID/AMB/50017 - POCI-01-0145-FEDER-007638). The authors acknowledge FCT financial support to A Alves (IF/00835/2013), AC Esteves (BPD/102572/2014) and C Felix (BD/97613/2013). The authors also thank the support of COST Action FA1303: Sustainable control of grapevine trunk diseases. COST Action is supported by the EU RTD Framework program and ESF provides the COST Office through an EC contract.

CHAPTER 5

Secondary metabolites produced by grapevine strains of
Lasiodiplodia theobromae grown at two different temperatures

ABSTRACT

Lasiodiplodia theobromae is a fungal plant pathogen that has been associated to Botryosphaeria dieback of grapevine. Despite several studies on *L. theobromae*, until now, the production of secondary metabolites by strains isolated from grapevines had not been reported.

In this work, the capacity to produce lipophilic metabolites of two strains of *L. theobromae* isolated from grapevine was studied (LA-SOL3 and LA-SV1). Although many typical metabolites with low molecular weight were identified from the crude extracts of both strains (*e.g.*, lasiolactols, substituted 2-dihydrofuranones, melleins, jasmonic acid, 3-indolcarboxylic acid, botryodiplodins), 3-*epi*-botryodiplodin was isolated for the first time as natural compound. Furthermore, a comparative study of metabolite production was conducted at 25 and 37 °C to understand the temperature effects on metabolic profiles.

Some metabolites were produced only by one strain (*e.g.*, (3*S*,4*S*)-4-acetyl-3-methyl-2-dihydrofuranone in LA-SOL3) and others at a specific temperature (*e.g.*, jasmonic acid at 25 °C, botryodiplodins at 37 °C).

Studies of phytotoxicity and cytotoxicity of pure compounds were conducted to clarify the influence of lipophilic metabolites on the biological activities of culture filtrates of both strains. Interestingly, *epi*-botryodiplodin is the most toxic compound for Vero and 3T3 cells.

KEYWORDS: Botryosphaeria dieback, secondary metabolites, phytotoxicity, cytotoxicity, grapevine, botryodiplodins

INTRODUCTION

The most widely cultivated and economically important fruit crop in the world is grapevine (*Vitis vinifera* L.) (Úrbez-Torres and Gubler, 2009). The main factors that can limit vineyard longevity and productivity include trunk diseases caused by fungal pathogens.

Over the past decades, several species of the family Botryosphaeriaceae have been recognized as important pathogens of grapevines (Phillips, 2002; van Niekerk et al., 2006; Pitt et al., 2010; Úrbez-Torres, 2011; Spagnolo et al., 2017). These pathogens invade primarily through pruning wounds on cordons and spurs of grapevines or through natural injuries (Úrbez-Torres and Gubler, 2009; Spagnolo et al., 2017).

In California, USA, the major grapevine-growing areas were infected by species of the family Botryosphaeriaceae (Úrbez-Torres et al., 2006) and some of these species were also reported to

cause grapevine cankers in other countries (Auger et al., 2004; van Nierkerk et al., 2004; Savocchia et al., 2007; Òrbez-Torres et al., 2008). Several *Lasiodiplodia* species, associated to the grapevine dieback, produce secondary metabolites that could play relevant roles in the disease (Andolfi et al., 2014; Andolfi et al., 2016; Masi et al., 2018). Among them, *Lasiodiplodia theobromae* (Pat.) Griffon & Maubl. is the most commonly found in vineyards in tropical and subtropical regions (Òrbez-Torres 2011; Rodriguez-Galvez et al., 2015). Although *L. theobromae* is the most representative species of *Lasiodiplodia* genus and it has been linked to Botryosphaeria dieback of grapevine (Òrbez-Torres 2011; Rodriguez-Galvez et al., 2015), there are no studies on secondary metabolites produced by *L. theobromae* strains from grapevine. It is known that *L. theobromae* biosynthesizes a variety of lipophilic and hydrophilic metabolites with different biological activities (Aldridge et al., 1971; Yang et al., 2000; Miranda et al., 2008; Kitaoka and Nabeta, 2009; Pandi et al., 2010; da Cunha et al., 2012) and it is able to grow between 9 °C and 39 °C infecting hosts in a wide range of temperatures (Dias et al., 1998; D'souza and Ramesh 2002; Saha et al., 2012; Jami et al., 2013; Félix et al., 2016). The symptoms caused by *L. theobromae* on grapevines suggest that phytotoxic metabolites may be involved in the virulence (Aldridge et al., 1971; Dias et al., 1998; Yang et al., 2000; D'souza and Ramesh 2002; Miranda et al., 2008; Kitaoka and Nabeta 2009; Pandi et al., 2010; da Cunha et al., 2012; Saha et al., 2012; Jami et al., 2013; Rodriguez-Galvez et al., 2015; Félix et al., 2016; Andolfi et al., 2011). Moreover, the production of fungal metabolites may be affected by abiotic factors, such as temperature, and the ability of *L. theobromae* to adapt to different environments may be an advantage to colonize new hosts or alter its virulence profile, resulting in impacts on the crops infected by this species. In fact, Paolinelli-Alfonso and his colleagues (2016) showed that heat stress facilitates *L. theobromae* colonization, since this fungus can degrade phenylpropanoid precursors and salicylic acid, compounds known to control host defense (Paolinelli et al., 2016).

In the present study, the capacity to produce lipophilic secondary metabolites of two strains of *L. theobromae* [LA-SOL3 (more virulent) and LA-SV1 (less virulent)] isolated from grapevine was investigated with attention to the effects of abiotic factors on metabolite profiles. In fact, to conduct a comparative study that evaluates how secondary metabolites' production is affected by temperature, these two strains of *L. theobromae* were grown at 25 and 37 °C. Furthermore, pure metabolites were tested for phytotoxicity and cytotoxicity.

MATERIALS AND METHODS

General Experimental Procedures

Optical rotations of pure metabolites were measured in chloroform or in methanol on a Jasco polarimeter (Tokyo, Japan). ^1H and ^{13}C NMR spectra were recorded at 400 and 100 MHz, respectively, in deuterated chloroform (CDCl_3) or in deuterated methanol (CD_3OD), on Bruker (Karlsruhe, Germany) spectrometers and the same solvents were used as internal standards. Analytical and preparative TLC were performed on silica gel plates (Kieselgel 60, F254, 0.25 and 0.5 mm, respectively, Merck, Darmstadt, Germany). The spots were visualized by exposure to UV radiation (253 nm), or by spraying first with 10 % sulfuric acid in methanol followed by heating at 110 °C for 10 min. Chromatography was performed on silica gel column (Merck, Kieselgel 60, 0.063–0.200 mm). ESI-TOF mass spectra were measured on an Agilent Technologies QTOF 6230 in the positive ion mode (Milan, Italy).

GC/MS measurements were performed using an Agilent 6850 GC equipped with an HP-5ms capillary column (5 % phenyl methyl poly siloxane stationary phase) and the Agilent 5973 Inert MS detector (used in the scan mode). GC/MS data were acquired on crude or purified metabolites after trimethylsilylation with *N,O*-bis(trimethylsilyl)-trifluoroacetamide (BSTFA). Samples were derivatized and analyzed according to the method previously reported (Guida et al., 2015, Salvatore et al., 2018).

Fungal Strains and Culture Filtrates Production

The *L. theobromae* strains LA-SOL3 and LA-SV1 used in this study were originally isolated from grapevines in Peru (Rodriguez-Galvez et al., 2015). Cultures were maintained at room temperature on Potato Dextrose Agar (PDA) medium (Merck, Germany). Before inoculations each strain was cultured on PDA at 25 °C for 4 days. Mycelium was scraped from PDA plates and suspended in 5 mL of sterilized ultra-pure water. This mycelial suspension was added to 1 L Erlenmeyers, containing 250 mL of Czapek medium amended with 2 % cornmeal (pH 5.7) and incubated for 21 days in the dark at 25 °C or 37 °C without agitation. Culture filtrates were obtained by filtering the culture through sterile 0.45 μm cellulose membranes in a vacuum system.

Extraction and purification of fungal metabolites

Culture filtrates (LA-SOL3₂₅ = 650 mL, LA-SOL3₃₇ = 1.6 L, LA-SV1₂₅ = 2.5 L, LA-SV1₃₇ = 1.0 L) were extracted 3 times with ethyl acetate. Each crude extract was dried with hydrochloric acid and evaporated under reduced pressure originating a brown oil residue (LA-SOL3CE₂₅ = 120.3 mg, LA-

SOL3CE₃₇ = 432.7 mg, LA-SOL3CE₃₇ = 432.7 mg, LA-SV1CE₂₅ = 413.9 mg, LA-SV1CE₃₇ = 524.4 mg). These extracts were purified by column and/or thin layer chromatography on silica gel (CC and/or TLC) producing the identified metabolites (Figure 5.1) as described in Supplementary material – chapter 5.

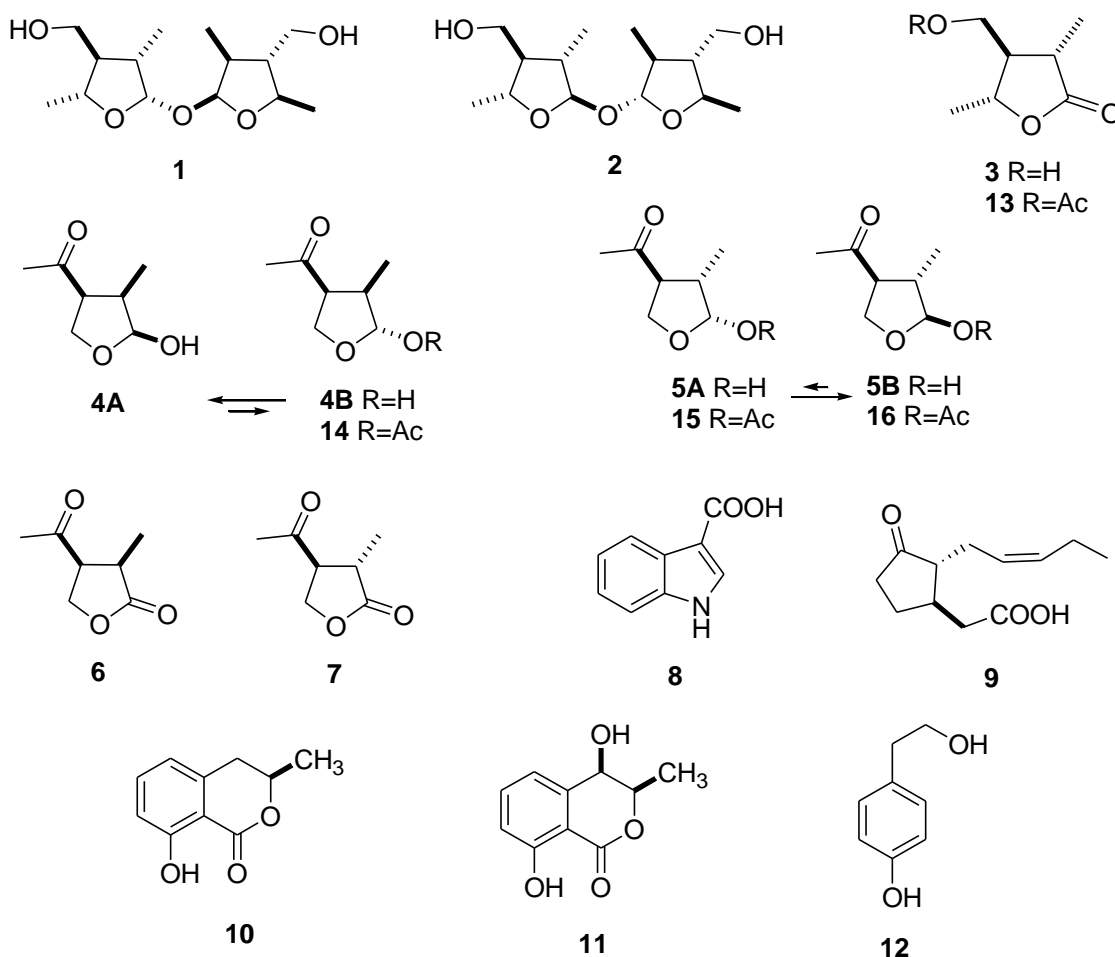


Figure 5.1 | Lasiolactols A and B (1 and 2), (3S,4R,5R)-4-hydroxymethyl-3,5-dimethyldihydro-2-furanone (3), botryodiplodin (4), epi-botryodiplodin (5), (3R,4S)- and (3S,4S)-4-acetyl-3-methyl-2-dihydrofuranones (6 and 7), 3-indolecarboxylic acid (8), (-)-jasmonic acid (9), (-)-mellein (10), (3R,4R)-cis-4-hydroxymellein (11), tyrosol (12), (3S,4R,5R)-4-hydroxymethyl-3,5-dimethyldihydro-2-furanone acetylate (13), botryodiplodin acetylate (14) and acetyl-epi-botryodiplodins (15 and 16).

Phytotoxicity Assays

Phytotoxicity was assessed on tomato cuttings and on tomato leaves. Phytotoxicity of culture filtrates, of strains LA-SOL3 and LA-SV1, diluted in distilled sterile water, were tested on tomato cuttings [1 %, 10 %, 25 %, 50 % (v/v) and without dilution]. Tomato stems of rootless plants (2 weeks old) were dipped in a vial with 2 mL of culture filtrate. After 24 h incubation at room temperature, the solution was replaced by 2 mL of sterile distilled water for additional 48 h. Sterile distilled water

and Czapek medium were used as controls. Using a 0-4 scale (0: no symptoms; 1: slight withering; 2: intermediate withering; 3: severe withering; 4: full withering), symptoms were recorded and converted to a percentage to evaluate the phytotoxic activity. All assays were conducted in triplicate.

For the leaf puncture assay, young tomato plant leaves punctured with a sterile needle were used. Metabolites were dissolved in methanol and then a stock solution (4 % methanol) was made with distilled water. A droplet (20 μL , 1 $\text{mg}\cdot\text{mL}^{-1}$) of the compound solution was applied on the adaxial surface of leaves. As control, a droplet of 4 % methanol was used. The leaves were kept in a moist chamber to prevent the droplets from drying and were observed daily. The visual symptoms were recorded after 10 days of incubation. The lesion diameter was expressed in mm. All assays were carried out in triplicate.

Cytotoxicity Assay on Mammalian Cells Culture

In vitro cytotoxicity was performed as previously reported with slight modifications (Félix et al., 2016, Duarte et al., 2015). Two cell lines were grown and maintained according to Ammerman et al., (2009): a Vero cell line (ECACC 88020401, African Green Monkey Kidney cells, GMK clone) and a 3T3 cell line (ECACC 86110401, mouse embryonic fibroblasts, A31 clone A31). The microtiter plates were incubated at 37 °C in 5 % CO_2 for 24 h. Vero and 3T3 cells were treated, for 20 h, with culture filtrates or pure metabolites (1:1 in DMEM - Dulbecco's Modified Eagle Medium). Two different concentrations of each metabolite were analyzed [1 $\text{mg}\cdot\text{mL}^{-1}$ and 0.5 $\text{mg}\cdot\text{mL}^{-1}$ in Phosphate Buffered Saline (PBS)]. After the incubation period, the medium was removed by aspiration and 50 μL of DMEM with 10 % resazurin (0.1 $\text{mg}\cdot\text{mL}^{-1}$ in PBS) was added to each well to assess cell viability. The microtiter plates were incubated at 37 °C in 5 % CO_2 during 3 h. The absorbance was read at 570 and 600 nm wavelengths in a microtiter plate spectrophotometer (Biotek Synergy). PBS and Czapek medium were used as controls.

RESULTS

Phytotoxicity of filtrates from cultures of *L. theobromae* strains LA-SOL3 and LA-SV1 (grown at 25 °C or 37 °C) was evaluated via assays on tomato stems of rootless plants (Figure 5.2).

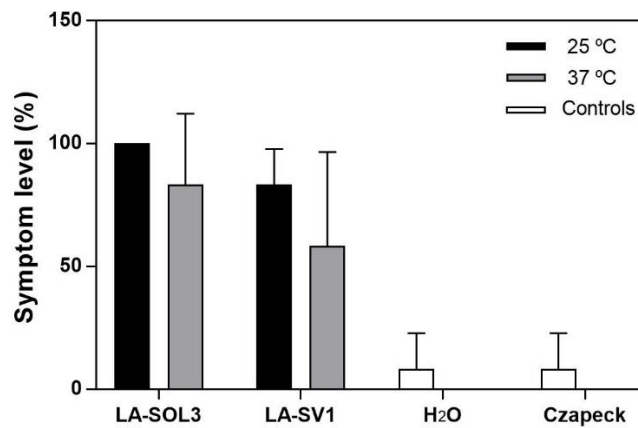


Figure 5.2 | Phytotoxicity assay on tomato stems using the filtrates of strains LA-SOL3 and LA-SV1 of *L. theobromae* grown at 25 °C and 37 °C. Data is shown as the average of 3 independent replicates for each condition.

In addition to phytotoxicity, cytotoxicity of culture filtrates of both strains, grown at 25 and 37 °C, to mammalian Vero and 3T3 cell lines, was also evaluated (Figure 5.3A and B).

Both strains were able to induce phytotoxicity (withering and dry leaves) inducing a higher level of toxicity when fungi were grown at 25 °C. At this temperature, LA-SOL3 strain seems to be more aggressive than LA-SV1, inducing more severe symptoms of phytotoxicity. Nevertheless, at 37 °C, LA-SV1 is more phytotoxic than strain LA-SOL3.

The culture filtrates of both strains grown at both temperatures, showed to be cytotoxic to both Vero and 3T3 cells (Figure 5.3A and B). However, the fibroblasts cells, 3T3, suffered higher mortality when exposed to LA-SOL3 and LA-SV1 culture filtrates than Vero cells. At 25 °C, LA-SV1 was the strain responsible for the higher levels of cell mortality, 80 % on 3T3 cells, but contrary, at 37 °C, this behavior was found for LA-SOL3 strain, reaching also values of near to 80 % on 3T3 cells.

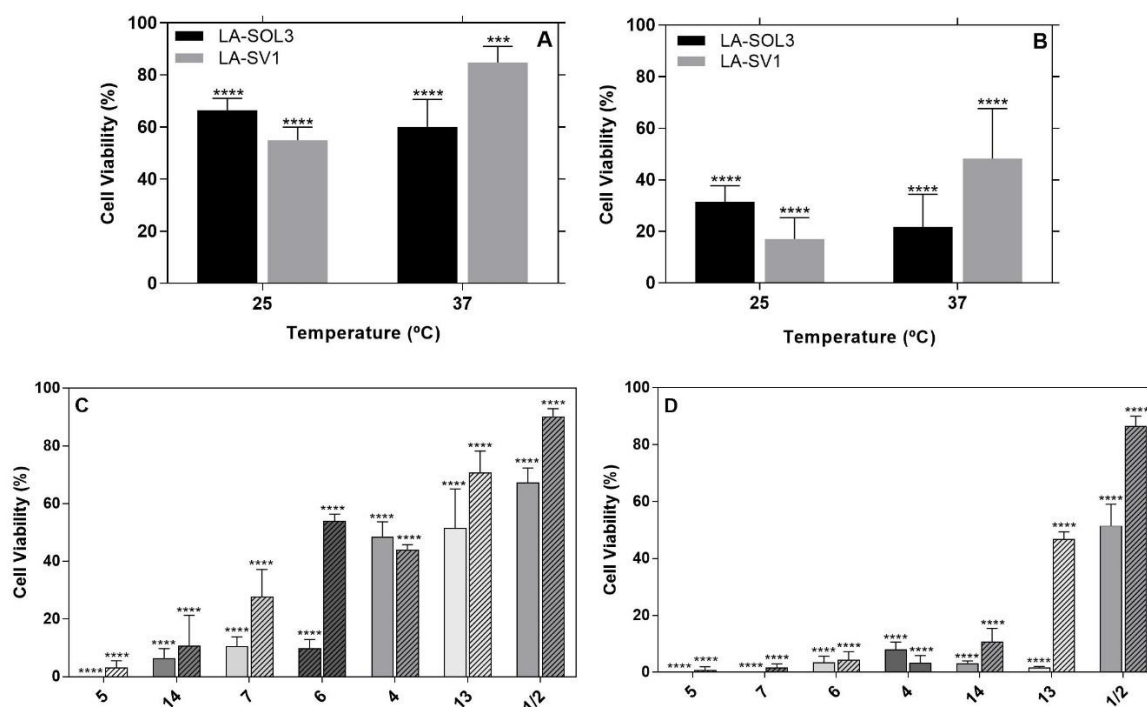


Figure 5.3 | Evaluation of cytotoxicity in Vero (A/C) and 3T3 (B/D) cells of culture filtrates (A/B) and pure metabolites (C/D) and derivatives from strains LA-SOL3 and LA-SV1 grown at 25 °C and 37 °C. Open and striped bars correspond to metabolite concentrations of 1 mg.mL⁻¹ and 0.5 mg.mL⁻¹, respectively. Data is presented as average \pm standard error. Two-way ANOVA, followed by a Bonferroni multiple comparison test was used to determine the statistical significance of cytotoxicity of each strain within the same temperature against the control (A/B) or between pure metabolites and control (C/D) (* p <0.05, ** p <0.01, *** p <0.001, **** p <0.0001).

In order to identify bioactive lipophilic compounds that may be involved in biological activities of culture filtrates of two strains, their crude extracts (LA-SOL3CE₂₅, LA-SOL3CE₃₇, LASV1CE₂₅, LASV1CE₃₇) were subjected to purification processes by combined column and TLC chromatography. All metabolites were identified by physical and spectroscopic techniques (*e.g.*, OR, ¹H and ¹³C NMR mono and bi-dimensional, ESI/TOF) and by comparison of the obtained data to those reported in the literature for: lasiolactols A and B (Andolfi et al., 2016), (3*S*,4*R*,5*R*)-hydroxymethyl-3,5-dimethyldihydro-2-furanone (Andolfi et al., 2014), (-)-botryodiplodin (Andolfi et al., 2014), *epi*-botryodiplodin (C-3 epimer of botryodiplodin) (Rehnberg et al., 1990), (3*S*,4*S*)- and (3*R*,4*S*)-4-acetyl-3-methyl-2-dihydrofuranones (Forzato et al., 2005), 3-indolecarboxylic acid (3-ICA) (Qian et al., 2014), (-)-jasmonic acid (Husain et al., 1993), (*R*)-mellein, *cis*-(3*R*,4*R*)-4-hydroxymellein (Cabras et al., 2006), and tyrosol (Evidente et al., 2010) (**1-12**, Figure 5.1).

In this study, the custom GC/MS library described by Félix et al., (2018) was improved adding mass spectra of derivatized pure metabolites **1**, **2**, **4**, **5**, and **10** obtained after purification processes of

crude extracts (Supplementary material – chapter 5). As an example, Figure 5.4A and B show the Total Ion Chromatograms (TICs) of LA-SOL3CE₂₅ and LA-SOL3CE₃₇, respectively.

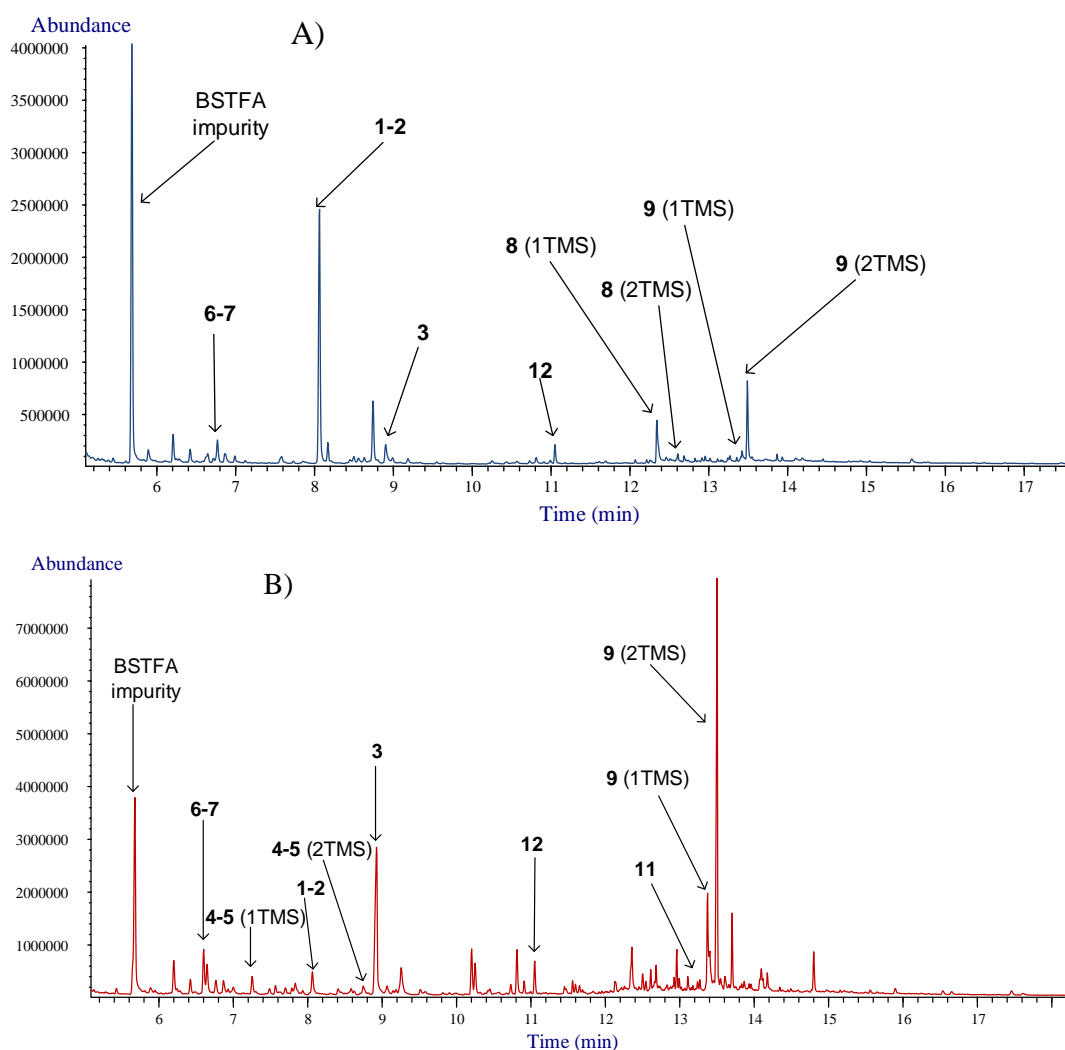


Figure 5.4 | Annotated total ion chromatograms (TIC) acquired by processing samples from LA-SOL3CE₂₅ (A) and LA-SOL3CE₃₇ (B).

Metabolites identified via GC/MS and spectroscopic techniques in the crude extracts of strains grown at 25 and 37 °C are listed in Table 5.1.

Table 5.1 | Distribution of secondary metabolites produced by strains of *Lasiodiplodia theobromae*, according to strain (LA-SOL3 and LA-SV1) and culture temperatures.

Code	Compound	Crude Extract (CE)			
		LA-SOL3CE ₂₅	LA-SOL3CE ₃₇	LA-SV1CE ₂₅	LA-SV1CE ₃₇
1-2	Lasiolactol A and B	+	+	+	+
3	(3 <i>S</i> ,4 <i>R</i> ,5 <i>R</i>)-4-Hydroxymethyl-3,5-dimethyldihydro-2-furanone	+	+	+	+
4	Botryodiplodin		+		+
5	<i>epi</i> -Botryodiplodin		+		+
6	(3 <i>R</i> ,4 <i>S</i>)-4-Acetyl-3-methyl-2-dihydrofuranone	+	+	+	+
7	(3 <i>S</i> ,4 <i>S</i>)-4-Acetyl-3-methyl-2-dihydrofuranone		+		
8	Indol-3-carboxylic acid	+	+	+	+
9	Jasmonic acid	+		+	
10	(-)-Mellein			+	+
11	(3 <i>R</i> ,4 <i>R</i>)-4-Hydroxymellein		+	+	
12	Tyrosol	+	+	+	+

The presence of compounds is indicated with “+”.

Both strains, at both growth temperatures studied (25 °C and 37 °C), produce lasiolactols A and B, (3*S*,4*R*,5*R*)-4-hydroxymethyl-3,5-dimethyldihydro-2-furanone, (3*R*,4*S*)-4-acetyl-3-methyl-2-dihydrofuranone, 3-indolecarboxylic acid, and tyrosol. On the other hand, some metabolites are strain or temperature specific. This is the case of jasmonic acid and botryodiplodins whose production was found to be temperature specific. In fact, the production of **9** by *L. theobromae* strains grown at 25 °C rather than 37 °C, is in accordance with that recently reported by our group for different strains of *L. theobromae* (Félix et al., 2018). Botryodiplodins' is produced by LA-SV1 and LA-SOL3 only when these are grown at 37 °C. Among the strain specific metabolites, (-)-mellein is produced only by LA-SV1 at both temperatures and (3*S*,4*S*)-4-acetyl-3-methyl-2-dihydrofuranon is produced only by LA-SOL3 at 37 °C (Table 5.1).

Botryodiplodins are present in solution as a mixture of hemiacetals (C-2 epimers). In order to confirm their structures, acetylation reactions were performed to obtain their acetyl-derivates. Acetylation of botryodiplodin, as expected, originates only the product (2*R*,3*R*,4*S*) isomer (Andolfi et al., 2014 and literature therein), as opposed to *epi*-botryodiplodin that originates both 2-*O*-acetyl derivatives (C-2 epimers). Therefore, it was possible to separate (2*R*,3*S*,4*S*)-, and (2*S*,3*S*,4*S*)-*epi*-botryodiplodin acetylates (**15** and **16**) and their ¹H, ¹³C NMR and COSY spectra make structure and stereostructure determination of possible derivatives. In particular, ¹H NMR spectrum of (2*R*,3*S*,4*S*)-*epi*-botryodiplodin acetylate is in agreement with previously reported spectra for the same compound (De Buyck et al., 2006). The main difference between protonic spectra of **15** and **16** is at the H-2 proton signal resonating as a broad singlet at δ 5.91 for the latter compound. The ESI-MS

spectrum of (2*R*,3*S*,4*S*)-*epi*-botryodiplodin acetylate recorded in the positive mode showed the potassium $[M + K]^+$ and sodiated clusters $[M + Na]^+$ at m/z 225 and 209, respectively; while ESI-MS spectrum of (2*S*,3*S*,4*S*)-*epi*-botryodiplodin acetylate showed the sodiated cluster $[M + Na]^+$ at m/z 209.

(3*S*,4*R*,5*R*)-4-Hydroxymethyl-3,5-dimethyldihydro-2-furanone (**3**) was also acetylated and its spectroscopic data were compared to its parent compound (Andolfi et al., 2014). In particular, 1H NMR spectrum of **13** showed, as only differences, the presence of a singlet at δ 2.11, attributed to acetyl group and the characteristic downfield shift of hydroxymethylene protons H_{2,8}, which resonant as double doublet at δ 4.26 ($J = 4.4$ and 11.5 Hz) and 4.18 ($J = 5.9$ and 11.5 Hz). The ESI-MS spectrum of **13** recorded in the positive mode showed the sodiated cluster $[M + Na]^+$, the pseudomolecular ion $[M + H]^+$ and the ion obtained from the loss of an acetate ion $[M + CH_3COO]^+$ at m/z 209, 187, and 127 respectively.

Phytotoxicity and cytotoxicity of pure compounds (**1**, **2**, **4-7**, and **13-14**) were evaluated, respectively, by a leaf puncture assay on tomato leaves (Table 5.2, Figure 5.5) and by an assay on mammalian cell cultures (Figure 5.3C and D).

Table 5.2 | Phytotoxicity of pure compounds (1-7 and 14) in leaf puncture assay on tomato leaves.

Code	Compound	Lesion size (mm)
14	Botryodiplodin acetylate	0.87 ± 0.15
5	<i>epi</i> -Botryodiplodin	0.73 ± 0.15
6	(3 <i>R</i> ,4 <i>S</i>)-4-Acetyl-3-methyl-dihydro-furan-2-one	0.5 ± 0.10
1-2	Lasiolactols A and B	0
3	(3 <i>S</i> ,4 <i>R</i> ,5 <i>R</i>)-4-Hydroxymethyl-3,5-dimethyldihydro-2-furanone acetylate	0
4	Botryodiplodin	0
7	(3 <i>S</i> ,4 <i>S</i>)-4-Acetyl-3-methyl-dihydro-furan-2-one	0
	Control (4% Methanol)	0

As reported by Felix et al., (2018), phytotoxicity and cytotoxicity of metabolites **3**, **8** and **9** were previously tested via same biological assays. Among the tested compounds, botryodiplodin acetylate, *epi*-botryodiplodin and (3*R*,4*S*)-4-acetyl-3-methyl-dihydro-furan-2-one show phytotoxicity.

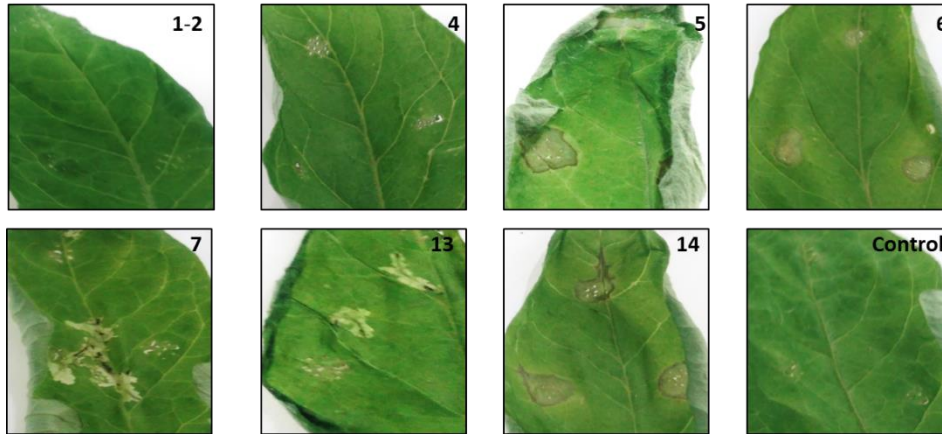


Figure 5.5 | Results of leaf puncture assay of the pure metabolites. 1-2: lasiolactols A and B; 4 botryodiplodin; 5: epi-botryodiplodin; 6: (3R,4S)-acetyl-3-methyl-dihydro-furan-2-one; 7: (3S,4S)-4-acetyl-3-methyl-dihydro-furan-2-one; 13: 4-hydroxymethyl-3,5-dimethyldihydro-2-furanone acetylate; 14: botryodiplodin acetylate; negative control: 4 % methanol.

The cytotoxicity assays on mammalian cell lines (Vero and 3T3 cells, Figure 5.3C and D) show that *epi*-botryodiplodin (**5**) and botryodiplodin acetylate (**14**) are the most cytotoxic compounds on Vero cells. Concerning the 3T3 cell line, all pure compounds induce more than 80 % of cell mortality, with the exception of lasiolactols A and B (**1** and **2**) that induce low toxicity to cells (cell mortality below 50 %).

DISCUSSION

Lasiodiplodia theobromae is a phytopathogenic fungus of the family *Botryosphaeriaceae*, well known to be involved in Botryosphaeria dieback of grapevine (Úrbez-Torres 2011, Rodríguez-Galvez et al., 2015). Despite all the available information about *L. theobromae*, there are no studies on the production of secondary metabolites by strains isolated from grapevines. Moreover, it is known that temperature is an important factor on the production of secondary metabolites by fungi. In particular, there is evidence that temperature affects *L. theobromae* protein and metabolite production (Félix et al., 2016, 2018). Within our recent activity aiming at the clarification of the effect of abiotic factors on the metabolic profiles of fungi, the present paper reports findings from the study of metabolite production at 25 and 37 °C by two strains of *L. theobromae* isolated from grapevine in Peru (Andolfi et al., 2014).

The culture filtrates produced by both strains grown at both temperatures (Rodríguez-Galvez et al., 2015) were evaluated for toxicity on tomato stems and on mammalian cells. Boosted by the preliminary investigation on the toxicity of culture filtrates, studies were conducted on the

production of secondary bioactive lipophilic metabolites that may be involved in the toxic activity of culture filtrates. Twelve metabolites, belonging to diverse classes of natural compounds, were identified. Findings show that the metabolite profiles depend on the strain and temperature (Table 5.1).

About biological activities of metabolites produced by *L. theobromae* strains grown at 25 and 37°C in this study, interesting results were obtained and discussed below for some representative compounds.

About **4-7**, they are structurally related and, for the first time, isolated from the same natural source. Botryodiplodin (**4**) is a natural mycotoxin with a variety of biological activities. It is a 2:3 mixture of (2*R*) and (2*S*) anomers and its absolute configuration is (2*R*/2*S*,3*R*,4*S*). Acetylation of **4** yielded as unique derivative the (2*R*,3*R*,4*S*)-2-*O*-acetylbotryodiplodin. Recently, botryodiplodin was isolated as a secondary metabolite produced by *Lasiodiplodia mediterranea* associated with grapevine declining in Sardinia (Italy) (Andolfi et al., 2014). Until now, none of the botryodiplodin stereoisomers was isolated from natural sources. In particular, studies speculated that *epi*-botryodiplodin could only be produced after treatment of botryodiplodin in ethyl acetate sodium bicarbonate (Fujimoto et al., 1980).

Epi-botryodiplodin (**5**), also present as a 1:2 mixture of 2*R* and 2*S* anomers, has the (2*R*/2*S*,3*S*,4*S*)-configuration. In the present paper, the acetylation of **5** that yield two 2-*O*-acetyl derivatives epimers at C-2 (**15** and **16**) is also reported. As previously reported (Andolfi et al., 2014), botryodiplodin turns out not to be a phytotoxic compound, but its epimerization on C3 and its acetylation give as products phytotoxic derivatives as showed in Table 5.2 and Figure 5.5 for **5** and **14**.

Interestingly, botryodiplodin and its acetylate derivative have the same cytotoxicity on 3T3 cells, conversely botryodiplodin is more toxic than acetylate botryodiplodin on Vero cells (Figure 5.3C and D). However, for Vero cells, *epi*-botryodiplodin was the most cytotoxic metabolite, inducing 100 % cell mortality (Figure 5.3C and D). The production of botryodiplodins at 37 °C could only be considered an important feature of fungal adaptation during host infection at higher temperatures than the current average environmental temperature.

Pure dihydrofuranolactones (**6** and **7**) were also tested. The C-3 stereochemistry has greater influence on the phytotoxicity than cytotoxicity because of the major toxicity of (3*R*,4*S*) isomer in the leaf puncture test (**6**, Table 5.2, Figure 5.5).

Lasiolactols (**1** and **2**), two dimeric γ -lactols, were isolated for the first time from *L. mediterranea* associated with grapevine decline in Sicily, Italy (Andolfi et al., 2016). Regarding the toxicity of these

compounds, no effect was visible in tomato leaves but lasiolactols induced 20-50 % cell mortality (Vero and 3T3 cells, respectively).

4-Hydroxymethyl-3,5-dimethyldihydro-2-furanone acetylate (**13**) is not toxic for tomato leaf and it is more cytotoxic for 3T3 cells than Vero cells in the same way as its parent compound (Andolfi et al., 2014, 2016, Félix et al., 2018).

(-)-Jasmonic acid (JA) is a phytotoxin associated to *L. theobromae* (Husain et al., 1993, Chanclud and Morel, 2016). Studies of toxicity on tomato plants and on mammalian cells show that JA is a potent phytotoxic and cytotoxic agent (Félix et al., 2018), which may contribute to the ability of *L. theobromae* to infect hosts. This toxin was identified in both strains, LA-SOL3 and LA-SV1, but only when these fungi were grown at 25 °C, which is in agreement with the results obtained earlier for other strains of *L. theobromae* (Félix et al., 2018).

3,4-Dihydroisocoumarins are lactonic natural products abundant in microbes and higher plants with many biological activities (Saeed et al., 2016). In particular, melleins are typical metabolites produced by several species of Botryosphaeriaceae, such as *L. theobromae* (Félix et al., 2018). Melleins' toxicity is due to the oxidative products of melanin precursors and to several phytotoxins that derive from DHN-melanin (Andolfi et al., 2011). In this study, the metabolite (-)-mellein (**10**) was identified in LA-SV1 strain grown at both temperatures. Although the phenotype of LA-SOL3 suggests the presence of melleins, no dihydroisocoumarins were identified. 3-ICA was produced by both strains grown at 25 and at 37 °C. It has been suggested that tryptophan is converted to 3-ICA via IAA (3-indoleacetic acid) in microorganisms (Qian et al., 2014 and literature therein). Recently, phytotoxic, cytotoxic, antioxidant and antimicrobial activities of 3-ICA were evaluated (Félix et al., 2018, Dzoyem et al., 2017). This metabolite showed to be toxic for tomato leaves and for different mammalian cell lines, especially to 3T3 cells, where 3-ICA was responsible by 100 % of cell mortality (Félix et al., 2018).

Tyrosol (**12**) is a well-known compound produced by plants and microorganisms and it is frequently isolated from Botryosphaeriaceae fungi (Andolfi et al., 2012).

In this study, it was produced by both strains grown at both temperatures. It is also known to contribute to biofilm formation by *Candida albicans*, which could be relevant for the infection process in this organism (Albuquerque and Casadevall 2012).

Different metabolic profiles of *L. theobromae* strains grown at 25 and 37 °C suggest that the production of secondary metabolites is temperature and strain dependent confirming what was previously reported (Félix et al., 2018).

Although our results show that abiotic factors, such as temperature, have an important role in the dynamics between host and pathogen, additional studies may be needed to clarify the role of hydrophilic compounds, with high and low molecular weight, as virulence agent.

ACKNOWLEDGEMENTS

Thanks are due, for the financial support to CESAM (UID/AMB/50017 - POCI-01-0145-FEDER-007638), to FCT/MEC through national funds, within the PT2020 Partnership Agreement and Compete 2020, Finanziamento delle Attività Base della Ricerca (FFABR) 2017 of Ministry of Education, University and Research (MIUR, Italy) This study was partially supported by FEDER funding through COMPETE program and by national funding through FCT within the research project ALIEN (PTDC/AGR-PRO/2183/2014 - POCI-01-0145-FEDER-016788). The authors acknowledge FCT financial support to A Alves (IF/00835/2013), AC Esteves (BPD/102572/2014) and C Félix (BD/97613/2013). The authors also thanks to COST Action FA1303: Sustainable control of grapevine trunk diseases. COST Action is supported by the EU RTD Framework program and ESF provides the COST Office through an EC contract.

CHAPTER 6

A multi-omics analysis of the grapevine pathogen *Lasiodiplodia theobromae* reveals that temperature affects the expression of virulence- and pathogenicity-related gene expression

ABSTRACT

Lasiodiplodia theobromae (Botryosphaeriaceae, Ascomycota) has been increasingly recognized as an important pathogen of grapevine (*Vitis vinifera* L.) and is typically found in tropical and subtropical regions.

This study aimed to understand how temperature affects the molecular mechanisms of pathogenicity of *L. theobromae*. This objective is part of the general question on the effect of the climate change on the behaviour of microbial pathogens. For that, a multi-omics approach, including genomics, transcriptomics, and proteomics was employed. The genome (Illumina HiSeq) of *L. theobromae* LA-SOL3 was sequenced. Furthermore, the transcriptome (Illumina TruSeq) and proteome (Orbitrap LC-MS/MS) of LA-SOL3 grown at 25 °C and 37 °C were analysed.

From the results, it is clear how a temperature increase affects the expression of a number of genes related to the virulence and pathogenicity. In fact, proteins related to pathogenicity and plant cell wall degradation, toxin synthesis, mitogen-activated kinases and proteins involved in the velvet complex are more expressed when the fungus is grown at 25 °C. At 37 °C, proteins related with pathogenicity were less common than at 25 °C, while proteins related with cell wall organization were more common. However, virulence factors, such as the virulence protein SSD1, known to contribute to host responses tolerance and colonization of human tissues, were expressed only at 37 °C: such proteins enlighten *L. theobromae* pathogenicity towards humans.

The integration of different omics approaches revealed important pathogenicity determinants of *L. theobromae*, improving the knowledge about the pathogenicity mechanisms of this species. The results also suggest that *L. theobromae* pathogenicity can be modulated by temperature and that it has the necessary machinery to infect hosts from different kingdoms.

KEYWORDS: temperature, transcriptome, proteome, plant cell wall degradation, toxins, phytopathogenicity

INTRODUCTION

The most widely cultivated and economically important fruit crop in the world is grapevine (*Vitis vinifera* L.) (Úrbez-Torres and Gubler, 2009). Among the primary factors that can limit vineyard longevity and productivity are trunk diseases caused by fungal pathogens.

Over the past decades, several species of the family Botryosphaeriaceae have been recognized as important pathogens of grapevine (Phillips, 2002; van Niekerk et al., 2006; Pitt et al., 2010; Úrbez-

Torres, 2011). Among these, *Lasiodiplodia theobromae* (Pat.) Griffon & Maubl. an emergent grapevine trunk disease agent especially in warmer climates, is frequently the species most commonly found in vineyards, as well as the most aggressive (Úrbez-Torres, 2011; Rodríguez-Gálvez et al., 2015).

Lasiodiplodia theobromae is a plant pathogenic fungus typically found in tropical and subtropical regions (Phillips et al., 2013). Although its optimal growth range of temperature is between 27 °C and 33 °C (Félix et al., 2016), it is easily found in different climates (D'souza and Ramesh, 2002), showing a great capacity to adapt to different environments. It has been associated to almost 500 hosts and a large number of diseases, especially in crops (Punithalingam, 1976). In humans, *L. theobromae* has been associated to several diseases with different levels of severity, from ocular infections to human death (Kindo et al., 2010; Saha et al., 2012a, 2012b; Woo et al., 2008; Summerbell et al., 2004).

The alterations on the climate, namely the increasing temperature (Galant et al., 2012; Piñeiro et al. 2010), can influence the behaviour of pathogens. Nonetheless, little effort has been directed to identify the impact of these alterations on microbial pathogen/host interactions, that ultimately can result in virulence changes (Eastburn et al., 2011; Gallana et al., 2013; Lindner et al., 2010).

Cell wall degrading enzymes, and other virulence factors are known to contribute to fungal pathogenicity (Gonzalez-Fernandez and Jorrín-Novó, 2012; King et al., 2011). The expression of these molecules in *L. theobromae* can be modulated by abiotic factors, such as temperature (Félix et al., 2016; Yan et al., 2017). A study by Úrbez-Torres et al. (2011) showed that the larger lesions caused by *L. theobromae* on grapevines were observed when the plants were grown at 35 °C, comparing with those grown at 30 °C. A similar result was obtained by Yan et al. (2017), where the largest lesions were observed at 35 °C when compared with 25 °C, suggesting that an increase of the temperature may influence the pathogenicity of this species (Paolinelli-Alfonso et al., 2016; Yan et al., 2017).

An approach that integrates multi-omics technologies is a powerful tool to understand the functional principles and the dynamics of cellular systems (Zhang et al., 2010; Assche et al., 2015). Omics approaches are not common to study fungi from the family Botryosphaeriaceae, but in the last years some studies in species of this family, such as *L. theobromae*, revealed important findings about the phylogeny, pathogen-host interactions and pathogenicity of the fungi (Dissanayake et al., 2016; Paolinelli et al., 2016; Uranga et al., 2017a; Uranga et al., 2017b; Yan et al., 2017).

The aim of this study was to understand how *in vitro* growth temperature affects the expression of virulence and pathogenicity-related genes expression in one strain of *L. theobromae* isolated from

grapevine, LA-SOL3. For this, we integrated genome and transcriptome sequencing, secretome and cellular proteome data to study the molecular basis of *L. theobromae* pathogenicity at different temperatures.

MATERIALS AND METHODS

Fungal strains and culture conditions

The strain used in this study was *L. theobromae* LA-SOL3, isolated from *Vitis vinifera* in Peru and that showed to be the most aggressive one in artificial inoculations trials of cv. Red Globe plants (Rodríguez-Gálvez et al., 2015). The culture was maintained on Potato Dextrose Agar (PDA) medium (Merck, Germany) at 25 °C.

DNA extraction, Genome sequencing and assembly

For DNA extraction the mycelium harvested from a culture grown on PDB at 25 °C for 3 days was ground in liquid nitrogen and DNA was extracted according to Möller et al. (1992).

Lasiodiplodia theobromae strain LA-SOL3 was sequenced by Illumina HiSeq at NXTGNT, Belgium. First, paired reads from sequencing were filtered by quality, then trimmed based on quality scores (modified Mott trimming algorithm, threshold=0.05) and reads shorter than 100 nt were discarded. Detected adaptor sequences were also trimmed and reads mapping to the Illumina internal control phage phiX were discarded. Assembly and scaffolding were achieved with CLC Genomics Workbench 9.0.1 (<https://www.qiagenbioinformatics.com/>) *de novo* assembly module with default settings, except for the minimum contig length (2000 nt) or word length (60 nt). Optimal word size was estimated using KmerGenie28 (Chikhi and Medvedev, 2013) prior to the assembly. The primary scaffolds were further refined by means of the SSPACE2 (Boetzer et al., 2011) scaffolder. The gapped regions in the re-scaffolded assembly were (partially) closed using GapFiller (Boetzer and Pirovano, 2012). Genome sequencing of *L. theobromae* LA-SOL3 generated into 38.8 million reads. After assembly, a total genome size of 43,925,482 bp was obtained, with 413 scaffolds and 79 gaps inside scaffolds, accounting for a total of 2,368 Ns (undetermined nucleotides). The N50-value was approximately 249 Mb.

Gene prediction and annotation

Before gene prediction, the genome was repeat-masked. RepeatModeler (v1.0.8) (Smit and Hubley, 2015) was used to build repeat libraries for the *L. theobromae* genome, which were then filtered to

exclude coding regions and simple repeats. RepeatMasker (v4.0.5) (Smit et al., 2015) was used to “hard mask” repeats and transposable elements in the genomes, using the curated repeat libraries, replacing repeats and transposable elements by strings of ‘N’s.

Gene prediction was achieved with BRAKER1 (v1) with the “fungus” option. RNA-seq paired-end reads from the GEO study GSE75978 (Paolinelli-Alfonso et al., 2016) were selected (SRR2994047, SRR2994048, SRR2994053, SRR2994054, SRR2994059, SRR2994060, SRR2994062 and SRR2994063) and used for mapping onto the assembled genome using HISAT2 (v2.0.5) (Kim et al., 2015) with default settings.

Gene product names were assigned based on predicted protein sequences with BLASTP against the UniProt-KB/SwissProt database (downloaded on March 1st, 2017), with an E-value threshold of 1e-3. Other functional annotations were added with InterProScan (v5.21-60) (Mulder and Apweiler, 2007), mapping accessions for InterPro, GO, CDD-3.14 and Pfam-30.0 as well as GO terms. Further functional analyses were carried out as described by Morales-Cruz et al. (2015).

Genome function analysis

Secreted proteins

In order to predict which gene products are secreted, the FunSec pipeline (v1.0) (<https://github.com/Lonewolfenrir/FunSec>) was used. Funsec integrates several software for features’ prediction: signal peptides and transmembrane regions with SignalP v4.1 (Petersen et al., 2011), TMHMM (Sonnhammer et al., 1998) and Phobius v1.01 (Käll et al., 2004); subcellular localization with WoLF PSORT v0.2 (Horton et al., 2007) and ProtComp v9.0 (<http://www.softberry.com/berry.phtml?topic=protcompan&group=help&subgroup=proloc>) and endoplasmic reticulum motifs with PS SCAN v1.86 (http://www.hpa-bioinfotools.org.uk/cgi-bin/ps_scan/ps_scanCGI.pl).

Enzymes

Although Enzyme Commission (EC) numbers and pathway information were provided by InterProScan analysis, the Ensemble Enzyme Prediction Pipeline (E2P2) was also used to annotate protein sequences. This ensemble-style pipeline is more thorough in that it used both single sequence (BLAST, E-value cutoff $\leq 1e-2$) and multiple sequence (Priam) models of enzymatic function. The results were divided into different categories based on their EC numbers.

Carbohydrate-degrading enzymes

Carbohydrate-degrading enzymes (CAZymes) were predicted with the web-based application dbCAN (HMMs 5.0) (Yin et al., 2012) with default settings, which searches the protein sequences in a multifasta file against the CAZy database (Cantarel et al., 2009).

Fungal peroxidases

Fungal peroxidases were predicted with the web-based BLAST application of fPoxDB: Fungal Peroxidase Database (Choi et al., 2014), against the Whole Predicted Peroxidases database, which had been last updated on April 18th, 2012, with an E-value threshold of 1e-5.

Synthetic gene clusters

Gene clusters encoding for secondary metabolites were predicted for the full genomes with the web-based application fungiSMASH (antiSMASH fungal version; v4) (Medema et al., 2011), with added GFF3-formatted files, obtained from gene prediction, and ran with default settings.

Cytochrome P450

Cytochrome P450 identification was pursued by BLAST against The Cytochrome P450 Homepage (Nelson, 2009) database, with an E-value threshold of 1e-5, against the fungal database, which had been last updated on August 12th, 2009.

Pathogen Host Interactions

A BLAST analysis was conducted against the Pathogen Host Interactions database (PHI-base) (Winnenburg et al. 2006), downloaded on February 2nd, 2017, against the whole proteome and the secreted protein datasets, with an E-value threshold of 1e-5.

Transporters

Transporters were identified with a BLAST analysis against the Transporter Classification Database (Saier et al., 2006), downloaded on January 14th, 2018, using an E-value threshold of 1e-5.

RNA extraction, library preparation and sequencing

The mycelium of each replicate (three replicates per condition) was ground in liquid nitrogen and total RNA was extracted using the Spectrum Plant Total RNA kit (Sigma), according to the manufacturer's instructions. Samples were incubated for 15 min with the DNase I digestion set (RNase-Free DNase Set, Qiagen). Integrity and quality analysis were done on a 2100 Bioanalyzer RNA (Agilent Technologies). Afterwards, samples were stored at -80 °C until cDNA library construction. RNA was sequenced at NXTGNT, Belgium, using the Illumina TruSeq Paired-End RNA

preparation kit v.2 (Illumina, San Diego, CA, USA). Reads were mapped to the genome of *L. theobromae* LA-SOL3 using the STAR aligning software (Dobin et al., 2013). Following the mapping step, the R/Bioconductor package edgeR (Robinson et al., 2010) was used to normalize gene counts and identify the differentially expressed genes (DEGs). The DEGs were determined using the “exactTest” function and adjusted using the Benjamin-Hochberg False Discovery Rate (FDR) correction to account for multiple comparisons.

A volcano analysis and clustering analysis of transcripts from the control group (25 °C) versus transcripts from the heat stressed fungus (37 °C) were performed to evaluate the quality of the tested samples and the similarity between them (Figure S6.1). All genes with a Counts Per Million (CPM) greater than 1 in at least 3 samples were used in the analysis. Fold Change (\log_2 FC >1 or <-1) and a False Discovery Rate (FDR <0.01) were used as statistical significance indexes.

Protein extraction and identification

For protein extraction, two plugs with 5 mm diameter from a 4 days old culture (grown at 25 °C) were inoculated into a 250 mL flask containing 50 mL of Potato Dextrose Broth (PDB, Merck, Germany) and incubated at 25 °C or 37 °C for 4 days. All assays were performed in triplicate. Culture supernatants were collected by gravitational filtration through filter paper and stored at -80 °C for extracellular protein analysis. Mycelia were washed with distilled water, frozen in liquid nitrogen and stored at -80 °C until intracellular protein analysis.

Extracellular fraction

The extracellular fraction of the proteome was obtained based on TCA/Acetone method (Fernandes et al. 2014). In order to discard precipitated polysaccharides, 35 mL of the extracellular medium was centrifuged (48,400 g, 1 h at 4 °C). One volume of cold TCA/Acetone [20%/80% (w/v)] with 0.14% (w/v) DTT was added to the supernatant obtained and incubated at -20 °C during 1 h. A centrifugation of 15,000 g (20 min, 4 °C) precipitated the proteins and the supernatant was removed. The pellet was washed with cold acetone (twice) and then with 10 mL of cold 80% acetone (v/v) in order to eliminate TCA traces. The residual acetone was air-dried. The final pellet was resuspended with 200 μ L of lysis buffer (7 M urea, 2 M thiourea, 4% CHAPS, 30 mM Tris) and stored at -80 °C.

Cellular fraction

Two plugs (5 mm) of strain LA-SOL3 were inoculated in PDB medium during 4 days at 25 °C and 37 °C. After this period, mycelia were washed with distilled water and grinded to a fine powder in a mortar in the presence of liquid nitrogen. A 15 mL tube was used to keep the powder and 10 mL

of 10 mM potassium-phosphate buffer (pH 7.4) containing 0.07 % DTT and cOmplete™ protease inhibitor cocktail (Roche) was added. All the samples were sonicated [1 min sonication, 2 min pause (3 min of sonication in total) (Branson, Sonifier 250) at 4 °C] and then agitated using an orbital agitator at minimum speed, during 2 h (4 °C) to induce protein dissociation from the cell wall debris. The homogenate was centrifuged (15000 g, 30 min, 4 °C) and the supernatant was collected. The remaining procedure was the same used to extracellular protein extraction (described above).

Protein Quantification

Protein concentration was determined with the 2-D Quant Kit (GE Healthcare, USA), according to the manufacturer's instructions. All the samples were quantified in triplicate.

Protein Separation

For both intra and extracellular proteins, 125 µg of sample were diluted (1:1) in loading buffer [2 % (v/v) 2-mercaptoethanol, 2 % (w/v) SDS, 8 M Urea, 100 mM Tris, 100 mM Bicine and traces of Bromophenol blue] and analysed by electrophoresis (Laemmli, 1970). Lab-casted SDS-PAGE gels ran at 2 W-2 h, 6 W-3 h on 12 % (w/v). The running buffer contained 100 mM Tris, 100 mM Bicine and 0.1 % (w/v) SDS. The samples were denatured at 100 °C for 5 min prior to electrophoresis. Gels were stained with Coomassie Brilliant Blue G-250 (CBB). After staining, gels were scanned on a GS-800 Calibrated Densitometer (Bio-Rad).

Tryptic Digestion, Mass Spectrometry Analysis, and Protein Identification

After ensuring the quality of the samples, these were electrophoresed and concentrated at the top of the separation gel (visualized as a unique band). This band was manually excised, and protein bands were destained in 200 mM ammonium bicarbonate (AB)/50 % acetonitrile for 15 min and 5 min in 100 % acetonitrile. Proteins were reduced by the addition of 20 mM dithiothreitol in 25 mM AB and incubated for 20 min at 55 °C. The mixture was cooled to room temperature, followed by alkylation of free thiols by the addition of 40 mM iodoacetamide in 25 mM AB in the dark, for 20 min. After that, protein bands were washed twice in 25 mM AB. Proteolytic digestion was performed by adding 12.5 ng.µL⁻¹ of trypsin (Promega, Madison, WI) in 25 mM AB, and incubated at 37 °C overnight. Protein digestion was stopped by addition of trifluoroacetic acid (TFA) at 1 % final concentration. Digested samples were dried in a speedvac.

A nano LC analysis was performed using a Dionex Ultimate 3000 nano UPLC (Thermo Scientific) with a C18 75 µm x 50 Acclaim Pepmam column (Thermo Scientific). Previously, the peptide mix was loaded in a 300 µm x 5 mm Acclaim Pepmap precolumn (Thermo Scientific) in 2 % acetonitrile/0.05 % TFA for 5 min at 5 µL.min⁻¹. Peptide separation was performed at 40 °C. Mobile

phase A was composed by water acidified with 0.1 % formic acid. Mobile phase B was composed by 20 % acetonitrile acidified with 0.1 % formic acid. Samples were separated at 300 nL.min⁻¹. Mobile phase B increased from 4 % to 45 % B in 60 min; 45-90 % B in 1 min, followed by a 5 min wash at 90 % B and a 15 min re-equilibration at 4 % B. The total time of chromatography was 85 min. Eluting peptide cations were converted to gas-phase ions by nano electrospray ionization and analysed in a Thermo Orbitrap Fusion (Q-OT-qIT, Thermo Scientific). Mass spectrometer was operated in positive mode. Survey scans of peptide precursors from 400 to 1,500 m/z were performed at 120 K resolution (at 200 m/z) with a 5 × 10⁵ ion count target. Tandem MS was performed by isolation at 1 Th with the quadrupole, CID fragmentation with normalized collision energy of 35, and rapid scan MS analysis in the ion trap. The AGC ion count target was set to 102 and the max injection time was 75 ms. Only those precursors with charge state 2–6 were sampled for MS2. The dynamic exclusion duration was set to 15 s with a 10 ppm tolerance around the selected precursor and its isotopes. Monoisotopic precursor selection was turned on. The instrument was run in top speed mode with 3 s cycles, meaning the instrument would continuously perform MS2 events until the list of non-excluded precursors diminishes to zero or 3 s, whichever is shorter.

The raw data were processed using Proteome Discoverer (version 2.1.0.81, Thermo Scientific). MS2 spectra were searched with SEQUEST engine against an in-house built database of proteins deduced from the genomic sequence. Peptides were generated from a tryptic digestion with up to one missed cleavages, carbamidomethylation of cysteines as fixed modifications, and oxidation of methionines as variable modifications. Precursor mass tolerance was 10 ppm and product ions were searched at 0 Da tolerance. Peptide spectral matches (PSM) were validated using percolator based on q-values at a 1 % FDR. With Proteome Discoverer software v. 2.1 (Thermo Scientific), peptide identifications were grouped into proteins according to the law of parsimony and filtered to 1 % FDR. The identified proteins were also filtered and considered for analysis only if present in 3 replicates and using at least 3 peptides for identification (Tables S6.1, S6.2, S6.3 and S6.4). The abundance level was obtained considering the temperature of 25 °C as control ($0.5 \geq FC \geq 2$).

RESULTS

Genome Analysis

Genome assembly

The genome of *L. theobromae* LA-SOL3 was sequenced into 38.8 million matched paired-end reads by Illumina sequencing (Table 6.1) and compared with the available genome of *L. theobromae* CSS-01s Yan et al. (2017). Assembly led to a genome size of 43.9 Mb with approximately 214 x coverage, divided into 413 scaffolds with minimum size of 2 Mb, a total of 79 gaps and 2,368 Ns (undetermined nucleotides), as well as a G+C content of 54.75 %. The N50 value was approximately 249 kb. RepeatMasker analysis, coupled with RepeatModeler and RepeatProteinMask, discovered an overall repeat content of 2.21 % of the genome. Gene prediction with BRAKER identified 12,785 genes, with an average length of 1,610 bp, thus accounting for a gene density of 291 genes/Mb and a total of 46.8 % of the genome covered by protein-coding genes. There was an average relation of 1 mRNA per gene, with an average of 2.8 exons and 1.8 introns per mRNA, and thus per gene.

Table 6.1 | General statistics of *L. theobromae* LA-SOL3 genome assembly, gene prediction and comparison with the available genome of *L. theobromae* CSS-01s (MDYX00000000.1).

<i>Lasiodiplodia theobromae</i>	LA-SOL3	CSS-01s (MDYX00000000.1)
Size (Mb)	43.9	43.3
Coverage	214 x	90 x
% G+C content	54.75	54.77
% Repeats	2.21	3.02
Number of genes	12785	12902
Average gene length (bp)	1610	1629
% of genome covered by genes	46.8	~48.5
% of genome covered by CDS	42.7	43.6
Gene density (genes/Mb)	291	297
Average exons per mRNA	2.8	2.8
Average exon length (bp)	510	506
Average introns per mRNA	1.8	1.8
Average intron length (bp)	86	88
Average mRNAs per gene	1	n.a.

n.a.: The average number of mRNAs per genes was not reported by Yan et al. (2017), nor the total number of mRNAs, therefore this statistic could not be calculated.

Genome functional analysis

Lasiodiplodia theobromae LA-SOL3 genome encodes 667 extracellular proteins. From these, 335 are enzymes (7.3 % of all enzymes encoded by the genome, Table 6.2). While the most represented enzymes have oxidoreductase, transferase or hydrolase functions, secreted enzymes are mainly hydrolases (Table 6.2), although some annotated genes were classified in more than one enzyme category.

Table 6.2 | Genes predicted to code for secreted enzymes by E2P2 in the genome of *L. theobromae* LA-SOL3.

Enzyme type	Total (n)	Secreted (n)
Oxidoreductases	1229	46
Transferases	962	7
Hydrolases	1486	237
Lyases	291	28
Isomerases	119	10
Ligases	192	0
Total	4579	335

One relevant group of hydrolases, CAZymes participate in the colonization and infection of plant pathogenic fungi, disassembling the plant cell wall (Lyu et al., 2015, Yan et al., 2017). In total, *L. theobromae* genome encodes for 789 enzymes CAZymes, including carbohydrate-binding modules (CBM). The largest number was annotated as glycoside hydrolases, accounting for 317 proteins (Figure 6.1A). About 272 genes coding for secreted proteins were annotated as CAZymes. Most of these were glycoside hydrolases (127) and no glycoside transferases were identified (Figure 6.1B).

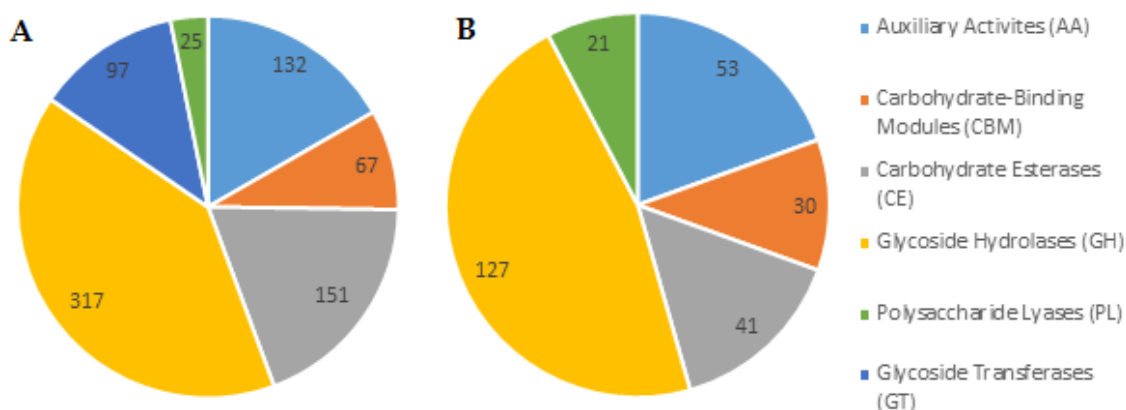


Figure 6.1 | Predicted CAZymes (A) and predicted secreted CAZymes (B) in the genome of *L. theobromae* LA-SOL3.

One of the main functions of plant pathogenic fungi peroxidases is related with the degradation of the lignin present in plant cell walls, contributing to the penetration of the pathogen inside the plant (Hammel and Cullen, 2008; Kellner et al., 2014).

Forty genes encode peroxidases, with a total of 69 functions (Table S6.1). The number of functions was higher than the number of proteins, since 14 genes were annotated with two or more peroxidase types.

Secondary gene cluster are responsible for the synthesis of relevant secondary metabolites. *Lasiodiplodia theobromae* LA-SOL3 genome encodes 52 secondary metabolite gene clusters – per type: 8 terpenes, 17 t1pks (type 1 poliketide synthases), 11 nrps (nonribosomal peptide-synthetase), 6 t1pks-nrps and 10 “other”. Of these, 7 clusters were found to have known homology to other described clusters (Table 6.3).

Table 6.3 | Metabolic gene clusters identified in the genome of *L. theobromae* LA-SOL3. NRPS - nonribosomal peptide-synthetase; T1PKS - type 1 polyketide synthases. Percentages reflect the proportion of common genes in the identified clusters with the most similar known cluster.

Type	Most similar known cluster
NRPS	Chaetocin (13%)
Terpene	PR toxin (50%)
NRPS	Hexadehydro-astechrome (HAS) (25%)
T1PKS	Brefeldin (20%)
T1PKS	Emericellin (50%)
T1PKS	Lasiodiplodin (71%)
T1PKS-NRPS	Fusaridone A (12%)

The function of cytochrome P450 enzymes in pathogenic fungi is usually related with their defense against toxic substances produced by the hosts. In fact, it is known that P450 is involved in the production of mycotoxins, as aflatoxins, and gibberellins (Črešnar et al., 2011). A total of 43 genes were annotated as coding for fungal cytochrome P450, within 23 different P450 families.

Table 6.4 | Fungal cytochrome P450 families predicted to be encoded by *L. theobromae* LA-SOL3. Cytochrome P450-encoding genes were predicted with BLASTP through The Cytochrome P450 Homepage portal (<http://drnelson.uthsc.edu/CytochromeP450.html>, last accessed November 2nd, 2017).

Family	Genes (n)
CYP504	13
CYP505	2
CYP5080	1
CYP531	1
CYP532	2
CYP545	1
CYP547	1
CYP548	1
CYP56	3
CYP570	1
CYP573	1
CYP578	2
CYP586	1
CYP596	1
CYP6001	1
CYP617	1
CYP620	1
CYP626	2
CYP633	1
CYP65	1
CYP664	1
CYP671	2
CYP682	2

Several studies suggest that transporters play a crucial role in pathogenicity of fungi, contributing to different functions such as the export of drugs from the cell (Yan et al., 2017) or the transport of

molecules involved in appressoria formation (Ciuffeti et al., 2014). In the genome of *L. theobromae* LA-SOL3, 1957 genes were annotated as coding for transporters (Table 6.5).

Table 6.5 | Genes predicted to code for transporters in the genome of *L. theobromae* LA-SOL3. Transporters' classes are according the classification of the Transporter Classification Database.

Transporter Class	Genes (n)
Channels and pores	166
Electrochemical potential-driven transporters	857
Primary active transporters	737
Accessory factors involved in transport	44
Transmembrane electron carriers	29
Group translocators	20
Incompletely characterized transport systems	104
Total	1957

Heat shock proteins (HSP) are known to be involved in several common biological activities, such as transcription, translation, protein folding, and aggregation and disaggregation of protein, protecting proteins from damages caused different types of biotic and abiotic stresses, as heat or osmotic alterations (Tiwari et al., 2015). Different families of HSP known to be involved in responses to heat stress were identified in the genome of *L. theobromae* (Table 6.6).

Table 6.6 | Predicted heat shock proteins involved in responses to heat stress in the genome of *L. theobromae* LA-SOL3.

Accession Code	HSP name	HSP Family
P15705	Heat shock protein STI1	HSP 70
P40920	30 kDa heat shock protein	HSP 30
P31540	Heat shock protein hsp98	HSP clpA/clpB
P22943	12 kDa heat shock protein	HSP 20
Q96UX5	Heat shock protein 78, mitochondrial	HSP clpA/clpB
O14368	Heat shock protein 16	HSP20

Transcriptomic Analysis

A transcriptomic analysis was carried out to characterize LA-SOL3 grown at 25 °C and 37 °C. Using class comparison statistical analysis (two-sample t-test, $p < 0.01$) a total of 1,580 transcripts were determined to be differentially expressed and 1,059 transcripts were annotated. An overview of the number of differentially expressed genes, and the proportion of up and down-regulated transcripts, showed a higher number of down-regulated transcripts at 37 °C (731 up- versus 849 down-regulated genes).

Differentially expressed genes at 37 °C were characterized concerning their Gene Ontology (GO) category, according to the biological process they are involved in (Table S6.6).

Comparing the up and down-regulated transcripts, it is possible to verify a different profile of transcripts species: heat stress leads to an increase of the number of transcripts related to primary metabolism and plant cell wall degradation, and to a decrease of transcripts related with stress response, carbohydrate metabolism and catabolism and transport functions (Figure 6.2).

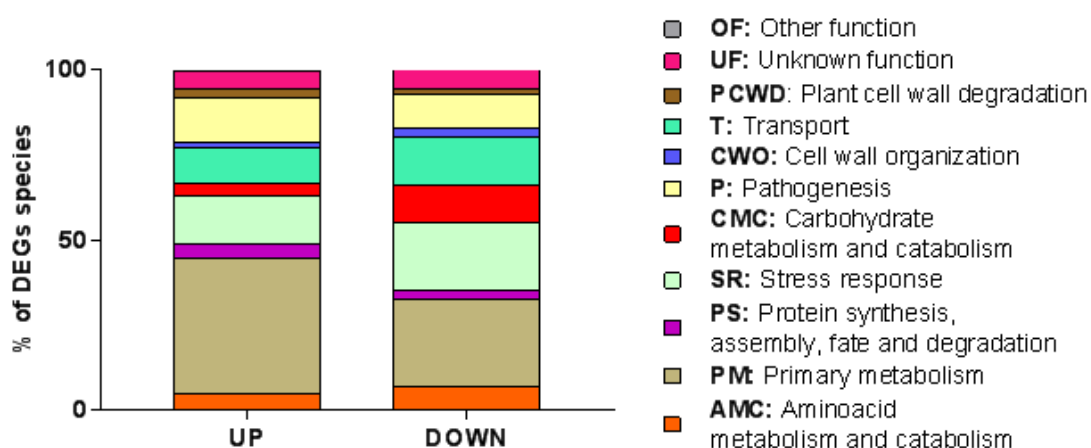


Figure 6.2 | Gene Ontology classification of the transcripts identified in *L. theobromae* LA-SOL3: up and down-regulated transcripts of the fungus grown at 37 °C in comparison with transcripts expressed by the fungus grown at 25 °C. The classification was obtained from the GO (biological process) of each gene product according to the Uniprot database (<http://www.uniprot.org/>).

Proteomic Analysis

In order to complement the data obtained by the genome and differential transcriptome, the secretome and cellular proteomes of *L. theobromae* LA-SOL3 under heat stress were analyzed by SDS-PAGE/LC-MS/MS and compared to those from LA-SOL3 grown under optimal growth temperature (25 °C) (Figure S6.2).

Growth temperature influenced both the secretome and the cellular proteome: growing at 25 °C induces a higher complexity of protein profiles.

A total of 269 proteins were identified in the secretome of the fungus grown at 25 °C and only 15 proteins in the secretome of the fungus grown at 37 °C. Regarding the cellular proteome, a significant higher number of proteins were identified: 1,312 proteins for 25 °C and 662 for 37 °C. In both cases, secretome and cellular proteome, the number of identified proteins was higher when the fungus was grown at optimal temperature (25 °C) (Figure 6.3-A).

The abundance level of the proteins was evaluated through the fold change (FC) ($0.5 \geq FC \geq 2$, Figure 6.3-B). No significantly up-regulated proteins were found in the secretome of the fungus grown at 37 °C and only 17 were identified in the cellular proteome. However, it was possible to identify 10 down-regulated proteins in the secretome and 241 in the cellular proteome, in the same condition.

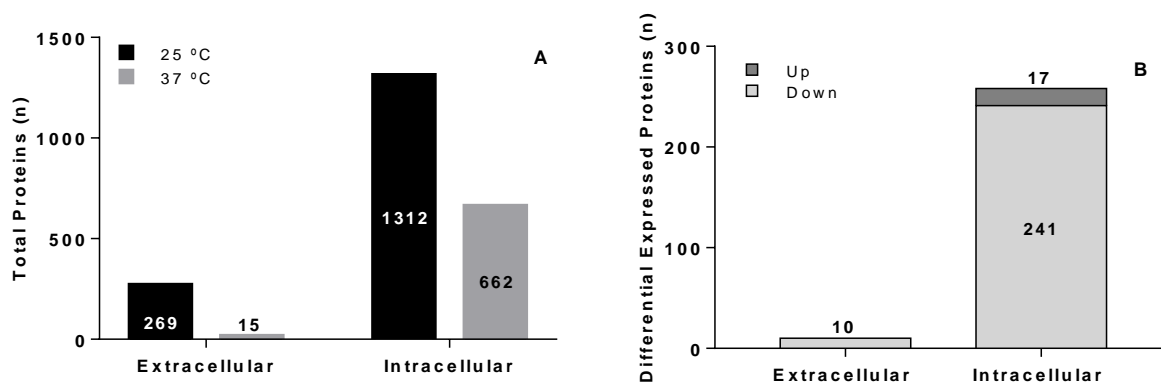


Figure 6.3 | Differential expression of proteins by *L. theobromae* LA-SOL3. Total number of identified extracellular and intracellular proteins (A) and up and down-regulated proteins expressed under heat stress (B). 25 °C corresponds to the control condition.

Differentially expressed proteins at 37 °C were characterized concerning their Gene Ontology (GO) category, according to the biological process they are involved in (Tables S6.7, S6.8). When *L. theobromae* LA-SOL3 grows at 37 °C, there is a considerable increase of extracellular proteins related with cell wall organization (CWO), primary metabolism (PM) and stress response (SR), while the proteins directly related to pathogenesis (P) were not detected (Figure 6.4).

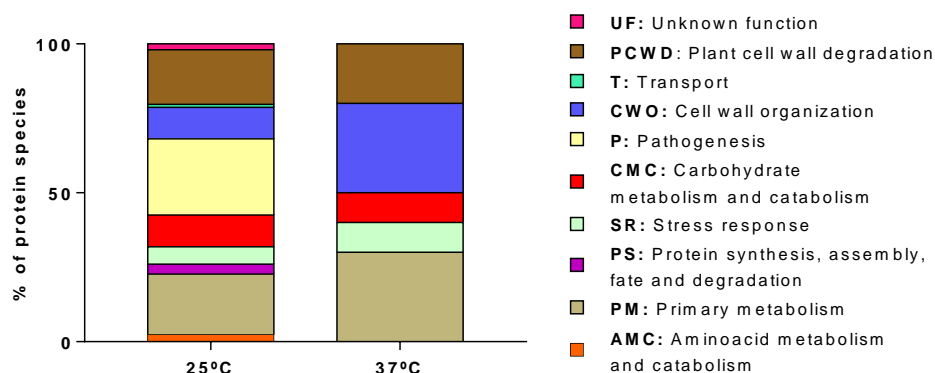


Figure 6.4 | Gene Ontology classification of the extracellular proteins identified in *L. theobromae* LA-SOL3: percentage of distinct species present in extracellular proteins at 25 °C and 37 °C. The classification was obtained from the GO (biological process) of each protein according to the Uniprot database (<http://www.uniprot.org/>).

The same analysis was performed for intracellular proteins (Figure 6.5). Proteins related with primary metabolism (PM) and proteins synthesis, assembly, fate and degradation (PS) were the most commonly found in the cellular proteome of LA-SOL3 grown at 25 °C and 37 °C, respectively.

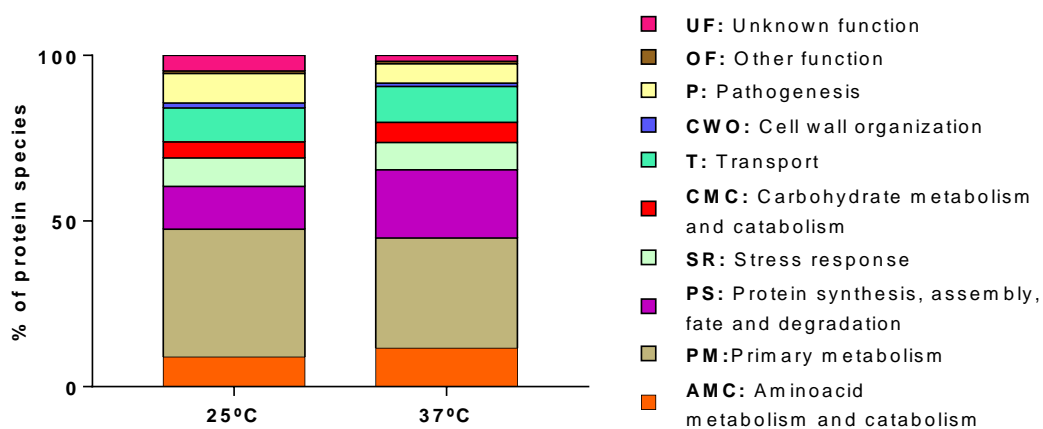


Figure 6.5 | Gene Ontology classification of the intracellular proteins identified in *L. theobromae* LA-SOL3: percentage of distinct species present in extracellular proteins at 25 °C and 37 °C. The classification was obtained from the GO (biological process) of each gene product according to the Uniprot database (<http://www.uniprot.org/>).

DISCUSSION

We performed a multi-omics approach (genomics, transcriptomics and proteomics) aiming to characterize both the molecular toolkit of *L. theobromae* LA-SOL3 and the gene expression associated to the plant-fungus interaction and pathogenicity under heat stress.

A global characterization of the proteins predicted to be encoded by the genome of *L. theobromae* strain LA-SOL3 and a comparison with the genome of *L. theobromae* strain CSS-01s is shown in Table 6.7.

Lasiodiplodia theobromae LA-SOL genome has 4075 genes that were annotated encoding for proteins described in PHI-base, to be involved in pathogenesis processes in plants (Table 6.7).

Table 6.7 | Genes predicted to be involved in pathogen-plant interaction in the genome of *L. theobromae* LA-SOL3 and comparison with *L. theobromae* CSS-01s (Yan et al., 2017).

	LA-SOL3	CSS-01s	Method
Total proteins	12785	12902	BRAKER1
Secreted proteins	677	937	FunSec
Enzymes	4579	-	E2P2
Secreted Enzymes	335	-	FunSec + E2P2
CAZymes	789	763	dbCAN
Secreted CAZymes	272	-	FunSec + dbCAN
Metabolic gene clusters	52	58	fungiSMASH
Cytochrome P450s	44	-	The Cytochrome P450 Homepage
Peroxidases	40	-	fPoxDB
Transporters	1957	2419	Transporter Classification Database
Pathogen-Host Interactions	4075	-	PHI-base

In the genome of strain CSS-01s, Yan et al. (2017) reported 937 secreted, accounting for about 7.26 % of their predicted proteome size. In LA-SOL3, we have identified 677 secreted proteins, about 5.30 % of our genome deduced proteome size. This difference may be related to the different strategies applied to identify secreted proteins. Yan et al. (2017) used SignalP, for signal peptides; TMHMM, for transmembrane regions; and TargetP (Emanuelsson et al., 2000), for subcellular localization. We used the new algorithm, FunSec, that although also integrating SignalP and TMHMM, additionally uses Phobius for signal peptide and transmembrane region prediction, both WoLF PSORT and ProtComp for subcellular localization, and finally PS SCAN for endoplasmic

reticulum motif finding. Therefore, FunSec is more accurate, performing a more stringent analysis, reducing the number of false positives and thus leading to a lower number of true positives. It is also plausible that it filters out many false negative proteins.

Genes encoding for hydrolases (Table 6.2) are the most common genes coding for secreted proteins on the genome of LA-SOL3. These secreted enzymes are known, not only to contribute to the nutrition of the fungus, but also to participate in cell wall degradation, and in plant-pathogen interactions as virulence factors (Chandrasekaran et al., 2016). The 44 phospholipases present in the genome of LA-SOL3 can play a role in plant cell wall degradation, hydrolyzing membrane phospholipids and leading to cell wall disruption (Ghannoum, 2000). Regarding CAZymes analysis, the most representative groups in the genome of *L. theobromae* strain LA-SOL3 are glycoside-hydrolases (GH), carbohydrate-esterases (CE) and carbohydrate-binding modules (CBM). CAZymes are responsible for the breakdown, biosynthesis/modification of glycoconjugates and of oligo- and polysaccharides (Lyu et al., 2015). Glycoside-hydrolases and carbohydrate-esterases are often known as cell wall degrading enzymes, since they play a central role in plant cell wall degradation (Lyu et al., 2015).

The superfamily of monooxygenases cytochromes P450 is also represented in the genome of *L. theobromae* with 43 genes. These enzymes are usually implicated in pathogenic fungi defense against antimicrobial substances produced by the hosts, leading to the production of mycotoxins, as aflatoxins, and gibberellins (Črešnar et al., 2011). These enzymes have the ability to modify these chemicals, facilitating fungal adaptation to different niches (Nierman et al., 2005). This may help to understand the large capacity of *L. theobromae* to adapt to different environments and its wide host range. All of the functions identified in the genome were also identified in the transcriptome and proteome. Specifically, the family of cytochrome P51 is widely distributed in all biological kingdoms. It is known to play a housekeeping role in fungi, in sterol biosynthesis, and has been considered a good antifungal target to control fungal diseases in crops and humans, inhibiting the synthesis of ergosterol (Chen et al., 2014). It was expected that genes and proteins of this family were identified, but although several genes and proteins related with sterol synthesis were identified, none of them belongs to the family of cytochrome P51.

Both transcriptomics and proteomics data revealed a high investment of the fungus in primary metabolism (Figures 6.2, 6.4 and 6.5). At 25 °C (Figure 6.4), the number of extracellular proteins involved in plant cell wall degradation (18.4 %) and pathogenesis (25.6 %) also stood out, while at 37 °C the percentage involved in pathogenesis decreased (proteins relevant for pathogenesis are described in Tables S6.9 and S6.10). However, transcriptomic data revealed an increase of gene

expression involved in pathogenesis. Previous studies showed that different strains of *L. theobromae* are cytotoxic to mammalian cells not only at 25 °C but also at 37 °C (Félix et al., 2016; Félix et al., 2018) and also phytotoxic to tomato plants (Félix et al., 2018). Previous results - *in vitro* assays in mammalian cells and in tomato cuttings - suggest that LA-SOL3 has the ability to be pathogenic at 37 °C. The absence of proteins involved in pathogenesis in the secretome could be related with the low number of proteins identified.

We observed that in the secretome at 37 °C there is an increase of the proteins related to cell wall organization (30 %). When grown at 25 °C, the optimum growth temperature of *L. theobromae* (Félix et al., 2016), the energy of the fungus was invested in proliferation, expressing cell wall degrading enzymes (CWDEs) and other virulence factors that can be used to penetrate and invade the host tissues (Félix et al., 2016). However, in stress conditions (37 °C), the energy is directed to guarantee the survival of the organism, and the maintenance of the cell wall integrity is crucial for that.

Specific groups of proteins with relevant functions for pathogenicity were identified in the transcriptome and proteome of LA-SOL3, particularly proteins involved in production of siderophores, toxins, allergens, mitogen-activated protein kinases (MAPKs), heat shock proteins, nudix effectors and proteins involved in the velvet complex (Table 6.8).

Table 6.8 | Functions identified in the transcriptome and proteome of strain LA-SOL3. Transcripts and proteins involved in the synthesis of relevant compounds for pathogenicity.

	Function	Contribution to pathogenicity	Reference
Siderophores	Iron-chelating ligands.	Intracellular iron storage	Renshaw et al., 2002
	Iron transport Compounds.	Suppress the growth of other microorganisms.	
Toxins	Polyketides that include a range of compounds as mycotoxins and spore pigments.	Toxic to plants and/or animals. Mode of action extremely variable, depending on the produced compound.	Gaffoor et al., 2005 Chauhan et al., 2016
	Sensitization with extraneous allergens. Fungal allergens are usually proteins, polysaccharides, or glycoproteins.	IgE-mediated hypersensitivity in humans. The major allergic manifestations are asthma, rhinitis, allergic bronchopulmonary	Fukutomi and Taniguchi, 2015

		mycoses, hypersensitivity pneumonitis.	
MAPKs	Mitogen-activated protein kinases that function as key signal transduction components.	Fungal MAPKs help to promote the penetration of host tissues governing appressorium formation and virulence.	Hamel et al., 2012 He et al., 2017
HSP	Involved in several common biological activities, such as transcription, translation, protein folding, and aggregation and disaggregation of proteins.	Involved in stress response. Different families of HSP are expressed depending on stress type, <i>e.g.</i> : pH, heat, cold or osmotic stress.	Tiwari et al., 2015
Nudix effectors	Sense and modulate levels of their substrates like nucleotide sugars, deoxyribonucleoside triphosphate and capped mRNAs to maintain proper cellular processes and physiological homeostasis.	Manipulation of host defense systems.	Dong and Wang, 2016
Velvet complex	Regulates fungal development and secondary metabolism.	Promotion of chromatin accessibility and expression of biosynthetic gene clusters involved pathogenicity as mycotoxins, pigments and hormones.	López-Berges et al., 2013 Niehaus et al., 2018

From those groups of proteins relevant for pathogenesis (Table 6.8), we highlight the presence of proteins involved in toxins' synthesis and of mitogen-activated protein kinases (MAPKs) that are more abundant in the cellular proteome of LA-SOL3 grown at 25 °C than at 37 °C, supporting the hypothesis that the fungus spends the energy in distinct functions, depending on temperature. MAPKs are associated with the regulation of specific responses in eukaryotic organisms to environmental alterations and to the presence of other organisms (Leng and Zhong, 2015). In the case of filamentous plant pathogenic fungi, MAPK pathways are known to be required not only for fungal growth but also for full virulence inside the host (Hamel et al. 2012; Leng and Zhong, 2015; He et al., 2017). The diverse functions of these kinases are well explored for the model organism of

fungi, *Saccharomyces cerevisiae*, where the pheromone response pathway, the high osmolarity glycerol pathway and the regulation of cell wall integrity pathway are well characterized (Zhao et al., 2007; Leng and Zhong et al., 2015). The pheromone response pathway is responsible for the regulation of the mating process by the *STE11-STE7-FUS3/KSS1* cascade. Among these genes, *STE11* is also involved in the osmolarity pathway, participating in filamentous growth of fungi in hyperosmotic conditions.

The MAPK pathway of *S. cerevisiae* that regulates the cell wall integrity is the *PKC1-SLT2* pathway that also promotes the cell wall biosynthesis (Zhao et al., 2007; Leng and Zhong et al., 2015). In *Magnaporthe grisea*, the *PMK1* (ortholog of *FUS3/KSS1*) is required for appressoria formation and infectious hyphae (Xu and Hamer, 1996; Leng and Zhong et al., 2015) and *OSM1* (orthologue of *HOG1*) essential for fungus survival under osmotic stress. The cell wall integrity and appressoria penetration in *M. grisea* is assisted by *MPS1* (orthologue of *STL2*) (Xu and Hamer, 1996; Dixon et al., 1999; Leng and Zhong et al., 2015).

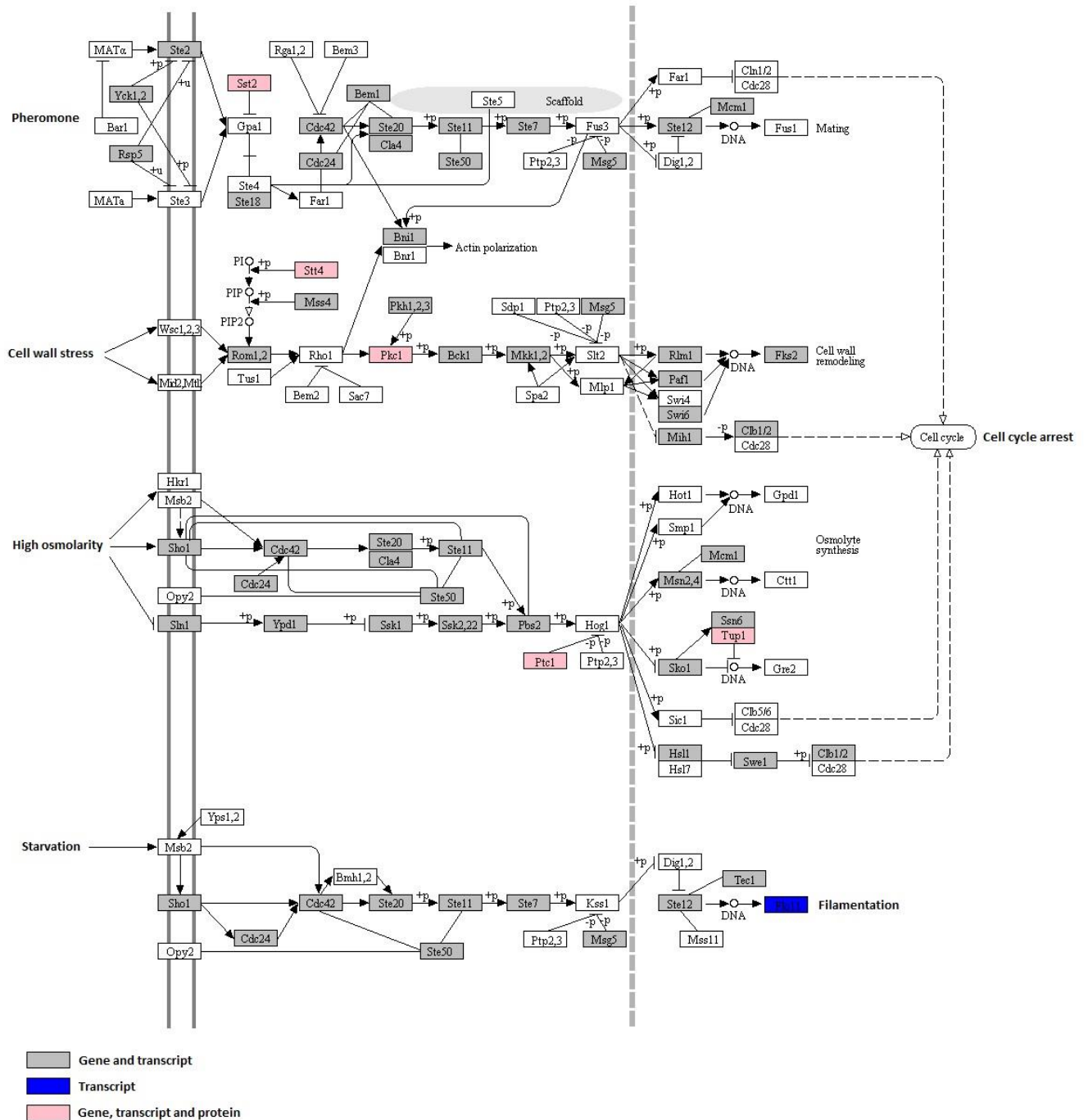


Figure 6.6 | Pathway map assigned for MAPKs signaling. Omics data obtained for LA-SOL3 are highlighted in pink (gene, transcript and protein levels), grey (gene and transcript levels) and blue (transcript level). This figure was adapted from KEGG software against a reference pathway.

In the present study, it should be highlighted the presence of the crucial genes for the cascades of phormone pathway identified for *S. cerevisiae* (*STE11-STE7-FUS3*) (Figure 6.6) and *M. grisea* (*PMK1*), as well as the genes involved in protection against high osmolarity for *S. cerevisiae* (*STE11-*

HOG1) (Figure 6.6) and *M. grisea* (*OSM1*). The presence of well-represented pathways of MAPKs signaling in *L. theobromae*, known to be involved in infection of host plants by filamentous fungi and also in protection of the fungus against stress, helps to explain how this species is able to infect a wide range of plant hosts and to proliferate in different conditions.

Several HSP related to heat response, as is the case of the family clpA/clpB (P31540) and family 70 (P15705) (Chatterjee and Tatu, 2017), were also identified in the genome, transcriptome and cellular proteome of this strain (Table 6.6). The velvet complex comprises different proteins that are responsible to regulate the production of secondary metabolites. The proteins involved in the velvet complex were identified in the transcriptome and in the cellular proteome of LA-SOL3 grown at 25 °C (López-Berges et al., 2013; Niehaus et al., 2018). It is known that the deletion of one of the proteins of the complex influences the production of determined gene clusters, *e.g.*, the deletion of LaeA protein promotes the decrease of virulence agents' production in *Fusarium fujikuroi* (Niehaus et al., 2018). Among these virulence agents are the genes and proteins involved in toxin synthesis, such as the synthesis of fusaric acid and of fusarin C, both identified in the genome, transcriptome and proteome in this study, and in the production of fumonisin and gibberellin, only identified at the genome and transcriptome and at all levels, respectively.

Other specific proteins with crucial roles in pathogenesis of fungi were also identified (Table 6.9).

Table 6.9 | Proteins with direct roles in pathogenesis of fungi identified in the proteome of *L. theobromae* strain LA-SOL3.

Accession number (UniProtKB)	Description	Secretome	Cellular Proteome	Function	Reference
P14010	4-aminobutyrate aminotransferase	-	25/37 °C	Metabolization of γ -aminobutyric acid to fulfil pathogen nitrogen requirements during infection and manipulates the plant metabolism to maintain/increase the concentration of nitrogen.	Fernandes, 2015
A9MYQ4	Gamma-aminobutyraldehyde dehydrogenase	-			
Q5AK62	Virulence protein SSD1	-	37 °C	Tolerance of host immune response, allowing the colonization of human tissues by <i>Candida albicans</i> .	Gank et al., 2008
C5FBW2	Tripeptidyl-peptidase	25 °C	-	Acidification of the microenvironment in the host, facilitating the nutrition and proliferation of the pathogen.	Reichard et al., 2006
Q70J59	SED2				Félix et al., 2016
D4ALG0	LysM domain-containing protein ARB_05157	25 °C	-	Manipulation of host immune responses to support pathogen Colonization.	Kombrink and Thomma, 2013 Akcapinar et al., 2015
O74238	Protein SnodProt1	25 °C	-	Cerato-platanin known to manipulate the immune response and cause necrosis in <i>Ceratocystis fimbriata</i> . In <i>Magnaphorte oryzae</i> a homologue is required for full virulence.	Brown et al., 2011

For the proteins described on Table 6.9, the expression at mRNA level was confirmed, with the exception of the virulence protein SSD1 and the Snodprot1 protein, that were only identified at protein level. However, the mRNA-protein correlation is not linear, since it can be affected by events, such as the degradation of the mRNA/protein or even bias in experimental procedure or quantification (Ponnala et al., 2014), which can lead to differences in identification/abundance level of compounds. It is important to highlight the presence of the virulence protein SSD1 only in the

cellular proteome of LA-SOL3 grown at 37 °C (Table 6.9). This protein is typically found in human infections caused by fungi, which is particularly relevant since *L. theobromae* is known to be a human opportunist (Kindo et al., 2010; Saha et al., 2012a, 2012b; Woo et al., 2008; Summerbell et al., 2004). Félix et al. (2016) have shown that the cytotoxicity, towards animal cells, of the secretome of *L. theobromae* varied with the fungus growth temperature. At 25 °C, almost no cytotoxic effect was observed, while at 37 °C cell mortality reached around 90 %. The authors suggested that the production of compounds toxic to mammalian cells is more pronounced when the fungus is grown 37 °C.

Other identified proteins/differentially genes expressed, such as allergens, aspartic proteases or proteins involved in toxin synthesis are often associated with human infections (Tables S6.9 and S6.10). Although LA-SOL3 was isolated from a plant, our data show that it has the machinery that enables it to colonize and infect different hosts. This machinery is over-expressed when the fungus is exposed to higher temperatures.

Recent studies revealed that genes identified in the transcriptome of *L. theobromae*, in the presence of shoots of grapevine, at different temperatures (25 °C and 35 °C) were induced during the infection process (Paolinelli et al., 2016; Yan et al., 2017). High temperatures induced the expression of genes with carbohydrate-binding modules, lysine motif domain and the glycosyl hydrolase families (Yan et al., 2017) and Paolinelli and co-authors found enzymes related with plant cell wall degradation up-regulated and an alteration on the metabolism of phenolic compounds in the presence of the heat stress. Enzymes with ability to degrade salicylic acid and phenylpropanoid precursors were up-regulated, suggesting that L-tyrosine catabolism pathway could help evading the host defense response (Paolinelli-Alfonso et al., 2016). In our study, we identified (in the transcriptome and in the secretome) gene products involved in the degradation of the plant cell wall up-regulated at 37 °C and also the molecules involved in the degradation of salicylic acid at 25 °C. The presence of the host in the study of Paolinelli and co-workers and the absence in our study could be the reason for the differences found in the abundance level of such molecules.

CONCLUSIONS

The analysis of *L. theobromae* LA-SOL 3 genome confirms that it has the molecular toolkit of a typical phytopathogen. We show that temperature modulates the expression of proteins, resulting in a higher abundance of pathogenesis-related proteins and several proteins involved in cell wall degradation at 25 °C. At 37 °C, the abundance of proteins related with pathogenicity decreased but

an increase of the proteins related with cell wall organization was observed, showing that different temperatures seems to define different metabolic priorities of the organism.

On the other hand, at 37 °C, *L. theobromae* expresses proteins known to be involved in human pathogenesis, which corroborates the known toxicity of this strain towards animal cells.

Future studies involving strains isolated from different hosts as well as studies in the presence of the host are crucial to complement the data obtained until the moment and improve the knowledge about the phytopathogen *L. theobromae*.

ACKNOWLEDGMENTS

This study was supported by FEDER funding through COMPETE program and by national funding through FCT within the research project ALIEN (PTDC/AGR-PRO/2183/2014 - POCI-01-0145-FEDER-016788) and the research unit CESAM (UID/AMB/50017 - POCI-01-0145-FEDER-007638). The authors acknowledge FCT financial support to A Alves (IF/00835/2013), AC Esteves (BPD/102572/2014), C Felix (BD/97613/2013) and M Gonçalves (BD/129020/2017).

CHAPTER 7

Multi-omics analyses reveal the molecular pathogenesis toolkit of
Lasiodiplodia hormozganensis, a cross-kingdom pathogen

ABSTRACT

Lasiodiplodia theobromae is a common fungal plant pathogen in tropical and subtropical regions where it is responsible to cause disease on a variety of plant hosts. Less frequently, it has also been reported as human opportunist, causing infections with different levels of severity.

The aim of this study was to understand the effect that temperatures have on the biology of *L. theobromae* strain CBS339.90, specifically on the molecular effectors of pathogenesis. For that, an integrated approach involving the sequencing of the genome, as well as the characterization of the transcriptome and proteome of CBS339.90 at 25 °C and 37 °C was carried out.

The genome of strain CBS339.90, previously identified as *L. theobromae*, was sequenced by Illumina HiSeq. The results show that strain CBS339.90 had been misidentified and is in fact *Lasiodiplodia hormozganensis*, which represents the first report of *L. hormozganensis* as a human opportunistic pathogen.

The transcriptome of *L. hormozganensis* CBS339.90 grown at 25 °C and 37 °C was sequenced by Illumina TruSeq. The secretome and cellular proteome at both temperatures were characterized by Orbitrap LC-MS/MS.

Functional analysis of the secretome of strain CBS339.90, grown at 25 °C, revealed a high percentage of proteins involved in the primary metabolism, carbohydrate metabolism and catabolism, plant cell wall degradation and pathogenesis. At 37 °C, a decrease of proteins related with carbohydrate metabolism and catabolism and plant cell wall degradation was found and an increase on stress response and pathogenesis related proteins was observed. For the cellular proteome, at both temperatures, the proteins involved in the primary metabolism were the most represented. Several pathways involved in the regulation of different processes crucial for pathogenesis in plants and in humans were also identified, such as mitogen-activated kinases pathways, cyclic adenosine-3',5'-monophosphate/protein kinase A pathway, velvet complex pathway and calcium-calcineurin pathway. Also, specific pathogenesis related proteins were identified: a phytotoxin cerato-platanin (snodprot1 protein), the aspartic protease, aspergillopepsin, and the virulence protein SSD1 were identified in the proteome of strain CBS339.90.

Collectively, data from the genome, transcriptome and proteome revealed that *L. hormozganensis* has, not only the genetic basis necessary to penetrate and infect plants and mammals, but also expresses different virulence determinants according to the temperature of growth, which supports the ability of this fungus to behave as a cross-kingdom pathogen.

KEYWORDS: temperature, transcriptome, proteome, cellular proteome, secretome, phytopathogenicity, human opportunist

INTRODUCTION

The family Botryosphaeriaceae comprises a wide range of pathogens, endophytes and saprobes, mostly to woody plants. These fungi are widely distributed, being absent only in polar regions (Phillips et al., 2017). *Lasiodiplodia* Ellis & Everh. is typically found in tropical and subtropical regions where it is responsible to cause a vast number of diseases on a variety of plant hosts (Rodríguez-Galvez et al., 2015; Dou et al., 2017; Prasher et al., 2017). As a plant pathogen, *Lasiodiplodia* spp. has the ability to cause branch dieback, stem cankers, seed and fruit decay, gum exudation, neck rot and foliage yellowing, leading to the plant death in several cases (Lima et al., 2013; Netto et al., 2014; Coutinho et al., 2017).

Lasiodiplodia theobromae (Pat.) Griffon & Maubl. is the most common species of *Lasiodiplodia* spp. in tropical regions and it is classified as the type species of the genus (Prasher et al., 2017). Although it was considered a weak pathogen for plants in the past, it is nowadays one of the major pathogens for several plant species (Lima et al., 2013; Netto et al., 2014; Rodríguez-Galvéz et al., 2015; Coutinho et al., 2017), counting with more than 500 hosts (Rodríguez-Galvéz et al., 2015). Over the past decades, it has also been classified as human opportunist causing, generally, ocular and skin infections with different levels of severity (Summerbell et al., 2004; Kindo et al., 2010; Saha et al., 2012a, b). A human death was also reported (Woo et al., 2008).

Increased environmental temperature due to climate changes (Piñeiro et al., 2010; Galant et al., 2012), can lead to alterations on the dynamic between microbial pathogens and their hosts leading to modifications in pathogen virulence or even to the infection of new hosts (Lindner et al., 2010; Félix et al., 2016). Detrimental interactions are usually associated to a restricted number of hosts and pathogens. However, for some pathogenic microorganisms, the ability to cause infection is extended to a variety of organisms including members of different biological kingdoms (Baarlen et al., 2007). One way to achieve stepped or quantitative alterations in virulence by fungi is the horizontal gene acquisition, facilitating pathogens in gaining new functions and allowing the colonization/competitiveness in specific niches. Bacteria and plants are the donors of fungal virulence genes, being bacteria possibly a more common source than plants (Gardiner et al., 2013). These host jumps can provoke the colonization of new hosts by the pathogen, which may result in heavy losses not only in agricultural field but also in human health.

The use of omics approaches as transcriptomics and proteomics to investigate the molecular patterns of pathogenesis and its relation to temperature is an advantage, since these approaches allow the identification of unknown mechanisms underlying environmental alterations (Lemos et al., 2010, Alves et al., 2015, Félix et al., 2016).

The aim of this study was to characterize the genome, transcriptome and proteome of CBS339.90 at two different temperatures, 25 °C and 37 °C, improve the knowledge about the interaction of the fungus with plant and human hosts and understand the effect that higher temperatures could induce on its behavior.

MATERIAL AND METHODS

Fungal strain and culture conditions

In this study, we used strain CBS339.90, isolated from a phaeohyphomycotic cyst of patient from Jamaica (Westerdijk Fungal Biodiversity Institute) and previously identified as *L. theobromae*. The identification of the strain was confirmed through a phylogenetic analysis of concatenated sequences of the rDNA internal transcribed spacer region (ITS) and translation elongation factor 1-alpha gene (*tef1-α*). Briefly, sequences from CBS339.90 were aligned with sequences from several *Lasiodiplodia* species retrieved from GenBank using Clustal X v. 1.83 (Thompson et al. 1997) and a Maximum Likelihood (ML) analysis was done using MEGA7 (Kumar et al. 2016). The best fitting DNA evolution model was determined with MEGA7 and selected based on the Akaike Information Criterion. ML analysis was performed on a Neighbour-Joining starting tree and the Nearest-Neighbour-Interchange was used as the heuristic method for tree inference. Robustness of the tree was assessed using 1,000 bootstrap replicates.

The culture was maintained on Potato Dextrose Agar (PDA) medium (Merck, Germany) at 25 °C. Mycelium of a culture grown on PDB at 25 °C for 3 days was ground in liquid nitrogen and DNA was extracted according Möller et al. (1992). For protein and RNA extraction, two plugs (5 mm diameter each) from a culture with 4 days were inoculated into a 250 mL flask containing 50 mL of Potato Dextrose Broth (PDB) and incubated at 25 °C and 37 °C for 4 days. All assays were performed in triplicate. Culture supernatants were collected by gravitational filtration through filter paper and stored at -80 °C for extracellular protein extraction. Mycelia were washed with distilled water and kept at -80 °C for cellular protein extraction. For RNA extraction, the supernatants were discarded and the fresh mycelia used to grind.

Genome Sequencing and Assembly

The genome sequence of CBS339.90 was obtained from 500 ng of genomic DNA using Illumina sequencing technology by NXTGNT (Ghent University, Ghent, Belgium). The DNA was fragmented to 800 bp using Covaris S2 sonication and a sequence library was made using the NEBNext Ultra DNA Library Prep Kit (New England BioLabs, Ipswich, MA, USA). During the library preparation, a size selection was performed just before the enrichment PCR using an Invitrogen 1 % E-gel to select for fragments between 700 and 1200 bp. Nine PCR cycles were used during the enrichment PCR. The libraries were equimolarly pooled and sequenced on an Illumina MiSeq sequencer, generating ~19E+06 2x300 bp paired-end reads. Base calling and primary quality assessments were performed using Illumina's Basespace genomics cloud computing environment. Reads were trimmed based on quality scores (modified Mott trimming algorithm, threshold=0.05) and reads shorter than 100 nt were discarded. Detected adaptor sequences were also trimmed and reads mapping to the Illumina internal control phage phiX were discarded. Assembly and scaffolding were achieved with CLC Genomics Workbench 9.0.1 (<https://www.qiagenbioinformatics.com/>), *de novo* assembly module with default settings, except for the minimum contig length (2000 nt) or word length (60 nt). Optimal word size was estimated using KmerGenie28 prior to the assembly. The primary scaffolds were further refined by means of the SSPACE2 scaffolder. The gapped regions in the re-scaffolded assembly were (partially) closed using GapFiller.

Gene prediction and annotation

Before gene prediction, the genome was repeat-masked: (1) RepeatModeler (v1.0.8) (Smit and Hubley, 2015) was used to build repeated libraries for the genome, which were then filtered to exclude coding regions and simple repeats and (2) RepeatMasker (v4.0.5) (Smit et al., 2015) was used to mask repeats and transposable elements in the genomes, using the curated repeat libraries, in a hard masking fashion (transforming repeats and transposable elements in strings of 'N's).

Gene prediction was achieved with BRAKER1 (v1) with the "fungus" option. RNA-seq paired-end reads from the GEO study GSE75978 (Paolinelli-Alfonso et al., 2016) were selected (SRR2994047, SRR2994048, SRR2994053, SEE2994054, SRR2994059, SRR2994060, SRR2994062, SRR2994063) and used for mapping onto the assembled genome using HISAT2 (v2.0.5) (Kim et al., 2015) with default settings.

Gene product names were assigned based on predicted protein sequences with BLASTP against the UniProt-KB/SwissProt database (01-03-2017), with an E-value threshold of 1e-3. Other functional annotations were added with InterProScan (v5.21-60) (Mulder and Apweiler, 2007), as well as GO

terms, which were further annotated with Blast2GO (pipeline v2.5.0). Further functional analyses were carried out as described by Morales-Cruz et al. (2015).

Genome functional analyses

Secreted Proteins

Potentially secreted proteins were identified using the FunSec pipeline (v1.0) (<https://github.com/Lonewolferrir/FunSec>) that integrates several tools for features' prediction: signal peptides and transmembrane regions with SignalP v4.1 (Petersen et al., 2011), TMHMM (Sonnhammer et al., 1998) and Phobius v1.01 (Käll et al., 2004); subcellular localization with WoLF PSORT v0.2 (Horton et al., 2007) and ProtComp v9.0 (<http://www.softberry.com/berry.phtml?topic=protcompan&group=help&subgroup=proloc>) and endoplasmic reticulum motifs with PS SCAN v1.86 (http://www.hpa-bioinfotools.org.uk/cgi-bin/ps_scan/ps_scanCGI.pl).

Enzymes

Although Enzyme Commission (EC) numbers and pathway information had been provided by InterProScan analysis, the Ensemble Enzyme Prediction Pipeline (E2P2) was also used to annotate protein sequences. This ensemble-style pipeline is more thorough in that it used both single sequence (BLAST, E-value cutoff $\leq 1e-2$) and multiple sequence (Priam) models of enzymatic function.

Carbohydrate-degrading enzymes

Carbohydrate-degrading enzymes (CAZymes) were predicted with the web-based application dbCAN (HMMs 5.0) (Yin et al., 2012) with default settings, which blasts the protein sequences in a multifasta file against the CAZy database (Cantarel et al., 2009).

Fungal peroxidases

Fungal peroxidases were predicted with the web-based blast application of fPoxDB: Fungal Peroxidase Database (Choi et al., 2014), against the Whole Predicted Peroxidases database, which had been last updated on 18-04-2012, with an E-value threshold of $1e-5$.

Synthetic gene clusters

Secondary metabolites' gene clusters were predicted for the full genomes with the web-based application fungiSMASH (antiSMASH fungal version; v4) (Medema et al., 2011), with added GFF3 files to consider for gene structures and ran with default settings.

Pathogen-Host Interactions

A blast analysis was conducted against the Pathogen Host Interactions database (PHI-base) (Winnenburg et al. 2006), downloaded on 28-02-2017, against the whole proteome and the secreted protein datasets, with an e-value threshold of $1e-5$.

RNA extraction, library preparation and sequencing

The mycelium of each replicate (three replicates per condition) was ground in liquid nitrogen and total RNA was extracted using the Spectrum Plant Total RNA kit (Sigma), according to the manufacturer's instructions. Samples were incubated for 15 min with the DNase I digestion set (RNase-Free DNase Set, Qiagen). Integrity and quality analysis were carried on a 2100 Bioanalyzer RNA (Agilent Technologies). After RNA isolation and quality assessment, samples were stored at -80°C until sequencing library preparation. Illumina mRNA sequencing libraries were made from 500 ng total RNA of each sample using the QuantSeq 3' mRNA-Seq Library Prep Kit (Lexogen, Vienna, Austria) according to manufacturer's protocol. Fourteen PCR cycles were used during the enrichment PCR. The size distribution, purity (absence of free adaptors) and quantity of the resulting libraries were measured using a High Sensitivity DNA chip (Agilent Technologies, Santa Clara, CA, US). The libraries were equimolarly pooled and sequenced in an Illumina Nextseq 500 high throughput flow cell, generating single-end 75bp reads. After sequencing, the data was demultiplexed using the sample specific nucleotide barcodes. Per sample, on average $38.3 \times 10^6 \pm 2.9 \times 10^6$ reads were generated. First, these reads were trimmed using cutadapt version 1.11 to remove the "QuantSEQ FWD" adaptor sequence (Martin, 2011). The trimmed reads were mapped to the genome of CBS339.90 using the STAR aligning software version 2.5.3a (Dobin et al., 2013). The RSEM software, version v1.2.31, was used to generate count tables (Li and Dewey, 2011). Only genes with accounts per million (cpm) above 1 in at least 3 samples were retained. EdgeR software (Robinson et al., 2010) was used to normalize gene counts and identify the differentially expressed genes (DEGs) using the empirical Bayes quasi-likelihood F-test, adjusted using the Benjamin-Hochberg False Discovery Rate (FDR) correction to account for multiple comparisons.

A volcano plot and clustering analysis of transcripts from the control group (25°C) versus transcripts from the heat stressed fungus (37°C) (Figure S7.1), were carried out to assess DEGs at 37°C using the R statistical computing software. Fold Change ($\log_2 \text{FC} > 1$ or < -1) and a False Discovery Rate (FDR < 0.01) were used as statistical significance indexes.

Proteomics

Extracellular Protein Fraction

Extracellular protein preparation was based on the TCA/Acetone method (Fernandes et al. 2014). In order to discard precipitated polysaccharides, 35 mL of the extracellular medium was centrifuged (48,400 g, 1 h at 4 °C). One volume of cold TCA/Acetone [20 %/80 % (w/v)] with 0.14 % (w/v) DTT was added to the supernatant and incubated at -20 °C for 1 h. Proteins were precipitated by centrifugation (15,000 g, 20 min, 4 °C) and the supernatant was removed. The pellet was washed with 10 mL of cold acetone (twice), centrifuged (15,000 g, 15 min, 4 °C) and washed with 10 mL of cold 80 % acetone (v/v). After centrifugation (15,000 g, 15 min, 4 °C), the residual acetone was air-dried. Protein pellet were resuspended in 200 µL of lysis buffer (7 M urea, 2 M thiourea, 4 % CHAPS, 30 mM Tris-base) and stored at -80 °C.

Cellular Protein Extraction

Two plugs (5 mm each) of strain CBS339.90 were inoculated in PDB for 4 days. After, mycelia were washed with distilled water, frozen with liquid nitrogen and grinded to a fine powder in a mortar. A 15 mL tube was used to keep the powder and 10 mL of 10 mM potassium-phosphate buffer (pH 7.4) containing 0.07 % DTT and cOmplete™ protease inhibitor cocktail (Roche) was added. All the samples were sonicated [1'' sonication, 2'' pause (3 minutes of sonication in total) (Branson, Sonifier 250) (4 °C)] and then agitated (2 h, 4 °C) to help the proteins to solubilize. The homogenate was centrifuged (15,000 g, 30 min, 4 °C) and the supernatant was collected. The remaining procedure was the same used for extracellular protein extraction (section – Extracellular Protein Fraction).

Protein Quantification

Protein concentration was determined with the 2-D Quant Kit (GE Healthcare, USA), according to the manufacturer's instructions. All the samples were quantified in triplicate.

Protein separation

For both intra and extracellular proteins, 125 µg were diluted (1:1) in loading buffer [2 % (v/v) 2-mercaptoethanol, 2 % (w/v) SDS, 8 M Urea, 100 mM Tris, 100 mM Bicine and traces of Bromophenol blue] and analysed by 1D-electrophoresis (Laemmli, 1970). Lab-casted SDS-PAGE gels (20 cm, 12% w/v) ran at 2 W-2 h, 6 W-3 h. The running buffer contained 100 mM Tris, 100 mM Bicine and 0.1 % (w/v) SDS. The samples were denatured at 100 °C for 5 min prior to electrophoresis. Proteins were stained with Colloidal Coomassie G-250. After staining, gels were scanned on a GS-800 Calibrated

Densitometer (Bio-Rad). After ensuring the quality of the samples, new electrophoresis was performed to concentrate samples at the top of the separation gel (visualized as a unique band). This band was manually excised and proteins were identified by Orbitrap LC mass spectrometry.

Tryptic Digestion, Mass Spectrometry Analysis, and Protein Identification

Briefly, protein bands were destained in 200 mM ammonium bicarbonate (AB)/50 % acetonitrile for 15 min followed by 5 min in 100 % acetonitrile. Proteins were reduced by 20 mM dithiothreitol in 25 mM AB and incubated for 20 min at 55 °C. The mixture was cooled to room temperature, followed by alkylation of free thiols by 40 mM iodoacetamide in 25 mM AB in the dark, for 20 min. After that, protein bands were washed twice in 25 mM AB. Proteolytic digestion was performed adding trypsin (Promega, Madison, WI), 12.5 ng.µL⁻¹ of enzyme in 25 mM AB, and incubated at 37 °C overnight. Protein digestion was stopped by addition of trifluoroacetic acid (TFA, 1 % final concentration). Digested samples were dried in a speedvac.

A nano LC analysis was performed in a Dionex Ultimate 3000 nano UPLC (Thermo Scientific) with a C18 75 µm x 50 Acclaim Pepmap column (Thermo Scientific). Previously, peptide mixture was loaded in a 300 µm x 5 mm Acclaim Pepmap precolumn (Thermo Scientific) in 2 % acetonitrile/0.05 % TFA for 5 min at 5 µL.min⁻¹. Peptide separation was performed at 40 °C for all runs in. Mobile phase A was composed by water acidified with 0.1 % formic acid. Mobile phase B was composed by 20 % acetonitrile acidified with 0.1 % formic acid. Samples were separated at 300 nL.min⁻¹. Mobile phase B increased to 4-45 % B for 60 min; 45-90 % B for 1 min, followed by a 5 min wash at 90 % B and a 15 min re-equilibration at 4 % B. The total time of chromatography was 85 min.

Eluting peptide cations were converted to gas-phase ions by nano electrospray ionization and analyzed in a Thermo Orbitrap Fusion (Q-OT-qIT, Thermo Scientific). Mass spectrometer was operated in positive mode. Survey scans of peptide precursors from 400 to 1500 m/z were performed at 120 K resolution (at 200 m/z) with a 5 × 10⁵ ion count target. Tandem MS was performed by isolation at 1 Th with the quadrupole, CID fragmentation with normalized collision energy of 35, and rapid scan MS analysis in the ion trap. The AGC ion count target was set to 102 and the max injection time was 75 ms. Only those precursors with charge state 2–6 were sampled for MS2. The dynamic exclusion duration was set to 15 s with a 10 ppm tolerance around the selected precursor and its isotopes. Monoisotopic precursor selection was turned on. The instrument was run in top speed mode with 3 s cycles, meaning the instrument would continuously perform MS2 events until the list of non-excluded precursors diminishes to zero or 3 s, whichever is shorter.

The raw data was processed using Proteome Discoverer (version 2.1.0.81, Thermo Scientific). MS2 spectra were searched with SEQUEST engine against an in-house built database of proteins deduced from the genomic sequence. Peptides were generated from a tryptic digestion with up to one missed cleavages, carbamidomethylation of cysteines as fixed modifications, and oxidation of methionines as variable modifications. Precursor mass tolerance was 10 ppm and product ions were searched at 0 Da tolerance. Peptide spectral matches (PSM) were validated using percolator based on q-values at a 1 % false discovery rate (FDR). With Proteome Discoverer software v. 2.1 (Thermo Scientific), peptide identifications were affiliated into proteins according to the law of parsimony and filtered to 1 % FDR. The identified proteins were also filtered and considered for analysis only if present in 3 replicates and using at least 3 peptides for identification (Tables S7.1, S7.2, S7.3 and S7.4). The expression level was obtained considering the temperature of 25 °C as control ($0.5 \geq FC \geq 2$).

Siderophores production

Siderophores' production was tested according to Pérez-Miranda and his colleagues (2007) with slight modifications. Strain CBS339.90 was grown in PDA medium for 24 h at 25 °C and 37 °C. After this period the plates were overlaid with CAS medium (Chrome azurol S) and incubated at 25 °C and 37 °C, respectively, for 4 h. Production of siderophores was detected as a change of colour of the overlay from blue to orange, purple or light yellow, allowing differentiating the type of siderophore production, hydroxamate, catechol or carboxylate, respectively.

RESULTS

Fungal strain identity

Phylogenetic analysis of concatenated ITS and *tef1- α* loci showed that strain CBS339.90, originally identified as *L. theobromae*, does in fact belong to the closely related but distinct species *L. hormozganensis*. As can be seen in Figure 7.1, it groups in the same clade as strain CBS124709 which is the ex-type strain of *L. hormozganensis*.

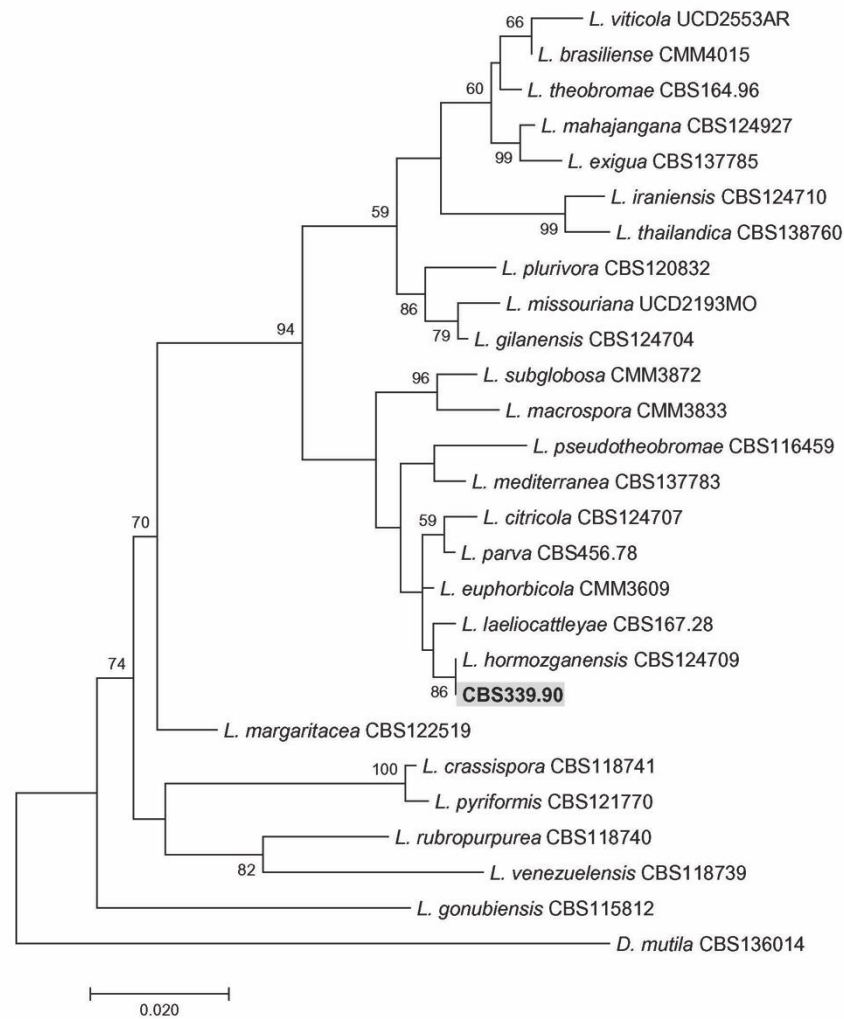


Figure 7.1 | Phylogenetic relationship of strain CBS339.90 and ex-type strains of several *Lasiodiplodia* species inferred using the Maximum Likelihood method based on the Tamura-Nei model. Bootstrap values (> 50%) are shown at the nodes. The tree is drawn to scale, with branch lengths measured in the number of substitutions per site. *Diplodia mutila* was used as outgroup to root the tree.

Genomic Analysis

Genome assembly

The genome of *L. hormozganensis* CBS339.90 was sequenced into 36.7 million matched paired-end reads by Illumina sequencing. Assembly led to a genome size of 43.2 Mb with approximately 222x coverage. The genome sequence was assembled into 356 scaffolds with a minimum size of approximately 2.2 Mb, a total of 86 gaps and 6015 N's (undetermined nucleotides), as well as a G+C content of 54.58 % (Table 1). The N50 value was approximately 291 kb. RepeatMasker analysis, coupled with RepeatModeler and RepeatProteinMask, discovered an overall repeat content of 2.26 % of the genome. Gene prediction with BRAKER identified 12,658 genes, with an average

length of 1,606 bp, thus accounting for a gene density of 293 genes per Mb and a total of 47.0 % of the genome covered by protein-coding genes. There was a mean relation of 1 mRNA per gene, with an average of 2.9 exons and 1.9 introns per mRNA, and thus per gene, similar to what was found by Yan et al. (2017) and Félix et al. (2018) for *L. theobromae*.

Table 7.1 | General statistics of the *Lasiodiplodia hormozganensis* CBS339.90 genome assembly and gene prediction.

<i>L. hormozganensis</i> CBS339.90	
Size (Mb)	43.2
Coverage	222x
% G+C content	54.58
% Repeats	2.26
Number of genes	12,658
Average gene length (bp)	1,606
% Genes	47.0
Gene density (genes/Mb)	293
mean exons per mRNA	2.9
Average exon length (bp)	507
mean introns per mRNA	1.9
Average intron length (bp)	86
mean mRNAs per gene	1

Genome functional analysis

A total of 52 secondary metabolite gene clusters were found: 9 terpenes, 16 t1pks (type 1 polyketide synthases), 11 nrps (nonribosomal peptide-synthetase), 5 t1pks-nrps and 11 “other”. From these clusters, 7 were found to have known homology to other described gene clusters (Table 7.2).

Table 7.2 | Metabolic gene clusters identified in the genome of *L. hormozganensis* CBS339.90. NRPS - nonribosomal peptide-synthetase; T1PKS - type 1 polyketide synthases. Percentage corresponds to the percentage of genes that present similarity to known gene clusters.

Type	Most similar known cluster
Terpene	PR toxin (50%)
NRPS	Aflatoxin (8%)

NRPS	Hexadecahydro-astechrome (HAS) (25%)
T1PKS	Brefeldin (20%)
T1PKS	Emericellin (50%)
T1PKS	Lasiodiplodion (71%)
T1PKS-NRPS	Fusaridone A (12%)

The genome of *L. hormozganensis* has 4,548 genes that were annotated as coding for enzymes annotated with EC numbers by the Ensemble Enzyme Prediction Pipeline (E2P2, Table 7.3). The most represented enzymes have oxidoreductase, transferase and hydrolase functions. It must be accounted that some genes were annotated with more than one function, while others were annotated as enzymes by E2P2 but with no EC numbers assigned. From these, 335 genes are predicted to code for secreted enzymes (approximately 50 % of the predicted secreted proteins). The majority of these were described as hydrolases.

Table 7.3 | Genes predicted to code for secreted enzymes by E2P2 in the genome of *L. hormozganensis* CBS339.90.

Enzyme type	Total (n)	Secreted (n)
Hydrolases	1470	236
Oxidoreductases	1213	44
Transferases	947	7
Lyases	277	30
Ligases	190	0
Isomerases	119	8
Total genes	4548	335

Lasiodiplodia hormozganensis genome encodes for 788 enzymes and carbohydrate-binding modules (CBM, Table 7.4). The largest number were annotated as glycoside hydrolases, accounting for 316 genes. From these, 271 genes code for secreted proteins were annotated as CAZymes. Most of these were glycoside hydrolases (128), while no glycoside transferases were identified.

Table 7.4 | Genes predicted to code for CAZymes in the genome of *L. hormozganensis* CBS339.90. CAZymes were predicted with the web-based application dbCAN (HMMs 5.0).

CAZyme type	Total proteome	Secreted enzymes
Glycoside Hydrolases (GH)	316	128
Carbohydrate Esterases (CE)	150	38
Auxiliary Activities (AA)	135	52
Glycoside Transferases (GT)	96	0
Carbohydrate-Binding Modules (CBM)	66	33
Polysaccharide Lyases (PL)	25	20
Total	788	271

One of the main functions of plant pathogenic fungi peroxidases is related with the degradation of the plant cell wall lignin, contributing to the penetration of the pathogen into the plant (Hammel and Cullen, 2008; Kellner et al., 2014). In the case of strain CBS339.90, 41 genes were annotated as coding for fungal peroxidases, with a total of 69 functions (Table 7.5). The number of functions is higher than the number of genes, because 13 genes were annotated with two or more peroxidase product types.

Table 7.5 | Genes predicted to code for fungal peroxidases in the genome of *L. hormozganensis* CBS339.90 using the web-based blast application of fPoxDB-Fungal Peroxidase Database, against the Whole Predicted Peroxidases database.

Peroxidase type	Genes (n)
New NoxA	6
Haloperoxidase (haem)	5
Linoleate diol synthase (PGHS like)	5
New NoxB	5
Other class II peroxidase	5
Atypical 2-Cysteine peroxiredoxin (type Q, BCP)	4
Cytochrome C peroxidase	4
Manganese peroxidase	4
New NoxC	4
1-Cysteine peroxiredoxin	3
Catalase	3
Hybrid Ascorbate-Cytochrome C peroxidase	3

Lignin peroxidase	3
Typical 2-Cysteine peroxiredoxin	3
Versatile peroxidase	3
Atypical 2-Cysteine peroxiredoxin (type II, type V)	2
Carboxymuconolactone decarboxylase (no peroxidase activity)	2
Catalase peroxidase	1
Fungi-Bacteria glutathione peroxidase	1
New Rbohs	1
NoxR	1
Prostaglandin H synthase (Cyclooxygenase)	1
DyP-type peroxidase D	0
New Doux	0
No haem, Vanadium chloroperoxidase	0

Several studies suggest that transporters play a crucial role in pathogenicity of fungi, contributing to different functions, such as the export of drugs from the cell (Yan et al., 2017) or the transport of molecules involved in appressoria formation (Ciuffeti et al., 2014). A total of 1,944 genes were annotated as coding for transporters (Table 7.6).

Table 7.6 | Genes predicted to code for transporters in the genome of *L. hormozganensis* CBS339.90, using the Transporter Classification Database.

Type	Number
Electrochemical potential-driven transporters	766
Primary active transporters	340
Incompletely characterized transport systems	323
Channels and pores	312
Accessory factors involved in transport	128
Group translocators	56
Transport electron carriers	19
Total	1,944

Heat shock proteins (HSP), known to be involved in several common biological activities, such as transcription, translation, protein folding, and aggregation and disaggregation of protein, are responsible to protect proteins from damages that can be caused by different types of biotic and

abiotic stresses (*e.g.* heat, pH, osmotic stress) (Tiwari et al., 2015). Different families of HSP known to be involved in responses to heat stress were identified in the genome of *L. hormozganensis* (Table 7.7).

Table 7.7 | Predicted heat shock proteins involved in responses to heat stress in the genome of *L. hormozganensis* CBS339.90.

Accession Code	HSP name	HSP Family
P40920	30 kDa heat shock protein	HSP 30
P31540	Heat shock protein hsp98	HSP clpA/clpB
P22943	12 kDa heat shock protein	HSP 20
Q96UX5	Heat shock protein 78, mitochondrial	HSP clpA/clpB
O14368	Heat shock protein 16	HSP 20

Pathogen-Host Interactions

In total, 4,021 genes were annotated as being proteins described in PHI-base, of which 1,848 were tested and confirmed to be responsible to be involved in pathogenicity. In Table 7.8, it is possible to find the number of genes encoding for proteins with different functions associated to host-pathogen interaction.

Table 7.8 | Genes predicted to have a role in the interaction pathogen-host in the genome of *L. hormozganensis* CBS339.90 and the respective method used for identification.

	Number (n)	Method
Total proteins	12,658	BRAKER1
Secreted proteins	698	FunSec
Enzymes	4,548	E2P2
Secreted Enzymes	335	FunSec + E2P2
CAZymes	788	dbCAN
Secreted CAZymes	271	FunSec + dbCAN
Secondary metabolism gene clusters	52	fungiSMASH
Peroxidases	41	fPoxDB
Transporters	1,944	Transporter Classification Database
Pathogen-Host Interactions	4,021 (1,848) ¹	PHI-base

¹1,848 genes were annotated with evidence of being involved in pathogenicity mechanisms.

Transcriptomic Analysis

An overview of the DEGs number and the proportion of up and down-regulated transcripts was performed and 1056 DEGs were identified, being 602 up-regulated and 454 down-regulated at 37 °C. From those, only the annotated DEGs (806 in total) were used on the functional analysis (Figure 7.2).

Genes differentially expressed at 37 °C were characterized concerning their Gene Ontology (GO) category, according to the biological process they are involved in (Table S7.5).

Regarding the expression level, it is possible to verify a different profile of transcripts species, with the DEGs related to primary metabolism (PM) and pathogenesis (P) being up-regulated and the DEGs related to amino acid metabolism and catabolism (AMC), stress response (SR), carbohydrate metabolism and catabolism (CMC), transport (T) and cell wall organization (CWO) down-regulated at 37 °C (Figure 7.2).

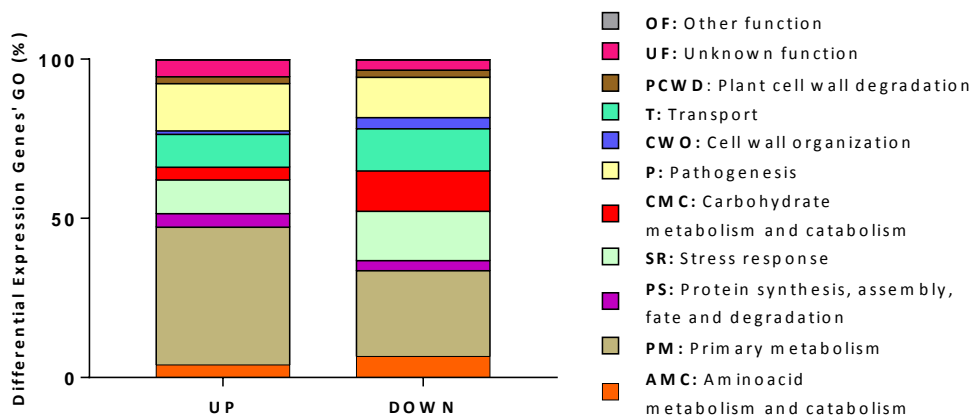


Figure 7.2 | Gene Ontology classification of the transcripts identified in strain CBS339.90: percentage of distinct species present in up and down-regulated transcripts in comparison with the fungus grown at 25 °C. The classification was obtained from biological process of each gene product according to the Uniprot database (<http://www.uniprot.org/>).

Proteomic Analysis

The secretome and cellular proteome of *L. hormozganensis* CBS339.90 were analyzed by SDS-PAGE/LC-MS/MS (Figure S7.2). Both the secretome and cellular proteome exhibited different profiles regarding fungus growth temperature.

A total of 95 proteins were identified in the secretome of *L. hormozganensis* grown at 25 °C and 59 in the secretome of *L. hormozganensis* grown at 37 °C (Figure 7.3A). From these, a total of 18 proteins were down-regulated and 2 proteins were up-regulated (Figure 7.3B, $0.5 \geq FC \geq 2$).

Regarding the cellular proteome, 636 proteins were identified at 25 °C and 482 at 37 °C (Figure 7.3A). A total of 23 proteins were found to be up-regulated and 47 down-regulated (Figure 7.3B) at 37 °C. As expected, a higher number of proteins was identified on the cellular proteome when compared with the secretome, especially at 25 °C.

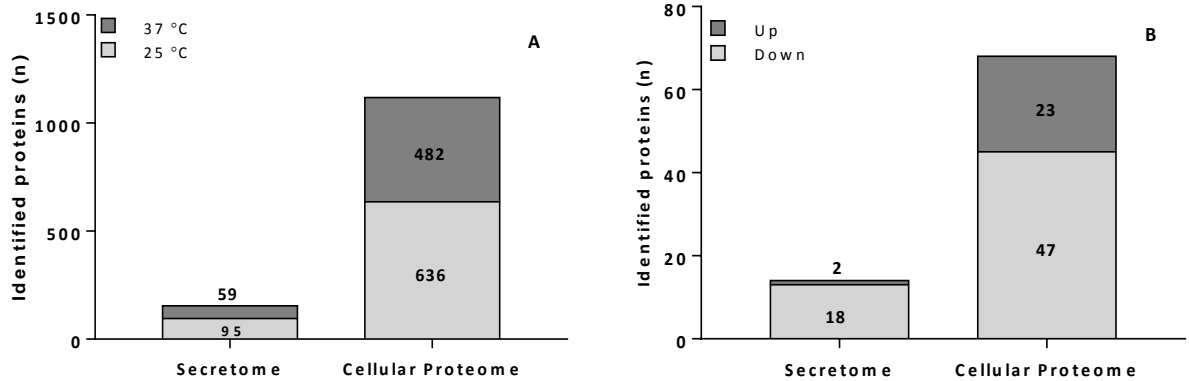


Figure 7.3 | Proteins identified in *L. hormozganensis* CBS339.90. Secretome and cellular proteome (A) and respective up and down-regulated proteins at 37 °C (B). Proteins were identified by LC-MS/MS and affiliated to proteins using Proteome Discoverer software.

The analysis of the functions of extracellular proteins was carried out using an enrichment analysis of the GO, according to their biological process (Figure 7.4). When *L. hormozganensis* grows at 25 °C, it mainly expresses proteins related with carbohydrate metabolism and catabolism (CMC), pathogenesis (P) and plant cell wall degradation (PCWD). At 37 °C, there is a decrease of proteins related with carbohydrate metabolism and catabolism and plant cell wall degradation and an increase on stress response (SR) and pathogenesis related proteins.

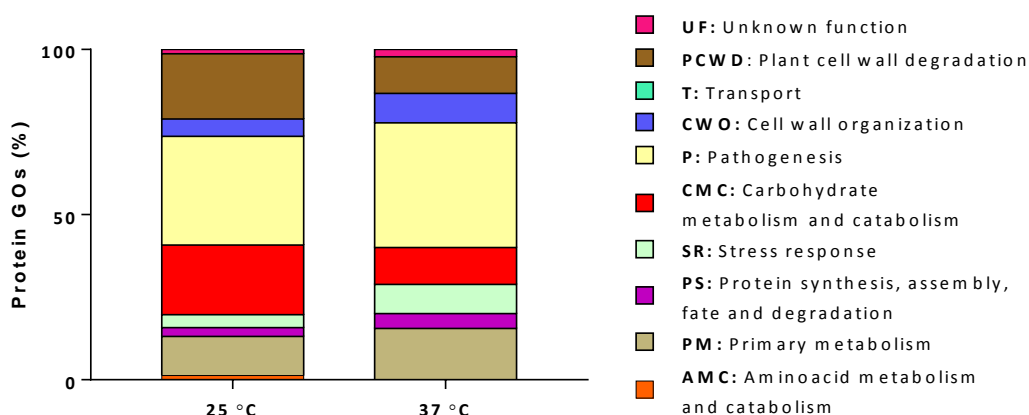


Figure 7.4 | Gene Ontology classification of the extracellular proteins identified in *L. hormozganensis* CBS339.90: percentage of distinct species present in extracellular proteins at 25 °C and 37 °C. The classification was obtained from biological process of each gene product according to Uniprot (<http://www.uniprot.org/>).

The same approach was used to analyze the cellular proteome of CBS339.90 (Figure 7.5). The cellular proteomes of *L. hormozganensis* CBS339.90 grown at 25 °C and at 37 °C are very similar. The most represented proteins are those related to primary metabolism (PM) and protein synthesis, assembly, fate and degradation (Figure 7.5).

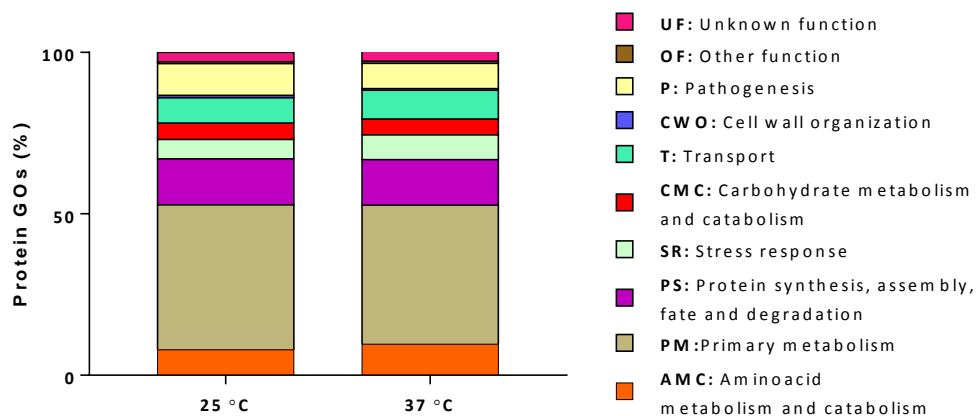


Figure 7.5 | Gene Ontology classification of the cellular proteins identified in CBS339.90: percentage of distinct species present in extracellular proteins at 25 °C and 37 °C. The classification was obtained from biological process of each gene product according to the Uniprot database (<http://www.uniprot.org/>).

Siderophores Production

The production of siderophores by *L. hormozganensis* CBS339.90 was also evaluated. Figure 7.6 shows that *L. hormozganensis* produces siderophores at 25 °C and at 37 °C. However, at 25 °C, only

a small orange halo is present near the inoculation plug, while at 37 °C, not only the orange halo is evident but also the color of the medium changed from blue to a light yellow. This suggests that different types of siderophores are being produced: at 25 °C siderophores from the type hydroxamate are being produced and at 37 °C the carboxylate type was also detected (Pérez-Miranda et al., 2007).

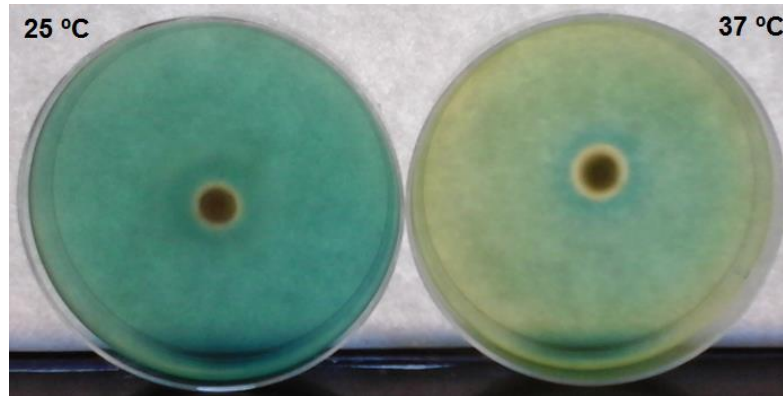


Figure 7.6 | Siderophores' production by strain CBS339.90 grown at 25 °C and 37 °C using O-CAS assay.

DISCUSSION

The genus *Lasiodiplodia* was, for a long time, an essentially monotypic genus composed of a single species *L. theobromae*. However, phylogenetic analysis of multilocus sequence data revealed that *L. theobromae* was in fact a complex of distinct cryptic species (Alves et al., 2008). Strain CBS339.90 was originally identified as *L. theobromae* (Alves et al., 2008) but here we shown that in fact it belongs to the species *L. hormozganensis* (Figure 7.1).

Lasiodiplodia hormozganensis was described for the first time in 2010 from Iran (Abdollahzadeh et al., 2010) and later from Australia (Sakalidis et al., 2011), Brazil (Marques et al., 2013; Netto et al., 2014) and Oman (UAE) (Al-Sadi et al., 2013; Al-Sadi et al., 2014) as a plant pathogen. This is the first time that *L. hormozganensis* is reported a human pathogen.

Several groups of genes relevant to pathogenesis were identified in the genome of *L. hormozganensis*. Gene clusters involved in toxin synthesis, hydrolases (1,515 genes), glycoside-hydrolases (316 genes), peroxidases (41 genes) and transporters (1,944 genes) were identified in the genome of CBS339.90, which enables *L. hormozganensis* with an immense toolbox of potential killing tools.

Carbohydrate-active enzymes are known to participate in the breakdown, biosynthesis, and modification of glycoconjugates and oligo- and polysaccharides (Lyu et al., 2015), being GH also known as cell wall degrading enzymes. These enzymes are responsible for different functions as

nutrition, cell wall degradation, and act as virulence factors in plant-pathogen interactions (Chandrasekaran et al., 2016). In plant cell wall degradation, the presence of fungal peroxidases that are involved in the degradation of the plant cell wall lignin, are a good improvement in the penetration of fungus in the plant (Hammel and Cullen, 2008; Kellner et al., 2014). The transport of molecules contributes to the development of the organism but also to pathogenicity (Yan et al., 2017). The transport of iron (Yan et al., 2017), the production of extracellular vesicles that work as virulence factors containers (Nosanchuck et al., 2008; Rodrigues et al., 2011) or the export of drugs from the cell (Yan et al., 2017) are some of the pathogenesis-related functions of transporters.

Comparing the analysis of the genome of *L. hormozganensis* with the most closely related available genomes of *L. theobromae* (Yan et al., 2017; Félix et al., 2018), the largest difference is related with the transporters identified. Although the total number of genes encoding for transporters in the genome of CBS339.90 is similar to the number found in the other genomes, their function shows a significant variability. More genes involved in channels and pores, translocators and accessories factors were identified in *L. hormozganensis*. This suggests different requirements of the two species concerning the transport of molecules between the cell and the environment.

The GO analysis of transcripts (Figure 7.2) and cellular proteins (Figure 7.5) shows that most proteins are involved in primary metabolism (Ene et al., 2014). On the contrary, the secretome (Figure 7.4) of *L. hormozganensis* exhibits a high percentage of proteins involved in pathogenesis processes, which increases when the fungus grows at 37 °C. Interestingly, opposite results were found by Félix et al. (2018) for a strain of *L. theobromae* isolated from grapevine that apparently does not express proteins directly related to pathogenesis at 37 °C. Previously, we have shown that the ability to cause toxicity to mammalian cells of *L. theobromae* (CAA019, isolated from coconut tree) and of *L. hormozganensis* CBS339.90 (previously identified as *L. theobromae*) was specific to *L. hormozganensis* CBS339.90 grown at 37 °C (Félix et al., 2016; Félix et al., 2018). The strain CAA019 only exhibited cytotoxic effect when grown at 25 °C and 30 °C for 96 h. After this period, the toxicity of the fungus decreases, suggesting that the expression of the toxic products is not continuous (Félix et al., 2016). On the contrary, *L. hormozganensis* CBS339.90 induces 90 % of cell mortality throughout growth time. This is in agreement with transcriptomics and proteomics data that show a higher expression of proteins related with plant cell wall degradation at 25 °C and a higher expression of proteins related with pathogenesis at 37 °C. The stress induced by growth at 37 °C – revealed the up-regulation of proteins related with stress response and the lower growth rate at 37 °C (Félix et al., 2016) – seems to favor pathogenesis towards animal cells.

Úrbez et al. (2011) showed that grapevines infected with *L. theobromae* developed larger lesions at 35 °C when comparing with the lower temperature tested, 30 °C (Úrbez-Torres et al., 2011). The same way, Yan et al. (2017) tested the interaction between *L. theobromae* and grapevines, concluding that the larger lesions were also found for the highest temperature tested (35 °C) and not to the lower (25 °C) (Yan et al., 2017). The data obtained from both studies, with mammalian cells and plants, suggest a molecular adaptation of *Lasiodiplodia* to higher temperatures and the trigger of specific molecules at each temperature. However, it should be highlighted that *in vitro* testing by Úrbez-Torres et al. (2011) and by Yan et al. (2017) exclude the mechanical barriers imposed by host penetration (since a mechanical opening was made in order to inoculate the fungus), which may be the cause to find a higher percentage of proteins related with PCWD at 25 °C.

A model based on transcriptomic data of *L. theobromae* (Paolinelli et al., 2016) suggests that in the presence of host (grapevine) the fungus has the ability to degrade salicylic acid and phenylpropanoid pathway precursors, produced by the host for protection, using the products as carbon sources. *Lasiodiplodia hormozganensis* also expresses the molecules involved in salicylic acid degradation. To overcome the first barrier, the same molecules identified by Paolinelli et al. (2016) involved in pectin degradation were identified in *L. hormozganensis* (xylosidase glycoside hydrolases and pectate lyases), contributing to the successful penetration of the fungus inside the host. Then, enzymes involved in the degradation of tyrosine/phenylalanine pathway (phenylpropanoid precursors) and of salicylic acid, produced by the plant host as defense mechanisms, were identified by Paolinelli et al. (2016) and in the present study: 4-hydroxyphenylpyruvate dioxygenase and fumarylacetoacetate hydrolase (degradation of tyrosine/phenylalanine), and salicylate hydroxylase and intradiol-ring-cleavage dioxygenases (degradation of salicylic acid) (Figure 7.7).

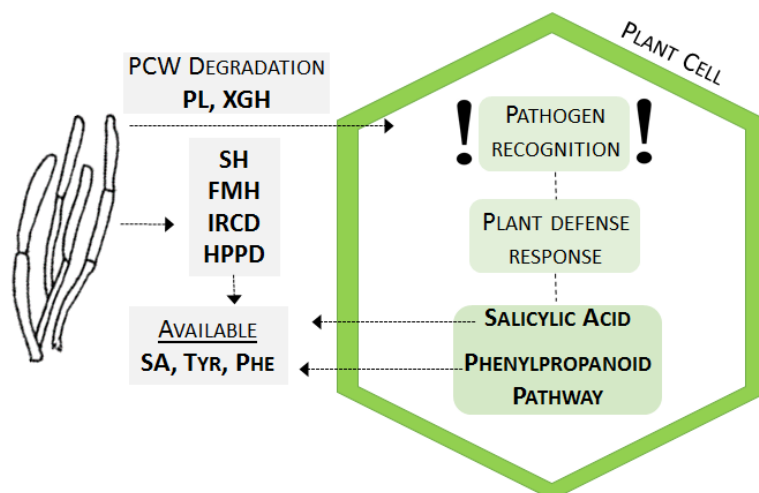


Figure 7.7 | Pathway of salicylic acid degradation by the fungus proposed by Paolinelli et al. (2016) for *L. theobromae* and identified in *L. hormozganensis* CBS339.90 (adapted from Paolinelli et al., 2016). PCW: plant cell wall; PL: pectate lyase, XGH: xylosidase glycoside hydrolase; SH: salicylate hydroxylase; FMH: fumarylacetoacetate hydrolase; IRCD: intradiol-ring cleavage dioxygenase; HPPD: 4-hydroxyphenylpyruvate dioxygenase; SA: salicylic acid; Tyr: tyrosine; Phe: phenylalanine.

However, in our work, no host tissue was used to study the salicylic acid degradation by CBS339.90, suggesting that this mechanism is active even in the absence of the host. The same scenario was found for a strain of *L. theobromae* isolated from grapevine and submitted to two different temperatures (25 °C and 37 °C) in the absence of the host (Félix et al., 2018). But, since no up-regulation of enzymes that could facilitate the fungal colonization (SH, FMH, XGH) were identified in this study under heat stress, as found by Paolinelli et al. (2016), the host could be key to trigger an increased expression of these enzymes.

For fungal pathogens, a rapid and fitting response of the fungus upon host tissue recognition is crucial (Choi et al., 2015). The first steps for a successful infection is the perception of the host conditions and the ability to adapt to the differences in nutrient availability, physical conditions (e.g. pH, oxygen and temperature) and overcome the host defense responses (Choi et al., 2015). For this, several pathways involved in regulation processes are activated, particularly the mitogen activated protein kinase (MAPK) pathways and the cyclic adenosine-3',5'-monophosphate (cAMP)/protein kinase A (PKA) pathway that play a key role in adaptation to nutrient availability (Hamel et al., 2012; Choi et al., 2015; He et al., 2017). Both pathways have an extreme importance in the virulence of several species of fungi capable to infect plants and animals, as the cases of *Cryptococcus neoformans*, a human opportunist and of *Ustilago maydis*, a plant pathogenic fungus. In both species, those pathways contribute to the penetration and dissemination inside the

respective host (Hamel et al., 2012; Choi et al., 2015). Globally, the cAMP pathway is activated when nutrients are available in the environment, such as glucose or amino acids. The presence of these nutrients is perceived by cell surface G-protein coupled receptors (GPCRs). An increase of intracellular cAMP is verified, and protein kinase A (PKA) is activated, resulting in phosphorylation of downstream target proteins (Choi et al., 2015). Those proteins can be transcription factors, enzymes or structural proteins that in animal and plant pathogens are responsible to regulate different processes, causing morphological alterations and the deployment of virulence factors (Choi et al., 2015). Mitogen activated proteins kinases cascades participate as key signal transducers, using also phosphorylation to conduct the information. In eukaryotes it usually consists in three interlinked protein kinases sequentially activated (Widman et al., 1999) that results in phosphorylation of substrates downstream, promoting specific responses (Hamel et al., 2012). One of these responses is related with the penetration of the fungus inside the host, contributing to the formation of the appressorium (Hamel et al. 2012; He et al., 2017). Several proteins that belong to these pathways were identified in the transcriptome and proteome of *L. hormozganensis* at both temperatures tested, as it was also found in the transcriptome and proteome of a strain isolated from grapevine of *L. theobromae* (Félix et al., 2018).

After the successful penetration of the pathogen, it is necessary to overcome the stress originated by the new environment and the defenses of the host. Nudix proteins and effectors have been reported in different plant pathogenic organisms, suggesting that this group might be relevant for a wide range of plant pathogens (Dong and Wang, 2016). Although the biological role of these effectors is poorly understood, they seem to manipulate the host defense systems. The best well-studied Nudix effectors promote an increase of the plant susceptibility and a decrease of reactive species around the invasion sites in the oomycete *Phytophthora sojae*, and elicit a hypersensitive response, like cell death in tobacco leaves, by the fungus *Colletotrichum truncatum* (Dong and Wang, 2016). Nudix proteins are also relevant for animal and human pathogens. In *Cryptococcus neoformans*, a Nudix hydrolase gene *YSA1* contributes to the virulence of the fungus, modulating the oxidative stress response and susceptibility to drugs (Dong and Wang, 2016). *Lasiodiplodia hormozganensis* expresses several proteins related with these effectors, specifically the *YSA1* gene, both at 25 °C and 37 °C. Another gene encoding for a Nudix hydrolase (NUDT1) was up-regulated in the transcriptome and only detected as a protein at 37 °C in the cellular proteome. The recent information showing that Nudix effectors contribute to the infection process across kingdoms reveals the importance of studying these molecules in a virulence mechanism that might be shared by plant and animal pathogens (Dong and Wang, 2016).

In order to help the pathogen to overcome biotic and abiotic stresses, heat shock proteins (HSPs) are expressed and are responsible for basal biological processes, as transcription, translational and posttranslational modifications and also protein folding and their aggregation/disaggregation (Tiwari et al., 2015). Different families of HSPs have different functions and when the fungus is submitted to thermal stress, there are specific families of HSPs that are expressed: HSP10, HSP30, HSP60, HSP90 and HSP104 (Tiwari et al., 2015). In this study, a HSP (P31540) involved in the protection of proteins that were subjected to a heat stress was identified in the genome, transcriptome and proteome of *L. hormozganensis* (Table 7.7). It was also possible to identify HSP60 and HSP70 in the transcriptome and in the cellular proteome, being up-regulated at the proteome level. HSP60 is usually activated and expressed in the presence of increasing temperatures, to control the possible damages in the proteins affected by the high temperature, while HSP 70 is not only related with response to pH stress but also seems to hyperactivate animal's immune systems, facilitating the infection by *C. albicans* (Brown et al., 2010; Tiwari et al., 2015).

Other groups of transcripts/proteins are required to guarantee the regulation of fungal development and its secondary metabolism, as is the case of Velvet complex (López-Berges et al., 2013). The Velvet complex is composed by several components, modulating chromatin accessibility and gene expression (López-Berges et al., 2013). In *Fusarium oxysporum*, a plant pathogenic fungus with the ability to infect humans, the components VeA and LaeA are crucial for full virulence on a mammalian host and VeA and VelB essential for early infection on tomato plants. Alone, LaeA showed to act during late infection stages, working in the colonization of the xylem vessels and consequently on vascular wilt symptoms (López-Berges et al., 2013). For *L. hormozganensis*, three different components of this complex were identified at both temperatures tested at the transcriptome level: *velB*, *velC* and *LaeA*. Although the component VeA was not identified by any approach used in this study, a homologous gene was identified in the genome of the fungus, *vel1*. Besides all the known functions, this component was also associated to growth of the human opportunist *Aspergillus fumigatus* at 37 °C (Lind et al., 2016).

Between the secondary metabolites produced, mycotoxins are relevant for the pathogenesis of fungi (Gaffoor et al., 2005; Chauhan et al., 2016). These polyketides can act by inhibiting the growth of other microorganisms, as other groups of fungi or bacteria, or leading to the toxicity of the host, promoting damages in tissue's host (Gaffoor et al., 2005). Several genes and proteins related with toxin biosynthesis were identified in this study. However, the production of aflatoxins should be highlighted. Although the similarity of the cluster gene associated to aflatoxins is low, several up-regulated proteins participating in the synthesis of these toxins were identified in the transcriptome

and proteome of *L. hormozganensis*. This type of toxins is produced by *Aspergillus flavus* and *A. parasiticus* (Chauhan et al., 2016) that are also responsible to cause disease in corn and derivative products, peanuts, cottonseed, milo, animal feed and majority of tree nuts. For animals, the contaminated food may also be a problem (Chauhan et al., 2016).

The nutrition of the pathogen inside the host is also of extreme importance, since without a proper up-take of nutrients, the development of the fungus is not possible. It is interesting to verify the presence of several genes and proteins involved in the up-take of iron and calcium through the expression of siderophores and calcium/calcineurin signaling network, respectively. Iron is an essential nutrient for life and is required for almost microorganisms and in fungi it could be important to serve as intracellular storage in mycelia and spores (Renshaw et al., 2002). Fe (III) is the most common form of iron in aerobic environments and usually forms insoluble hydroxides and oxyhydroxides that are unavailable to microorganisms. To up-take iron, microorganisms need to solubilize Fe (III), which is usually achieved by the production of siderophores (Renshaw et al., 2002). These iron-chelating ligands are an advantage to the producer, promoting the enhancement of its growth and limiting the available iron for other microorganisms and consequently its growth (Renshaw et al., 2002). For most microorganisms, it is true that they have the capacity to produce and transport several siderophores, which is important to allow the growth in different environmental conditions. This is also true in this case, where different transporters of iron were identified in the transcriptome and proteome and the CAS assay showed the expression of different types of siderophores (Figure 7.6). Regarding pathogenicity, all of these characteristics are a huge advantage in the competition by iron with other microorganisms and also in the acquisition of the necessary iron even in adverse conditions, as inside a host (Renshaw et al., 2002).

The calcineurin pathway consists of several transporters, channels, pumps and other proteins/enzymes involved in the up-take of calcium. This pathway influences several processes, such as morphogenesis, stress response and pathogenesis in eukaryotes (Chen et al., 2010; Liu et al., 2015). Specifically, in fungal pathogens, it is used to survive and to effectively propagate within the host, contributing to cell wall integrity, growth at elevated temperatures, alkaline pH, cation homeostasis, mating, azole resistance and morphogenesis (Chen et al., 2010; Liu et al., 2015). Thus, it is an important signaling pathway not only for plant pathogenic fungi but also for human pathogenic fungi (Chen et al., 2010; Liu et al., 2015). The general pathway in fungi starts with the activation of both subunits of calcineurin, the catalytic (Cna1) and the regulatory (Cnb1). This activation is mediated by Ca²⁺-calmodulin, when there is a Ca²⁺ ion flux from the external environment or intracellular organelles. The activated form of calcineurin is responsible to remove

phosphate from the downstream transcription factor (Crz1) and binding to calcineurin-dependent response elements. The transcription of genes involved in processes such as cell wall synthesis or oxidative stress resistance are then activated (Chen et al., 2010; Shapiro et al., 2011; Liu et al., 2015). In this work, the entire pathway was identified in the transcriptome at both temperatures, resembling the pathway identified for *C. albicans* (Chen et al., 2010; Shapiro et al., 2011; Liu et al., 2015).

Other specific proteins identified should be considered relevant for pathogenesis, as is the case of the proteins involved in γ -aminobutyric acid degradation. In this work, a 4-aminobutyrate aminotransferase (P14010) was identified at 25 °C and 37 °C in the cellular proteome of the fungus. It has been suggested that the metabolization of γ -aminobutyric acid contributes to fulfil pathogen nitrogen requirements during infection and manipulate the plant metabolism to maintain the necessary concentration of nitrogen to the survival of the fungus (Fernandes, 2015). The important phytotoxin, from the family of cerato-platanins, protein SnodProt1 (O74238) was also identified in the secretome of this fungus. SnodProt1 from *Ceratocystis fimbriata* is able to manipulate the immune response of the plant and cause its necrosis. Also, a homologue is required for full virulence in *Magnaporthe oryzae* (Brown et al., 2011). The virulence protein SSD1 (Q5AK62) was also identified in the cellular proteome of CBS339.90, but only at 37 °C. This protein is known to be crucial for the pathogenesis of *C. albicans* by promoting resistance to the host immune defense, facilitating the colonization of human tissues (Gank et al., 2008). In *L. theobromae*, these proteins were already identified in the same conditions (Félix et al., 2018), suggesting that *L. hormozganensis* has several mechanisms similar to successful plant and human pathogens.

CONCLUSIONS

The conjugation of different “omics” revealed that *L. hormozganensis* CBS339.90 has the ability to adequate its behavior to changing environmental conditions, in this case the increasing temperature, in order to guarantee its survival and growth in a stringent environment. When subjected to the temperature of 25 °C, primary metabolism, metabolism of carbohydrates and plant cell wall degradation are favored. At 37 °C, there is an increase of proteins related with pathogenicity and stress response, suggesting a modulation of the fungus molecular pathways by temperature.

Several proteins important for pathogenesis in plants and humans were identified at mRNA and protein level, such as the cerato-platanin SnodProt1, at 25 °C and 37 °C, known to contribute to the

plant infection; and virulence proteins as SSD1 (expressed at 37 °C) known to participate in human infections. Also, several pathways known to contribute to pathogenesis were identified, as MAPKs, cAMP/PKA, calcium/calcineurin or degradation of salicylic acid.

Strain CBS339.90 of *L. hormozganensis* showed to be rich in several molecular mechanisms that allow it to infect organisms from different kingdoms, as plants and humans.

ACKNOWLEDGMENTS

This study was supported by FEDER funding through COMPETE program and by national funding through FCT within the research project ALIEN (PTDC/AGR-PRO/2183/2014 - POCI-01-0145-FEDER-016788) and the research unit CESAM (UID/AMB/50017 - POCI-01-0145-FEDER-007638). The authors acknowledge FCT financial support to A Alves (IF/00835/2013), AC Esteves (BPD/102572/2014), C Felix (BD/97613/2013) and M Gonçalves (BD/129020/2017).

CHAPTER 8

Proteomic study of two strains of *Lasiodiplodia theobromae*
submitted to different temperatures

ABSTRACT

The family Botryosphaeriaceae counts with pathogens with a wide range of plants hosts, several of them economically relevant. *Lasiodiplodia theobromae* (Pat.) Griffon & Maubl. is a member of this family, typically found in the tropics and subtropics, and commonly associated to vineyards and coconut palms diseases, causing serious damages in these crops. As a phytopathogen, *L. theobromae* counts with more than 500 hosts and is able to tolerate different climates, suggesting a wide adaptability to different environments. In the last decades, it has also been considered a human opportunist.

Slight changes on the environment (*e.g.* increase of temperature) may influence the dynamic between the pathogen and its hosts. Although there is no information regarding the consequences of such alterations, the impact on the interaction host-pathogen can ultimately lead to virulence changes and eventually to the infection of new hosts – which becomes of particular relevance given the current scenario of global climate changes. Several studies conducted on *L. theobromae* showed that the expression of secondary metabolites and proteins such as cell wall degrading enzymes, and other molecules involved in pathogenesis mechanisms, is modulated by temperature.

The aim of this work was to characterize the molecular patterns of pathogenesis of *L. theobromae* under thermal stress. For that, the proteome of two strains of *L. theobromae* isolated from different hosts, CAA019 – isolated from a coconut tree – and LA-SV1 – isolated from a grapevine – submitted to increasing temperatures was compared.

The results show that protein profiles are strain and temperature dependent, with more expression of pathogenesis-related proteins identified at 25 °C and proteins related to cell wall organization and stress response at 37 °C. The majority of the proteins relevant for pathogenesis is shared by both strains. Among these, are aspartic proteases, phospholipases, the snodprot1 protein and the effector protein PevD1 (secretome), as well as proteins involved in the mitogen activated protein kinases pathways, in cyclic adenosine-3',5'-monophosphate/protein kinase A pathway, nudix effectors, in mycotoxin synthesis and in melanin synthesis (in the cellular proteome). Proteins involved in jasmonic acid synthesis, a known phytotoxic and cytotoxic metabolite were identified only at 25 °C, and the SSD1 protein, known to contribute to the colonization of humans by *C. albicans*, was identified only at 37 °C.

Nonetheless, some of the proteins identified were exclusive to each strain. The extracellular LysM effector expressed by CAA019 deserves attention, due to its contribution to the manipulation of the host immune defenses. LA-SV1, expresses a protein involved in tryptacin synthesis at both temperatures. This metabolite can act as a toxin to lung cells and protect the fungus against

phagocytes, and therefore maybe involved in the pathogenesis mechanisms of LA-SV1 towards animal cells.

The results suggest that different strains of *L. theobromae* share similar pathways involved in pathogenesis, but use different adaptation pathways to increased temperature, expressing different proteins according to the growth conditions. Proteins related with pathogenesis in plants and humans were identified in both strains and temperatures, explaining the cross-kingdom pathogenesis of *L. theobromae*.

KEYWORDS: Botryosphaeriaceae, pathogenesis, secretome, cellular proteome, virulence factors, gene expression, adaptation pathways

INTRODUCTION

Species of the family Botryosphaeriaceae include relevant pathogens in a wide diversity of economically relevant woody and horticultural plant hosts (Punithalingam 1980; Slippers and Wingfield 2007; Slippers et al. 2014; Li et al., 2015).

Vineyard and coconut productivity are of extreme importance in several countries: vineyard is the most cultivated crop in the world (Úrbez-Torres and Gubler, 2009) and coconut culture has significant economic value in Brazil (Rosado et al., 2016). Diseases caused by fungal pathogens are among the primary factors that can limit the vineyard and coconut longevity and productivity.

Over the past decades, several species of the family Botryosphaeriaceae have been recognized as important pathogens of grapevine (Phillips, 2002; van Niekerk et al., 2006; Pitt et al., 2010; Úrbez-Torres, 2011). Among these, *Lasiodiplodia theobromae* (Pat.) Griffon & Maubl. is one of the species most commonly found in vineyards (Úrbez-Torres, 2011; Rodríguez-Gálvez et al., 2015). In coconut palms, stem-end rot is the major postharvest disease of coconut in Brazil and *L. theobromae* is the only species associated with this pathology.

Lasiodiplodia theobromae is usually found in tropical and subtropical regions (Alves et al., 2008; Phillips et al., 2013) and its optimal growth temperature is between 27 °C and 33 °C (D'souza and Ramesh, 2002). However, it has a large tolerance to different climates (D'souza and Ramesh, 2002), suggesting an ability to adapt to different environments. It is responsible to cause serious damages in plants, especially in crops (Rodríguez-Gálvez et al., 2015; Phillips et al., 2013), but it was also associated to human infections, being considered a human opportunist (de Hoog et al. 2000).

One of the major climate alterations is the increase of the average temperature (Galant et al., 2012; Piñeiro et al. 2010). Little is known about the consequences of these alterations, but the impact on

host-pathogen interactions could ultimately lead to virulence changes and eventually to the colonization of new hosts (Eastburn et al., 2011; Gallana et al., 2013; Lindner et al., 2010).

Some studies conducted on *L. theobromae* showed the importance of increasing temperatures for the pathogenicity of these organisms (Félix et al., 2016; Félix et al., 2018; Yan et al., 2017). The expression of several molecules involved in pathogenesis, such as cell wall degrading enzymes, inhibitory proteins, secondary metabolites, and others is modulated by temperature (Gonzalez-Fernandez and Jorrín-Novo, 2012; King et al., 2011; Félix et al., 2016; Félix et al., 2018c). Larger lesions in grapevine caused by *L. theobromae* were observed at higher temperatures (Úrbez-Torres et al., 2011; Yan et al., 2017). Also, transcriptomics and proteomics analyses at different temperatures showed that several mechanisms involved in pathogenesis (Paolinelli-Alfonso et al., 2016; Félix et al., 2018a), primary metabolism and cell wall organization are influenced by temperature (Félix et al., 2018a), showing a regulation of the fungus dependent on the environmental conditions.

The aim of this work was to understand the effect of heat stress (25 °C and 37 °C) in the molecular mechanisms related with pathogenesis, characterizing and comparing the proteome of two strains of *L. theobromae* isolated from different hosts, CAA019 – isolated from a coconut tree, and LA-SV1 – isolated from a grapevine.

MATERIALS AND METHODS

Fungal strains and culture conditions

The strains used in this study were LA-SV1, isolated from *Vitis vinifera* in Peru (Rodríguez-Gálvez et al., 2015) and CAA019, isolated from *Cocos nucifera* L. in Brazil (Alves et al., 2008). The cultures were maintained on Potato Dextrose Agar (PDA) medium (Merck, Germany). For protein and RNA extraction, two plugs with 5 mm diameter, from a culture with 4 days, were inoculated into a 250 mL flask containing 50 mL of Potato Dextrose Broth (PDB) and incubated at 25 °C or at 37 °C for 4 days. All assays were performed in triplicate. Culture supernatants were collected by gravitational filtration through filter paper and stored at -80 °C for extracellular protein extraction. Mycelia were washed with distilled water and kept at -80 °C for cellular protein extraction, and for RNA extraction were washed and immediately used.

Radial Growth

Fungal growth was evaluated based on the development of the mycelium in PDA. The plates were inoculated with a 5 mm-diameter agar plug from an actively growing fungal culture in PDA at 1 cm

from the border of the plate and incubated at 5 °C, 15 °C, 20 °C, 25 °C, 30 °C, 35 °C, 37 °C or 40 °C. After 96 h, the colony radius was measured. Assays were carried out in triplicate and data is presented as mean \pm standard deviation.

RNA extraction and cDNA synthesis

Mycelium from each condition (3 biological replicates) was crushed in liquid nitrogen and total RNA was extracted using the Spectrum Plant Total RNA kit (Sigma), according to the manufacturer's instructions. Samples were incubated for 15 min with the DNase I digestion set (RNase-Free DNase Set, Qiagen). RNA integrity and quality analysis was carried out on a 2100 Bioanalyzer RNA (Agilent Technologies). After RNA isolation and quality assessment, samples were stored at -80 °C. cDNA was synthesized using the Nzy First-Strand cDNA Synthesis Kit (Nzytech), according to the manufacturer's instructions.

Extracellular Protein Extraction

A TCA/Acetone method was used in protein extraction according to Fernandes et al. 2014. The resuspension of the protein pellet was made with 200 μ L of lysis buffer (7 M urea, 2 M thiourea, 4 % CHAPS, 30 mM Tris-base) and stored at -80 °C in aliquots of 30 μ L.

Cellular Protein Extraction

Two plugs (5 mm) of each strain were inoculated in PDB medium during 4 days at 25 °C and 37 °C. Cellular protein extraction was performed according to Félix et al., 2018a.

Protein Quantification

Protein concentration was determined using the 2-D Quant Kit (GE Healthcare, USA), according to the manufacturer's instructions. All the samples were quantified in triplicate.

Protein separation by electrophoresis

For all the samples in test, 125 μ g of sample were diluted (1:1) in loading buffer [2 % (v/v) 2-mercaptoethanol, 2 % (w/v) SDS, 8 M Urea, 100 mM Tris, 100 mM Bicine and traces of Bromophenol blue] and analyzed by electrophoresis (Laemmli, 1970). The analysis by SDS-PAGE was as described earlier Félix et al., 2018a.

Tryptic Digestion, Mass Spectrometry Analysis, and Protein Identification

All the procedure was performed according to Félix and co-authors (Félix et al., 2018a).

MS2 spectra were searched with SEQUEST engine against an in-house built database of proteins deduced from the genomic sequence (Félix et al., 2018a). The identified extracellular and cellular proteins of both strains were also filtered and considered for analysis only if present in 3 replicates and using at least 3 peptides for identification (Tables S8.1 – S8.8). The expression level was obtained considering the temperature of 25 °C as control ($0.5 \geq FC \geq 2$).

Primer design for target genes used for qPCR

Using proteomic data of CAA019 and LA-SV1 strains of *L. theobromae*, 4 target genes were selected according to their pattern of expression and functional annotation (Table 8.1). The sequence of the reference gene primers used was obtained from the work of Paolinelli and co-authors (2016) and the sequences of the target genes were used to design specific primers.

Table 8.1 | Reference and target genes and respective primers.

Protein Name	Gene	Expression Strain/condition	Primer Sequence (5'-3')	Amplicon length (bp)	Reference
Elongation Factor	<i>EF1α</i>	Reference gene	FW TCGTCTGGGTTCCGGCAAAAT RV CGCGTTAGCCATTGCTCGTA	126	Paolinelli et al., 2016
Low-redox potential peroxidase	<i>LnP</i>	LA-SV1, secretome	FW CCATCATCCTCGCCAAGG RV GGATGGAATGTCGTTGTCG	203	Present study
Endo-1,4-beta-xylanase B	<i>xlnB</i>	CAA019, secretome	FW CGTCACCTACACCAACGG RV CGATCAGAGGGCTGGTGG	185	Present study
Virulence protein SSD1	<i>SSD1</i>	CAA019, cellular proteome	FW CCTGCACATTGCGCATCG RV GCCCATGTTGACATACTGC	214	Present study
Peroxiredoxin TSA1-A	<i>TSA1</i>	LA-SV1, cellular proteome	FW CGACTTCAAGGTCACCGC RV CGAGCAGGCTGTACTCGG	221	Present study

Protein validation by Quantitative PCR (qPCR)

All reactions were performed in a CFX96 Real-Time thermocycler (BioRad) using the NzySpeedy qPCR Green Master Mix (2x) (Nzytech). For each reaction, 5 μ L of the Master Mix, 0.5 μ L of each primer (10 μ M, forward and reverse), 4.2 μ L of nuclease-free water and 0.5 μ L of template cDNA (0.1-0.5 μ g) was used. The PCR program used was: 95 °C - 3 min, 40 cycles of 95 °C - 15 s and 60 °C - 30 s. After this step the fluorescence was read and, at the end of the program, the temperature suffered an increase from 65 °C to 95 °C at a rate ramp of 0.1 °C/s, allowing the melting curves evaluation. Cq values were calculated by the threshold method with BIO-RAD CFX Manager software and used to compare the expression between reference and target genes.

RESULTS

The radial growth of the strains CAA019 and LA-SV1 of *L. theobromae* was evaluated at 8 different temperatures, ranging from 5 °C to 40 °C (Figure 8.1). Both strains were unable to grow at 5 and at 40 °C and showed maximum radial growth between 25 °C and 30 °C on PDA (considered the best growth temperatures for these strains from this point forward).

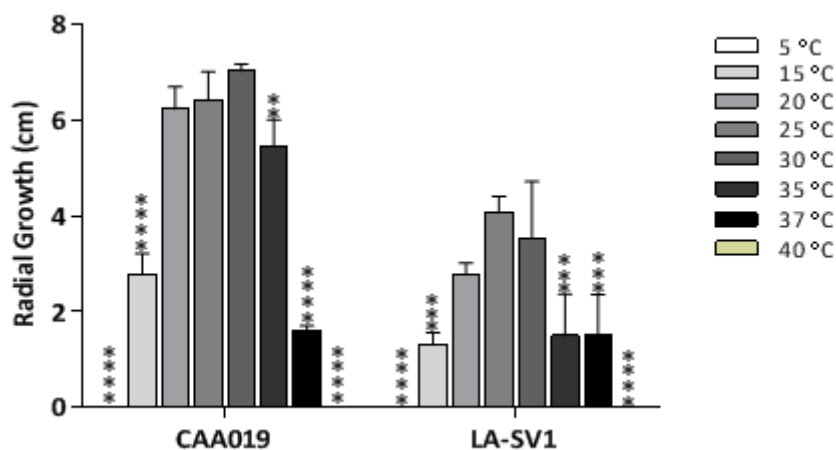


Figure 8.1 | Radial growth of the strains CAA019 and LA-SV1 in PDA medium after 96 h of incubation at 8 different temperatures. Data is presented as average \pm standard error. A two-way ANOVA (**** $p < 0.0001$, *** $p < 0.001$, ** $p < 0.01$, * $p < 0.05$) followed by a Sydak's post-test, was used to determine the statistical significance between the temperature of 30 °C and the other temperatures for each strain.

The secretome and cellular proteome of the strains CAA019 and LA-SV1 under heat stress (grown at 37 °C) was analyzed by SDS-PAGE/LC-MS/MS and compared to those grown at 25 °C (control temperature) (Figure S8.1). The growth temperature influenced protein profiles, mostly in the cellular proteome, where the profiles between temperatures and strains from different hosts seems to be more variable.

A total of 205 proteins were identified on the secretome of strain CAA019 grown at 25 °C and 159 proteins on the secretome of strain CAA019 grown at 37 °C. Regarding the cellular proteome, a higher number of proteins were identified: 508 proteins at 25 °C and 368 at 37 °C (Figure 8.2A). For strain LA-SV1, 89 proteins were identified in the secretome of the fungus grown at 25 °C and 76 in the secretome at 37 °C. A higher number of proteins was identified in the cellular proteome of LA-SV1 strain: at 25 °C, 778 proteins were identified and at 37 °C a total of 994 proteins were found (Figure 8.2B). Strain CAA019 expresses more proteins at 25 °C than at 37 °C, in both fractions.

Contrarily, strain LA-SV1 expresses a similar number of secreted proteins at both temperatures and a higher number at 37 °C in the cellular proteome.

The expression level of the proteins was evaluated through the fold change (FC) ($0.5 \geq FC \geq 2$) (Figure 8.2B/D). For strain CAA019, 35 proteins are down-regulated and 15 up-regulated in the secretome. In the cellular proteome of this fungus, 64 proteins were down-regulated and only 5 proteins up-regulated (Figure 8.2B). Contrary to strain CAA019, strain LA-SV1 presented more up-regulated proteins than down-regulated proteins, counting with 19 up-regulated proteins in the secretome and 169 in the cellular proteome, and only 4 proteins down-regulated in the secretome and 31 in the cellular proteome (Figure 8.2D).

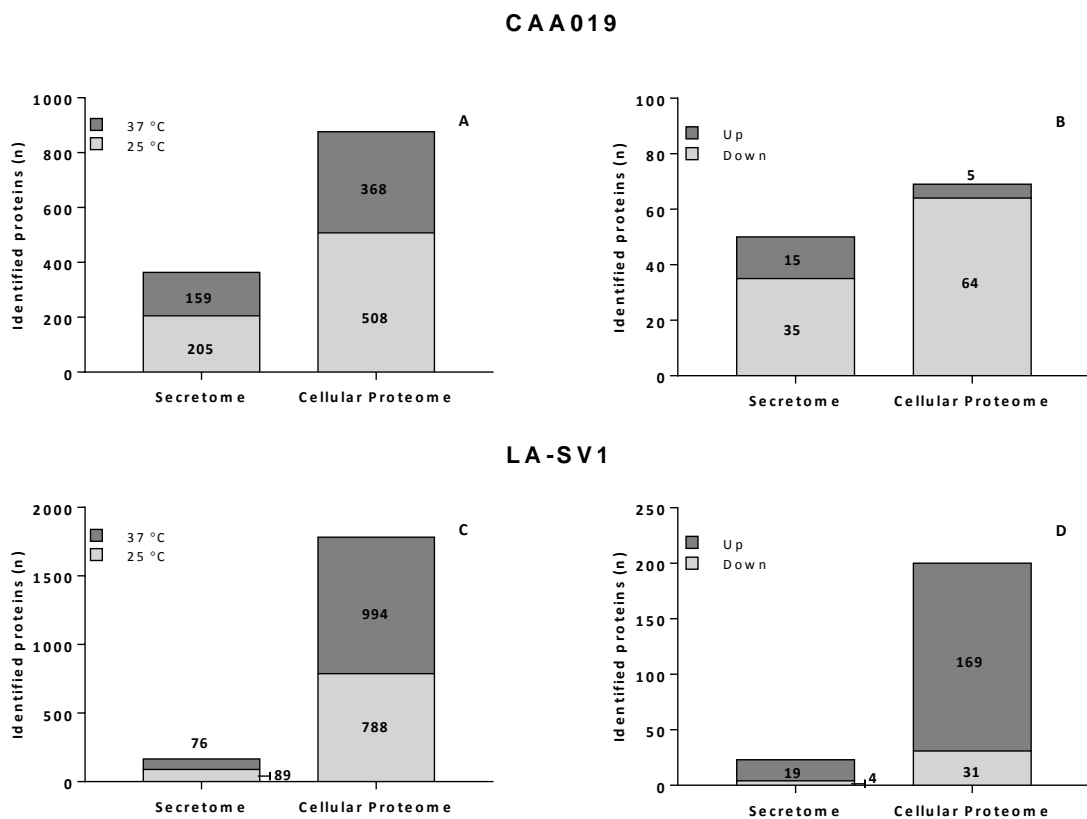


Figure 8.2 | Proteins identified in the secretome and in the cellular proteome of strains CAA019 (A) and LA-SV1 (C). Up and down-regulated proteins in the secretome and in the cellular proteome of strains CAA019 (B) and LA-SV1 (D).

Proteins from the secretome and cellular proteome from both strains grown at 25 °C and 37 °C were characterized concerning their function (Tables S8.9-S8.12). When strain CAA019 is grown at 37 °C, there is an increase of extracellular proteins related with cell wall organization (CWO), primary metabolism (PM) and stress response (SR), while the proteins directly related to

pathogenesis (P), plant cell wall degradation (PCWD) and carbohydrate metabolism and catabolism (CMC) decrease (Figure 8.3A). The secretome of LA-SV1 is less affected by temperature than the secretome of CAA019 (Figure 8.3B). It should be highlighted the presence of more proteins related to pathogenesis in the strain isolated from grapevine, LA-SV1 (33.8 % of proteins identified at 25 °C and 29.0 % identified at 37 °C) than in the strain isolated from the coconut tree, CAA019, (26.6 % of proteins involved in pathogenesis identified at 25 °C and 23.0 % at 37 °C).

Regarding the cellular proteome of strain CAA019, the main alterations verified is an increase of the proteins related to primary metabolism (PM) and stress response (SR) at 37 °C and a decrease of proteins involved in transport (T) and carbohydrate metabolism and catabolism (CMC) (Figure 8.3C). In the case of strain LA-SV1, similar profiles at both temperatures were obtained (Figure 8.3D).

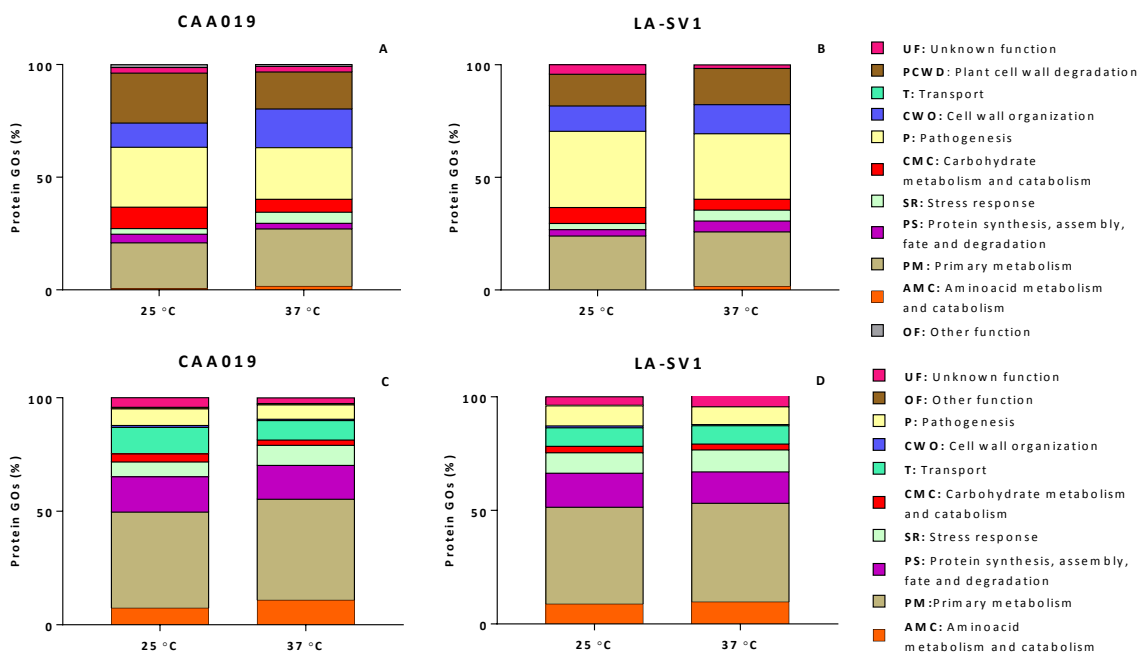


Figure 8.3 | Gene Ontology classification of the extracellular and cellular proteins identified in *L. theobromae* strains CAA019 and LA-SV1: percentage of distinct species present in extracellular (A/B) and cellular proteins at 25 °C and 37 °C (C/D). The classification was obtained from the GO (biological process) of each protein according to the Uniprot database (<http://www.uniprot.org/>).

The secretome of the two strains, grown at both temperatures includes 43 common proteins (Figure 8.4A): forty-one (41) proteins are specific of strain CAA019 and only 3 of strain LA-SV1.

Regarding the cellular proteome, 158 proteins were identified in all conditions, whereas 11 proteins were found to be specific of CAA019 and 201 specific of LA-SV1 (Figure 8.4B).

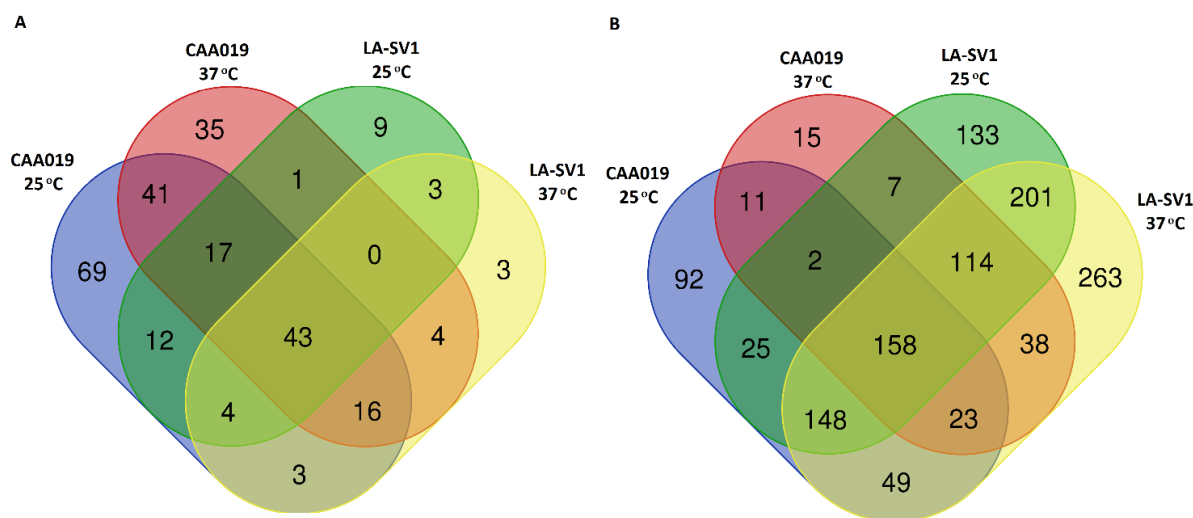


Figure 8.4 | Venn diagrams showing the common and specific proteins between the strains of *L. theobromae* CAA019 and LA-SV1 grown at 25 °C and 37 °C - secretome (A) and cellular proteome (B).

Two proteins identified in each strain (one from the secretome and other from cellular proteome) with different expression levels were selected for further analysis by real-time PCR (Figure 8.5). The endo-1,4- β -xylanase B (P48824) identified in the secretome and the virulence protein SSD1 (Q5AK62) identified in the cellular proteome of strain CAA019 were selected due to their relevance to pathogenesis and exclusive identification at 37 °C (Figure 8.5A). The expression of the low-redox potential peroxidase (C0IW58) - identified in the secretome at 37 °C - and the expression of the peroxiredoxin TSA1-A (Q9Y7F0) - up-regulated at 37 °C in the cellular proteome of strain LA-SV1 were also analyzed (Figure 8.5B). Gene expression was detected at 25 °C and 37 °C, for all genes, with higher expression at 37 °C for the virulence protein SSD1 (Q5AK62) and for the peroxiredoxin TSA1-A (Q9Y7F0). The expression of endo-1,4- β -xylanase B (P48824) and low-redox potential peroxidase (C0IW58) was higher at 25 °C, contrary to the results obtained by proteomics.

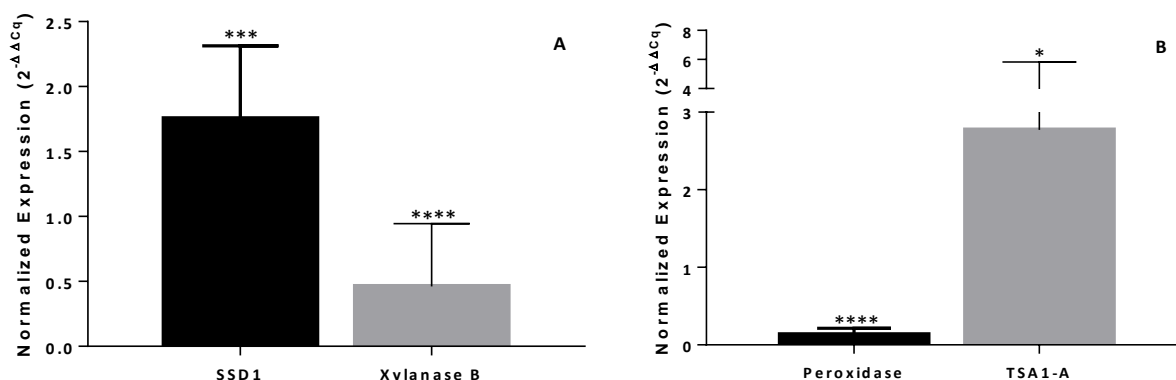


Figure 8.5 | Target genes encode: a virulence protein SSD1 (Q5AK62) and an endo-1,4- β -xylanase B (P48824) in strain CAA019 (A) and a low-redox potential peroxidase (COIW58) and a peroxiredoxin TSA1-A (Q9Y7F0) in strain LA-SV1 (B). A t-test was conducted using the ΔCq value of each gene at two conditions tested, 25 °C and 37 °C, using the temperature of 25 °C as control (* $p < 0.05$, ** $p < 0.01$, *** $p < 0.001$, **** $p < 0.0001$).

DISCUSSION

Functional analysis of proteins expressed by strain CAA019 shows that there is an increase of extracellular proteins related with cell wall organization (CWO), primary metabolism (PM) and stress response (SR) at 37 °C. Such profile suggests the need for proteins involved in the survival of the organism, such as proteins required for the maintenance of the cell wall integrity or an efficient protection against the stress generated by high temperature. The expression of proteins directly related to pathogenesis (P), plant cell wall degradation (PCWD) and carbohydrate metabolism and catabolism (CMC) decreased at 37 °C (Figure 8.3A), suggesting that phytopathogenesis is favored at 25 °C. Although common to the tropics, the optimal temperature of *L. theobromae* is 25-30°C (Félix et al., 2016) which is in accordance to the protein profile identified. The proteins identified are compatible with an effort on fungus dissemination, through the expression of plant cell wall degrading enzymes (CWDEs) and other virulence determinants that allow the penetration and invasion of the host (Félix et al., 2016; Félix et al., 2018a).

Interestingly the secretome of strain LA-SV1 seems to be more stable regarding the growth temperature when compared to the secretome of strain CAA019 (Figure 8.3B). At 37 °C, LA-SV1 seems to invest its energy in the expression of proteins related to stress response (SR) and protein synthesis, assembly, fate and degradation (PS). A higher percentage of pathogenesis-related proteins was identified in LA-SV1 for both temperatures, when compared with CAA019 strain. Previous studies had already shown that CAA019 cytotoxicity to mammalian cells is specific of the

temperatures 25 °C and 30 °C (96 h), being almost absent at 37 °C (Félix et al., 2016). Furthermore, CAA019 is more phytotoxic to tomato cuttings when grown at 25 °C than when grown at 37 °C (Félix et al., 2018c).

Some of the proteins expressed by both strains have key roles in pathogenesis processes. It is the case of *snodprot1* protein (O74238), down-regulated in CAA019 strain and up-regulated in LA-SV1. *Snodprot1* protein is a phytotoxin from the cerato-platanins family, known to manipulate the immune system of the plant and cause necrosis (Brown et al., 2012). This protein is also present in the secretome of another strain of *L. theobromae* isolated from grapevine (Félix et al., 2018a) and in a strain of the closely-related species *Lasiodiplodia hormozganensis* isolated from a human patient (Félix et al., 2018b), suggesting that the expression of this phytotoxin is common in strains of *L. theobromae* and in closely-related species. Also, phospholipases were identified (more expressed at 25 °C, in both strains), contributing for plant cell wall degradation, leading to cell disruption (Ghannoum, 2000) and helping, this way, in the penetration of the fungus inside the host. Several aspartic proteases were also identified in both strains and temperatures. Some of the aspartic proteases identified [*e.g.* *sedolisin* (Q70J59)] were up-regulated at 37 °C, in both strains. These enzymes are not only involved in physiological functions, but also play a crucial role in the pathogenesis of plants and humans, participating in the dissemination and evasion of the hosts (Duarte et al., 2016; Rawling and Bateman, 2009; Monod et al., 2002). Their presence at both temperatures and in other strains of *L. theobromae* (Félix et al., 2016; Félix et al., 2018a), could help explaining the efficient infection mechanism of this pathogen in humans.

The effector protein *pevD1* (G0Y276) was identified in all conditions, with the exception of the strain LA-SV1 grown at 37 °C. This elicitor was isolated from *Verticillium dahlia*, a fungal pathogen, and it is known to trigger a hypersensitive response in tobacco plants and cotton (Bu et al. 2014). In the other hand, it was also found in endophytic fungi, contributing to the protection of the plant. Thus, this effector protein has been studied as a possible contribution to control diseases in plant, especially in cotton (*Gossypium hirtusum*) (Bu et al., 2014). Nevertheless, the exact function of this protein in *L. theobromae* remains unclear.

LysM effectors, expressed by strain CAA019, LysM domain-containing protein ARB_05157 (D4ALG0), expressed at both temperatures and the LysM domain-containing protein ARB_00327 (D4AVW3), expressed at 25 °C, contribute to the manipulation of the host immune responses and physiology, and consequently to host colonization by fungus (Kombrink et al., 2013).

Globally, since a large percentage of proteins related with pathogenesis were identified (in both strains at both temperatures), the ability to secrete this type of proteins seems to be inherent to the species, and that the infection efficiency appears to be host- and temperature independent.

Regarding the protein validation through real-time pPCR, only two of the four selected proteins presented similar expression between mRNA and protein: virulence protein SSD1 (Q5AK62) and peroxiredoxin TSA-1 (Q9Y7F0). The expression of endo-1,4- β -xylanase B (P48824) and low-redox potential peroxidase (C0IW58) was higher at 25 °C, contrary to the results obtained by proteomics. However, it is known that transcription and translation processes don't have a linear relation (Maier et al., 2009). Different mechanisms generate several systems that enhance or repress the synthesis of proteins from a certain copy number of mRNA molecules. Also, different events may disrupt continuous transcription and translation, as alterations of conditions (Maier et al., 2009).

Both strains (Figure 8.4B) express mitogen activated protein kinases (MAPKs), as well as proteins from the cyclic adenosine-3',5'-monophosphate (cAMP)/protein kinase A (PKA) pathway. Both pathways are essential for the virulence of several phyto- and human-pathogenic fungi, as is the case of the phytopathogenic fungus *Ustilago maydis*, or of the human opportunist *Cryptococcus neoformans*. Both in *U. maydis* and *C. neoformans*, these pathways are activated in the presence of nutrients, contributing to the penetration (appressorium formation) and dissemination of fungi inside the host (Hamel et al., 2012; Choi et al., 2015). Félix and co-authors identified several proteins related to both pathways in *L. theobromae* LA-SOL3 (Félix et al., 2018a) and in *L. hormozganensis* CBS339.90 (Félix et al., 2018b). The expression of these proteins - know to contribute to the infection process of plants by several filamentous fungi and to the protection of fungi against stress conditions (He et al., 2017) - partially explain the wide range of niches that are colonized by *L. theobromae*, as well as the wide range of hosts that this species is able to infect.

Proteins related to stress response, specifically heat shock proteins (HSPs), were identified in the cellular proteome of both strains at both temperatures. These proteins help the pathogen to overcome biotic and abiotic stresses (Tiwari et al., 2015). Different families of HSPs are associated to different functions and when the fungus is submitted to thermal stress, there are specific families of HSP that are expressed: HSP10, HSP30, HSP60, HSP90 and HSP104 (Tiwari et al., 2015). We identified proteins from families HSP30, HPS60, HSP70 and HSP90. Curiously, family HSP30, involved in energy conservation during stress conditions (Tiwari et al., 2015), was only identified at 37 °C in both strains.

The production of antibiotics and mycotoxins is also of extreme importance in fungal pathogenesis and survival (Gaffoor et al., 2005; Spikes et al., 2008; Chauhan et al., 2016), inhibiting the growth of

other microorganisms or leading to the toxicity in host tissues (Gaffoor et al., 2005; Spikes et al., 2008). We identified several proteins involved in antibiotics' synthesis: bacilysin (P39640) in CAA019, granaticin (P16543) and bacilysin (P39640) in LA-SV1. Also, proteins involved in the biosynthesis of aflatoxins (in both strains) and of fusarin C and gliotoxins (in LA-SV1), were identified in the cellular proteome. The biosynthesis of gliotoxins is especially interesting. In *C. albicans*, gliotoxin has antithrombotic properties and immunosuppressive functions, contributing to the survival of the fungus in the blood stream of humans during infection (Bertling et al., 2010). In *A. fumigatus*, the contribution of gliotoxin to the infection is mostly seen in immunosuppressed hosts that maintains phagocytic cell functions. This toxin may also be an advantage in the fungi normal ecological niche, where the competition with other microorganisms is constant (Spikes et al., 2008). The functions associated to this mycotoxin, seem to favor the infection of immunocompromised organisms, which is in agreement with the fact that *L. theobromae* is a human opportunist. The degradation of γ -aminobutyric acid was proposed to be relevant for pathogenesis, fulfilling the pathogen nitrogen requirement during the infection process and manipulating the plant metabolism to maintain the necessary concentration of nitrogen available to fungus development (Fernandes et al., 2015). Both strains, at both temperatures, were able to express proteins involved in the catabolic process of γ -aminobutyric acid, as was the case of other strains of *L. theobromae* and *L. hormozganensis* (Félix et al., 2018a; Félix et al., 2018b). These results, combined with previous results, suggest that *L. theobromae* is well adapted to plants and that this mechanism could be used by the fungus to guarantee the supply of nitrogen during growth. In fact, several strains of *L. theobromae* are able to express proteins related with γ -aminobutyric acid catabolism even in stressful temperatures.

The secondary metabolite scytalone is produced by several fungi and participates as a precursor in the synthesis of dihydronaphthalene (DHN)-melanin, involved in melanin pathway. The toxicity of the oxidative products of melanin precursors can induce injuries in the hosts, contributing to the pathogenesis of the fungus (Jacobson et al., 2000). Although it was never identified in *L. theobromae*, it was already identified in the closely-related species *L. hormozganensis*, strain CBS339.90 (first identified as *L. theobromae*) (Félix et al., 2018b). Both CAA019 and LA-SV1 express a scytalone dehydratase (Q00455), known to be involved in melanin biosynthesis. Other proteins involved in this pathway were also identified: a heptaketide hydrolyase *ayg1* (Q4WZB3) and a conidial pigment polyketide synthase *alb1* (Q4WZA8). In addition, a gene involved in melanin biosynthesis and that codifies a scytalone dehydratase, *SDC1*, is present in the genome of LA-SOL3

strain of *L. theobromae*. These data suggest that, although never identified in *L. theobromae*, the pathway that leads to scytalone synthesis is present in these strains.

Among plants, animals and fungi, oxylipins (polyunsaturated fatty acids) are commonly used as communication signals to elicit biological responses (Fischer and Keller, 2016). Previous studies showed that oxylipins are related to basic fungal development, quorum sensing, mycotoxins production and to several host-pathogen interactions (Fischer and Keller, 2016). In addition, fungi also produce oxylipins to modify plant and mammalian host responses (Fischer and Keller, 2016). In plants, the expression of fungal oxylipins is crucial for niche establishment. In fact, tissue invasion by *Magnaphorte oryzae* is compromised when an oxylipin producing monooxygenase is deleted (Patkar et al., 2016). In the presence of mammalian cells, specific fungal oxylipins can be modified by the host cells, leading to the generation of potent immune system-modulating oxylipins (Fischer and Keller, 2016). Strain CAA019 produces oxylipins at 25 °C, which is in agreement with previous results that show that CAA019 is cytotoxic to mammalian cells when grown at 25 °C (Félix et al., 2016). In addition, CAA019 phytotoxicity to tomato cuttings is also higher at this temperature (Félix et al., 2018).

Nudix effectors, only detected on LA-SV1, help to overcome the stress of the new environment after the penetration of the fungus inside the host. These proteins are known to collaborate in the pathogenesis process of several plant pathogenic organisms by manipulating the host immune defenses. In *Phytophthora sojae*, these effectors promote an increase of the plant susceptibility and a decrease of reactive species around the invasion sites (Dong and Wang, 2016). The proteins involved in the velvet complex should be referred due to its importance in fungal development and secondary metabolism, promoting chromatin accessibility and expression of genes involved in mycotoxins, pigments and hormones synthesis (López-Berges et al., 2013; Niehaus et al., 2018). In LA-SV1 strain, only the subunit *LaeA* was identified at both temperatures. However, the genome *L. theobromae* LA-SOL3 has all of the subunits (*VeA*, *VelB*, *VelC* and *Lae1*). Additionally, previous studies on different strains of *L. theobromae* (Félix et al., 2018a) and of *L. hormozganensis* (Félix et al., 2018b) revealed the presence of the other subunits of the velvet complex, suggesting that, although not detected, the other subunits may be expressed by this strain. In *Fusarium oxysporum*, the *LaeA* subunit showed to be relevant during late infections stages, acting in the colonization of the xylem vessels and, therefore, on vascular wilt symptoms (López-Berges et al., 2013). Also specific to LA-SV1, proteins involved in tryptacidin synthesis were identified at both temperatures. This metabolite was originally identified in *Aspergillus fumigatus* and was shown to be active against protozoa (Balan et al., 1964) and to be a potent toxin to lung cells (Gauthier et al., 2012). A

recent study suggested that this metabolite could have a protective function against phagocytes not only in the environment but also during the infection process (Mattern et al., 2015).

Temperature specific proteins were also identified in both strains. From those, proteins related with jasmonic acid synthesis in both strains, grown at 25 °C. This metabolite is a phytotoxin (Husain et al., 1993) and recently, its production by pathogenic fungi showed to lead to the inhibition of the defense pathway of plants, facilitating the infection process (Tsukada et al., 2010; Chanclud and Morel, 2016). *In vitro* assays with *L. theobromae* strains showed that this metabolite is phytotoxic to tomato plants and cytotoxic to mammalian cells (Félix et al., 2018).

The virulence protein SSD1 (Q5AK62) was identified in the cellular proteome of both strains, but only when these were grown at 37 °C. This protein participates in the pathogenesis process of *C. albicans*, facilitating the colonization of humans, since they allow *C. albicans* to tolerate the host immune defenses and this way persist inside the host (Gank et al., 2008). In previous studies on *L. theobromae* (Félix et al., 2018a) and the closely-related species *L. hormozganensis* (Félix et al., 2018b), this protein was already detected in the same conditions. All together, the data suggests that SSD1 protein is a recurrent mechanism used by the species in the presence of heat stress.

CONCLUSIONS

The proteomic approach used in this study revealed that strains of *L. theobromae*, isolated from different hosts, have the capacity to adapt to increasing temperatures, by regulating the expression of proteins involved with cell wall organization, stress response or even pathogenesis and plant cell wall degradation.

Strain CAA019 showed a higher variability of expressed proteins when submitted to different temperatures than LA-SV1. In the secretome, the majority of relevant proteins identified for the pathogenesis of this fungus was common to both strains (cerato-platanin snodprot1 protein, aspartic proteases, phospholipases or the effector protein PevD1). However, the identification of one protein, the LysM effector, in the secretome of CAA019 should be highlighted, since it contributes to the manipulation of the host immune helping the colonization of the fungus. In the cellular proteome, proteins related with MAPKs pathways, cAMP/PKA pathways, HSP, mycotoxins or melanin biosynthesis were also identified in both strains, showing a high investment of the cell in the expression of pathogenicity key molecules. The presence of proteins involved in oxylipin synthesis in CAA019 at 25 °C, or tryptacidin synthesis in LA-SV1 at both temperatures also stood out. Proteins involved in the biosynthesis of jasmonic acid were identified in both strains, but not at 37 °C, which may help to justify the higher phytotoxicity of these strains at 25 °C. At 37 °C, the SSD1

protein, a virulence factor identified in both strains, is typically found during the infection process by *C. albicans*, facilitating the colonization of the fungus.

Data suggests that both strains share very similar infection mechanisms but that they have the ability to adapt to different temperatures, expressing different molecules concerning the growth temperature. Proteins related both with pathogenesis in plants and in humans were identified in both strains and temperatures, explaining the dual capability of *L. theobromae* to infect both plants and humans.

ACKNOWLEDGMENTS

This study was supported by FEDER funding through COMPETE program and by national funding through FCT within the research project ALIEN (PTDC/AGR-PRO/2183/2014 - POCI-01-0145-FEDER-016788) and the research unit CESAM (UID/AMB/50017 - POCI-01-0145-FEDER-007638). The authors acknowledge FCT financial support to A Alves (IF/00835/2013), AC Esteves (BPD/102572/2014), and C Félix (BD/97613/2013).

CHAPTER 9

General Discussion

FINAL CONSIDERATIONS

The pathogenicity mechanisms of generalist and opportunistic fungi, as *L. theobromae*, is of extreme importance to identify potential targets that allow the control of the diseases and consequently the associated losses.

There is a general lack of information regarding the consequences of, even small, alterations of the climate on the dynamics between a host and a microbial pathogen (Gallana et al., 2013).

The specialization of a pathogen to a host or environment may lead to a decrease of the capacity to thrive in different environments or hosts. A study with *Aspergillus flavus* and insects, suggested that continued pathogenicity promotes the decrease of living as a saprobe (Scully and Bidochka, 2005). A shift between a plant infection and a human infection requires an adaptation, or at least tolerance, to the new environment's conditions, as the elevated temperature, and not all microorganisms are prepared to survive in such different conditions (Parker and Gilber, 2004). In *L. theobromae*, it is known that this shift occurs, and the increase of the average global temperature seems to lead this opportunistic fungus to co-evolve not only with plants but also with human hosts, potentially turning this species also a relevant human pathogen. Thus, it is crucial to characterize and improve the knowledge on the behavior, especially regarding pathogenicity, of strains isolated from different hosts of *L. theobromae* under different temperatures (environmental temperature – 25 °C – and human body temperature – 37 °C).

The number of available reports describing the use of omics approaches to study *L. theobromae*, are still scarce. Furthermore, only recently the first genome sequence of *L. theobromae* was released (Paolinelli et al., 2016, Uranga et al., 2017; Yan et al., 2017). With this work, we have incremented the number of sequenced and annotated genomes of *Lasiodiplodia* complementing the information available.

All strains of *L. theobromae* used in the study presented evidences of pathogenicity. The integrated omics analysis showed that the behavior of this species seems to be affected by the original host. When submitted to the same conditions, the tested strains of *L. theobromae* showed variability in their protein/metabolite expression profiles. Moreover, the increasing temperature of growth also induced the expression of different molecules. Globally, the temperature of 25 °C showed to promote an investment of energy in tasks related with growth and dissemination of the fungus. On the contrary, the stress temperature of 37 °C seems to be responsible for the fungus to canalize the energy to self-protection. The exception is the strain isolated from a human patient, where the temperature of 37 °C seems to promote the pathogenesis more than the temperature of 25 °C. Reinforcing these hypothesis, *in vitro* assays using plants and mammalian cells revealed an interesting behavior of these strains: strains

isolated from plants were mostly toxic to plants at 25 °C, while the strain isolated from the human patient was toxic mostly to mammalian cells at 37 °C. The production of phytotoxic secondary metabolites only at 25 °C, such as jasmonic acid, also helps to explain this ability of *L. theobromae*.

A vast arsenal of molecules and pathways were identified as being part of the mechanisms of pathogenicity of the species *L. theobromae*, contributing to processes from the early stage of host recognition until their dissemination inside the host (Figure 9.1).

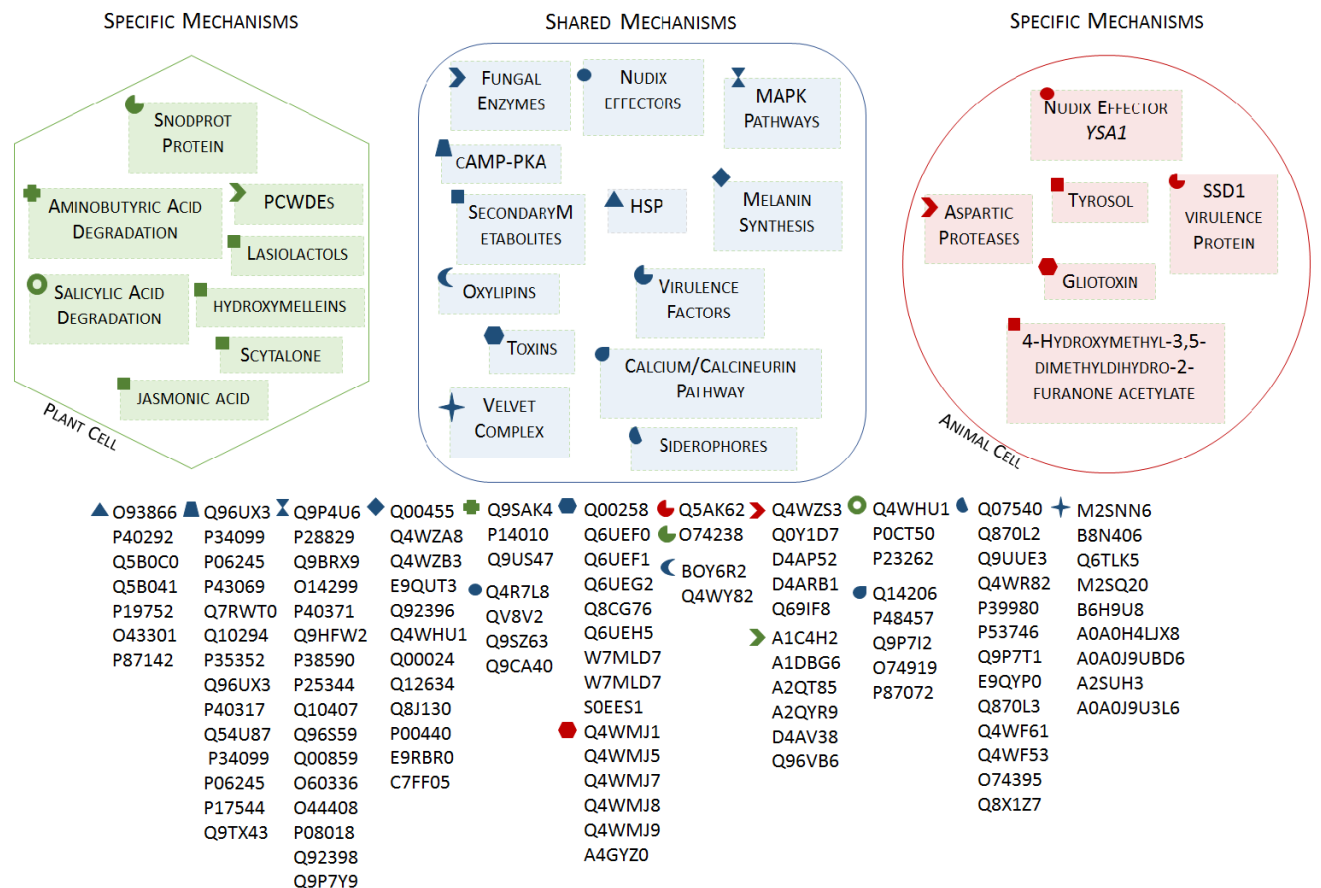


Figure 9.1| Schematic representation main metabolites, transcripts/proteins and pathways potentially involved in various stages of an infection process in plants and humans identified in *L. theobromae* and *L. hormozganensis*.

The presence of MAPKs pathways is of extreme importance for the penetration and dissemination of several pathogenic fungi inside the host. In *Magnaporthe grisea*, three classes of MAPKs are expressed, contributing for the appressoria formation and infectious hyphae, fungal survival under osmotic stress and also cell wall integrity and appressoria penetration (Xu and Hamer, 1996; Leng and Zhong et al., 2015). A similar mechanism, including these three classes of MAPKs, was identified in *L. theobromae*. The presence of these well-represented

pathways of MAPKs signaling helps explaining how this species is able to infect a wide range of plant hosts and to proliferate in different conditions.

To overcome the stress originated by the new environment and the defenses of the hosts, different strategies are used by pathogenic fungi. Between them, heat shock proteins are known to participate in basal biological processes, as translational modifications and protein folding, in the presence of biotic and abiotic stresses (Tiwari et al., 2015). In this study, several families of HSPs were identified, especially, families involved in the response to thermal and pH stress, known to facilitate the infection of plant and human tissues (Brown et al., 2010; Tiwari et al., 2015). Different nudix effectors were also identified. These effectors are believed to manipulate the host defense system of several plants and also the oxidative stress response and susceptibility to drugs in humans (Dong and Wang, 2016), helping the pathogen to persist inside the host. Interestingly, from all the strains in study, only *L. hormozganensis*, isolated from a human patient, expressed at 37 °C a nudix hydrolase (gene *YSA1*), known to be directly related with human pathogenesis (Dong and Wang, 2016).

Oxylipins in fungi are used as communication signals, participating in several host-pathogen interactions and being responsible to modify plant and mammalian host responses (Fischer and Keller, 2016). Not present in all strains, CAA019 was the only strain producing these molecules at 25 °C, reinforcing the hypothesis of each strain having its own molecular profile and that each strain responds to temperature changes in a way that is unique to itself. Strain CAA019 also revealed higher levels of toxicity to tomato cuttings and mammalian cells at 25 °C.

Despite the fact that the initial stages of an infection process are crucial, the nutrition of the pathogen after entering the host is also essential. One of the essential elements for the nutrition of fungi is iron, important to serve as intracellular storage in mycelia and spores (Renshaw et al., 2002). However, Fe (III), the most common form of iron in aerobic environment, is usually unavailable to microorganisms, being the up-take of iron dependent on the production of siderophores. The transport of iron was well represented in *L. theobromae* at both temperatures, corroborating the ability of this species to survive in hostile conditions. Also, proteins involved in the degradation of γ -aminobutyric acid were identified in all strains and may be related with the uptake of carbon originated by this process of degradation. In *Diplodia corticola*, the degradation pathway of γ -aminobutyric acid was identified in a pathogenic strain, suggesting that γ -aminobutyric acid might be the triggering factor between a latent state and a pathogenic one (Fernandes, 2015). Although detected in the genome of both species, the expression of several molecules from the pathway calcium/calcineurin were only detected in CBS339.90. In fungal pathogens, calcium is used to survive and to effectively propagate within the host, contributing to different biological activities, as cell wall integrity and growth at

elevated temperatures (Chen et al., 2010; Liu et al., 2015). Thus, it is an important signaling pathway not only for plant pathogenic fungi but also for human pathogenic fungi (Chen et al., 2010; Liu et al., 2015).

After the successful colonization of the host, the next stage is the regulation of fungal development and its secondary metabolism, assisted in this case by the velvet complex, composed by several components with specific functions. Globally, the velvet complex acts in the modulation of chromatin accessibility and gene expression (López-Berges et al., 2013). In all strains investigated, this complex was well represented. This is especially true in CBS339.90, where all the components were expressed, including the gene *vel1*, previously associated to the growth of the human opportunist *Aspergillus fumigatus* at 37 °C (Lind et al., 2016). Although, not identified by proteomics or transcriptomics, the analysis of the genomes of both species (*L. theobromae* - LA-SOL3 and *L. hormozganensis* - CBS339.90) shows that all main components that participate in this pathway are present.

The synthesis of (DHN)-melanin is of extreme importance to pathogenic fungi. The toxicity of the oxidative products of melanin precursors can induce injuries in the hosts (Jacobson et al., 2000) and also protect the fungus against abiotic stresses, as high temperature (Rehnstrom and Free, 1996). Several molecules involved in the synthesis of melanins were expressed by the strains of *L. theobromae* and *L. hormozganensis*. Indeed, the phytotoxin scytalone (precursor in the synthesis of (DHN)-melanin) was identified in CBS339.90 at both temperatures. This phytotoxin was identified for the first time in *L. theobromae* in this work (Félix, 2018). However, the misidentification of the species showed that this secondary metabolite is in fact produced by *L. hormozganensis*, being also the first time that this phytotoxin is identified in this species. Different melleins, toxins known to participate in the pathogenesis of different plants (Andofi et al., 2011) were identified in strains CBS339.90 and LA-SV1, also at both temperatures, suggesting that the production of mellein among strains of this species seems to be an established mechanism to participate in pathogenicity events. The production of toxins is another mechanism from the secondary metabolism of several fungi that can be beneficial by suppressing the host defenses but also allowing the up-take of cellular components (as nutrients), mostly by necrotrophic fungi. Several molecules associated to toxins' synthesis are expressed by the strains of *L. theobromae* and *L. hormozganensis*. Among them, the synthesis of gliotoxin should be highlighted, since it is a toxin known to be produced by fungi phylogenetically separated involved in several animal mycoses (Tsunawaki et al., 2004; Spikes et al., 2008; Bertling et al., 2010). The functions associated to this mycotoxin, seem to favor the

infection of immunocompromised organisms (Spikes et al., 2008; Bertling et al., 2010), which is in agreement with *L. theobromae* and *L. hormozganensis* being human opportunists.

Specific virulence factors were also identified in the studied strains, as is the case of the phytotoxin from the family of cerato-platanins, protein SnodProt1 (O74238) identified in the secretome of all strains. In other microorganisms, SnodProt1 is able to manipulate the immune response of the plant, causing necrosis of the plant (Brown et al., 2011). The expression of SnodProt1 at 25 and 37 °C suggests that it may have an important role in the pathogenesis of this fungus, even when exposed to increasing temperatures.

The virulence protein SSD1 (Q5AK62) was identified in the cellular proteome of all strains, but only at 37 °C. This protein is known to contribute for the pathogenesis of *C. albicans*, promoting resistance to the host immune defense and facilitating the colonization of human tissues (Gank et al., 2008). It is interesting to understand that virulence determinants relevant not only for plant pathogenesis but also to human pathogenesis were found in all tested strains and temperatures. Although virulence determinants related to phytopathogenesis seem to be easily found at both temperatures, human pathogenesis determinants are more frequent at 37 °C and in the strain isolated from a human patient.

Recent studies including *L. theobromae* under heat stress and in the presence of host (grapevine) concluded that higher temperatures seem to favor its pathogenicity (Úrbez-Torres et al., 2011; Paolinelli et al., 2016; Yan et al., 2017). In fact, the transcriptome of *L. theobromae* UCD256Ma revealed the ability to degrade the salicylic acid produced by grapevine, even at 35 °C. This mechanism –degradation of salicylic acid - is extremely relevant for the pathogenesis of this fungus in plants, since it can use the products from degradation of salicylic acid and phenylpropanoid precursors as carbon sources to guarantee its growth (Paolinelli et al., 2016). We also identified this mechanism although no hosts were used, all the strains were grown only in PDA medium, suggesting that *L. theobromae* and *L. hormozganensis* may have a constitutive expression of these proteins. However, the recognition of the host may, in fact, induce an over expression of these proteins, which could be in the origin of the expression differences between the present study and the study of Paolinelli (Paolinelli et al., 2016).

The initial hypothesis of this study were the following:

- The pathogenicity of *L. theobromae* is modulated/affected by its original host.
- The pathogenicity of *L. theobromae* is modulated/affected by the growth temperature.
- Different temperatures favor the infection of different hosts by *L. theobromae*.

The results, although may not be final (in a sense that more questions were raised), allow to suggest that the pathogenicity of the tested strains of *L. theobromae* and *L. hormozganensis* is

modulated by its original host and growth temperature. The strains share very similar infection mechanisms, but distinct profiles of genes, proteins and metabolites were identified in different strains under similar conditions. However, following the available data from the different omics, this plasticity seems to be mostly at the phenotypic level. When submitted to different temperatures, the behavior of the strains also changed, clearly defining different priorities concerning the growth temperature. The results also allowed to understand that different temperatures seem to favor the infection of different hosts. Proteins and metabolites related both with pathogenesis in plants and in humans were identified in all strains and temperatures, explaining the dual capability of *Lasiodiplodia* to infect both plants and humans. However, it should be highlighted the exclusive ability of the strain isolated from a human patient to express more pathogenicity-related proteins at 37 °C and not at 25 °C (as obtained for all the strains isolated from plants) as well as the expression of specific transcripts/proteins at 37 °C involved in potential relevant mechanisms of pathogenicity.

FUTURE PERSPECTIVES

Despite the contribution of the present work to the knowledge of *L. theobromae* and *L. hormozganensis* biology, especially regarding its pathogenesis, the results obtained are just a piece of the puzzle.

In the future, several directions should be taken to completely unveil the mechanisms used by these species during infection processes. For that, it would be precious the use of a higher number of strains of *L. theobromae* and *L. hormozganensis* isolated from distinct hosts and geographical locations, including hosts from different kingdoms. In the present study, only one strain isolated from human was available, but for a robust conclusion about the infection process in humans, a higher number is crucial. In fact, strains of *L. theobromae* isolated from human patients should also be characterized.

Although the literature and results obtained in this study suggest that higher temperatures seems to facilitate the infection of plants (*e.g.* grapevines) and humans (*e.g.* keratitis), a study using more test temperatures would be valuable to fully understand the effect of temperature on *Lasiodiplodia*.

The integration of omics approaches is a powerful tool to identify potential virulence determinants that can be used to the development of new strategies of controlling diseases caused by these fungi. An interactomics approach would be useful as a next step to visualize the possible interactions between the identified proteins and have a more accurate view of relevant proteins. Thus, an interesting perspective to follow, after this multi-omics analysis, would be

perform knockout experiences using the potential targets identified in the study to prove the function and involvement of such targets in the infection process and their possible use in disease control strategies.

REFERENCES

- Abdi, H. (2003). Multivariate analysis. In M. Lewis-Beck, A. Bryman, & T. Futing (Eds): *Encyclopaedia for research methods for the social sciences*. Thousand Oaks: Sage.
- Abdollahzadeh, J., Javadi, A., Goltapeh, M. E., Zare, R., and Phillips, A. J. L. (2010). Phylogeny and morphology of four new species of *Lasiodiplodia* from Iran. *Persoonia*. 25, 1–10. doi:10.3767/003158510X524150
- Abou-Mansour, E., Débieux, J. L., Ramírez-Suero, M., Bénard-Gellon, M., Magnin-Robert, M., Spagnolo, A., Chong, J., Farine, S., Bertsch, C., L'Haridon, F., Serrano, M., Fontaine, F., Rego, C., and Larignon, P. (2015). Phytotoxic metabolites from *Neofusicoccum parvum*, a pathogen of *Botryosphaeria* dieback of grapevine. *Phytochemistry*. 115, 1, 207-215. doi: 10.1016/j.phytochem.2015.01.012
- Akcapinar, G. B., Kappel, L., Sezerman, O. U., and Seidl-seiboth, V. (2015). Molecular diversity of LysM carbohydrate-binding motifs in fungi. *Curr Genet*. 61, 103–113. doi: 10.1007/s00294-014-0471-9
- Albuquerque, P., and Casadevall, A. (2012). Quorum sensing in fungi—a review. *Med Mycol*. 50, 337–345.
- Aldridge, D. C., Galt, S., Giles, D., Turner, W. B. (1971). Metabolites of *Lasiodiplodia theobromae*. *J Chem Soc C*. 1623–1627. doi: 10.1039/J39710001623
- Al-Nasiry, S., Geusens, N., Hanssens, M., Luyten, C. & Pijnenborg, R. (2007). The use of Alamar Blue assay for quantitative analysis of viability, migration and invasion of choriocarcinoma cells. *Human Reprod*. 22(5), 1304-1309.
- Al-Sadi, A. M., Al-Ghaithi, A. G., Al-Fahdi, N., and Al-Yahyai, R. (2014). Characterization and pathogenicity of fungal pathogens associated with root diseases of *Citrus* in Oman. *Int J Agri Biol*. 371-376.
- Al-Sadi, A. M., Al-Wehaibi, A. N., Al-Shariqi, R. M., Al Hammadi, M. S., Al-Hosni, I. A., and Al-Ghaithi, A. G. (2013). Population genetic analysis reveals diversity in *Lasiodiplodia* species infecting date palm, *Citrus*, and mango in Oman and the UAE. *Plant Dis*. 97, 10, 1363-1369. doi: 10.1094/PDIS-03-13-0245-RE
- Alves, A., Crous, P. W., Correia, A., and Phillips, A. J. L. (2008). Morphological and molecular data reveal cryptic speciation in *Lasiodiplodia theobromae*. *Fungal Divers*. 28, 1–13.
- Alves, E., Esteves, A. C., Correia, A., Cunha, A., Faustino, M. A., Neves, M. G., et al. (2015). Protein profiles of *Escherichia coli* and *Staphylococcus warneri* are altered by photosensitization with cationic porphyrins. *Photochem Photobiol. Sci*. 14, 1169–1178. doi: 10.1039/c4pp00194j
- Ammerman, N. C., Beier-Sexton, M., and Azad, A. F. (2009). Growth and maintenance of Vero cell lines. *Curr. Protoc. Microbiol. Appendix 4:Appendix 4E*. doi: 10.1002/9780471729259.mca04es11

- Andolfi, A., Basso, S., Giambra, S., Conigliano, G., Lo Piccolo, S., Alves, A., and Burruano, S. (2016). Lasiolactols A and B produced by the grapevine fungal pathogen *Lasiodiplodia mediterranea*. *Chem Biodiv.* 13, 395–402. doi: 10.1002/cbdv.201500104
- Andolfi, A., Maddau, L., Cimmino, A., Linaldeddu, B. T., Basso, S., Deidda, A., Serra, S., and Evidente, A. (2014). Lasiojasmonates A–C, three jasmonic acid esters produced by *Lasiodiplodia* sp., a grapevine pathogen. *Phytochemistry.* 103, 145–153. doi: 10.1016/j.phytochem.2014.03.016
- Andolfi, A., Maddau, L., Cimmino, A., Linaldeddu, B.T., Franceschini, A., Serra, S., Basso, S., Melck, D., and Evidente, A. (2012). Cyclobotryoxide, a phytotoxic metabolite produced by the plurivorous pathogen *Neofusicoccum austral.* *J Nat Prod.* 75, 1785–1791. doi: 10.1021/np300512m
- Andolfi, A., Mugnai, L., Luque, J., Surico, G., Cimmino, A., and Evidente, A. (2011). Phytotoxins produced by fungi associated with grapevine trunk diseases. *Toxins.* 3, 1569–1605. doi: 10.3390/toxins3121569
- Araujo, R., and Rodrigues, A. G. (2004). Variability of germinative potential among pathogenic species of *Aspergillus*. *J Clin Microbiol.* 42, 4335–4337. doi: 10.1128/JCM.42.9.4335-4337.2004
- Arsenault, G. P., Althaus, J. R., and Divekar, P. V. (1969). Structure of the antibiotic botryodiplodin—use of chemical ionization mass spectrometry in organic structure determination. *J Chem Soc Chem Commun.* 23, 1414–1415.
- Assche, R. V., Broeckx, V., Boonen, K., Maes, E., Haes, W. D., Schoofs, L., and Temmerman, L. (2015). Integrating -omics: Systems biology as explored through *C. elegans* research. *J Mol Biol.* 427, 3441–3451. doi: 10.1016/j.jmb.2015.03.015
- Auger, J., Esterio, M., Ricke, G., and Pérez, I. (2004). Black dead arm and basal canker of *Vitis vinifera* cv. Red Globe caused by *Botryosphaeria obtusa* in Chile. *Plant Dis.* 88, 1286. doi: 10.1094/PDIS.2004.88.11.1286A
- Azevedo, J.S.N., Ramos, I., Araújo, S., Oliveira, C.S., Correia, A., Henriques, I.S. (2012). Spatial and temporal analysis of estuarine bacterioneuston and bacterioplankton using culture-dependent and culture-independent methodologies. *Antonie van Leeuwenhoek.* 101(4), 819–835. doi: 10.1007/s10482-012-9697-z
- Baarden, P. V., Belkum, A. V., Summerbell, R. C., Crous, P. W., and Thomma, B. P. H. J. (2007). Molecular mechanisms of pathogenicity: how do pathogenic microorganisms develop cross-kingdom host jumps? *FEMS Microbiol Rev.* 31, 239–277. doi: 10.1111/j.1574-6976.2007.00065.x
- Badenoch, P., Wetherall, B., Woolley, M., and Coster, D. (2008). Newer emerging pathogens of ocular non-sporulating molds (NSM) identified by polymerase chain reaction (PCR)-based DNA sequencing technique targeting internal transcribed spacer (ITS) region. *Curr Eye Res.* 33, 10, 905–906. doi: 10.1080/02713680701864780
- Balan, J., Ebringer, L., Nemec, P. (1964). Trypacidin a new antiprotozoal antibiotic. *Naturwissenschaften.* 51, 9, 227.

- Banerjee, A. C., Kundu, A., and Ghosh, S. K. (2003). Genetic manipulation of filamentous fungi. Roussos, S. ed. *New horizons in biotechnology*. Kluwer Academic Publishers, Dordrecht (Neth), 193–198. doi: 10.1007/978-94-017-0203-4_17
- Barros, R., R., O., Oliveira, R., A., Gottschalk, L., M., F., and Bon, E., P., S. (2010). Production of cellulolytic enzymes by fungi *Acrophialophora nainiana* and *Ceratocystis paradoxa* using different carbon sources. *Appl Biochem Biotechnol*. 161, 448–454. doi: 10.1007/s12010-009-8894-3
- Baskarathevan, J., Jaspers, M. V., Jones, E. E., Ridgway, H. J. (2012). Incidence and distribution of botryosphaeriaceous species in New Zealand vineyards. *Eur J Plant Pathol*. 132, 549–560. doi: 10.1007/s10658-011-9900-5
- Bebber, D. P., Ramotowski, M. A. T., Gurr, S. J. (2013) Crop pests and pathogens move polewards in a warming world. *Nat Climate Change*. 3, 985–988. doi: 10.1038/nclimate1990
- Benedict, K., Malcolm, R., Vallabhaneni, S., Jackson, B. R., and Chiller, T. (2017). Emerging issues, challenges, and changing epidemiology of fungal disease outbreaks. *Lancet Infect Dis*. 17, e403–12. doi: org/10.1016/S1473-3099(17)30443-7
- Bennett, J. W. (1998). Mycotechnology: the role of fungi in biotechnology. *J Biotechnol*. 66, 101-107. doi.org/10.1016/S0168-1656(98)00133-3
- Bertling, A., Niemann, S., Uekötter, A., Fegeler, W., Lass-Flörl, C., von Eiff, C., and Kehrel, B. E. (2010). *Candida albicans* and its metabolite gliotoxin inhibit platelet function via interaction with thiols. *Thromb Haemost*. 104, 270–278. doi: 10.1160/TH09-11-0769
- Blackwell, M. (2011). The fungi: 1, 2, 3... 5.1 million species? *Am J Bot*. 98, 426–438.
- Bliska, J. B., Casadevall, A. (2009). Intracellular pathogenic bacteria and fungi—a case of convergent evolution? *Nat. Rev. Microbiol*. 7(2), 165–171. doi; 10.1038/nrmicro2049
- Boetzer, M., and Pirovano, W. (2012). Toward almost closed genomes with GapFiller. *Genome Biol*. 13, R56. doi: 10.1186/gb-2012-13-6-r56
- Boetzer, M., Henkel, C. V., Jansen, H. J., Butler, D., and Pirovano, W. (2011). Scaffolding pre-assembled contigs using SSPACE. *Bioinformatics*. 27, 578–579. doi: 10.1093/bioinformatics/btq683
- Borderie, V. M., Bourcier, T. M., Poirot, J. L, Baudrimont, M., de Saint-Maur, P. P., and Laroche, L. (1997). Endophthalmitis after *Lasiodiplodia theobromae* corneal abscess. *Graefe's Arch Clin Exper Ophthalmol*. 235, 259–261.
- Braaksma, M., nad Punt, P. J. (2008). *Aspergillus* as a cell factory for protein production: controlling protease activity in fungal production. Goldman, G. H., Osmani, S. A. eds *The Aspergilli: genomics, medical aspects, biotechnology, and research methods*. CRC Press, Boca Raton, 441–455.
- Bregar, O., Mandelc, S., Celar, F., Javornik, B. (2012). Proteome analysis of the plant pathogenic fungus *Monilinia laxa* showing host specificity. *Food Technol Biotechnol*. 50(3), 326–333.

- Brown, A. J. P., Leach, M. D., and Nicholls, S. (2010). The relevance of heat shock regulation in fungal pathogens of humans. *Virulence*. 1, 4, 330-332.
- Brown, N. A., Antoniw, J., Hammond-Kosack, K. E. (2012). The predicted secretome of the plant pathogenic fungus *Fusarium graminearum*: A refined comparative analysis. *PLoS ONE*. 7,4, e33731. doi: 10.1371/journal.pone.0033731
- Brown, N. F., Wickham, M. E., Coombes, B. K., and Finlay, B. B. (2006). Crossing the line: selection and evolution of virulence traits. *PLoS Pathog*. 2, e42. doi: 10.1371/journal.ppat.0020042
- Bu, B., Qiu, D., Zeng, H., Guo, H., Yuan, J., and Yang, X. (2014). A fungal protein elicitor PevD1 induces Verticillium wilt resistance in cotton. *Plant Cell Rep*. 33, 461. doi: 10.1007/s00299-013-1546-7
- Burgess, T. I., and Wingfield, M. J. (2002). Quarantine is important in restricting the spread of exotic anthropogenic introduction. *Trends Ecol Evol*. 20, 420-421. doi: 10.1016/j.tree.2005.05.002
- Byers, B. R., and Arceneaux, J. E. (1998). Microbial iron transport: iron acquisition by pathogenic microorganisms. *Metal Ions Biol Syst*. 35, 37-66.
- Cabras, A., Mannoni, M. A., Serra, S., Andolfi, A., Fiore, M., and Evidente, A. (2006). Occurrence, isolation and biological activity of phytotoxic metabolites produced in vitro by *Sphaeropsis sapinea*, pathogenic fungus of *Pinus radiata*. *Eur J Plant Pathol*. 115, 187-193. doi: 10.1007/s10658-006-9006-7
- Cantarel, B., L., Coutinho, P. M., Rancurel, C., Bernard, T., Lombard, V., and Henrissat, B. (2009). The Carbohydrate-Active EnZymes database (CAZy): an expert resource for Glycogenomics. *Nucleic Acids Res*. 37, D233-8. doi: 10.1093/nar/gkn663
- Carvalhais, V., Cerveira, F., Vilanova, M., Cerca, N., Vitorino, R. (2015). An immunoproteomic approach for characterization of dormancy within *Staphylococcus epidermidis* biofilms. *Mol Immunol*. 65(2), 429-435. doi: 10.1016/j.molimm.2015.02.024
- Carvalho, A., and Goldman, G. H. (2017). Editorial: An omics perspective on fungal infection: toward next-generation diagnosis and therapy. *Front Microbiol*. 8, 85. doi: 10.3389/fmicb.2017.00085
- Casadevall, A., and Pirofski, L. (2003). The damage-response framework of microbial pathogenesis. *Nat Rev Microbiol*. 1, 17-24. doi: 10.1038/nrmicro732
- Castro-Ochoa, L. D., Rodríguez-Gómez, C., Valerio-Alfaro, G., Ros, R. O. (2005). Screening, purification and characterization of the thermoalkalophilic lipase produced by *Bacillus thermoleovorans* CCR11. *Enzyme Microb Technol* 37, 648-654. doi: 10.1016/j.enzmictec.2005.06.003
- Chaffin, W.L., López-Ribot, J.L., Casanova, M., Gozalbo, D., Martínez, J. P. (1998). Cell wall and secreted proteins of *Candida albicans*; identification, function, and expression. *Microbiol. Mol. Biol. Rev*. 62(1), 130-180.

- Chanclud, E., and Morel, J. B. (2016). Plant hormones: a fungal point of view. *Mol Plant Pathol.* 17, 1289-1297. doi: 10.1111/mpp.12393
- Chandrasekaran, M., and Sathiyabama, M. (2014). Production, partial purification and characterization of protease from a phytopathogenic fungi *Alternaria solani* (Ell. and Mart.) Sorauer. *J. Basic Microbiol.* 54, 763–774. doi: 10.1002/jobm.201200584
- Chandrasekaran, M., Thangavelu, B., Chun, S. C., and Sathiyabama, M. (2016). Proteases from phytopathogenic fungi and their importance in phytopathogenicity. *J Gen Plant Pathol.* 82, 233–239. doi: 10.1007/s10327-016-0672-9
- Chatterjee, S., Tatu, U. (2017). Heat shock protein 90 localizes to the surface and augments virulence factors of *Cryptococcus neoformans*. *PLoS Negl Trop Dis.* 11, 8, e0005836. doi: 10.1371/journal.pntd.0005836
- Chauhan, N. M., Washe, A. P., and Minota, T. (2016). Fungal infection and aflatoxin contamination in maize collected from Gedeo zone, Ethiopia. *SpringerPlus*, 5, 753. doi: 10.1186/s40064-016-2485-x
- Chen, S., Chen, D., Cai, R., Cui, H., Long, Y., Lu, Y., Li, C., and She, Z. (2016). Cytotoxic and antibacterial preussomerins from the mangrove endophytic fungus *Lasiodiplodia theobromae* ZJ-HQ1. *J Nat Prod.* 79, 9, 2397-2402. doi: 10.1021/acs.jnatprod.6b00639
- Chen, W., Lee, M., Jefcoate, C., Kim, S., Chen, F., and Yu, J. (2014). Fungal cytochrome P450 monooxygenases: their distribution, structure, functions, family expansion, and evolutionary origin. *Genome Biol Evol.* 6, 7, 1620–1634. doi: 10.1093/gbe/evu132
- Chen, Y., Kozubowski, L., Cardenas, M. E., and Heitman, J. (2010). On the roles of calcineurin in fungal growth and pathogenesis. *Curr Fungal Infect Rep.* 4, 244–255. doi: 10.1007/s12281-010-0027-5
- Chikhi, R., and Medvedev, P. (2013). Informed and automated k-mer size selection for genome assembly. *Bioinformatics.* doi: 10.1093/bioinformatics/btt310
- Choi, J., Jung, W. H., and Kronstad, J. W. (2015). The cAMP/protein kinase A signaling pathway in pathogenic basidiomycete fungi: connections with iron homeostasis. *J Microbiol.* 53, 9, 579–587. doi: 10.1007/s12275-015-5247-5
- Cimmino, A., Andolfi, A., Abouzeid, M., and Evidente, A. (2013). Polyphenols as fungal phytotoxins, seed germination stimulants and phytoalexins. *Phytochem Rev.* 12, 653. doi: 10.1007/s11101-013-9277-5
- Cimmino, A., Cinelli, T., Masi, M., Reveglia, P., da Silva, M. A., Mugnai, L., Michereff, S. J., Surico, G., and Evidente, A. (2017). Phytotoxic lipophilic metabolites produced by grapevine strains of *Lasiodiplodia* species in Brazil. *J Agric Food Chem.* 65, 6, 1102-1107. doi: 10.1021/acs.jafc.6b04906
- Cobos, R., Barreiro, C., Mateos, R., and Coque, J. (2010). Cytoplasmic- and extracellular-proteome analysis of *Diplodia seriata*: a phytopathogenic fungus involved in grapevine decline. *J Proteome Sci.* 8, 46-62. doi: 10.1186/1477-5956-8-46

- Corrêa, R. C. G., Rhoden, S. A., Mota, T. R., Azevedo, J. L., Pamphile, J. A., de Souza, C. G. M., Polizeli, M. d. L. T. d. M., Bracht, A., and Peralta, R. M. (2014). Endophytic fungi: expanding the arsenal of industrial enzyme producers. *J Ind Microbiol Biotechnol.* 41, 1467. doi: 10.1007/s10295-014-1496-2
- Correia, K. C., Silva, M. A., de Moraes, M. A. Jr., Armengol, J., Phillips, A. J. L., Câmara, M. P. S., and Michereff, S. J. (2016). Phylogeny, distribution and pathogenicity of *Lasiodiplodia* species associated with dieback of table grape in the main Brazilian exporting region. *Plant pathology* 65, 92–103. doi: 10.1111/ppa.12388
- Costa, L., Esteves, A. C., Correia, A., Moreirinha, C., Delgadillo, I., Cunha, Â., Almeida, A. (2014). SDS-PAGE and IR spectroscopy to evaluate modifications in the viral protein profile induced by a cationic porphyrinic photosensitizer. *J Virol Methods.* 209, 103–109. doi: 10.1016/j.jviromet.2014.09.013
- Coutinho, B. L., Freire, F. C. O., Lima, C. S., Lima, J. S., Goncalves, F. J. T., Machado, A. R., Silva, A. M. S., and Cardoso, J. E. (2017). Diversity of genus *Lasiodiplodia* associated with perennial tropical fruit plants in northeastern Brazil. *Plant Pathol.* 66, 90–104. doi: 10.1111/ppa.12565
- Črešnar, B., and Petrič, Š. (2011). Cytochrome P450 enzymes in the fungal kingdom. *Biochim Biophys Acta.* 1814, 29–35. doi: 10.1016/j.bbapap.2010.06.020
- Crous, P. W., Slippers, B., Wingfield, M. J., Rheeder, J., Marasas, W. F. O., Philips, A. J. L., Alves, A., Burgess, T., Barber, P., Groenewald, J. Z. (2006). Phylogenetic lineages in the Botryosphaeriaceae. *Stud Mycol.* 55, 235–53.
- Cruz, A., Areias, D., Duarte, A., Correia, A., Suzuki, S., Mendo, S. (2013). *Aeromonas molluscorum* Av27 is a potential tributyltin (TBT) bioremediator; phenotypic and genotypic characterization indicates its safe application. *Antonie van Leeuwenhoek* 104(3), 385–396. doi: 10.1007/s10482-013-9961-x
- Culibrk, L., Croft, C. A., Tebbutt, S. J. (2016). Systems biology approaches for host–fungal interactions: an expanding multi-omics frontier. *OMICS.* 20, 3, 127-138. doi: 10.1089/omi.2015.0185
- D’souza, A. D., and Ramesh, M. (2002). Senescence in fungi. *Resonance* 7, 51–55. doi: 10.1007/BF02896308
- da Cunha, M. A. A., Turmina, J. A., Ivanov, R. C., Barroso, R. R., Marques, P. T., Fonseca, E. A. I., Fortes, Z. B., Dekker, R. F. H., Khaper, N., and Barbosa, A. M. (2012). Lasiodiplodin, an exocellular (1-6)-b-D-glucan from *Lasiodiplodia theobromae* MMPI: production on glucose, fermentation kinetics, rheology and anti-proliferative activity. *J Ind Microbiol Biotechnol.* 39, 1179–1188. doi: 10.1007/s10295-012-1112-2
- De Buyck, L., Forzato, C., Ghelfi, F., Mucci, A., Nitti, P., Pagnoni, U. M., Parsons, A. F., Pitacco, G., and Roncaglia, F. (2006). A new and effective route to (+/-)-botryodiplodin and (+/-)-epi-botryodiplodin acetates using a halogen atom transfer Ueno-Stork cyclization. *Tetrahedron Lett.* 47, 7759–7762. doi: 10.1016/j.tetlet.2006.08.121

- de Groot, M. J. A., Bundock, P., Hooykaas, P. J. J., and Beijersbergen, A. G. M. (1998). *Agrobacterium tumefaciens*-mediated transformation of filamentous fungi. *Nature Biotechnol.* 16, 839–842. doi: 10.1038/nbt0998-839
- de Hoog, G. S., Guarro, J., Gen, e. J., Figueras, M. J., (2000). *Atlas of Clinical Fungi*, 2nd edn. Centraalbureau voor Schimmelcultures/Universitat Rovira i Virgili, Utrecht/Reus.
- De Lucca, A. J. (2007). Harmful fungi in both agriculture and medicine. *Revista Iberoamericana de Micologia.* 24, 1, 3-13.
- Dekker, M. (2003). *Handbook of fungal biotechnology*. Dilip, K. Arora ed., New York, 600p.
- Dellagi, A., Rigault, M., Segond, D., Roux, C., Kraepiel, Y., Cellier, F., Briat, J. F., Gaymard, F., and Expert, D. (2005). Siderophore mediated up-regulation of *Arabidopsis* ferritin expression in response to *Erwinia chrysanthemi* infection. *Plant J.* 43, 262–272. doi: 10.1111/j.1365-313X.2005.02451.x
- Dhandhukia, P. C., Thakkar, V.R. (2007). Standardization of growth and fermentation criteria of *Lasiodiplodia theobromae* for production of jasmonic acid. *Afr J Biotechnol.* 6, 6, 707-712.
- Dias, M., and Souza, D. S. (1998). Principais doenças da videira. Informe Agropecuário, Belo Horizonte 194, 76-84.
- Dissanayake, A. J., Phillips, A. J. L., Li, X. H., and Hyde, K. D. (2016). Botryosphaeriaceae: Current status of genera and species. *Mycosphere.* 7, 7, 1001–1073, doi: 10.5943/mycosphere/si/1b/13
- Dix, A., Vlais, S., Guthke, R., and Linde, J. (2016). Use of systems biology to decipher host-pathogen interaction networks and predict biomarkers. *Clin Microbiol Infect.* 22, 600–606. doi: 10.1016/j.cmi.2016. 04.014
- Dixon, K. P., Xu, J. R., Smirnov, N., Talbot, N. J. (1999). Independent signaling pathways regulate cellular turgor during hyperosmotic stress and appressorium-mediated plant infection by the rice blast fungus *Magnaporthe grisea*. *Plant Cell.* 11, 2045–2058.
- Do Vale, L. H., Gomez-Mendoza, D. P., Kim, M. S., Pandey, A., Ricart, C. A., Edivaldo, X. F., and Sousa, M. V. (2012). Secretome analysis of the fungus *Trichoderma harzianum* grown on cellulose. *Proteomics.* 12(17), 2716-2728. doi: 10.1002/pmic.201200063
- Dobin, A., Davis, C. A., Schlesinger, F., Drenkow, J., Zaleski, C., Jha, S., Batut, P., Chaisson, M., and Gingeras, T. R. (2013). STAR: ultrafast universal RNA-seq aligner. *Bioinformatics.* 29, 1, 15–21. doi: 10.1093/bioinformatics/bts635
- Dong, S., Wang, Y. (2016). Nudix Effectors: A common weapon in the arsenal of plant pathogens. *PLoS Pathog.* 12, 8, e1005704. doi:10.1371/journal.ppat.1005704
- Donnio, A., Desbios, N., Boiron, P., Théodose, R., Mouniee, D., Thoumazet, F., and Merle, H. (2006). Mycotic keratitis and endophthalmitis caused by unusual fungi: *Lasiodiplodia theobromae*. *J Fr Ophtalmol.* 29, e4.
- Dou, Z. P., He, W., and Zhang, Y. (2017). Does morphology matter in taxonomy of *Lasiodiplodia*? An answer from *Lasiodiplodia hyalina* sp. Nov. *Mycosphere.* 8, 2, 1014–1027. doi: 10.5943/mycosphere/8/2/5

- Duarte, A. S., Cavaleiro, E., Pereira, C., Merino, S., Esteves, A. C., Duarte, E. P., Correia, A. C. (2015). *Aeromonas piscicola* AH-3 expresses an extracellular collagenase with cytotoxic properties. *Lett Appl Microbiol.* 60(3), 288–297. doi: 10.1111/lam.12373
- Duarte, A. S., Correia, A., and Esteves, A. (2016). Bacterial collagenases – a review. *Crit Ver Microbiol.* 42, 106–126. doi:10.3109/1040841X.2014.904270
- Duarte, A. S., Duarte, E. P., Correia, A., Pires, E., and Barros, M. T. (2009). Cardosins improve neuronal regeneration after cell disruption: a comparative expression study. *Cell Biol Toxicol.* 25, 99–108. doi: 10.1007/s10565-008-9058-x
- Duarte, A., Rosa, N., Duarte, E. P., Pires, E., Barros, M.T. (2006). Cardosins; a new and efficient plant enzymatic tool to dissociate neuronal cells for the establishment of cell cultures. *Biotechnol Bioeng.* 97(4), 991–996. doi: 10.1002/bit.21259
- Duarte, X., Anderson, C. T., Grimson, M., Barabote, R. D., Strauss, R. E., Gollahon, L. S., and San Francisco, M. J. D. (2000). *Erwinia chrysanthemi* strains cause death of human gastrointestinal cells in culture and express an intimin-like protein. *FEMS Microbiol Lett.* 190, 81–86.
- Dulbecco, R., Freeman, G. (1959). Plaque production by the polyoma virus. *Virology.* 8, 3, 396-7.
- Dzoyem, J. P., Melong, R., Tsamo, A. T., Maffo, T., Kapche, D. G., Ngadjui, B. T., McGaw, L. J., and Eloff, J. N. (2017). Cytotoxicity, antioxidant and antibacterial activity of four compounds produced by an endophytic fungus *Epicoccum nigrum* associated with *Entada abyssinica*. *Revista Brasileira de Farmacognosia.* 27, 251–253. doi: 10.1016/j.bjp.2016.08.01
- Eastburn, D. M., McElrone, A. J., and Bilgin, D. D. (2011). Influence of atmospheric and climatic change on plant-pathogen interactions. *Plant Pathol.* 60, 54–69. doi: 10.1111/j.1365-3059.2010.02402.x
- Ene, I. V., Brunke, S., Brown, A. J. P., and Hube, B. (2014). Metabolism in fungal pathogenesis. *Cold Spring Harb Perspect Med.* 4, a019695. doi: 10.1101/cshperspect.a019695
- Eng, F., Haroth, S., Feussner, K., Meldau, D., Rekhter, D., Ischebeck, T., Brodhun, F., and Feussner, I. (2016). Optimized jasmonic acid production by *Lasiodiplodia theobromae* reveals formation of valuable plant secondary metabolites. *PLoS ONE* 11, 12. doi: 10.1371/journal.pone.0167627
- Esteves, A. C., Saraiva, M., Correia, A., and Alves, A. (2014). Botryosphaerales fungi produce extracellular enzymes with biotechnological potential. *Can J Microbiol.* 60, 332–42. doi: 10.1139/cjm-2014-0134
- Evidente, A., Andolfi, A., and Cimmino, A. (2011). Relationships between the stereochemistry and biological activity of fungal phytotoxins. *Chirality.* 23,9, 674-693. doi: 10.1002/chir.20966
- Evidente, A., Punzo, B., Andolfi, A., Cimmino, A., Melck, D., and Luque, J. (2010). Lipophilic phytotoxins produced by *Neofusicoccum parvum*, a grapevine canker agent. *Phytopathol Mediterr.* 49, 74–79. doi: 10.14601/Phytopathol_Mediterr-5433
- Facchini, F., D., A., Vici, A., C., Pereira, M., G., Jorge, J., A., and Polizeli, M., L., T., M. (2015). Enhanced lipase production of *Fusarium verticillioides* by using response surface methodology and wastewater pretreatment application. *J Biochem Tech.* 6(3), 996-1002.

- Félix C., Duarte, A. S., Vitorino, R., Guerreiro, A. C. L., Domingues, P., Correia, A. C. M., Alves, A., and Esteves, A. C. (2016). Temperature modulates the secretome of the phytopathogenic fungus *Lasiodiplodia theobromae*. *Front Plant Sci.* 7:1096. doi: 10.3389/fpls.2016.01096
- Félix, C., Libório, S., Nunes, M., Félix, R., Duarte, A. S., Alves, A., and Esteves, A. C. (2018). *Lasiodiplodia theobromae* as a producer of biotechnologically relevant enzymes. *Int J Mol Sci.* 19, 29. doi: 10.3390/ijms19020029
- Félix, C., Meneses, R., Gonçalves, M. F. M., Tillerman, L., Duarte, A. S., Jorrín-Novo, J. V., de Peer, Y. V., Deforce, D., Nieuwerburgh, F. V., Esteves, A. C., and Alves, A. (2018a). A multi-omics analysis of the grapevine pathogen *Lasiodiplodia theobromae* reveals that temperature affects the expression of virulence and pathogenicity-related gene expression. *In preparation*
- Félix, C., Meneses, R., Gonçalves, M. F. M., Tillerman, L., Duarte, A. S., Jorrín-Novo, J. V., de Peer, Y. V., Deforce, D., Nieuwerburgh, F. V., Alves, A., and Esteves, A. C. (2018b). Multi-omics analyses reveal the molecular pathogenesis toolkit of *Lasiodiplodia hormozganensis*, a cross-kingdom fungal pathogen. *In preparation*
- Félix, C., Salvatore, M. M., DellaGreca, M., Meneses, R., Duarte, A. S., Salvatore, F., Naviglio, D., Gallo, M., Jorrín-Novo, J. V., Alves, A., Andolfi, A., and Esteves, A. C. (2018) (*in press*). Production of toxic metabolites by two strains of *Lasiodiplodia theobromae*, isolated from a coconut tree and a human patient. *Mycologia*. doi: 10.1080/00275514.2018.1478597
- Fernandes, I. (2015). Infection mechanism of *Diplodia corticola*. PhD thesis. Aveiro University, Portugal.
- Fernandes, I., Alves, A., Correia, A., Devreese, B., and Esteves, A. (2014). Secretome analysis identifies potential virulence factors of *Diplodia corticola*, a fungal pathogen involved in cork oak (*Quercus suber*) decline. *Fungal Biol.* 118, 516–523. doi: 10.1016/j.funbio.2014.04.006
- Filler, S. G., Swerdloff, J. N., Hobbs, C., and Lockett, P. M. (1995). Penetration and damage of endothelial cells by *Candida albicans*. *Infect Immun.* 63, 976–983.
- Fischer, G. J. and Keller, N. P. (2016). Production of cross-kingdom oxylipins by pathogenic fungi: An update on their role in development and pathogenicity. *J Microbiol.* 54, 3, 254–264. doi: 10.1007/s12275-016-5620-z
- Forzato, C., Furlan, G., Nitti, P., Pitacco, G., Marchesan, D., Coriani, S., and Valentin, E. (2005). A combined experimental and computational strategy in the assignment of absolute configurations of 4-methyl-5-oxo-tetrahydrofuran-3-carboxylic acids and their esters. *Tetrahedron Asymmetry* 16, 3011–3023. doi:10.1016/j.tetasy.2005.08.018
- Fujimoto, Y., Kamiya, M., Tsunoda, H., Ohtsubo, K., and Tatsuno, T. (1980). Recherche toxicologique des substances metaboliques de *Penicillium carneo-lutescens*. *Chem Pharm Bull.* 28, 1062–1066.
- Fukutomi, Y., and Taniguchi, M. (2015). Sensitization to fungal allergens: Resolved and unresolved issues. *Allergol Int.* 64, 321–331. doi: 10.1016/j.alit.2015.05.007

- Gaffoor, I., Brown, D. W., Plattner, R., Proctor, R. H., Qi, W., Trail, F. (2005). Functional analysis of the polyketide synthase genes in the filamentous fungus *Gibberella zeae* (anamorph *Fusarium graminearum*). *Eukaryot Cell*, 1926–1933. doi:10.1128/EC.4.11.1926–1933.2005
- Galant, A., Koester, R. P., Ainsworth, E. A., Hicks, L. M., and Jez, J. M. (2012). From climate change to molecular response: redox proteomics of ozone- induced responses in soybean. *New Phytol.* 194, 220–229. doi:10.1111/j.1469- 8137.2011.04037.x
- Gallana, M., Ryser-Degiorgis, M. P., Wahli, T., and Segner, H. (2013). Climate change and infectious diseases of wildlife: altered interactions between pathogens, vectors and hosts. *Curr. Zool.* 59, 427–437. doi: 10.1093/czoolo/59.3.427
- Gank, K. D., Yeaman, M. R., Kojima, S., Yount, N. Y., Park, H., Edwards, J. E., Filler, S. G., and Fu, Y. (2008). SSD1 is integral to host defense peptide resistance in *Candida albicans*. *Eukaryot Cell.* 7, 8, 1318–1327. doi: 10.1128/EC.00402-07
- Gardiner, D. J., Waring, P., and Howlett, B. J. (2005). The epipolythiodioxopiperazine (ETP) class of fungal toxins: mode of action, functions and biosynthesis. *Microbiol.* 151, 1021–1032. doi: 10.1099/mic.0.27847-0
- Gardiner, D. M., Kazan, K., and Manner, J. M. (2013). Cross-kingdom gene transfer facilitates the evolution of virulence in fungal pathogens. *Plant Science.* 210, 151– 158. doi: 10.1016/j.plantsci.2013.06.002
- Gauthier, G. M., and Keller, N. P. (2013). Crossover fungal pathogens: the biology and pathogenesis of fungi capable of crossing kingdoms to infect plants and humans. *Fungal Genet Biol.* 61, 146–157. doi: 10.1016/j.fgb.2013.08.016
- Gauthier, T., Wang, X., Sifuentes Dos Santos, J., Fysikopoulos, A., Tadrist, S., Canlet, C., Artigot, M. P., Loiseau, N., Oswald, I. P., Puel, O. (2012). Trypacidin, a spore-borne toxin from *Aspergillus fumigatus*, is cytotoxic to lung cells. *PLoS One.* 7, 2, e29906. doi: 10.1371/journal.pone.0029906
- Ghannoum, M. (2000). Potential role of phospholipases in virulence and fungal pathogenesis. *Clin Microbiol Rev.* 122–143. doi: 0893-8512/00/\$04.0010
- Gibson, D. M., King, B. C., Hayes, M. L., and Bergstrom, G. C. (2011). Plant pathogens as a source of diverse enzymes for lignocellulose digestion. *Curr. Opin. Microbiol.* 14, 264–270. doi: 10.1016/j.mib.2011.04.002
- Gonawardena, S. A. S., Ranasinghe, K. E., Arseculeratne, S. N., Seimon, C. R., and Ajello, L. (1994). Survey of mycotic and bacterial keratitis in Sri Lanka. *Mycopathologia.* 127, 77–81.
- Gonzalez-Fernandez, R., and Jorrín-Novo, J. V. (2012). Contribution of proteomics to the study of plant pathogenic fungi. *J Proteome Res.* 11, 3–16. doi: 10.1021/pr200873p
- Gonzalez-Fernandez, R., Valero-Galván, J., Gómez-Gálvez, F. J., Jorrín-Novo, J.V. (2015). Unraveling the in vitro secretome of the phytopathogen *Botrytis cinerea* to understand the interaction with its hosts. *Front. Plant Sci.* 6, 836. doi; 10.3389/fpls.2015.00839

- Gu, H. J., Kim, Y. J., Lee, H. J., Dong, S. H., Kim, S. W., Huh, H. J., and Ki, C. (2016). Invasive Fungal Sinusitis by *Lasiodiplodia theobromae* in a Patient with Aplastic Anemia: An extremely rare case report and literature review. *Mycopathologia*. 181, 901–908. doi: 10.1007/s11046-016-0062-z
- Guégan, S., Garcia-Hermoso, D., Sitbon, K., Ahmed, S., Moguelet, P., Dromer, F., and Lortholary, O. (2016). Ten-year experience of cutaneous and/or subcutaneous infections due to Coelomycetes in France. The French Mycosis Study Group Open Forum Infectious Diseases. doi: 10.1093/ofid/ofw106
- Guida, M., Salvatore, M. M., and Salvatore, F. (2015). A Strategy for GC/MS quantification of polar compounds via their silylated surrogates: silylation and quantification of biological amino acids. *J Anal Bioanal Tech*. 6, 263–279. doi: 10.4172/2155-9872.1000263
- GuoQing Li, G., Arnold, R. J., Liu, F., Li, J., and Chen, S. (2015). Identification and pathogenicity of *Lasiodiplodia* Species from *Eucalyptus urophylla* x *grandis*, *Polyscias balfouriana* and *Bougainvillea spectabilis* in Southern China. *J Phytopathol*. 163, 956–967. doi: 10.1111/jph.12398
- Hahn, H. P. (1997). The type-4 pilus is the major virulence associated adhesin of *Pseudomonas aeruginosa* – a review. *Gene*. 192, 99–108.
- Hamasaki, T., Nagayama, K., and Hatsuda, K. (1976). A new metabolite, l-Alanyl-l-tryptophan anhydride from *Aspergillus chevalieri*. *Agric Biol Chem*. 40, 2487. doi: 10.1271/bbb1961.40.2487
- Hamel, L., Nicole, M., Duplessis, S., and Ellisc, B. E. (2012). Mitogen-activated protein kinase signalling in plant-interacting fungi: distinct messages from conserved messengers. *The Plant Cell*. 24, 1327–1351. doi: 10.1105/tpc.112.096156
- Hankin, L., and Anagnostakis, S. L. (1975). Use of solid media for detection of enzyme production by fungi. *Mycologia* 67(3), 597-607.
- Hasin, Y., Seldin, M., and Lusic, A. (2017). Multi-omics approaches to disease. *Genome Biol*. 18, 83. doi: 10.1186/s13059-017-1215-1
- Hayward, A. C., and Waterston, J. M. (1965). *Agrobacterium tumefaciens*. In: CMI descriptions of pathogenic fungi and bacteria, No. 42. Commonwealth Mycological Institute, Kew, Surrey.
- He, P., Wang, Y., Wang, X., Zhang, X., and Tian, C. (2017). The Mitogen-activated protein kinase CgMK1 governs appressorium formation, melanin synthesis, and plant infection of *Colletotrichum gloeosporioides*. *Front Microbiol*. 8, 2216. doi: 10.3389/fmicb.2017.02216
- Heurlier, K., D'enervaud, V., Haenni, M., Guy, L., Krishnapillai, V., and Haas, D. (2005). Quorum-sensing-negative (lasR) mutants of *Pseudomonas aeruginosa* avoid cell lysis and death. *J Bacteriol*. 187, 4875–4883. doi: 10.1128/JB.187.14.4875-4883.2005
- Horton, P., Park, K., Obayashi, T., Fujita, N., Harada, H., Adams-collier, C. J., and Nakai, K. (2007). WoLF PSORT: protein localization predictor. *Nucleic Acids Res*. 35, W585-7. doi: 10.1093/nar/gkm259

- Howard, R. J. and Valent, B. (1996). Breaking and entering: host penetration by the fungal rice blast pathogen *Magnaporthe grisea*. *Annu Rev Microbiol.* 50, 491–512. doi: 10.1146/annurev.micro.50.1.491
- Hua, C., Zhao, J., and Guo, H. (2018). Trans-Kingdom RNA silencing in plant–fungal pathogen interactions. *Mol Plant.* 11, 235–244. doi: 10.1016/j.molp.2017.12.001
- Hua, X., Zhao, J., DeGrado, W. F., and Binns, A. N. (2013). *Agrobacterium tumefaciens* recognizes its host environment using ChvE to bind diverse plant sugars as virulence signals. *PNAS.* 110, 2, 678–683. doi: 10.1073/pnas.1215033110
- Hube, B. (2004). From commensal to pathogen: stage- and tissue specific gene expression of *Candida albicans*. *Curr Opin Microbiol.* 7, 336–341. doi: 10.1016/j.mib.2004.06.003
- Hube, B. (2009). Fungal adaptation to the host environment. *Curr. Opin. Microbiol.* 12(4), 347–349. doi: 10.1016/j.mib.2009.06.009
- Hummel, J., Strehmel, N., Selbig, J., Walther, D., and Kopka, J. (2010). Decision tree supported substructure prediction of metabolites from GC-MS profiles. *Metabolomics.* 6, 2, 322–333. doi: 10.1007/s11306-010-0198-7
- Hunter, S., Jones, P., Mitchell, A., Apweiler, R., Attwood, T.K., Bateman, A., Yong, S.Y. (2012). InterPro in 2011; new developments in the family and domain prediction database. *Nucleic Acids Res.* 40(D1), 306–312. doi: 10.1093/nar/gkr948
- Husain, A., Ahmad, A., and Agrawal, K. P. (1993). (-)-Jasmonic acid, a phytotoxic substance from *Botryodiplodia theobromae*: characterization by NMR spectroscopic methods. *J Nat Prod.* 56, 2008–2011. doi: 10.1021/np50101a025
- Ishibashi, Y., and Matsumoto, Y. (1984). Intravenous miconazole in the treatment of keratomycosis. *Am J Ophthalmol.* 97, 646–647.
- Islam, M., Haque, M., Islam, M., Emdad, E., Halim, A., Hossen, Q., and Alam, M. (2012). Tools to kill; genome of one of the most destructive plant pathogenic fungi *Macrophomina phaseolina*. *BMC Genomics.* 13(1), 493. doi: 10.1186/1471-2164-13-493
- Jacobson, E. S. (2000). Pathogenic roles for fungal melanins. *Clin Microbiol Rev.* 13, 708–717.
- Jami, F., Slippers, B., Wingfield, M. J., and Gryzenhout, M. (2013). Greater Botryosphaeriaceae diversity in healthy than associated diseased *Acacia karroo* tree tissues. *Aust. Plant Pathol.* 42, 421–430. doi:10.1007/s13313-013-0209-z
- Johnson, L. (2008). Iron and siderophores in fungal–host interactions. *Mycol Res.* 112, 170–183. doi: 10.1016/j.mycres.2007.11.012
- Käll, L., Krogh, A., and Sonnhammer, E. L. (2004). A Combined Transmembrane Topology and Signal Peptide Prediction Method. *J Mol Biol.* 338, 1027–1036. doi: 10.1016/j.jmb.2004.03.016
- Kaplan, F., Kopka, J., Haskell, D. W., Zhao, W., Schiller, K. C., Gatzke, N., Sung, D. W., and Guy, C. L. (2004). Exploring the temperature-stress metabolome of *Arabidopsis*. *Plant Physiol.* 136, 4159–4168. doi: 10.1104/pp.104.052142

- Karkowska-Kuleta, J., Rapala-Kozik, M., and Kozik, A. (2009). Fungi pathogenic to humans; molecular bases of virulence of *Candida albicans*, *Cryptococcus neoformans* and *Aspergillus fumigatus*. *Acta Biochim. Pol.*, 56(2), 211–224.
- Kashima, T., Takahashi, K., Matsuura, H., and Nabeta, K. (2009). Biosynthesis of resorcylic acid lactone lasiodiplodin in *Lasiodiplodia theobromae*. *Biosci Biotechnol Biochem.* 73(5), 1118–1122. doi: 10.1271/bbb.80878
- Kellner, H., Luis, P., Pecyna, M. J., Barbi, F., Kapturska, D., Krüger, D., Zak, D. R., Marmeisse, R., Vandenbol, M., and Hofrichter, M. (2014). Widespread occurrence of expressed fungal secretory peroxidases in forest soils. *PLoS ONE* 9, 4, e95557. doi: 10.1371/journal.pone.0095557
- Khan, M. S. A., Ahmad, I., Aqil, F., Owais, M., Shahid, M., and Musarrat, J. (2010). Virulence and pathogenicity of fungal pathogens with special reference to *Candida albicans*. *Combating fungal infections.* 21-45. doi: 10.1007/978-3-642-12173-9_2k
- Khang, T., and Lau, C. (2015), Getting the most out of RNA-seq data analysis. *Peer J.* 3, e1360; doi: 10.7717/peerj.1360
- Khurana, E., Fu, Y., Colonna, V, Um, X. J., Kang, H. M., Lappalainen, T., Sboner, A., Lochovsky, L., Chen, J., Harmanci, A., Das, J., Abyzoy, A., Balasubramanian, S., Beal, K., Chakravarty, D., Challis, D., Chen, Y., Clarke, D., Clarke, L., Cunningham, F., Evani, U. S., Flicek, P., Fragoza, R., Garrison, E., Gibbs, R., Gumus, Z. H., Herrero, J., Kitabayashi, N., Kong, Y., Lage, K., Liliashvili, V., Lipkin, S. M., MacArthur, D. G., Marth, G., Muzny, D., Pers, T. H., Ritchie, G. R. S., Rosenfeld, J. A., Sisu, C., Wei, X., Wilson, M., Xue, Y., Yu, F., Dermitzakis, E. T., Yu, H., Rubin, M. A., Tyler-Smith, C. and Gerstein, M. (2013). Integrative annotation of variants from 1092 humans: Application to Cancer Genomics. *Science.* 342, 6154, 1235587. doi: 10.1126/science.1235587
- Kikot, G. E., Hours, R. A., and Alconada, T. M. (2009). Contribution of cell wall degrading enzymes to pathogenesis of *Fusarium graminearum*: a review. *J Basic Microbiol.* 49, 231–241. doi: 10.1002/jobm.200800231
- Kim, D., Langmead, B., and Salzberg, S. L. (2015). HISAT: a fast spliced aligner with low memory requirements. *Nat Methods.* 12, 357–360. doi: 10.1038/nmeth.3317
- Kind, T. (2014). AMDIS - Automated mass spectral deconvolution and identification system.
- Kindo, A. J., Pramod, C., Anita, S., and Mohanty, S. (2010). Maxillary sinusitis caused by *Lasiodiplodia theobromae*. *Indian J Med Microbiol.* 28, 167–169. doi: 10.4103/0255-0857.62499
- King, B. C., Waxman, K. D., Nenni, N. V., Walker, L. P., Bergstrom, G. C., and Gibson, D. M. (2011). Arsenal of plant cell wall degrading enzymes reflects host preference among plant pathogenic fungi. *Biotechnol. Biofuels* 4,4. doi: 10.1186/1754-6834-4-4
- Kombrink, A., and Thomma, B. P. H. J. (2013). LysM effectors: secreted proteins supporting fungal life. *PLoS Pathog.* 9, 12, e1003769. doi: 10.1371/journal.ppat.1003769
- Kotogán, A., Németh, B., Vágvölgyi, C., Papp, T., and Takó, M. (2014). Screening for extracellular lipase enzymes with transesterification capacity in *Mucoromycotina* strains. *Food Technol Biotechnol.* 52(1), 73–82.

- Kubicek, C. P., Starr, T. L., and Glass, N. L. (2014). Plant cell wall-degrading enzymes and their secretion in plant-pathogenic fungi. *Annu Rev Phytopathol.* 52, 427–51. doi: 10.1146/annurev-phyto-102313-045831
- Kumamoto, C. A., and Vences, M. D. (2005). Contributions of hyphae and hypha-co-regulated genes to *Candida albicans* virulence. *Cell Microbiol* 7, 1546–1554. doi: 10.1111/j.1462-5822.2005.00616.x
- Kumar, S., Stecher, G., and Tamura, K. (2016). MEGA7: Molecular Evolutionary Genetics Analysis Version 7.0 for Bigger Datasets. *Mol Biol Evol.* 33, 7, 1870–1874. doi: 10.1093/molbev/msw054
- Kunik, T., Tzfira, T., Kapulnik, Y., Gafni, Y., Dingwall, C., and Citovsky, V. (2001). Genetic transformation of HeLa cells by *Agrobacterium*. *Proc Natl Acad Sci USA.* 98, 1871–1876. doi: 10.1073/pnas.98.4.1871
- Lacroix, B., Tzfira, T., Vainstein, A., and Citovsky, V. (2006). A case of promiscuity: *Agrobacterium's* endless hunt for new partners. *Trends Genet.* 22, 29–37. doi: 10.1016/j.tig.2005.10.004
- Laemmli, U. K. (1970). Cleavage of structural proteins during the assembly of the head of bacteriophage T4. *Nature* 227, 680–685. doi:10.1038/227680a0
- Latgé, J. (2007). The cell wall: a carbohydrate armour for the fungal cell. *Mol Microbiol.* 66, 2, 279–290. doi:10.1111/j.1365-2958.2007.05872.x
- Laverde, S., Moncada, L. H., Restrepo, A., and Vera, C. L. (1973). Mycotic keratitis; 5 cases caused by unusual fungi. *Sabouraudia*, 11, 119–123.
- Lekhanont, K., Nonpassopon, M., Nimvorapun, N., and Santanirand, P. (2015). Treatment with intrastromal and intracameral voriconazole in 2 eyes with *Lasiodiplodia theobromae* keratitis: case reports. *Medicine.* 94, e541. doi: 10.1097/MD.0000000000000541
- Lemos, M. F., Soares, A. M., Correia, A. C., and Esteves, A. C. (2010). Proteins in ecotoxicology—how, why and why not? *Proteomics.* 10, 873–887. doi: 10.1002/pmic.200900470
- Leng, Y., and Zhong, S. (2015). The role of Mitogen-Activated Protein (MAP) Kinase signaling components in the fungal development, Sstress response and virulence of the fungal cereal pathogen *Bipolaris sorokiniana*. *PLoS ONE.* 10, 5, e0128291. doi: 10.1371/journal.pone.0128291
- Li, G. Q., Arnold, R. J., Liu, F. F., Li, J. Q., and Chen, S. F. (2015). Identification and pathogenicity of *Lasiodiplodia* species from *Eucalyptus urophyllaxgrandis*, *Polyscias balfouriana* and *Bougainvillea spectabilis* in southern China. *J Phytopathol.* 163, 956–967. doi: 10.1111/jph.12398
- Li, S. T., Yiu, E. P., Wong, A. H., Chun-Ting, J., Lester, Y., and Yu, W. (2016). Successful treatment of *Lasiodiplodia theobromae* keratitis – assessing the role of Voriconazole. *Case Rep Ophthalmol.* 7, 179-185. doi: 10.1159/000449369
- Lima, J. S., Moreira, R. C., Cardoso, J. E., Martins, M. V. V., and Viana, F. M. P. (2013). Cultural, morphological and pathogenic characterization of *Lasiodiplodia theobromae* associated with tropical fruit plants. *Summa Phytopathol.* 39, 81–8. doi: 10.1590/S0100-54052013000200001

- Lind, A. L., Smith, T. D., Saterlee, T., Calvo, A. M., and Rokas, A. (2016). Regulation of secondary metabolism by the velvet complex is temperature-responsive in *Aspergillus*. *G3: Genes, Genomes, Genetics*. 4023-4033. doi: 10.1534/g3.116.033084.
- Lindner, M., Maroschek, M., Netherer, S., Kremer, A., Barbati, A., Garcia- Gonzalo, J., Seidl, R., Delzon, S., Corona, P., Kolstrom, M., Lexer, M. J., Marchetti, M. (2010). Climate change impacts, adaptive capacity, and vulnerability of European forest ecosystems. *For Ecol Manage.* 259, 698–709. doi: 10.1016/j.foreco.2009.09.023
- Liu, S., Hou, Y., Liu, W., Lu, C., Wang, W., and Sun, S. (2015). Components of the calcium-calcineurin signaling pathway in fungal cells and their potential as antifungal targets. *Eukaryot Cell*. 14, 324–334. doi: 10.1128/EC.00271-14.
- López-Berges, M. S., Hera, C., Sulyok, M., Schäfer, K., Capilla, J., Guarro, J., and Pietro, A. D. (2013). The velvet complex governs mycotoxin production and virulence of *Fusarium oxysporum* on plant and mammalian hosts. *Mol Microbiol*. 87, 1, 49–65. doi: 10.1111/mmi.12082
- Lynch, M., and Conery, J. S. (2003). The origins of genome complexity. *Science*. 302, 1401–1404. doi: 10.1126/science.1089370
- Lyu, X., Shen, C., Fu, Y., Xie, J., Jiang, D., Li, G., and Cheng, J. (2015). Comparative genomic and transcriptional analyses of the carbohydrate-active enzymes and secretomes of phytopathogenic fungi reveal their significant roles during infection and development. *Sci Rep*. 5, 15565, 1-16. doi: 10.1038/srep15565
- Macchione, M. M., Merheb, C. W., Gomes, E., and da Silva, R. (2008). Protease production by different thermophilic fungi. *Appl. Biochem. Biotech.* 146(1-3), 223-230. doi: 10.1007/s12010-007-8034-x
- MacDonald, G. M., Bennett, K. D., Jackson, S. T., Parducci, L., Smith, F. A., Smol, J. P., Willis, K. J. (2008). Impacts of climate change on species, populations and communities; palaeobiogeographical insights and frontiers. *Prog Phys Geogr*. 32, 2, 139–172. doi: 10.1177/0309133308094081
- Mandelc, S. Javornik, B. (2015). The secretome of vascular wilt pathogen *Verticillium albo-atrum* in simulated xylem fluid. *Proteomics*. 15; 787-797. doi:10.1002/pmic.201400181
- Maier, T., Guell, M., and Serrano, L. (2009). Correlation of mRNA and protein in complex biological samples. *FEBS Letters*. 583, 3966-3973. doi: 10.1016/j.febslet.2009.10.036
- Chavent, M., Kuentz, V., Labenne, A., Liquet, B., and Saracco, J. (2017). PCAmixdata: multivariate analysis of mixed data. R package version 3.0.
- Marques, M. W., Lima, N. B., de Moraes Jr, M. A., Barbosa, M. A. G., Souza, B. O., Michereff, S. J., Phillips, A.J.L., and Câmara, M. P. S. (2013). Species of *Lasiodiplodia* associated with mango in Brazil. *Fungal Divers*. doi:10.1007/s13225-013-0231-z
- Masi, M., Cimmino, A., Reveglia, P., Mugnai, L., Surico, G., and Evidente, A. (2018). Advances on fungal phytotoxins and their role in grapevine trunk diseases. *J Agric Food Chem*. doi: 10.1021/acs.jafc.8b00773.

- Maslen, M. M., Collis, T., and Stuart, R. (1996). *Lasiodiplodia theobromae* isolated from a subcutaneous abscess in a Cambodian immigrant to Australia. *J Med Vet Mycol.* 34, 279–283.
- Matsumoto, M., and Nago, H. (1994). (R)-2-octeno- δ -lactone and other volatiles produced by *Lasiodiplodia theobromae*. *Biosc Biotechnol and Biochem.* 58, 7, 1262-1266. doi: 10.1271/bbb.58.1262
- Mattern, D. J., Schoeler, H., Weber, J., Novohradská, S., Kraibooj, K., Dahse, H., Hillmann, F., Valiante, V., Thilo, M., and Brakhage, A. (2015). Identification of the antiphagocytic trypacidin gene cluster in the human-pathogenic fungus *Aspergillus fumigatus*. *Appl Microbiol Biotechnol.* 99, 10151–10161. doi: 10.1007/s00253-015-6898-1
- Medema, M. H., Bink, K., Cimermantic, P., de Jager, V., Zakrzewski, P., Fischbach, M. A., Weber, T., Takano, E., and Breitling, R. (2011). antiSMASH: rapid identification, annotation and analysis of secondary metabolite biosynthesis gene clusters in bacterial and fungal genome sequences. *Nucleic Acids Res.* 39, W339–W346. doi: 10.1093/nar/gkr466
- Mehl, J., Wingfield, M. J., Roux, J., and Slip, B., (2017). Invasive everywhere? Phylogeographic analysis of the globally distributed tree pathogen *Lasiodiplodia theobromae*. *Forests.* 8(5), 145. doi: 10.3390/f8050145
- Miller, G. L. (1959). Use of dinitrosalicylic acid reagent for determination of reducing sugar. *Anal Chem.* 31(3), 426-428. doi: 10.1021/ac60147a030
- Miranda, C. C. B. O., Dekker, R. F. H., Serpeloni, J. M., Fonseca, E. A. I., Cólus, I. M. S., and Barbosa, A. M. (2008). Anticlastogenic activity exhibited by botryosphaeran, a new exopolysaccharide produced by *Botryosphaeria rhodina* MAMB-05. *Int J Biol Macromol.* 42, 172–177. doi: 10.1016/j.ijbiomac.2007.10.010
- Mohan, M. Shalin, S. C., Kothari, A., Rico, J. C. C., Caradine, K., and Burgess, M. (2016). *Lasiodiplodia* species fungal osteomyelitis in a multiple myeloma patient. *Transpl Infect Dis.* 0, 1-4. doi: 10.1111/tid.12573
- Möller, E. M., Bahnweg, G., Sandermann, H., and Geiger, H. H. (1992). A simple and efficient protocol for isolation of high molecular weight DNA from filamentous fungi, fruit bodies, and infected plant tissues. *Nucl Acids Res.* 22, 6115-6116.
- Monod, M., Capoccia, S., Léchenne, B., Zaugg, C., Holdom, M., and Jousson, O. (2002). Secreted proteases from pathogenic fungi. *Int J Med Microbiol.* 292, 405–419. doi: 10.1078/1438-4221-00223
- Morales-Cruz, A., Amrine, K. C. H., Blanco-Ulate, B., Lawrence, D. P., Travadon, R., Rolshausen, P. E., Baumgartner, K., and Cantu, D. (2015). Distinctive expansion of gene families associated with plant cell wall degradation, secondary metabolism, and nutrient uptake in the genomes of grapevine trunk pathogens. *BMC Genomics* 16-469. doi: 10.1186/s12864-015-1624-z
- Mulder, N., and Apweiler, R. (2007). InterPro and InterProScan: tools for protein sequence classification and comparison. *Methods Mol Biol.* 396, 59-70. doi: 10.1007/978-1-59745-515-2_5.

- Murphy, C., Powlowski, J., Wu, M., Butler, G., Tsang, A. (2011). Curation of characterized glycoside hydrolases of fungal origin. *Database*, 2011, 1–14. doi; 10.1093/database/bar020
- Nelson, D. R. (2009). The Cytochrome P450 Homepage. *Hum genomics*. 4, 59–65
- Netto, M. S. B., Assunção, I. P., and Lima, G. S. A. (2014). Species of *Lasiodiplodia* associated with papaya stem-end rot in Brasil. *Fungal Divers*. 67, 127–41. doi: 10.1007/s13225-014-0279-4
- Nguyen, N. (2008). Importance of secreted lipases for virulence of the phytopathogenic fungus *Fusarium graminearum*. 1-110. *Annu Rev of Ecol Evol Syst*. 35, 675–700. doi: 10.1146/annurev.ecolsys.34.011802.132339
- Niehaus, E., Rindermann, L., Janevska, S., Münsterkötter, M., Güldener, U., Tudzynski, B. (2018). Analysis of the global regulator Lae1 uncovers a connection between Lae1 and the histone acetyltransferase HAT1 in *Fusarium fujikuroi*. *Appl Microbiol Biotechnol*. 102, 279–295. doi: 10.1007/s00253-017-8590-0
- Nierman, W. C., Pain, A., Anderson, M. J., Wortman, J. R., Kim, H. S., Arroyo, J., Berriman, M., Abe, K., Archer, D. B., Bermejo, C., Bennett, J., Bowyer, P., Chen, D., Collins, M., Coulsen, R., Davies, R., Dyer, P. S., Farman, M., Fedorova, N., Fedorova, N., Feldblyum, T. V., Fischer, R., Fosker, N., Fraser, A., García, J. L., García, M. J., Goble, A., Goldman, G. H., Gomi, K., Griffith-Jones, S., Gwilliam, R., Haas, B., Haas, H., Harris, D., Horiuchi, H., Huang, J., Humphray, S., Jiménez, J., Keller, N., Khouri, H., Kitamoto, K., Kobayashi, T., Konzack, S., Kulkarni, R., Kumagai, T., Lafon, A., Latgé, J. P., Li, W., Lord, A., Lu, C., Majoros, W. H., May, G. S., Miller, B. L., Mohamoud, Y., Molina, M., Monod, M., Mouyna, I., Mulligan, S., Murphy, L., O'Neil, S., Paulsen, I., Peñalva, M. A., Perteua, M., Price, C., Pritchard, B. L., Quail, M. A., Rabbinowitsch, E., Rawlins, N., Rajandream, M. A., Reichard, U., Renauld, H., Robson, G. D., Rodriguez de Córdoba, S., Rodríguez-Peña, J. M., Ronning, C. M., Rutter, S., Salzberg, S. L., Sanchez, M., Sánchez-Ferrero, J. C., Saunders, D., Seeger, K., Squares, R., Squares, S., Takeuchi, M., Tekaia, F., Turner, G., Vazquez de Aldana, C. R., Weidman, J., White, O., Woodward, J., Yu, J. H., Fraser, C., Galagan, J. E., Asai, K., Machida, M., Hall, N., Barrell, B., and Denning, D. W. (2005). Genomic sequence of the pathogenic and allergenic filamentous fungus *Aspergillus fumigatus*. *Nature*. 438, 1151–1156. doi: 10.1038/nature04332
- Nosanchuk, J. D., and Casadevall, A. (2006). Impact of melanin on microbial virulence and clinical resistance to antimicrobial compounds. *Antimicrob Agents Chemother*. 50, 3519–3528. doi: 10.1128/AAC.00545-06
- Nosanchuk, J. D., Nimrichter, L., Casadevall, A., and Rodrigues, M. L. (2008). A role for vesicular transport of macromolecules across cell walls in fungal pathogenesis. *Commun Integr Biol*. 1, 1, 37–39.
- Nouguier, R., Gastaldi, S., Stien, D., Bertrand, M., Villar, F., Andrey, O., and Renaud, P. (2003). Synthesis of (±)- and (-)-botryodiplodin using stereoselective radical cyclizations of acyclic esters and acetals. *Tetrahedron: Asymmetry* 14, 3005–3018. doi: 10.1016/j.tetasy.2003.06.004
- Nucci, M., and Marr, K. A. (2005). Emerging Fungal Diseases. *Clin Infect Dis*. 41, 521–6. doi: 1058-4838/2005/4104-0017\$15.00

- Pahl, H. L., Krauss, B., Schulze-Osthoff, K., Decker, T., Traenckner, E. B., Vogt, M., Myersfl, C., Parksfl, T., Warring, P., Miihlbacher, A., Czernilofiky, A., and Baeuerle, P. A. (1996). The immunosuppressive fungal metabolite gliotoxin specifically inhibits transcription factor NF-kappaB. *J Exp Med.* 183, 1829–1840.
- Pandi, M., Kumaran, R. S., Choi, Y., Kim, H. J., Muthumary, J., (2011). Isolation and detection of taxol, an anticancer drug produced from *Lasiodiplodia theobromae*, an endophytic fungus of the medicinal plant *Morinda citrifolia*. *Afr J Biotechnol.* 10, 8, 1428–1435. doi: 10.5897/AJB10.950
- Pandi, M., Manikandan, R., and Muthumary, J. (2010). Anticancer activity of fungal taxol derived from *Botryodiplodia theobromae* Pat., an endophytic fungus, against 7, 12 dimethyl benz(a)anthracene (DMBA)-induced mammary gland carcinogenesis in Sprague dawley rats. *Biomed Pharmacother.* 64, 48–53. doi: 10.1016/j.biopha.2009.03.001.
- Paolinelli-Alfonso, M., Galindo-Sánchez, C. E., Hernandez-Martinez, R. (2016). Quantitative real-time PCR normalization for gene expression studies in the plant pathogenic fungi *Lasiodiplodia theobromae*. *J Microbiol Methods.* 127, 82–88. doi: 10.1016/j.mimet.2016.05.021
- Paolinelli-Alfonso, M., Villalobos-Escobedo, J. M., Rolshausen, P., Herrera-Estrella, A., Galindo-Sánchez, C., López-Hernández, J. F., and Hernandez-Martinez R. (2016). Global transcriptional analysis suggests *Lasiodiplodia theobromae* pathogenicity factors involved in modulation of grapevine defensive response. *BMC Genomics.* 17, 615. doi: 10.1186/s12864-016-2952-3
- Papacostas, L. J., Henderson, A., Choong, K., Sowden, D. (2015). An unusual skin lesion caused by *Lasiodiplodia theobromae*. *Med Mycol Case Rep.* 8, 44–46. doi: 10.1016/j.mmcr.2015.03.002
- Park, M., Do, E., and Jung, W. H. (2013). Lipolytic enzymes involved in the virulence of human pathogenic fungi. *Mycobiology.* 41, 2, 67-72. doi: 10.5941/MYCO.2013.41.2.67
- Parker, I. M., and Gilbert, G. S. (2004). The evolutionary ecology of novel plant–pathogen interactions. *Annu Rev Ecol Evol Syst.* 35, 675–700. doi: 10.1146/annurev.ecolsys.34.011802.132339
- Patkar, R., Benke, P., Qu, Z., Chen, Y., Yang, F., Swarup, S., and Naqvi, N. (2015). A fungal monooxygenase-derived jasmonate attenuates host innate immunity. *Nat Chem Biol.* 11, 733–740. doi: 10.1038/nchembio.1885
- Pérez-Miranda, S., Cabirol, N., George-Téllez, R., Zamudio-Rivera, L. S., and Fernández, F. J. (2007). O-CAS, a fast and universal method for siderophore detection. *J Microbiol. Methods* 70, 127–131. doi: 10.1016/j.mimet.2007.03.023
- Petersen, T. N., Brunak, S., von Heijne, G., and Nielsen, H. (2011). SignalP 4.0: discriminating signal peptides from transmembrane regions. *Nat Methods* 8, 785–786.
- Peterson, R., Grinyer, J., and Nevalainen, H. (2011). Extracellular hydrolase profiles of fungi isolated from koala faeces invite biotechnological interest. *Mycol. Prog.* 10, 207–218. doi: 10.1007/s11557-010-0690-5
- Pflugfelder, S. C., Flynn, H. W., Zwickey, T. A., Forster, R. K., Tsiligianni, A., Culbertson, W. W., and Mandelbaum, S. (1988). Exogenous fungal endophthalmitis. *Ophthalmology.* 95, 19–30.

- Phillips, A. J. L. (2002). Botryosphaeria species associated with diseases of grapevines in Portugal. *Phytopathol Mediterr.* 41, 3–18. doi:10.14601/Phytopathol_Mediterr-1655
- Phillips, A. J. L., Alves, A., Abdollahzadeh, J., Slippers, B., Wingfield, M. J., Groenewald, J. Z., and Crous, P. W. (2013). The Botryosphaeriaceae: genera and species known from culture. *Stud Mycol.* 76, 51–167. doi: 10.3114/sim0021
- Phillips, A. J. L., Alves, A., Pennycook, S. R., Johnston, P. R., Ramaley, A., Akulov, A., and Crous, P. W. (2008). Resolving the phylogenetic and taxonomic status of dark-spored teleomorph genera in the Botryosphaeriaceae. *Persoonia.* 21, 29–55. doi: 10.3767/003158508X340742
- Piñeiro, C., Cañas, B., and Carrera, M. (2010). The role of proteomics in the study of the influence of climate change on sea food products. *Food Res Int.* 43, 1791–1802. doi: 10.1016/j.foodres.2009.11.012
- Pitt, W. M., Huang, R., Steel, C. C., and Savocchia, S. (2010). Identification, distribution and current taxonomy of Botryosphaeriaceae species associated with grapevine decline in New South Wales and South Australia. *Aus J Grape Wine Res.* 16, 258–271.
- Pohlert, T. (2014). The pairwise multiple comparison of mean ranks package (PMCMR). R package, version 4.1.
- Ponnala, L., Wang, Y., Sun, Q., and Wijk, K. J. v. (2014). Correlation of mRNA and protein abundance in the developing maize leaf. *Plant J.* 78, 3, 424–440. doi: 10.1111/tpj.12482
- Prasher, I. B., and Dhanda, R. K. (2017). *Lasiodiplodia hormozganensis*: First report as an endophyte and a new record for India. *Kavaka.* 48, 2, 59-60.
- Punithalingam, E. (1976). *Botryodiplodia theobromae*. C.M.I. Descript. Fungi Bact. 519, 1–2.
- Punithalingam, E. (1980). Plant diseases attributed to *Botryodiplodia theobromae* Pat. Vaduz, Liechtenstein, J. Cramer.
- Puttana, S. T. (1967). Mycotic infections of the cornea. *J All-India Ophthalmol. Soc.* 15, 11–18.
- Qian, C. D., Fu, Y. H., Jiang, F. S., Xu, Z. H., Cheng, D. Q., Ding, B., Gao, C. X., and Ding, Z. S. (2014). *Lasiodiplodia* sp. ME4-2, an endophytic fungus from the floral parts of *Viscum coloratum*, produces indole-3-carboxylic acid and other aromatic metabolites. *BMC Microbiol.* 14: 297, 1-7. doi: 10.1186/s12866-014-0297-0
- R Core Team (2015). R: A language and environment for statistical computing. Vienna: R Foundation for Statistical Computing.
- Ramirez-Suero, M., Benard-Gellon, M., Chong, J., Laloue, H., Stempien, E., Abou-Mansour, E., Fontaine, F., Larignon, P., Mazet-Kieffer, F., Farine, S., and Bertsch, C. (2014). Extracellular compounds produced by fungi associated with *Botryosphaeria dieback* induce differential defence gene expression patterns and necrosis in *Vitis vinifera* cv. Chardonnay cells. *Protoplasma.* 251, 6, 1417-26. doi: 10.1007/s00709-014-0643-y.
- Ratledge, C., and Dover, L. G. (2000). Iron metabolism in pathogenic bacteria. *Annu Rev Microbiol.* 54, 881–941. doi: 10.1146/annurev.micro.54.1.881

- Rawlings, N. D., and Bateman, A. (2009). Pepsin homologues in bacteria. *BMC Genomics*. 10, 437. doi: 10.1186/1471-2164-10-437
- Rebell, G., and Forster, R. K. (1976). *Lasiodiplodia theobromae* as a cause of keratomycoses. *Sabouraudia*. 14, 155–170.
- Rehnberg, N., and Magnusson, G. (1990). General conjugate-addition method for the synthesis of enantiomerically pure lignans. Total synthesis of (-)-and (+)-burseran,(-)-dehydroxycubebin,(-)-trichostin,(-)-cubebin,(-)-5"-methoxyhinokinin, and (-)-hinokinin. *J Org Chem*. 55, 4340-4349.
- Rehnstrom, A. L., and Free, S. J. (1996). The isolation and characterization of melanin-deficient mutants of *Monilinia fructicola*. *Physiol Mol Plant Pathol*. 49, 321–330. doi: 10.1006/pmpp.1996.0057
- Reichard, U., Léchenne, B., Asif, A. R., Streit, F., Grouzmann, E., Jousson, O., and Monod, M. (2006). Sedolisins, a new class of secreted proteases from *Aspergillus fumigatus* with endoprotease or tripeptidyl-peptidase activity at acidic pHs. *Appl. Environ. Microbiol*. 72, 1739–1748. doi:10.1128/AEM.72.3.1739-1748.2006
- Reignault, Ph., Valette-Collet, O., and Boccara, M. (2008). The importance of fungal pectinolytic enzymes in plant invasion, host adaptability and symptom type. *Eur J Plant Pathol*. 120, 1–11. doi: 10.1007/s10658-007-9184-y
- Reis, H., Pfiffi, S., and Hahn, M. (2005). Molecular and functional characterization of a secreted lipase from *Botrytis cinerea*. *Mol Plant Pathol*. 6(3), 257-267. doi: 10.1111/J.1364-3703.2004.00280.X
- Renshaw, J. C., Robson, G. D., Trinci, A. P. J., Wiebe, M. G., Livens, F. R., Collison, D., and Taylor, R. J. (2002). Fungal siderophores: structures, functions and applications. *Mycol Res*. 106, 10, 1123–1142. doi: 10.1017/S0953756202006548
- Restrepo, A., Arango, M., Velez, H., and Uribe, L. (1976). The isolation of *Botryodiplodia theobromae* from a nail lesion. *Sabouraudia*. 14, 1–4.
- Rigling, D. (1995). Isolation and characterization of *Cryphonectria parasitica* mutants that mimic a specific effect of hypovirulence-associated dsRNA on laccase activity. *Can J Botany*. 73(10), 1655-1661. doi:10.1139/b95-179
- Robinson, M. D., McCarthy, D. J., and Smyth, G. K. (2010). edgeR: a Bioconductor package for differential expression analysis of digital gene expression data. *Bioinformatics*. 26, 1,139-140. doi:10.1093/bioinformatics/btp616.
- Rodrigues, M. L., Nosanchuk, J. D., Schrank, A., Vainstein, M. H., Casadevall, A., and Nimrichter, L. (2011). Vesicular transport systems in fungi. *Future Microbiol*. 6, 11, 1371–1381. doi: 10.2217/fmb.11.112
- Rodríguez-Gálvez, E., Guerrero, P., Barradas, C., Crous, W., and Alves, A. (2017). Phylogeny and pathogenicity of *Lasiodiplodia* species associated with dieback of mango in Peru. *Fungal Biol*. 121, 452-465. doi: 10.1016/j.funbio.2016.06.004

- Rodríguez-Gálvez, E., Maldonado, E., and Alves, A. (2015). Identification and pathogenicity of *Lasiodiplodia theobromae* causing dieback of table grapes in Peru. *Eur J Plant Pathol.* 141, 477–489. doi: 10.1007/s10658-014-0557-8
- Rosado, A. W. C., Machado, A. R., Freire, F. C. O., and Pereira, O. L. (2016). Phylogeny, identification, and pathogenicity of *Lasiodiplodia* associated with postharvest stem-end rot of coconut in Brazil. *Plant Dis.* 100, 561-568. doi: 10.1094/PDIS-03-15-0242-RE
- Rosas, A. L., and Casadevall, A. (2001). Melanization decreases the susceptibility of *Cryptococcus neoformans* to enzymatic degradation. *Mycopathologia* 151, 53–56.
- Rukachaisirikul, R., Arunpanichlert, J., Sukpondma, Y., Phongpaichit, S., and Sakayaroj, J. (2009). Metabolites from the endophytic fungi *Botryosphaeria rhodina* PSU-M35 and PSU-M114. *Tetrahedron.* 65, 10590-10595. doi: 10.1016/j.tet.2009.10.084
- Ryder, L. S., and Talbot, N. J. (2015). Regulation of appressorium development in pathogenic fungi. *Curr Opin Plant Biol.* 26, 8–13. doi: 10.1016/j.pbi.2015.05.013
- Saeed, A. (2016). Isocoumarins, miraculous natural products blessed with diverse pharmacological activities. *Eur J Med Chem.* 116, 290–317. doi: 10.1016/j.ejmech.2016.03.025
- Sagnolo, A., Mondello, V., Larignon, P., Villaume, S., Rabenoelina, F., Clément, C., and Fontaine, F. (2017). Defense responses in grapevine (cv. Mourvèdre) after inoculation with the *Botryosphaeria* dieback pathogens *Neofusicoccum parvum* and *Diplodia seriata* and their relationship with flowering. *Int J Mol Sci.* 18, 393. doi: 10.3390/ijms18020393
- Saha, S., Sengupta, J., Banerjee, D., and Khetan, A. (2012a). *Lasiodiplodia theobromae* keratitis: a case report and review of literature. *Mycopathologia* 174, 335–339. doi: 10.1007/s11046-012-9546-7
- Saha, S., Sengupta, J., Banerjee, D., and Khetan, A. (2012b). *Lasiodiplodia theobromae* keratitis: a rare fungus from eastern India. *Microbiol Res.* 3, 82–83. doi: 10.4081/mr.2012.e19
- Saier, M. H., Tran, C. V., and Barabote, R. D. (2006). TCDB: the Transporter Classification Database for membrane transport protein analyses and information. *Nucleic Acids Res.* 34(Database issue), D181-D186. doi: 10.1093/nar/gkj001.
- Sajith, S., Priji, P., Sreedevi, S., and Benjamin, S. (2016). An overview on fungal cellulases with an industrial perspective. *J Nutr Food Sci.* 6, 461. doi: 10.4172/2155-9600.1000461
- Sakalidis, M. L., Hardy, StJ., Hardy, G. E., and Burgess, T. I. (2011). Endophytes as potential pathogens of the baobab species *Androsoria gregorii*: a focus on the *Botryosphaeriaceae*. *Fungal Ecol.* 1-14. doi: 10.1016/j.funeco.2010.06.001
- Salihu, A., and Alam, Md. Z. (2014). Thermostable lipases: an overview of production, purification and characterization. *Biosci Biotechnol Res Asia* 11 (3), 1095-1107.
- Salvatore, M. M., DellaGreca, M., Nicoletti, R., Salvatore, F., Vinale, F., Naviglio, D., and Andolfi, A. (2018). Talarodiolide, a new 12-membered macrodiolide, and GC/MS investigation of culture filtrate and mycelial extracts of *Talaromyces pinophilus*. *Molecules.* 23, 950. doi: 10.3390/molecules23040950.

- Samudio, M., Lapsing, F., Farina, N., Franco, A., Mino de Kaspar, H., and Giusiano, G. (2014). Keratitis by *Lasiodiplodia theobromae*: a case report and literature review. *Rev Chilena Infectol.* 31, 750–754. doi: 10.4067/S0716-1018201400060001
- Santos, A. L., Moreirinha, C., Lopes, D., Esteves, A. C., Henriques, I., Almeida, A., Delgadillo, I. (2013). Effects of UV radiation on the lipids and proteins of bacteria studied by mid-infrared spectroscopy. *Environ Sci Technol.* 47, 6306–6315. doi: 10.1021/es400660g
- Savocchia, S., Steel, C. C., Stodart, B. J., and Somers, A. (2007). Pathogenicity of *Botryosphaeria* species isolated from declining grapevines in sub tropical regions of Eastern Australia. *Vitis* 46, 27-32. doi:10.1094/PDIS-93-6-0584
- Scholthof, K. (2007). The disease triangle: pathogens, the environment and society. *Nat Rev Microbiol.* 5, 152-156.
- Scully, L. R., and Bidochka, M. J. (2005). Serial passage of the opportunistic pathogen *Aspergillus flavus* through an insect host yields decreased saprobic capacity. *Can J Microbiol.* 51, 185–189. doi: 10.1139/w04-124
- Shapiro, R. S., Robbins, N., and Cowen, L. E. (2011). Regulatory circuitry governing fungal development, drug resistance, and disease. *Microbiol Mol Biol Rev.* 75, 2, 1092-2172. doi: 10.1128/MMBR.00045-10
- Slippers, B., Boissin, E., Phillips, A. J. L., Groenewald, J. Z., Lombard, L., Wingfield, M. J., Postma, A., Burgess, T., and Crous, P. W. (2013). Phylogenetic lineages in the *Botryosphaeriales*: a systematic and evolutionary framework. *Studies in Mycology* 76, 31–49. doi: 10.3114/sim0020
- Slippers, B., and Wingfield, M. J. (2007). Botryosphaeriaceae as endophytes and latent pathogens of seed-borne tree pathogens in the southern hemisphere. *Int Forest Rev.* 4, 56–65. doi: 10.1016/j.fbr.2007.06.002
- Slippers, B., Burgess, T. I., Pavlic, D., Ahumada, R., Maleme, H., Mohali, S. R., Rodas, C. A., Wingfield, M. J. (2009). A diverse assemblage of Botryosphaeriaceae infects *Eucalyptus* in native and non-native environments. *Southern Forests.* 71, 101-110. doi: 10.2989/SF.2009.71.2.3.818
- Slippers, B., Roux, J., Wingfield, M. J., Van der Walt, F. J. J., Jami, F., Mehl, J. W. M., Marais, G. J. (2014). Confronting the constraints of morphological taxonomy in the Botryosphaeriales. *Persoonia* 33, 155–168. doi: 10.3767/003158514X684780
- Slippers, B., Stenlid, J., and Wingfield, M. J. (2005). Emerging pathogens: fungal host jumps following the globally distributed tree pathogen *Lasiodiplodia theobromae*. *Forests.* 8, 145. doi: 10.3390/f8050145
- Slippers, B., Wingfield, M. J. (2007). Botryosphaeriaceae as endophytes and latent pathogens of woody plants: diversity, ecology and impact. *Fungal Biol Rev.* 21, 90–106. doi: 10.1016/j.fbr.2007.06.002
- Smit, A., Hubley, R., and Green, P. (2015). RepeatMasker. Open-4.0 Available at: <http://www.repeatmasker.org/>. (Accessed: 6th June 2017)

- Sonnhammer, E. L., von Heijne, G., and Krogh, A. (1998). A hidden Markov model for predicting transmembrane helices in protein sequences. *Proceedings Int Conf Intell Syst Mol Biol.* 6, 175–82.
- Spikes, S., Xu, R., Nguyen, K., Chamilos, G., Kontoyiannis, D. P., Jacobson, R. H., Ejzykowitz, D. E., Chiang, L. Y., Filler, S. G., and May, G., S. (2008). Gliotoxin production in *Aspergillus fumigatus* contributes to host-specific differences in virulence. *J Infect Dis.* 197, 479–86. doi: 10.1086/525044
- St Leger, R. J., Joshi, L., and Roberts, D. W. (1997). Adaptation of proteases and carbohydrases of saprophytic, phytopathogenic and entomopathogenic fungi to the requirements of their ecological niches. *Microbiol.* 143, 1983-1992.
- Stein, S. E. (1999). An integrated method for spectrum extraction and compound identification from gas chromatography/mass spectrometry data. *J Am Soc Mass Spectr.* 10, 8, 770-781.
- Stein, S. E. (2017). NIST Standard Reference Database 1A v17.
- Summerbell, R. C., Krajden, S., Levine, R., and Fuksa, M. (2004). Subcutaneous phaeohyphomycosis caused by *Lasiodiplodia theobromae* and successfully treated surgically. *Med Mycol.* 42, 543–547. doi: 10.1080/136937804000 05916
- Suryanarayanan, T. S., Thirunavukkarasu, N., Govindarajulu, M. B., and Gopalan, V. (2012). Fungal endophytes: an untapped source of biocatalysts. *Fungal Divers.* 54(1), 19-30. doi: 10.1007/s13225-012-0168-7
- Thew, M. R. J., and Franzco, B. T. (2008). Fungal keratitis in far north Queensland, Australia. *Clin Experiment Ophthalmol.* 36, 721–724. doi: 10.1111/j.1442-9071.2008.01879.x
- Thomas, O. A., Kuriakose, T., Kirupashanker, M. P., and Maharajan, V. S. (1991). Use of lactophenol cotton blue mounts of corneal scraping as an aid to the diagnosis of mycotic keratitis. *Diagn Microbiol Infect Dis.* 14, 219–224.
- Thomma, B. P. H. J., Penninckx, I. A. M. A., Broekaert, W. F., and Cammue, B. P. A. (2001). The complexity of disease signaling in *Arabidopsis*. *Curr Opin Immunol.* 13, 63–68.
- Thompson, J.D., Gibson, T.J., Plewniak, F., Jeanmougin, F., and Higgins, D.G. (1997). The ClustalX windows interface: flexible strategies for multiple sequence alignment aided by quality analysis tools. *Nucleic Acids Research* 25: 4876–4882.
- Tiwari, S., Thakur, R., and Shankar, J. (2015). Role of heat-shock proteins in cellular function and in the biology of fungi. *Biotechnol Res Int.* 1-11. doi: 10.1155/2015/132635
- Tóth, A., Németh, T., Csonka, K., Horváth, P., Vágvolgyil, C., Vizler, C., Nosanchuck, J. D., and Gácsér, A. (2014). Secreted *Candida parapsilosis* lipase modulates the immune response of primary human macrophages. *Virulence.* 5(4), 555–562. doi: 10.4161/viru.28509
- Tsukada, K., Takahashi, K., and Nabeta, K. (2010). Biosynthesis of jasmonic acid in a plant pathogenic fungus, *Lasiodiplodia theobromae*. *Phytochem.* 71, 2019-2023. doi:10.1016/j.phytochem.2010.09.013

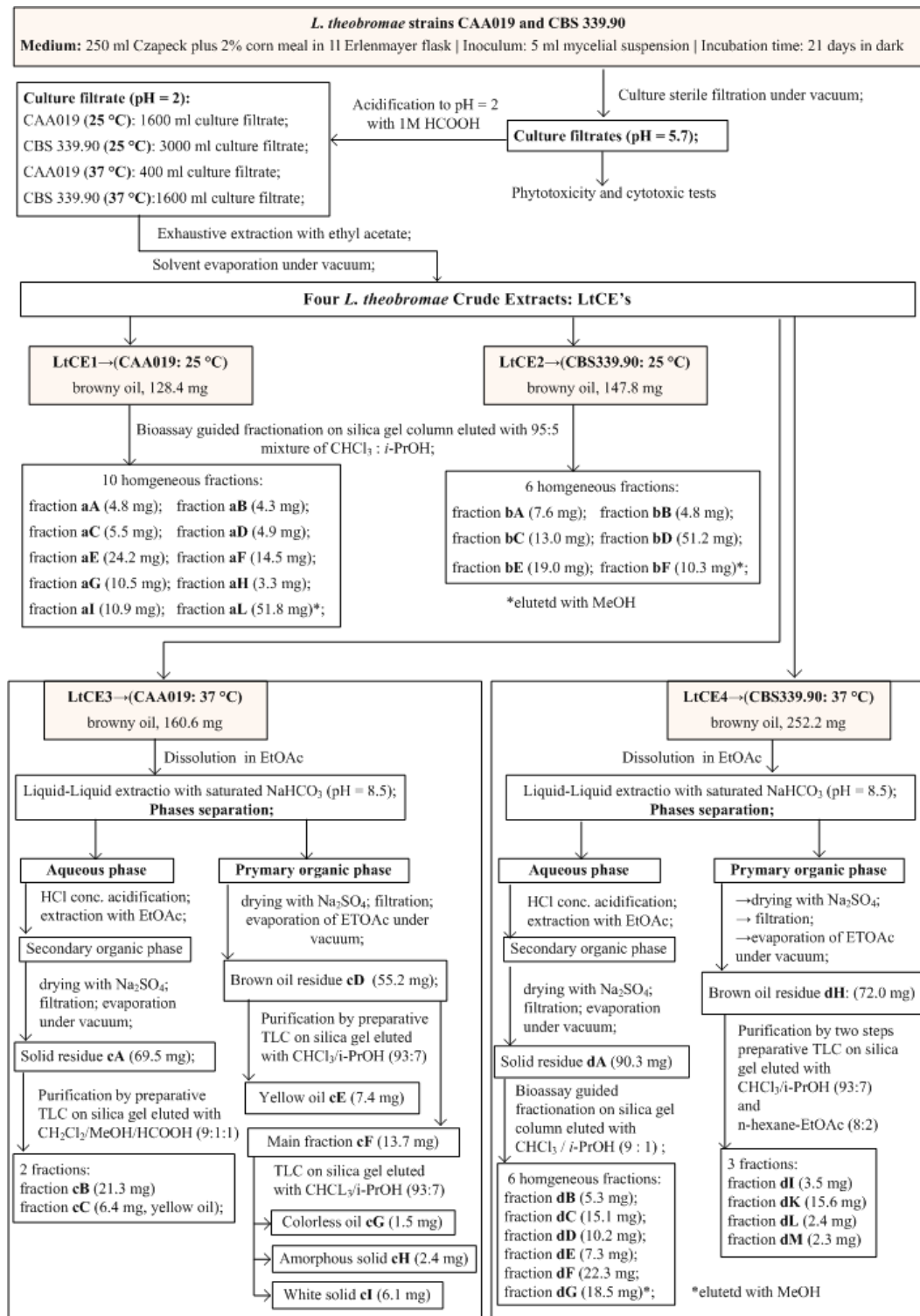
- Tsunawaki, S., Yoshida, L. S., Nishida, S., Kobayashi, T., and Shimoyama, T. (2004). Fungal metabolite gliotoxin inhibits assembly of the human respiratory burst NADPH oxidase. *Infect Immun.* 72, 3373–3382. doi: 10.1128/IAI.72.6.3373-3382.2004
- Úranga, C. C., Ghassemian, M., and Hernández-Matínez, R. (2017). Novel proteins from proteomic analysis of the trunk disease fungus *Lasiodiplodia theobromae* (Botryosphaeriaceae). *Biochimie Open.* 4, 88e98. doi: 10.1016/j.biopen.2017.03.001
- Úrbez-Torres, J. R. (2011). The status of Botryosphaeriaceae species infecting grapevine. *Phytopathol. Mediterr.* 50, S5–S45. doi: 10.14601/Phytopathol_Mediterr-9316
- Úrbez-Torres, J. R., and Gubler, W. D. (2009). Pathogenicity of Botryosphaeriaceae species isolated from grapevine cankers in California. *Plant Dis.* 93(6), 584-592. doi: 10.1094/PDIS-93-6-0584
- Úrbez-Torres, J. R., Castro-Medina, F., Mohali, S. R., and Gubler, W. D. (2016). Botryosphaeriaceae species associated with cankers and dieback symptoms of *Acacia mangium* and *Pinus caribaea var. hondurensis* in Venezuela. *Plant Dis.* 100, 2455-2464. doi: 10.1094/PDIS-05-16-0612-RE
- Úrbez-Torres, J. R., Leavitt, G. M., Guerrero, J. C., Guevara, J., and Gubler, W. D. (2008). Identification and pathogenicity of *Lasiodiplodia theobromae* and *Diplodia seriata*, the causal agents of bot canker disease of grapevines in Mexico. *Plant Dis.* 92, 519-529. doi:10.1094/PDIS-92-4-0519
- Úrbez-Torres, J. R., Leavitt, G. M., Voegel, T. M., and Gubler, W. D. (2006). Identification and distribution of *Botryosphaeria spp.* associated with grapevine cankers in California. *Plant Dis.* 90, 1490-1503. doi:10.1094/PD-90-1490
- Valenton, M. J., Rinaldi, M. G., and Butler, E. E. (1975). A corneal abscess due to the fungus *Botryodiplodia theobromae*. *Can J Ophthalmol.* 10, 416–418.
- Van der Does, H. C., and Rep, M. (2007). Virulence genes and the evolution of hosts specificity in plant-pathogenic fungi. *Mol Plant Microbe Interact.* 20, 1175–1182. doi: 10.1094/MPMI-20-10-1175
- van Niekerk, J. M., Crous, P. W., Groenewald, J. Z., Fourie, P. H., and Halleen, F. (2004). DNA phylogeny, morphology and pathogenicity of Botryosphaeria species on grapevines. *Mycologia* 96, 781-798.
- van Niekerk, J. M., Fourie, P. H., Halleen, F., and Crous, P. W. (2006). *Botryosphaeria spp.* as grapevine trunk disease pathogens. *Phytopathol Mediterr.* 45, S43–S54. doi: 10.14601/Phytopathol_Mediterr-1843
- Vandamme, E. J. (2003). Bioflavours and fragrances via fungi and their enzymes. *Fung Div.* 13, 153-166.
- Vandesompele, J. qPCR guide. 2009: <http://www.bio-rad.com/en-pt/applications-technologies/qpcr-assay-design-optimization?ID=LUSO7RIVK#3> (Accessed 4 Dec 2017).

- Vögele, R. T., and Mendgen, K. (2003). Rust haustorium: nutrient uptake and beyond. *New Phytol* 159, 93–100. doi: 10.1046/j.1469-8137.2003.00761.x
- Voigt, C. A., Schafer, W., and Salomon, S. (2005). A secreted lipase of *Fusarium graminearum* is a virulence factor required for infection of cereals. *The Plant J.* 42, 364–375. doi: 10.1111/j.1365-313X.2005.02377.x
- Wasylnka, J. A., and Moore, M. M. (2002). Uptake of *Aspergillus fumigatus* conidia by phagocytic and nonphagocytic cells *in vitro*: quantitation using strains expressing green fluorescent protein. *Infect Immun.* 70, 3156–3163.
- Weiberg, A., Wang, M., Lin, F. M., Zhao, H., Zhang, Z., Kaloshian, I., Huang, H. D., and Jin, H. (2013). Fungal small RNAs suppress plant immunity by hijacking host RNA interference pathways. *Science.* 342, 118–123. doi: 10.1126/science.1239705.
- Weinberg, E. D. (2000). Modulation of intramacrophage iron metabolism during microbial cell invasion. *Microbes Infect.* 1, 85–89. doi: 10.1016/S1286-4579(00)00281-1
- Wicklow, D. T. (1988). Metabolites in the coevolution of fungal chemical defense systems. *Coevolution of fungi with plants and animals* (Pirozynski KA & Hawksworth DL, eds), pp. 173–202. Academic Press, London.
- Widmann, C., Gibson, S., Jarpe, M. B., and Johnson, G. L. (1999). Mitogen-activated protein kinase: conservation of a three-kinase module from yeast to human. *Physiol Rev.* 79, 143–180.
- Winnenburg, R., Baldwin, T. K., Urban, M., Rwalings, C., Kohler, J., and Hammond-Kosack, K. E. (2006). PHI-base: a new database for pathogen host interactions. *Nucleic Acids Res.* 34, D459–D464. doi: 10.1093/nar/gkj047
- Woo, P. C. Y., Lau, S. K. P., Ngan, A. H. Y., Tse, H., Tung, E. T. K., and Yuen, K. Y. (2008). *Lasiodiplodia theobromae* pneumonia in a liver transplant recipient. *J Clin Microbiol.* 46, 380–384. doi:10.1128/JCM.01137-07
- Wood, D. W., Setubal, J. C., Kaul, R., Monks, D. E., Kitajima, J. P., Okura, V. K., Zhou, Y., Chen, L., Wood, G. E., Almeida, N. F. Jr., Woo, L., Chen, Y., Paulsen, I. T., Eisen, J. A., Karp, P. D., Bovee, D. Sr., Chapman, P., Clendenning, J., Deatherage, G., Gillet, W., Grant, C., Kutayavin, T., Levy, R., Li, M. J., McClelland, E., Palmieri, A., Raymond, C., Rouse, G., Saenphimmachak, C., Wu, Z., Romero, P., Gordon, D., Zhang, S., Yoo, H., Tao, Y., Biddle, P., Jung, M., Krespan, W., Perry, M., Gordon-Kamm, B., Liao, L., Kim, S., Hendrick, C., Zhao, Z. Y., Dolan, M., Chumley, F., Tingey, S. V., Tomb, J. F., Gordon, M. P., Olson, M. V., Nester, E. W. (2001). The genome of the natural genetic engineer *Agrobacterium tumefaciens* C58. *Science.* 294. 2317–2323. doi: 10.1126/science.1066804
- Xu, J. R., and Hamer, J. E. (1996). MAP kinase and cAMP signaling regulate infection structure formation and pathogenic growth in the rice blast fungus *Magnaporthe grisea*. *Genes Dev.* 10, 2696–2706.
- Yan, J. Y., Zhao, W. S., Chen, Z., Xing, Q. K., Zhang, W., Chethana, K. W. T., Xue, M. F., Xu, J. P., Phillips, A. J. L., Wang, Y., Liu, J. H., Liu, M., Zhou, Y., Jayawardena, R. S., Manawasinghe, I. S., Huang, J. B., Qiao, G. H., Fu, C. Y., Guo, F. F., Dissanayake, A. J., Peng, Y. L., Hyde, K. D., and Li, X.

- H. (2017). Comparative genome and transcriptome analyses reveal adaptations to opportunistic infections in woody plant degrading pathogens of Botryosphaeriaceae. *DNA Res.* 0, 1-16. doi: 10.1093/dnares/dsx040
- Yang, D., Chen, Q., Chertov, O., and Oppenheim, J. J. (2000). Human neutrophil defensins selectively chemoattract naive T and immature dendritic cells. *J Leukoc Biol.* 68, 9–14.
- Yang, Q., Asai, M., Matsuura, H., and Yoshihara, T. (2000). Potato micro-tuber inducing hydroxylasiodiplodins from *Lasiodiplodia theobromae*. *Phytochemistry* 54, 489– 494. doi: 10.1016/S0031-9422(00)00156-4
- Yike, I. (2011). Fungal proteases and their pathophysiological effects. *Mycopathologia.* 171, 5, 299-323. doi: 10.1007/s11046-010-9386-2
- Zhang, L., Ni, H., Du, X., Wang, S., Ma, X. W., Nurnberger, T., Guo, H. S., and Hua, C. (2017). The *Verticillium*-specific protein VdSCP7 localizes to the plant nucleus and modulates immunity to fungal infections. *New Phytol.* 215, 368–381. doi: 10.1111/nph.14537
- Zhang, T., Jin, Y., Zhao, J. H., Gao, F., Zhou, B. J., Fang, Y. Y., and Guo, H. S. (2016). Host-induced gene silencing of the target gene in fungal cells confers effective resistance to the cotton wilt disease pathogen *Verticillium dahliae*. *Mol Plant.* 9, 939–942. doi: 10.1016/j.molp.2016.02.008
- Zhang, W., Li, F., and Nie, L. (2010). Integrating multiple ‘omics’ analysis for microbial biology: application and methodologies. *Microbiol.* 156, 287-301. doi: 10.1099/mic.0.034793-0
- Zhang, Z., Qin, G., Li, B., and Tian, S. (2014). Knocking out *Bcsas1* in *Botrytis cinerea* impacts growth, development, and secretion of extracellular proteins, which decreases virulence. *MPMI.* 27, 6, 590-600. doi: 10.1094/MPMI-10-13-0314-R
- Zhao, X., Mehrabi, R., and Xu, J. R. (2007). Mitogen-activated protein kinase pathways and fungal pathogenesis. *Eukaryot Cell.* 6, 1701–1714. doi: 10.1128/EC.00216-07

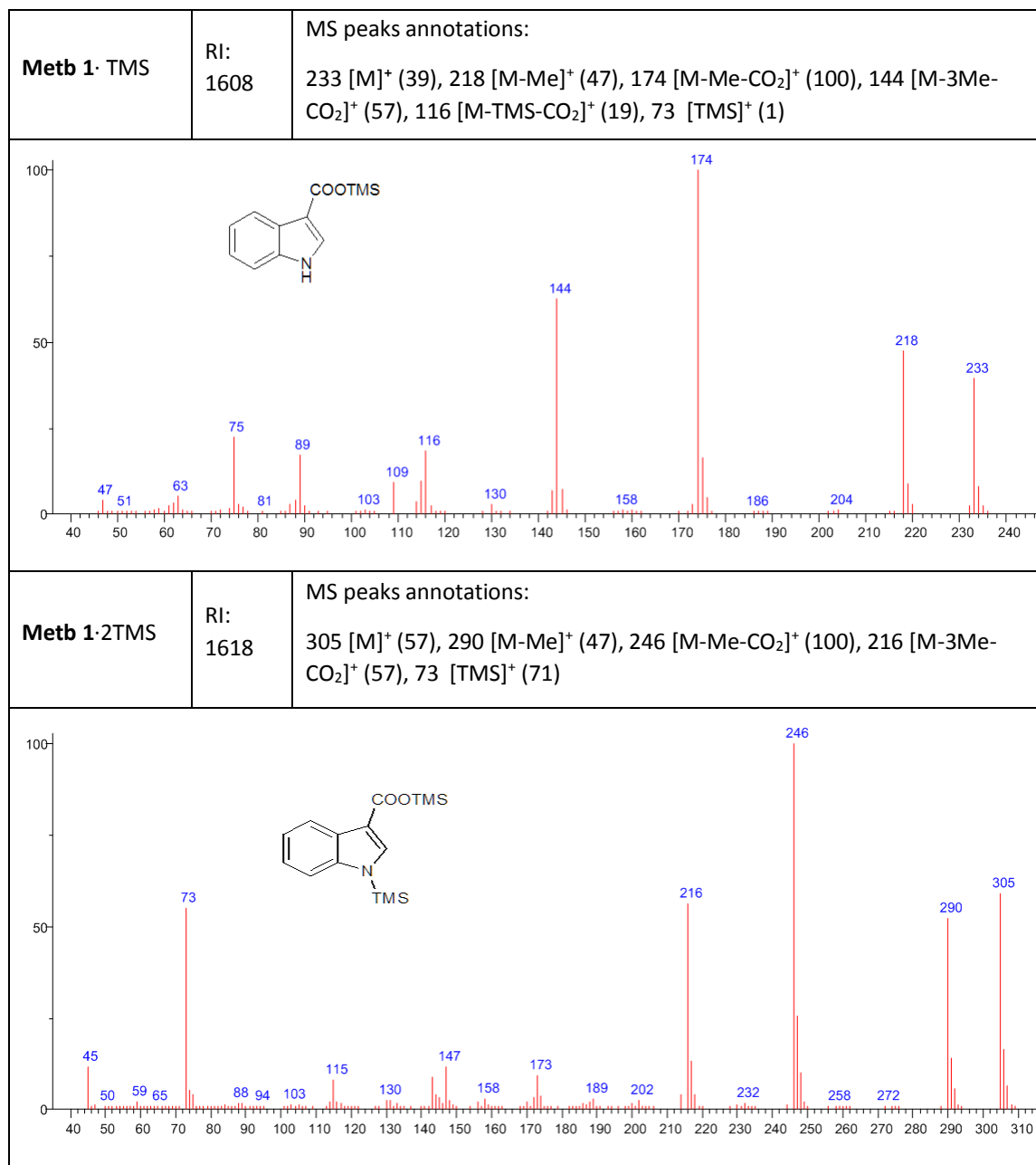
SUPPLEMENTARY MATERIAL

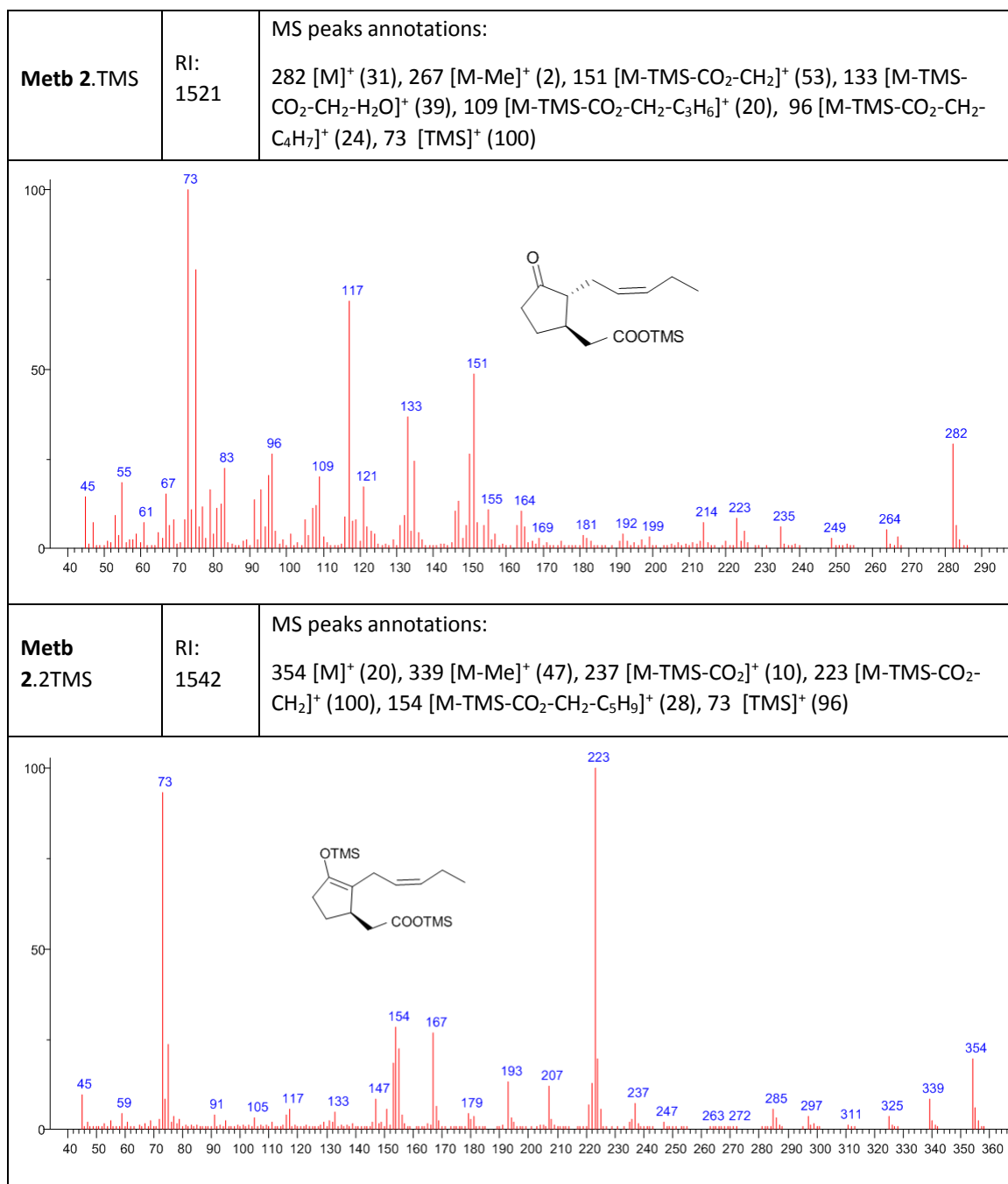
CHAPTER 4



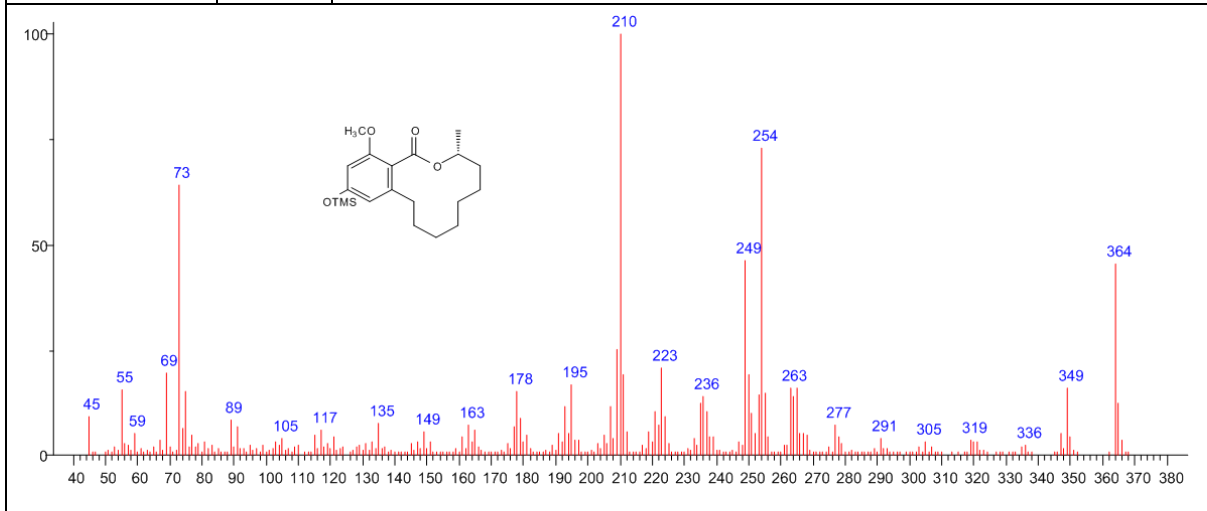
Supplementary Figure S4.1 | Isolation paths of metabolites from *L. theobromae* crude extracts 25 °C (LtCE1 and LtCE2) and 37 °C (LtCE3 and LtCE4).

Supplementary Table S4.1 | Mass spectra of identified metabolites. RI represents the Kovats non isothermal retention index on HP5MS 30 m capillary column. Panel "MS peaks annotations" reports mass, formula (in square brackets) and normalized abundance (in round brackets) of identified fragments in mass spectra whenever available; the molecular ion is always represented by M; Me indicates methyl (-CH₃); TMS represents -Si(CH₃)₃; abundance is normalized taking abundance of base peak equal 100; for instance array 233 [M]⁺ (39) represents a molecular ion with integer mass of 233 Dalton present in a mass spectrum at an abundance 39% the abundance of base peak; analogously array 218 [M-Me]⁺ (47) represents ion of mass 218 Dalton and abundance 47 which has been formed from the molecular ion by loss of a methyl fragment (15 Dalton).

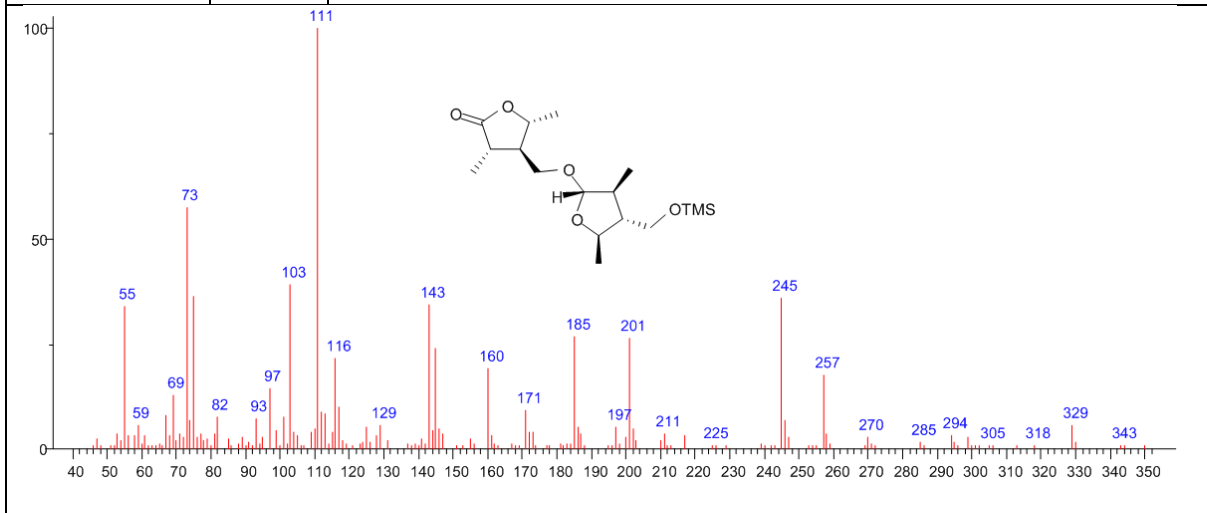




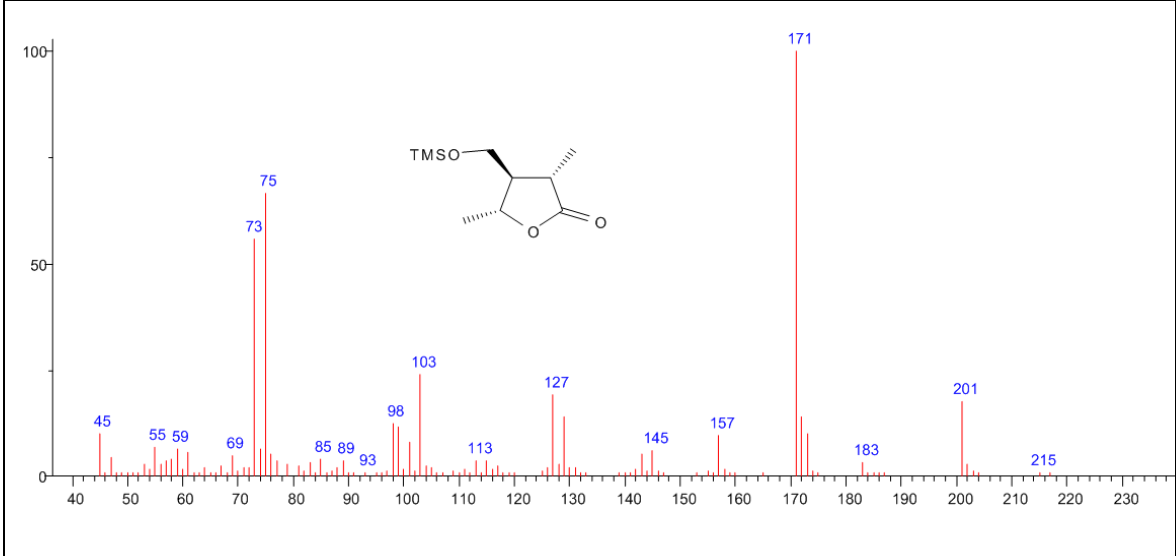
Metb 3.TMS	RI: 1753	MS peaks annotations: 364 [M] ⁺ (51), 349 [M-Me] ⁺ (17), 291 [M-TMS] ⁺ (5), 277 [M-TMS-CH ₂] ⁺ (10), 254 (72), 210 (100), 73 [TMS] ⁺ (61)
-------------------	-------------	---



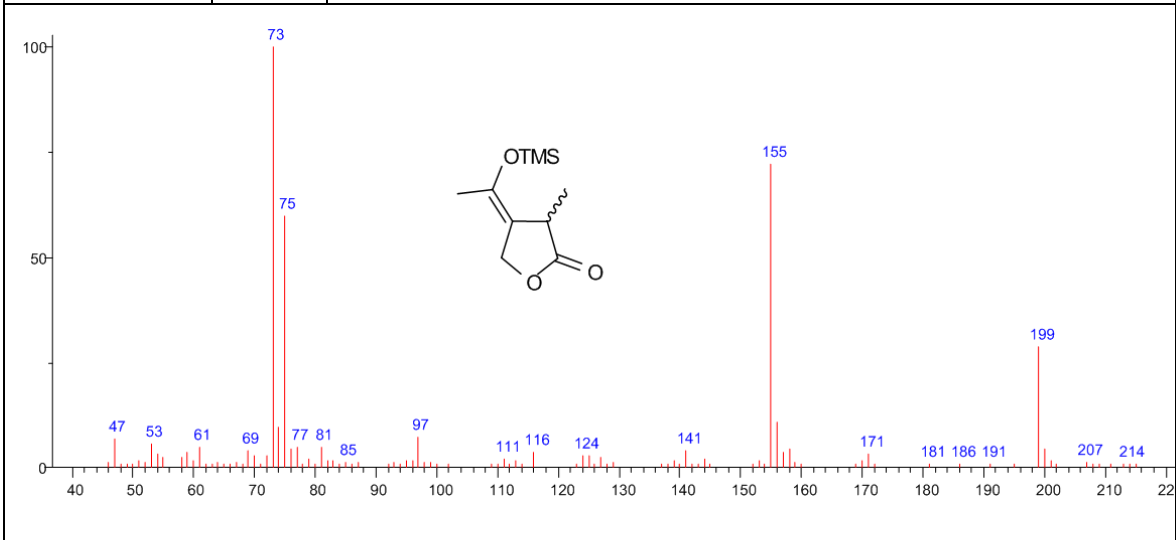
Metb 4.TMS	RI: 1602	344 [M] ⁺ (1), 329 [M-Me] ⁺ (6), 271 [M-TMS] ⁺ (2), 245 (30), 145 [C ₇ H ₁₃ O ₃] ⁺ (25), 111 [C ₇ H ₁₁ O] ⁺ (100), 73 [TMS] ⁺ (65)
-------------------	----------	--

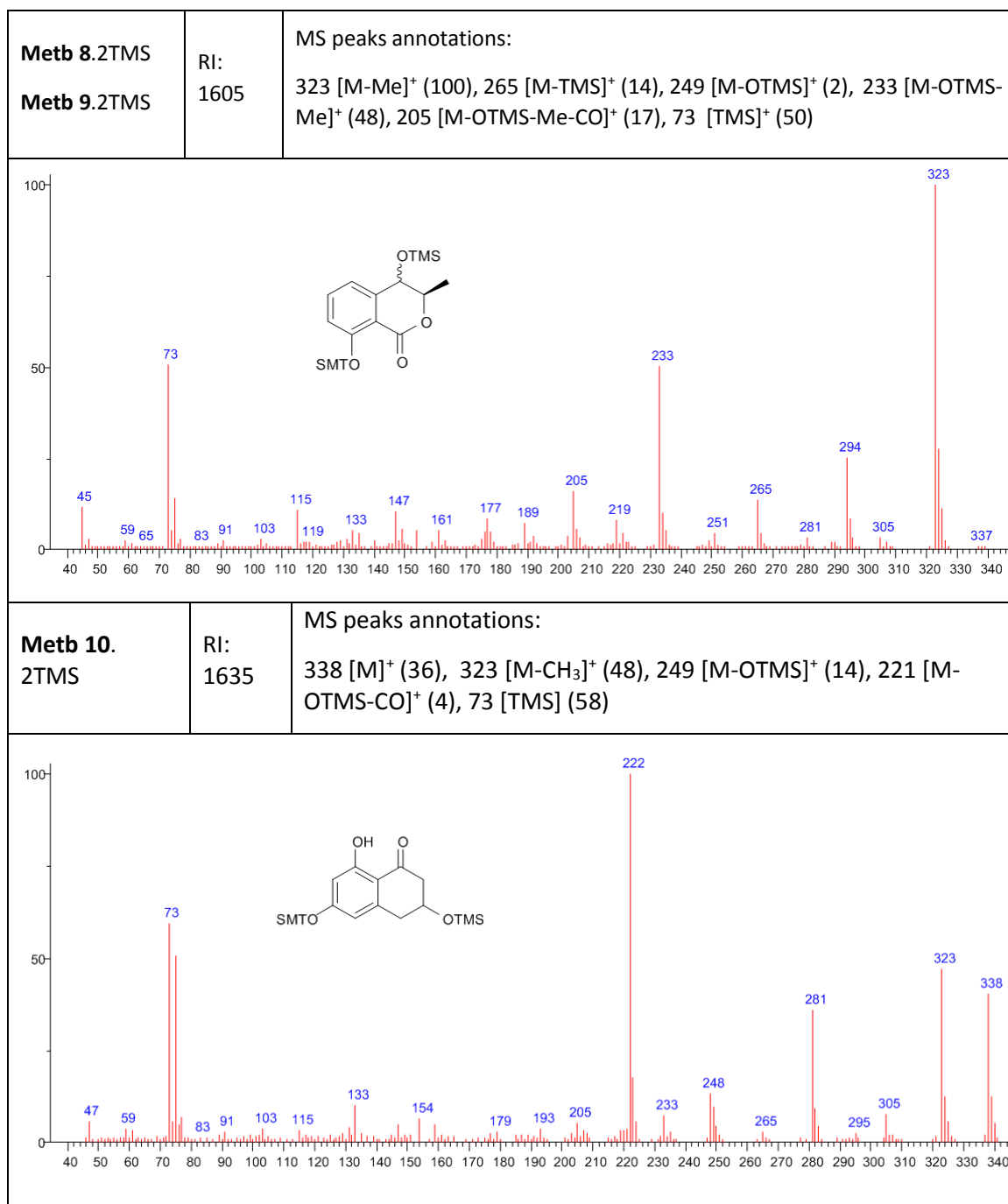


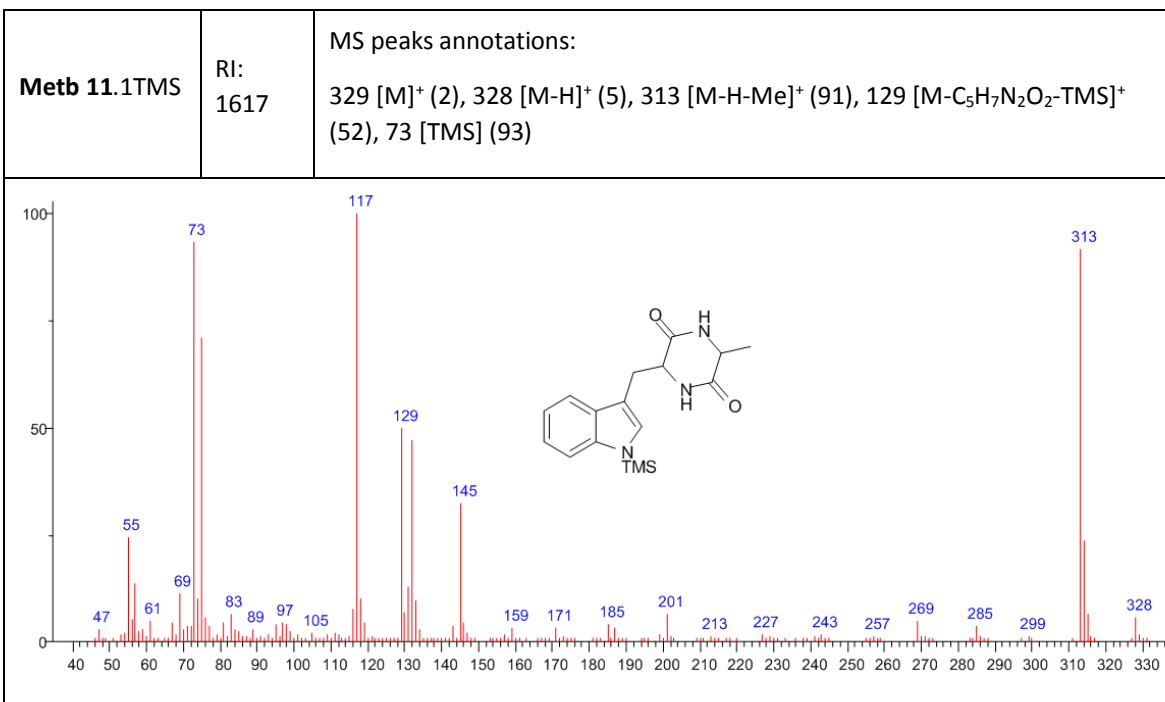
Metb 5.TMS	RI: 1255	MS peaks annotations: 201 [M-Me] ⁺ (17), 183 [M-Me-H ₂ O] ⁺ (3), 171 [M-2Me] ⁺ (100), 157 [M-2Me-CH ₂] ⁺ (10), 143 [M-TMS] ⁺ (5), 129 [M-TMS-CH ₂] ⁺ (14), 73 [TMS] ⁺ (56)
-------------------	-------------	---



Metb 6. TMS Metb 7. TMS	RI: 1115	MS peaks annotations: 199 [M-Me] ⁺ (31), 155 [M-Me-CO ₂] ⁺ (72), 73 [TMS] ⁺ (100)
--	-------------	---







CHAPTER 5

Metabolite purification of strain LA-SOL3 grown at 25 °C

The freeze-dried culture filtrates (from 650 mL) were dissolved in 80 mL of pure water and extracted 3 times with an equal volume of EtOAc. The crude extracts were combined, dried with Na₂SO₄, and evaporated under reduced pressure originating a brown oil residue (LA-SOL3CE₂₅, 120.3 mg). This extract was fractionated by silica gel chromatography (CC) (30 x 1.5 cm) eluted with CHCl₃/*i*-PrOH (9:1) to yield 7 fractions (A 4.6 mg, B 2.4 mg, C 6.7 mg, D 14.5 mg, E 5.9 mg, F 23.4 mg, G 12.8 mg). The residue of fraction D was dissolved in EtOAc and then washed with a saturated solution of NaHCO₃ to remove jasmonic acid [**9**, Figure 5.1, 5.3 mg; *R_f* 0.44 on TLC on silica gel eluted with CHCl₃/*i*-PrOH (92:8, v/v)]. The organic phase was dried with Na₂SO₄, and evaporated under reduced pressure originating the amorphous solid (3*S*,4*R*,5*R*)-4-hydroxymethyl-3,5-dimethyldihydro-2-furanone [**3**, Figure 5.1, 6.7 mg, *R_f* 0.60 on TLC on silica gel eluted with CHCl₃/*i*-PrOH (92:8, v/v)]. Fraction F was purified by preparative TLC on silica gel eluted with CHCl₃/*i*-PrOH (9:1). Two more metabolites were obtained as amorphous solid and yellow oil, respectively, and identified as 3-ICA [3-indolecarboxylic acid, **8**, Figure 5.1, 3.5 mg; *R_f* 0.38 on TLC on silica gel eluted with CHCl₃/*i*-PrOH (9:1)] and lasiolactols A and B [**1** and **2**, Figure 5.1, 12.4 mg; *R_f* 0.33 on TLC on silica gel eluted with CHCl₃/*i*-PrOH (9:1)].

Metabolite purification of strain LA-SOL3 grown at 37 °C

The freeze-dried culture filtrate (from 1.6 L) was dissolved in 200 mL of ultrapure water and extracted with same volume of EtOAc as previously described for LA-SOL3 grown at 25 °C. The crude extract (LA-SOL3CE₃₇, 432.7 mg), obtained as a brown oil, was fractionated by CC on silica gel (45 x 1.5 cm) eluted with CHCl₃/*i*-PrOH (9:1, v/v) originating 9 homogeneous fractions (A 3.3 mg, B 4.3 mg, C 6.3 mg, D 5.6 mg, E 64.0 mg, F 18.3 mg, G 16.4 mg, H 102.3 mg, I 12.3 mg). The residue of fraction B, an amorphous solid, was identified as (*R*)-mellein (**10**, Figure 5.1, *R_f* 0.69 on TLC on silica gel eluted with CHCl₃). The residue of fraction C, a yellow oil, was identified as (3*S*,4*S*)-4-acetyl-3-methyl-2-dihydrofuranone [**7**, Figure 5.1, *R_f* 0.85 on TLC on silica gel eluted with CHCl₃/*i*-PrOH (95:5, v/v)], and the residue of fraction D, a yellow oil, was identified as (3*R*,4*S*)-4-acetyl-3-methyl-2-dihydrofuranone [**6**, Figure 5.1, *R_f* 0.84 on TLC on silica eluted with CHCl₃/*i*-PrOH (95:5, v/v)]. Fraction E, after purification by preparative TLC on silica gel eluted with *n*-hexane/EtOAc (1:1, v/v), produced a yellow oil identified as botryodiplodin (**4**, Figure 5.1, 22.3 mg *R_f* 0.24) and an amorphous solid identified as *epi*-botryodiplodin [**5**, Figure 5.1, 16.8 mg *R_f* 0.26 on TLC on silica gel eluted with *n*-hexane/EtOAc (1:1, v/v)]. The residue from fraction F was further purified by preparative TLC on

silica gel eluted with $\text{CHCl}_3/i\text{-PrOH}$ (92:8, v/v), originating (3*S*,4*R*,5*R*)-4-hydroxymethyl-3,5-dimethyldihydro-2-furanone (**3**, Figure 5.1, 13.4 mg) and an amorphous solid identified as tyrosol [**12**, Figure 5.1, 3.2 mg, R_f 0,52 on TLC on silica gel eluted with $\text{CHCl}_3-i\text{-PrOH}$ (92:8, v/v)]. The residue from fraction G, an amorphous solid, was identified as 3-ICA. Finally, the fraction H, obtained as yellow oil, was identified as a mixture of lasiolactols A and B (**1** and **2**, Figure 5.1).

Metabolite purification of strain LA-SV1 grown at 25 °C

The freeze-dried culture filtrates (from 2.5 L) were dissolved in 250 mL of ultrapure water and extracted with same volume of EtOAc, as previously described for LA-SOL3 grown at 25 °C. The crude extract (LA-SV1CE₂₅, 413.9 mg), obtained as brown oil residue, was submitted to fractionation by CC (45 x 1.5 cm) on silica gel eluted with $\text{CHCl}_3/i\text{-PrOH}$ (9:1, v/v) originating 8 fractions (A 10.3 mg, B 5.5 mg, C 15.2 mg, D 6.1 mg, E 135.1 mg, F 36.5 mg, G 185.5 mg, and H 9.1 mg). The residue from fraction A was further purified by preparative TLC on silica gel eluted with CHCl_3 and identified as (*R*)-mellein (**10**, Figure 5.1, 2.0 mg). The residue of fraction B was identified as (3*S*,4*S*)-4-acetyl-3-methyl-2-dihydrofuranone (**7**, Figure 5.1). The residue of fraction C was purified by preparative TLC on silica gel eluted with a mixture of *n*-hexane/EtOAc (1:1, v/v), originating an amorphous solid identified as *cis*-(3*R*,4*R*)-4-hydroxymellein [**11**, Figure 5.1, 3.2 mg R_f 0.45 on TLC on silica gel eluted with *n*-hexane/EtOAc (1:1, v/v)]. The residue of fraction E (30.5 mg) was dissolved in EtOAc and then washed with a saturated solution of NaHCO_3 to remove jasmonic acid (7.5 mg). The organic phase was dried with Na_2SO_4 , and evaporated under reduced pressure giving **3** (Figure 5.1, 12.4 mg). The residue of fraction F was identified as jasmonic acid. Finally, the residue of fraction G (yellow oil) was obtained and identified as a mixture of lasiolactols A and B.

Metabolite purification of strain LA-SV1 grown at 37 °C

The freeze-dried culture filtrate (from 1.0 L) was dissolved in 200 mL of ultrapure water and extracted with the same volume of EtOAc as previously reported for LA-SOL3 grown at 25 °C. The crude extract (LA-SV1CE₃₇, 524.4 mg), obtained as brown oil, was fractionated by CC (45 x 1.5 cm) on silica gel, eluted with $\text{CHCl}_3/i\text{-PrOH}$ 9:1 (v/v), originating 11 fractions (A 2.8 mg, B 11.6 mg, C 13.6 mg, D 22.5 mg, E 116.0 mg, F 35.4 mg, G 47.1 mg, H 7.4 mg, I 33.5 mg, L 113.8 mg, and M 9.6 mg). The residue of fraction B was identified as (*R*)-mellein. The residue of fraction C was identified as (3*S*,4*S*)-4-acetyl-3-methyl-2-dihydrofuranone (**7**, Figure 5.1). Part of the residue of fraction E (37.4 mg) was further purified by preparative TLC on silica gel eluted with *n*-hexane/EtOAc 1:1, v/v (three times) originating botryodiplodin and *epi*-botryodiplodin (7.4 and 8.3 mg, respectively). The residue of fraction F was identified as 3-ICA. Finally, the residue of fraction L, yellow oil, was identified as a mixture of lasiolactols A and B.

Acetylation of epibotryodiplodin (5)

epi-Botryodiplodin (6.4 mg), dissolved in pyridine (30 μ L), was converted into the corresponding 2-*O*-acetyl derivatives by acetylation with Ac₂O (30 μ L) at room temperature for 12 h. The reaction was stopped by addition of MeOH, and the azeotrope formed by addition of benzene was evaporated in a N₂ stream. The oily residue (7.3 mg) was purified by TLC on silica gel, eluent toluene-EtOAc (1:1, v/v), yielding derivatives **15** (2.3 mg, *Rf* 0.52) and **16** (3.2 mg, *Rf* 0.49) as oils.

(2R)-*epi*-Botryodiplodin acetylate (15)

¹H NMR (400 MHz, in CDCl₃): δ 1.11 (3H, d, *J* = 6.8 Hz, CH₃C-3), 2.10 (3H, s, CH₃COO), 2.25 (3H, s, CH₃CO), 2.61 (1H, m, H-3), 3.13 (1H, dt, *J* = 9.0, 10.0 Hz, H-4), 3.98 (1H, t, *J* = 9.0 Hz, H-5), 4.31 (1H, t, *J* = 9.0 Hz, H-5), 6.27 (1H, d, *J* = 4.5 Hz, H-2); ¹³C NMR (100 MHz, in CDCl₃): δ 12.1 (CH₃C-3), 21.2 (CH₃COO), 30.3 (CH₃CO), 41.5 (C-3), 56.0 (C-4), 70.0 (C-5), 99.8 (C-2), 170.2 (COO), 207.0 (CO); ESIMS (+) *m/z* 225 [M+K]⁺, 209 [M+Na]⁺.

(2S)-*epi*-Botryodiplodin acetylate (16)

¹H NMR (400 MHz, in CDCl₃): δ 1.25 (3H, d, *J* = 7.2 Hz, CH₃C(3)), 2.05 (3H, s, CH₃COO), 2.25 (3H, s, CH₃CO), 2.70 (1H, m, H-3), 2.84 (1H, m, H-4), 4.29 (1H, t, *J* = 8.1 Hz, H-5), 4.23 (1H, t, *J* = 8.1 Hz, H-5), 5.91 (1H, brs, H-2); ¹³C NMR (100 MHz, in CDCl₃): δ 17.8 (CH₃C-3), 22.5 (CH₃COO), 30.2 (CH₃CO), 42.8 (C-3), 58.4 (C-4), 68.9 (C-5), 104.0 (C-2), 166.1 (COO), 206.5 (CO); ESIMS (+), *m/z* 209 [M+Na]⁺.

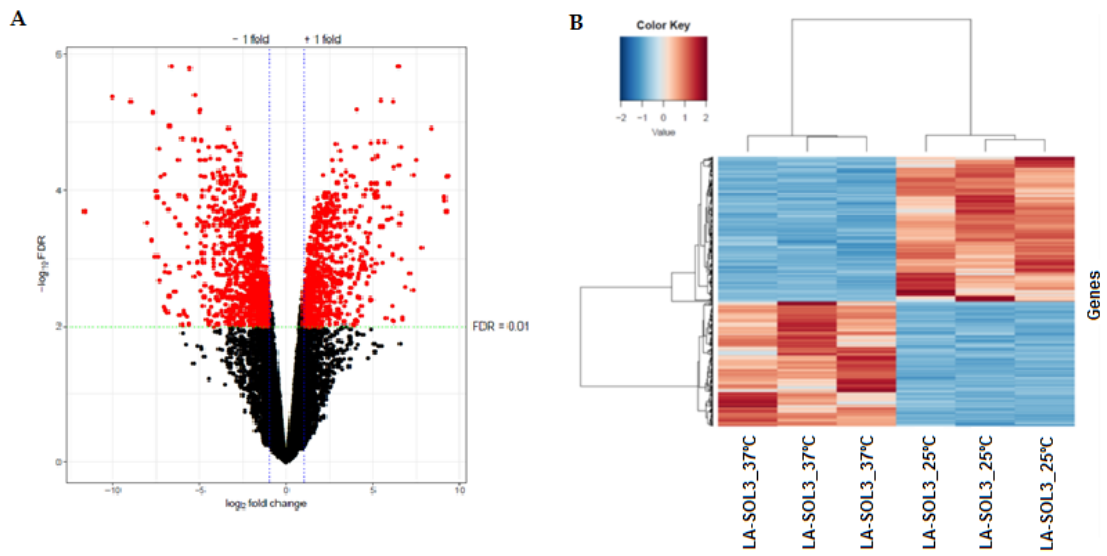
Acetylation of 4-Hydroxymethyl-3,5-dimethyldihydro-2-furanone (3)

4-Hydroxymethyl-3,5-dimethyldihydro-2-furanone (4.9 mg), dissolved in pyridine (30 μ L), Ac₂O was added to solution. The reaction (room temperature for 12 h), was stopped with MeOH and work up as above reported. The oily residue (6.2 mg) was purified by TLC on silica gel, eluent *n*-hexane-EtOAc (6:4), yielding derivative **13** (5.1 mg, *Rf* 0.23) as an oil. ¹H NMR (400 MHz, in CDCl₃): δ 4.28 (1H, m, H-5), 4.26 (1H, dd, *J* = 4.4, 11.5 Hz, H-8a), 4.18 (1H, dd, *J* = 5.9, 11.5 Hz, H-8b), 2.52 (1H, m, H-3), 2.11 (3H, s, COCH₃), 2.03 (1H, m, H-4), 1.48 (3H, d, *J* = 6.1, Hz, H₃-6), 1.32 (3H, d, *J* = 7.6 Hz, H₃-7). ESI MS(+) *m/z*: 209 [M+Na]⁺, 187 [M+H]⁺, 127 [M+CH₃COO]⁺.

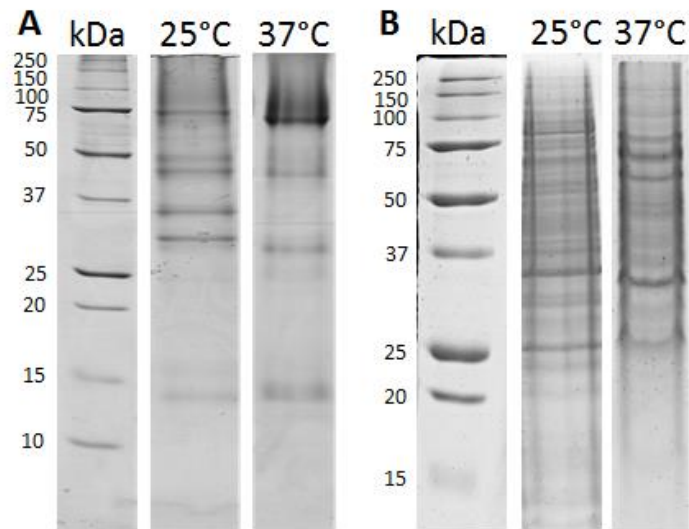
Acetylation of botryodiplodin (4)

(3*R*,4*S*)-Botryodiplodin (5.3 mg) was acetylated with pyridine (30 μ L) and Ac₂O (30 μ L) in the same conditions above reported to convert **5** in the corresponding 2-*O*-acetyl derivatives. Also, the reaction work-up is the same and the residue was purified by TLC on silica gel, eluent *n*-hexane-AcOEt (1:1, v/v), originating (2*R*,3*R*,4*S*)-botryodiplodin acetate (**14**, 4.3 mg, *Rf* 0.56), whose physic and spectroscopic data were comparable to those previously reported (Arsenault et al. 1969).

CHAPTER 6



Supplementary Figure S6.1 | Volcano plot (A) and hierarchical cluster analysis (B) of the expression profiles of differentially expressed genes between 25 °C and 37 °C. Genes and samples were hierarchically clustered using Pearson correlation.



Supplementary Figure S6.2 | One-DE gel of extracellular medium (A) and mycelium (B) of LA-SOL3 strain grown at 25 °C and 37 °C for 4 days.

Supplementary Table S6.1 | Genes predicted to code for fungal peroxidases in the genome of *L. theobromae* LA-SOL3. Peroxidases were predicted with the web-based BLAST application of fPoxDB: Fungal Peroxidase Database.

Peroxidase	Genes (n)
New NoxA	6
Other class II peroxidase	6
Haloperoxidase (haem)	5
Linoleate diol synthase (PGHS like)	5
New NoxC	4
Atypical 2-Cysteine peroxiredoxin (type Q, BCP)	4
Cytochrome C peroxidase	4
Manganese peroxidase	4
New NoxB	4
1-Cysteine peroxiredoxin	3
Catalase	3
Hybrid Ascorbate-Cytochrome C peroxidase	3
Lignin peroxidase	3
Typical 2-Cysteine peroxiredoxin	3
Versatileperoxidase	3
Atypical 2-Cysteine peroxiredoxin (type II, type V)	2
Carboxymuconolactone decarboxylase (no peroxidase activity)	2
Prostaglandin H synthase (Cyclooxygenase)	1
New Rbohs	1
Fungi-Bacteria glutathione peroxidase	1
NoxR	1
New_Doux	0
DyP-type peroxidase D	0
No haem, Vanadium chloroperoxidase	0

The following tables (S6.2, S6.3, S6.4, S6.5, S6.6, S6.7 and S6.8) are deposited in an excel file named “Supplementary Material Chapter 6”:

Supplementary Table S6.2 | Proteins identified in the secretome of LA-SOL3 strain at 25 °C.

Supplementary Table S6.3 | Proteins identified in the cellular proteome of LA-SOL3 strain at 25 °C.

Supplementary Table S6.4 | Proteins identified in the secretome of LA-SOL3 strain at 37 °C.

Supplementary Table S6.5 | Proteins identified in the cellular proteome of LA-SOL3 strain at 37 °C.

Supplementary Table S6.6 | Up and down-regulated genes at 37 °C identified in LA-SOL3 strain and correspondent GO biological process.

Supplementary Table S6.7 | Up and down-regulated proteins ($0.5 \geq FC \geq 2$) identified in the secretome of LA-SOL3 strain and correspondent GO biological process.

Supplementary Table S6.8 | Up and down-regulated proteins ($0.5 \geq FC \geq 2$) identified in the cellular proteome of LA-SOL3 strain and correspondent GO biological process.

Supplementary Table S6.9 | Potentially relevant proteins identified in the secretome of strain LA-SOL3 grown at 25 °C and 37 °C.

GO Category	Accession code	Description	Gene names	Temperature (°C)
PATHOGENESIS	B8NM69	Peptidase S41 family protein ustP (EC 3.4.-.-)	ustP AFLA_095010	25
	C5FBW2	Tripeptidyl-peptidase SED2 (EC 3.4.14.10)	SED2 MCYG_00184	25
	C5FW30	Carboxypeptidase S1 homolog A (EC 3.4.16.6)	SCPA MCYG_06933	25
	C9SPU8	Probable zinc metalloprotease VDBG_06923 (EC 3.4.-.-)	VDBG_06923	25
	D4ALG0	LysM domain-containing protein ARB_05157	ARB_05157	25
	D4ALQ5	Probable extracellular glycosidase ARB_05253 (EC 3.2.-.-)	ARB_05253	25
	D4AP52	Carboxypeptidase S1 homolog B (EC 3.4.16.6)	SCPB ARB_06019	25
	D4APQ6	Probable thioredoxin reductase ARB_06224 (EC 1.8.1.9)	ARB_06224	25
	D4AQA7	Probable serine carboxypeptidase ARB_06414 (EC 3.4.16.-)	ARB_06414	25
	D4ARB1	Probable dipeptidyl-peptidase 5 (EC 3.4.14.-)	DPP5 ARB_06651	25
	D4AYB4	Antigenic thaumatin-like protein ARB_01183	ARB_01183	25
	D4AYS6	Probable extracellular serine carboxypeptidase (EC 3.4.-.-)	ARB_01345	25
	D4B327	Probable pathogenesis-related protein ARB_02861	ARB_02861	25
	D4B5N0	Metalloprotease A-like protein ARB_03789 (EC 3.4.17.-)	ARB_03789	25
	D7UQ40	Bifunctional solanapyrone synthase (EC 1.1.3.42) (Prosolanapyrone-II oxidase)	sol5	25
	G3XMD0	FAD-linked oxidoreductase azaL (EC 1.-.-.-)	azaL ASPNIDRAFT_132654	25
	M1W428	Thioredoxin reductase tcpT (EC 1.8.1.-)	tcpT CPUR_02681	25
	O42630	Vacuolar protease A (EC 3.4.23.25)	pep2 AFUA_3G11400	25
	O42799	Allergen Asp f 7	AFUA_4G06670	25
	O64411	Polyamine oxidase (EC 1.5.3.14) (EC 1.5.3.15)	PAO	25
	O74238	Protein SnodProt1	SNOG_13722	25
	P11838	Endothiapepsin (EC 3.4.23.22)	EAPA EPN-1	25
	P24665	Aspergillopepsin-2 (EC 3.4.23.19)		25
	P29717	Glucan 1,3-beta-glucosidase (EC 2.4.1.-) (EC 3.2.1.58)	XOG1 EXG EXG1 XOG CAALFM_C102990CA Ca49C10.05	25
	P34946	Carboxypeptidase S1 (EC 3.4.16.6)		25/37
	P36196	Acetylcholinesterase (EC 3.1.1.7)	ACHE	25
	P39105	Lysophospholipase 1 (EC 3.1.1.5)	PLB1 YMR008C YM8270.10C	25
	P42893	Endothelin-converting enzyme 1 (EC 3.4.24.71)	Ece1	25
	P52719	Carboxypeptidase cpdS (EC 3.4.16.-)	cpdS	25
	P58099	C5a peptidase (EC 3.4.21.110)	scpA SPy_2010 M5005_Spy1715	25
	P64744	Sphingomyelinase (EC 3.1.4.12)	BQ2027_MB0912	25

	P79085	Major allergen Alt a 1	ALTA1	25
	P86325	Carboxylesterase (EC 3.1.1.1)		25
	Q00668	Putative sterigmatocystin biosynthesis peroxidase stcC (EC 1.11.1.-)	stcC AN7823	25
	Q03168	Lysosomal aspartic protease (EC 3.4.23.-)	AAEL006169	25
	Q0D1P3	Multicopper oxidase terE (EC 1.-.-)	terE ATEG_00141	25
	Q0V1D7	Neutral protease 2 homolog SNOG_02177 (EC 3.4.24.39)	SNOG_02177	25
	Q4WFX9	Probable leucine aminopeptidase 2 (EC 3.4.11.-)	lap2 AFUA_3G00650	25
	Q4WNV0	Aspartic-type endopeptidase ctsD (EC 3.4.23.-)	ctsD AFUA_4G07040	25
	Q4WZS3	Putative aspergillopepsin A-like aspartic endopeptidase AFUA_2G15950 (EC 3.4.23.-)	AFUA_2G15950	25
	Q5AZ42	Probable dipeptidyl peptidase 4 (EC 3.4.14.5)	dpp4 AN6438	25
	Q70J59	Tripeptidyl-peptidase sed2 (EC 3.4.14.10)	sed2 sedB AFUA_4G03490	25
	Q871C5	Extracellular metalloprotease NCU07200 (EC 3.4.24.-)	B8G12.220 NCU07200	25
	Q8RJP2	Rhamnogalacturonate lyase (EC 4.2.2.23)	rhiE Dda3937_01465	25
	Q92396	Tyrosinase (EC 1.14.18.1)	TYR	25
	Q9DDE3	Acetylcholinesterase (EC 3.1.1.7)	ache	25
	Q9Y7F0	Peroxiredoxin TSA1-A (EC 1.11.1.15)	TSA1 TSA1A CAALFM_C306180CA CaO19.7417	25
STRESS RESPONSE	B0Y004	Cell wall protein phiA (Major allergen phiA)	phiA AFUB_045170	25
	B9W4V6	Aromatic peroxygenase (EC 1.11.2.1)	APO1	25
	C0IW58	Low-redox potential peroxidase (EC 1.11.1.7)	LnP	25
	D4AUF1	WSC domain-containing protein ARB_07867	ARB_07867	25
	D4AUF4	WSC domain-containing protein ARB_07870	ARB_07870	25
	G0Y276	Effector protein PevD1		25
	P29141	Minor extracellular protease vpr (EC 3.4.21.-)	vpr BSU38090 ipa-45r	25
	Q3HRQ2	Aldehyde oxidase GLOX (EC 1.2.3.1)	GLOX	25
	Q4WNS8	Protein ecm33	ecm33 AFUA_4G06820	25
	Q4WXZ5	Ribonuclease T2-like (EC 3.1.27.1)	rny1 AFUA_3G11220	25
	Q86WA6	Valacyclovir hydrolase (EC 3.1.-.-)	BPHL MCNAA	25
	Q877A8	Catalase B (EC 1.11.1.6)	catB AO090120000068	25

	B5Y008	Oxygen-dependent choline dehydrogenase (EC 1.1.99.1) (EC 1.2.1.8)	betA KPK_3995	37
CELL WALL DEGRADATION	A1C4H2	Probable endo-beta-1,4-glucanase D (EC 3.2.1.4)	eglD ACLA_059790	25
	A1DBG6	Probable beta-glucosidase btgE (EC 3.2.1.21)	btgE NFIA_098360	25
	A1DBS6	Probable endo-beta-1,4-glucanase D (EC 3.2.1.4)	eglD NFIA_099510	25
	A1DME8	Probable endo-beta-1,4-glucanase B (EC 3.2.1.4)	eglB NFIA_053150	25
	A1DMR8	Probable beta-glucosidase F (EC 3.2.1.21)	bgfF NFIA_054350	25/37
	A1DMV3	Probable feruloyl esterase B-2 (EC 3.1.1.73)	faeB-2 NFIA_054700	25
	A2QT85	Probable arabinan endo-1,5-alpha-L-arabinosidase A (EC 3.2.1.99)	abnA An09g01190	25
	A2QYR9	Probable 1,4-beta-D-glucan cellobiohydrolase C (EC 3.2.1.91)	cbhC An12g02220	25
	B8MW97	probable endo-beta-1,4-glucanase B (EC 3.2.1.4)	eglB AFLA_087870	25
	B8MXJ7	Probable endo-beta-1,4-glucanase D (EC 3.2.1.4)	eglD AFLA_077840	25
	B8NJF4	Probable beta-glucosidase D (EC 3.2.1.21)	bgfD AFLA_066750	25
	B8NMD3	Probable arabinan endo-1,5-alpha-L-arabinosidase C (EC 3.2.1.99)	abnC AFLA_123690	25
	B8NPT0	Probable feruloyl esterase B-2 (EC 3.1.1.73)	faeB-2 AFLA_001440	25
	D4AJR9	Endo-1,3(4)-beta-glucanase ARB_04519 (EC 3.2.1.6)	ARB_04519	25
	D4AV38	Probable secreted lipase ARB_00047 (EC 3.1.1.1)	ARB_00047	25
	D4AZ24	Probable endo-1,3(4)-beta-glucanase ARB_01444 (EC 3.2.1.6)	ARB_01444	25
	D4AZ78	Secreted lipase ARB_01498 (EC 3.1.1.3)	ARB_01498	25
	P07982	Endoglucanase EG-II (EC 3.2.1.4)	egl2	25
	POC1A6	Pectate lyase L (EC 4.2.2.2)	pell	25
	P23360	Endo-1,4-beta-xylanase (EC 3.2.1.8)	XYNA	25/37
	P23550	Endoglucanase B (EC 3.2.1.4)	celB	25
	P41365	Lipase B (EC 3.1.1.3) (CALB)		25
	P43317	Endoglucanase-5 (EC 3.2.1.4)	egl5	25
	P45699	Putative endoglucanase type K (EC 3.2.1.4)		25
	P53626	Glucan endo-1,3-beta-glucosidase BGN13.1 (EC 3.2.1.39)	bgn13.1	25
	P55332	Endo-1,4-beta-xylanase A (EC 3.2.1.8)	xlnA AN3613	25
	Q01738	Cellobiose dehydrogenase (EC 1.1.99.18)	CDH-1; CDH-2	25

Q0CEF3	Probable beta-glucosidase L (EC 3.2.1.21)	bglL ATEG_07931	25
Q0CMT2	Probable 1,4-beta-D-glucan cellobiohydrolase B (EC 3.2.1.91)	cbhB ATEG_05002	25
Q0CTD7	Probable beta-glucosidase A (EC 3.2.1.21)	bglA bgl1 ATEG_03047	25
Q2U7D2	Probable alpha-L-arabinofuranosidase axhA (EC 3.2.1.55)	axhA AO090701000885	25
Q45071	Arabinoxylan arabinofuranohydrolase (EC 3.2.1.55)	xynD BSU18160	25
Q5B9F2	Probable beta-glucosidase L (EC 3.2.1.21)	bglL AN2828	25
Q5ZNB1	Endo-1,4-beta-xylanase D (Xylanase D) (EC 3.2.1.8)	xynD	25
Q92194	Acetylxylan esterase A (EC 3.1.1.72)	axeA aceA	25
Q96VB6	Endo-1,4-beta-xylanase F3 (EC 3.2.1.8)	xynF3 xlnF3 AO090001000208	25
Q96WQ9	Probable endo-beta-1,4-glucanase D (EC 3.2.1.4)	eglD cel61A AKAW_08531	25
Q99034	Acetylxylan esterase (EC 3.1.1.72)	axe1	25

Supplementary Table S6.10 | Potentially relevant proteins identified in the cellular proteome of strain LA-SOL3 grown at 25 °C and 37 °C.

GO Category	Accession	Description	Gene names	Temperature (°C)
PATHOGENESIS	A1CFL1	Alcohol dehydrogenase patD (EC 1.1.1.1)	patD ACLA_093590	25
	A1CFL2	Dehydrogenase patE (EC 1.1.-.-)	patE ACLA_093600	25
	A4GYZ0	Glutathione S-transferase gliG (EC 2.5.1.18)	gliG AFUA_6G09690	25
	A7UX13	Hercynylcysteine sulfoxide lyase (EC 4.4.1.-) (egt-2 NCU11365	25
	B2WKF1	Carboxypeptidase Y homolog A (EC 3.4.16.5)	cpyA PTRG_10461	25/37
	B6HJU2	Glandicoline B O-methyltransferase roqN (EC 3.1.1.-)	roqN gmt Pc21g15440	25
	B8N406	Secondary metabolism regulator laeA (EC 2.1.1.-)	laeA AFLA_033290	25
	B8NM69	Peptidase S41 family protein ustP (EC 3.4.-.-)	ustP AFLA_095010	25
	B9WYE6	Versiconal hemiacetal acetate reductase (EC 1.1.1.353)	vrda	25
	B9WZX1	Tryprostatin B 6-hydroxylase (EC 1.14.13.176)	ftmP450-1 ftmC	25
	C5FBW2	Tripeptidyl-peptidase SED2 (EC 3.4.14.10) (Sedolisin-B)	SED2 MCYG_00184	25
	C5P4Z8	Subtilisin-like protease CPC735_031240 (EC 3.4.21.-)	CPC735_031240	25
	D4ARB1	Probable dipeptidyl-peptidase 5 (EC 3.4.14.-) (Dipeptidyl-peptidase V) (DPP V) (DppV)	DPP5 ARB_06651	25
	D4B1R0	Probable glutamate carboxypeptidase ARB_02390 (EC 3.4.17.21)	ARB_02390	25
	D4B5N0	Metalloprotease A-like protein ARB_03789 (EC 3.4.17.-)	ARB_03789	25
	D7PHZ0	Aldolase vrtJ (EC 4.1.2.-)	vrtJ	25
	E9FCP6	Aldo-keto reductase dtxS3 (EC 1.1.1.-)	dtxS3 MAA_10045	25/37
	E9QUT3	Hydroxynaphthalene reductase arp2 (EC 1.1.-.-)	arp2 AFUA_2G17560	25
	J4UHQ8	Glutathione S-transferase-like protein OpS6 (EC 2.5.1.-)	OpS6 BBA_08184	25
	M1W428	Thioredoxin reductase tcpT (EC 1.8.1.-)	tcpT CPUR_02681	25
	M2SNN6	Secondary metabolism regulator LAE1 (EC 2.1.1.-)	LAE1 COCHEDRAFT_1197809	25
	N4WHA7	Reducing polyketide synthase PKS2 (EC 2.3.1.-)	PKS2 COCC4DRAFT_45941	25
	N4WQZ8	Probable esterase TOX9 (EC 3.1.2.-)	TOX9 COCC4DRAFT_155492	25
	N4WW42	Dehydrogenase RED3 (EC 1.1.1.1)	RED3 COCC4DRAFT_155403	25
	O42630	Vacuolar protease A (EC 3.4.23.25)	pep2 AFUA_3G11400	25/37
	O43301	Heat shock 70 kDa protein 12A	HSPA12A KIAA0417	25
	O74225	Heat shock protein hsp88	hsp88 NCU05269	25/37
	O74238	Protein SnodProt1	SNOG_13722	25
	O93806	Glucosamine 6-phosphate N-acetyltransferase (EC 2.3.1.4)	GNA1	25
	O93866	Heat shock 70 kDa protein	HSP70	25/37
	P11838	Endothiapepsin (EC 3.4.23.22)	EAPA EPN-1	25
	P14010	4-aminobutyrate aminotransferase (EC 2.6.1.19)	gatA AN2248	25/37
	P15705	Heat shock protein ST11	ST11 YOR027W OR26.17	25
P29702	Protein farnesyltransferase/geranylgeranyltransferase type-1 subunit alpha (EC 2.5.1.58) (EC 2.5.1.59alpha)	FNTA	25	
P29717	Glucan 1,3-beta-glucosidase (EC 2.4.1.-) (EC 3.2.1.58)	XOG1 EXG EXG1 XOG CAALFM_C102990CA	25	
P31540	Heat shock protein hsp98	hsp98 NCU00104	25	

P34946	Carboxypeptidase S1 (EC 3.4.16.6)		25
P38624	Proteasome subunit beta type-1 (EC 3.4.25.1)	PRE3 YJL001W J1407	25/37
P38677	Carboxy-cis,cis-muconate cyclase (EC 5.5.1.5)	NCU04071	25
P39640	Dihydroanticiapsin 7-dehydrogenase (EC 1.1.1.385)	bacC ywfD BSU37720 ipa-82d	25
P40108	Aldehyde dehydrogenase (EC 1.2.1.3)	CLAH10 CLAH3	25/37
P40850	Protein MKT1	MKT1 YNL085W N2302	25/37
P42059	Minor allergen Cla h 7	CLAH7 CLAH5	25/37
P54006	Protein TOXD	TOXD	25
P62998	Ras-related C3 botulinum toxin substrate 1 (p21-Rac1)	RAC1	25
P75863	Uncharacterized protein YcbX	ycbX b0947 JW5126	25
P78417	Glutathione S-transferase omega-1 (GSTO-1) (EC 2.5.1.18)	GSTO1 GSTTLP28	25
P79085	Major allergen Alt a 1	ALTA1	25
P86029	Catechol 1,2-dioxygenase (EC 1.13.11.1)	HQD2 CAALFM_C402230CA	25
P87017	5'-hydroxyaverantin dehydrogenase (EC 1.1.1.352)	afIH adhA P875_00052989-1	25
P87216	Protein vip1	vip1 SPAC10F6.06	25/37
Q00258	Norsolorinic acid reductase A (EC 1.1.1.-)	afIE norA P875_00052990	25/37
Q00278	Norsolorinic acid ketoreductase (EC 1.1.1.349)	afID nor-1 P875_00052988	25
Q00455	Scytalone dehydratase (EC 4.2.1.94)	SCD1 Cob_03011	25
Q00859	Mitogen-activated protein kinase (EC 2.7.11.24)	MAPK	25/37
Q05533	Inositol monophosphatase 2 (EC 3.1.3.25)	INM2 IMP2 YDR287W	25
Q07505	Putative carboxymethylenebutenolidase (EC 3.1.1.45)	YDL086W	25/37
Q0CCX5	Questin oxidase (EC 1.-.-)	gedK ATEG_08459	25
Q0CJ62	6-methylsalicylic acid decarboxylase atA (EC 1.-.-)	atA ATEG_06272	25/37
Q12634	Tetrahydroxynaphthalene reductase (EC 1.1.1.252)	MGG_02252	25
Q2YDM1	ADP-ribosylation factor-like protein 1	ARL1	25
Q47317	N(6)-hydroxylysine O-acetyltransferase (EC 2.3.1.102)	iucB	25/37
Q49W60	Probable nitronate monooxygenase (EC 1.13.12.16)	SSP1854	25
Q4R7L8	Peroxisomal NADH pyrophosphatase NUDT12 (EC 3.6.1.22)	NUDT12 QtsA-14876	25/37
Q4V8V2	Nucleoside diphosphate-linked moiety X motif 17 (EC 3.6.1.-)	nudt17 zgc:114128	25
Q4W946	2-oxoglutarate-Fe(II) type oxidoreductase (EC 1.14.11.-)	encD AFUA_4G00230	25
Q4WHU1	Probable 4-hydroxyphenylpyruvate dioxygenase 1 (EC 1.13.11.27)	AFUA_2G04200	25/37
Q4WMJ1	N-methyltransferase gliN (EC 2.1.1.-)	gliN AFUA_6G09720	25
Q4WMJ5	O-methyltransferase gliM (EC 2.1.1.-)	gliM AFUA_6G09680	25
Q4WMJ7	Nonribosomal peptide synthetase gliP (EC 6.3.2.-)	gliP NRPS10 pesK AFUA_6G09660	25
Q4WMJ8	Dipeptidase gliJ (EC 3.4.13.19)	gliJ AFUA_6G09650	25
Q4WMJ9	Probable aminotransferase gliI (EC 2.6.1.-)	gliI AFUA_6G09640	25
Q4WQZ7	O-methyltransferase tpcA (EC 2.1.1.-)	tpcA tynA AFUA_4G14580	25/37
Q4WZB3	Heptaketide hydrolyase ayg1 (EC 3.7.1.-)	ayg1 AFUA_2G17550	25

Q4WZS3	Putative aspergillopepsin A-like aspartic endopeptidase AFUA_2G15950 (EC 3.4.23.-)	AFUA_2G15950	25
Q54DU5	von Willebrand factor A domain-containing protein DDB_G0292028	DDB_G0292028	25
Q5A599	Histidine protein kinase NIK1 (EC 2.7.13.3)	NIK1 COS1 HIK1 CAALFM_C702800WA	25
Q5AG40	Vacuolar protein sorting-associated protein 4	VPS4 CAALFM_C503090WA	25
Q5ANB1	White-opaque regulator 2	WOR2 CAALFM_C305170WA	25
Q6F4M7	Hydroxyquinol 1,2-dioxygenase (EC 1.13.11.37)	npcC	25
Q6Q875	Oxidoreductase sirO (EC 1.1.1.-)	sirO	25
Q6UEF0	NADH-dependent flavin oxidoreductase nadA (EC 1.-.-.-)	nadA P875_00053008	25/37
Q6UEF1	Oxidoreductase Afly (EC 1.-.-.-)	afly hypA P875_00053033	25
Q6WP50	Presilphiperfolan-8-beta-ol synthase (EC 4.2.3.74) (Botrydial synthesis protein 2)	BOT2 CND15	25
Q6Z965	12-oxophytodienoate reductase 7 (EC 1.3.1.42)	OPR7 OPR13 LOC_Os08g35740 OsJ_27573	25
Q88RC0	Glutarate-semialdehyde dehydrogenase DavD (EC 1.2.1.20)	davD PP_0213	25
Q8CG76	Aflatoxin B1 aldehyde reductase member 2 (EC 1.1.1.n11)	Akr7a2 Afar Akr7a5	25
Q92250	Farnesyl pyrophosphate synthase (EC 2.5.1.10)	fpp fpps 123A4.020 NCU01175	25
Q92398	Mitogen-activated protein kinase spm1 (EC 2.7.11.24)	spm1 pmk1 SPBC119.08	25/37
Q93XW5	Nitrile-specifier protein 5	NSP5 At5g48180 MIF21.7	25
Q96VN5	Triosephosphate isomerase (EC 5.3.1.1)	TPI1 TPI PAAG_02585	25/37
Q975C8	Acryloyl-coenzyme A reductase (EC 1.3.1.84)	STK_04800	25
Q9CA40	Nudix hydrolase 1 (EC 3.6.1.55)	NUDT1 NUDX1 At1g68760 F14K14.13	25
Q9N1F5	Glutathione S-transferase omega-1 (EC 2.5.1.18)	GSTO1	25
Q9P6C8	Alcohol dehydrogenase 1 (EC 1.1.1.1)	adh-1 B17C10.210 NCU01754	25/37
A9MYQ4	Gamma-aminobutyraldehyde dehydrogenase (EC 1.2.1.19)	prp SPAB_01688	25/37
Q9US47	Putative succinate-semialdehyde dehydrogenase C1002.12c [NADP(+)] (EC 1.2.1.16)	SPAC1002.12c	25
Q9UUN9	Aldehyde reductase 2 (EC 1.1.1.2)		25
Q9UW21	Oxysterol-binding protein-like protein OBPalph	OBPALPHA C5_01775C_B CaO19.10709/10710	25
Q9Y885	Putative branched-chain-amino-acid aminotransferase TOXF (EC 2.6.1.42)	TOXF	25/37
S0EE84	Cytochrome P450 monooxygenase FUS8 (EC 1.-.-.-)	FUS8 FFUJ_10051	25
W7MLD7	Fusarin C synthetase (EC 2.3.1.-)	FUS1 FVEG_11086	25
W7MWX4	Putative aldehyde dehydrogenase FUS7 (EC 1.2.1.3)	FUS7 FVEG_11080	25
A1CNW6	Probable Xaa-Pro aminopeptidase ACLA_020440 (EC 3.4.11.9)	ACLA_020440	25/37
B8N4P0	Probable carboxypeptidase AFLA_037450 (EC 3.4.17.-)	AFLA_037450	37
B8N8Q9	NADPH dehydrogenase afvA (EC 1.6.99.1)	afvA AFLA_108540	25/37

STRESS RESPONSE

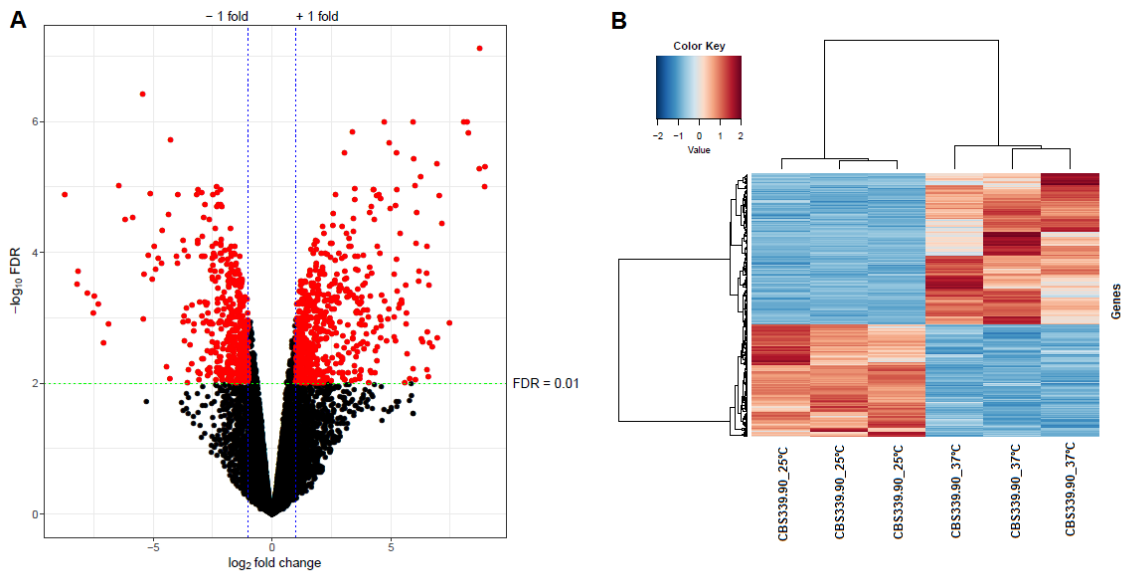
G3XMB9	Ketoreductase azaE (EC 1.-.-.-)	azaE ASPNI DRAFT_212676	37
G3XMC4	Non-reducing polyketide synthase azaA (EC 2.3.1.-)	azaA ASPNI DRAFT_56946	37
J4UHQ6	Orsellinic acid synthase (EC 2.3.1.-)	OpS1 PKS9 BBA_08179	37
O65679	Probable pinosresinol-lariciresinol reductase 3 (EC 1.23.1.-)	PLR3 At4g34540 T4L20.120	37
O93868	NADP-dependent mannitol dehydrogenase (EC 1.1.1.138)	mtdH	37
O94246	Putative glutamate--cysteine ligase regulatory subunit	SPCC737.06c	25/37
P42893	Endothelin-converting enzyme 1 (EC 3.4.24.71)	Ece1	25/37
P53619	Coatomer subunit delta	ARCN1 COPD	25/37
Q01398	Haloacetate dehalogenase H-1 (EC 3.8.1.3)	dehH1	37
Q0DA50	Zinc finger CCCH domain-containing protein 45	Os06g0677700 LOC_Os06g46400	37
Q0U6E8	Mannitol-1-phosphate 5-dehydrogenase (EC 1.1.1.17)	mpd1 SNOG_12666	25/37
Q0U6G5	Probable Xaa-Pro aminopeptidase PEPP (EC 3.4.11.9)	PEPP SNOG_12649	25/37
Q10166	Hydrolase C26A3.11 (EC 3.5.-.-)	SPAC26A3.11	25/37
Q2UpZ7	Aspartyl aminopeptidase (EC 3.4.11.21)	dapA AO090005001447	37
Q59KZ1	Aminopeptidase 2 (EC 3.4.11.-)	APE2 CAALFM_C104400CA	37
Q5AK62	Virulence protein SSD1	SSD1 CAALFM_C504730CA	37
Q6ZXC1	Probable inactive dehydrogenase easA	easA cpox3	25/37
A1VUV0	2-hydroxy-6-oxo-6-phenylhexa-2,4-dienoate hydrolase (EC 3.7.1.8)	bphD Pnap_4141	25
B0XPP3	Metacaspase-1A (EC 3.4.22.-)	casA AFUB_007090	25
B8N8R1	Aromatic peroxygenase (AaP) (EC 1.11.2.1)	APO1	25
B9W4V6	Low-redox potential peroxidase (EC 1.11.1.7)	LnP	25
C0IW58	Short chain dehydrogenase gsfK (EC 1.-.-.-)	gsfK	25
D7PI11	O-methyltransferase gsfB (EC 2.1.1.-)	gsfB	25
D7PI16	Short chain dehydrogenase gsfE (EC 1.-.-.-)	gsfE	25
D7PI19	E3 ubiquitin-protein ligase TRIP12 (EC 2.3.2.26)	trip12 si:ch211-272f3.4	25
F1RCR6	LanC-like protein GCR2	GCR2 GPCR At1g52920 F14G24.19	25
F4IEM5	Gibberellin 20-oxidase-like protein (EC 1.14.11.-)	At5g51310 MWD22.26	25
F4KBY0	Epoxide hydrolase A (EC 3.3.2.10)	ephA Rv3617 LH57_19705	25
I6YGS0	Putative monooxygenase Rv1533 (EC 1.13.12.-)	Rv1533	25
O06179	Putative alpha,alpha-trehalose-phosphate synthase [UDP-forming] 106 kDa subunit (EC 2.4.1.15)	SPAC2E11.16c SPACUNK4.16c	25
O14081	Peroxiredoxin Asp f3 (EC 1.11.1.15)	aspf3 AFUA_6G02280	25
O43099	Mitogen-activated protein kinase-binding protein 1	MAPKBP1 JNKBP1 KIAA0596	25
O60336	GTP-binding protein gtr2	gtr2 SPCC777.05	25
O74544	Mitochondrial protein import protein mas5	mas5 SPBC1734.11	25
O74752	GTP-binding protein rhb1	rhb1 SPBC428.16c	25/37
O94363	Serine/threonine-protein kinase srk1 (EC 2.7.11.1)	srk1 SPCC1322.08	25

O94524	Zeta-crystallin	CRYZ	25
O94547	Superoxide dismutase [Mn], mitochondrial (EC 1.15.1.1)	SOD2 YHR008C	25
O97764	Exportin-1	xpo1 caf2 crm1	25
P00447	Aromatic-L-amino-acid decarboxylase (EC 4.1.1.28)	Ddc	25/37
P14068	Granaticin polyketide synthase putative ketoacyl reductase 2 (EC 1.3.1.-)	gra-orf6	25/37
P14173	Allantoicase (EC 3.5.3.4)	alc-1 alc B8B8.070 NCU01816	25
P16543	Thioredoxin-1	TRX1 TRX2 YLR043C	25
P18407	Ubiquitin-activating enzyme E1 1 (EC 6.2.1.45)	UBA1 YKL210W	25
P22217	Fumarate reductase 1 (FRDS1) (EC 1.3.1.6)	FRD1 FRDS FRDS1 YEL047C SYGP-ORF35	25
P22515	Peroxiredoxin PRX1, mitochondrial (EC 1.11.1.15)	PRX1 YBL064C YBL0503 YBL0524	25
P32614	Bifunctional epoxide hydrolase 2 (EC 3.3.2.10)	EPHX2	25
P34227	Fatty acid repression mutant protein 2	FRM2 YCL026C-A YCLX08C YCLX8C	25/37
P34913	Probable quinone oxidoreductase (EC 1.6.5.5)	ZTA1 YBR046C YBR0421	25
P37261	6-phosphogluconate dehydrogenase, decarboxylating 1 (EC 1.1.1.44)	GND1 YHR183W	25/37
P38230	Dihydroxy-acid dehydratase, mitochondrial (EC 4.2.1.9)	ILV3 YJR016C J1450	25
P38720	Heat shock protein 90	hsp90 hsp1 AFUA_5G04170	25/37
P39522	scyllo-inositol 2-dehydrogenase (EC 1.1.1.370)	iolX yisS yucG yuxD BSU10850	25
P40292	Protein phosphatase 2C homolog 1 (EC 3.1.3.16)	ptc1 SPCC4F11.02	25/37
P40332	Thioredoxin	trx NCU05731	25
P40371	Cystathionine beta-synthase (EC 4.2.1.22)	cysB DDB_G0267386	25
P42115	Amine oxidase (EC 1.4.3.4)	mao	25/37
P46794	60S ribosomal protein L26-1	RPL26A At3g49910 F3A4.4 T16K5.260	25
P49253	Thioredoxin reductase (EC 1.8.1.9)	cys-9 NCU08352	25/37
P51414	Isoflavone reductase homolog P3 (EC 1.3.1.-)	At1g75280 F22H5.17	25
P51978	Zinc finger protein ZPR1	ZPR1 YGR211W	25/37
P53303	Glutamine--fructose-6-phosphate aminotransferase [isomerizing] (GFAT) (EC 2.6.1.16)	GFA1 CAALFM_C302280CA	25
P53373	26S proteasome non-ATPase regulatory subunit 4 homolog	RPN10 MBP1 MCB1 At4g38630 F20M13.190 T9A14.7	25/37
P53704	Succinyl-CoA:3-ketoacid coenzyme A transferase 1, mitochondrial (EC 2.8.3.5)	OXCT1 OXCT SCOT	25
P55034	Aldo/keto reductase slr0942 (EC 1.1.1.184)	slr0942	25
P55809	Disulfide-bond oxidoreductase YfcG (EC 1.8.4.-)	yfcG b2302 JW2299	25
P74308	Bifunctional epoxide hydrolase 2 (EC 3.3.2.10)	Ephx2	25
P77526	Epoxide hydrolase B (EC 3.3.2.10)	MT1988	25
P80299	4-nitrophenylphosphatase (PNPPase) (EC 3.1.3.41)	pho2 SPBC15D4.15	25
P95276	O-methyltransferase MdmC (EC 2.1.1.-)	mdmC	25/37

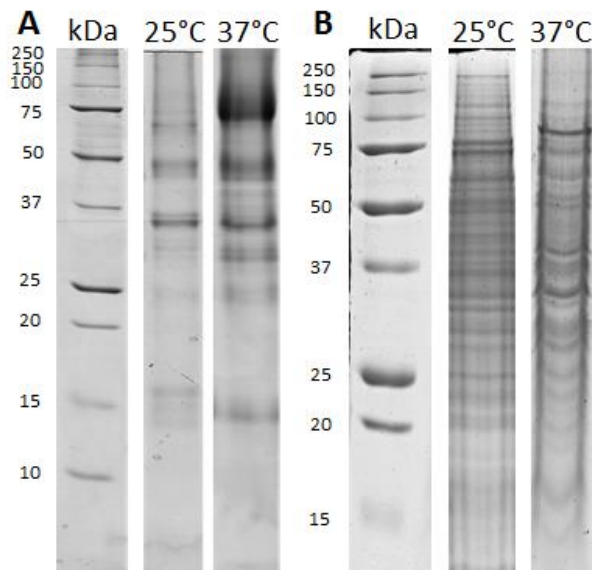
Q00472	Calcium/calmodulin-dependent protein kinase cmkA (EC 2.7.11.17)	cmkA AN2412	25
Q00719	Nitronate monooxygenase (EC 1.13.12.16)	ncd-2 G17A4.200 NCU03949	25/37
Q00771	Glutamate decarboxylase (GAD) (EC 4.1.1.15)	GAD1 YMR250W YM9920.04	25
Q01284	DNA damage tolerance protein RHC31	AOS1 RHC31 YPR180W P9705.5	25/37
Q04792	Frataxin homolog, mitochondrial (EC 1.16.3.1)	YFH1 YDL120W	25
Q06624	Beta-lactamase domain-containing protein 2	lact-2 ZK945.1	25
Q07540	Phospholipase D1 (EC 3.1.4.4)	pld1 SPAC2F7.16c	25
Q09621	Probable peptide methionine sulfoxide reductase (EC 1.8.4.11)	mxr1 SPAC29E6.05c SPAC30.09c	25
Q09706	Catalase-peroxidase (EC 1.11.1.21)	katG ATEG_08422	25/37
Q09859	eIF-2-alpha kinase activator gcn1 (Translational activator gcn1)	gcn1 SPAC18G6.05c	25
Q0CD12	Damage response protein 1	DAP1 YPL170W P2515	25
Q10105	Small glutamine-rich tetratricopeptide repeat-containing protein 2	SGT2 YOR007C UNF346	25/37
Q12091	Nucleolar protein 56	NOP56 SIK1 YLR197W L8167.9	25
Q12118	Bleomycin hydrolase (EC 3.4.22.40)	BLMH	25
Q12460	Thiopurine S-methyltransferase (EC 2.1.1.67)	tpm Nmul_A2259	25
Q13867	Oxygen-dependent coproporphyrinogen-III oxidase, mitochondrial (EC 1.3.3.3)	Cpox Cpo	25
Q2Y650	Survival factor 1	SVF1 FGRRES_05072 FGSG_05072	25
Q3B7D0	Cytochrome c peroxidase, mitochondrial (EC 1.11.1.5)	CCP1 FGRRES_01245 FGSG_01245	25
Q4ICI6	Mitogen-activated protein kinase HOG1 (EC 2.7.11.24)	HOG1	25/37
Q4ING3	Ribonuclease T2-like (EC 3.1.27.1)	rny1 AFUA_3G11220	25/37
Q4W6D3	2-amino-3-carboxymuconate-6-semialdehyde decarboxylase (EC 4.1.1.45)	acmsd DDB_G0286525	25
Q4WXZ5	Heat shock protein 60	hsp60 AN6089	25
Q54LN9	Heat shock 70 kDa protein	AN6010	25
Q5B041	Inorganic pyrophosphatase (EC 3.6.1.1)	ipp1 AN2968	25/37
Q5B0C0	Homoserine dehydrogenase (EC 1.1.1.3)	AN2882	25/37
Q5B912	Acyl-CoA ligase easD (EC 6.2.1.-)	easD AN2549	25/37
Q5B998	Quinone oxidoreductase (EC 1.6.5.5)	Cryz	25
Q5BA81	Translationally-controlled tumor protein homolog	NCU06464	25
Q6AYT0	Flavoheomprotein (EC 1.14.12.17)	hmp fhp BB3091	25
Q7RYV5	Glutathione reductase (EC 1.8.1.7)	gtr-1 glr1 B10C3.130 NCU03339	25
Q7WHW5	Catalase B (EC 1.11.1.6)	catB AO090120000068	25/37
Q873E8	2,4-dichlorophenol 6-monooxygenase (EC 1.14.13.20)	tfdB	25/37
Q877A8	cAMP-dependent protein kinase regulatory subunit	pkaR AFUA_3G10000	25
Q8KN28	O-acetyl-ADP-ribose deacetylase MACROD1 (EC 3.2.2.-) (EC 3.5.1.-)	MACROD1 LRP16	25

Q96UX3	Galactinol synthase 2 (EC 2.4.1.123)	GOLS2 At1g56600 F25P12.95	25/37
Q9BQ69	Nitronate monooxygenase (EC 1.13.12.16)	PA1024	25
Q9FXB2	Glycine-rich RNA-binding protein 4, mitochondrial	RBG4 GR-RBP4 GRP4 MRBP1B At3g23830 F14O13_2	25
Q9I4V0	Uncharacterized protein C1711.08	SPBC1711.08	25
Q9LIS2	Copper amine oxidase 1 (EC 1.4.3.21)	cao1 spao1 SPAC2E1P3.04	25
Q9P782	Glutathione S-transferase kappa 1 (EC 2.5.1.18) (GST 13-13) (GST class-kappa) (GSTK1-1) (hGSTK1) (Glutathione S-transferase subunit 13)	GSTK1 HDCMD47P	25/37
Q9P7F2	Superoxide dismutase [Mn], mitochondrial (EC 1.15.1.1)	sod-2 18F11.030 NCU01213	25
Q9Y2Q3	Acyltransferase LovD (EC 2.3.1.238)	lovD	25
Q9Y783	Peroxiredoxin TSA1-A (EC 1.11.1.15)	TSA1 TSA1A CAALFM_C306180CA	25
Q9Y7D1	DnaJ homolog 1, mitochondrial	AN10778	25
Q9Y7F0	Thiamine thiazole synthase	sti35 FOXG_10428	25/37
C8V213	Glutathione hydrolase-like YwrD proenzyme (EC 2.3.2.2)	ywrD BSU36100	37
J9N5G7	30 kDa heat shock protein	hsp30 NCU09364	37
O05218	Mitochondrial FAD-linked sulfhydryl oxidase ERV1 (EC 1.8.3.2)	ERV1 YGR029W	25/37
O74180	Trehalose-phosphatase (EC 3.1.3.12)	TPS2 PFK3 YDR074W YD8554.07	37
P19752	Probable coatomer subunit gamma	sec21 SPAC57A7.10c	37
P27882	Formate dehydrogenase (EC 1.17.1.9)	aciA AN6525	37
P31688	Curved DNA-binding protein (42 kDa protein)	cdb4 SPAC23H4.09	37
P41751	ATP-dependent (S)-NAD(P)H-hydrate dehydratase (EC 4.2.1.93)	SNOG_04206	37
P85978	Phosphatidylserine decarboxylase proenzyme 1, mitochondrial (EC 4.1.1.65)	PSD1 CAALFM_C100610WA	37
P87140	THO complex subunit 4D	ALY4 DIP2 THO4D At5g37720 K12B20.19	25/37
Q03134	N-acyl-phosphatidylethanolamine-hydrolyzing phospholipase (EC 3.1.4.54)	Napepld Mbldc1	25/37
Q09184	Heat shock protein 78, mitochondrial	HSP78 CAALFM_C203390CA	25/37
Q0UBT2	Stomatin-like protein 2, mitochondrial	STOML2 SLP2 HSPC108	25/37
Q0UVK8	ATP-dependent (S)-NAD(P)H-hydrate dehydratase (EC 4.2.1.93)	SNOG_04206	37
Q5ABC5	Phosphatidylserine decarboxylase proenzyme 1, mitochondrial (EC 4.1.1.65)	PSD1 CAALFM_C100610WA	37
Q6NQ72	THO complex subunit 4D	ALY4 DIP2 THO4D At5g37720 K12B20.19	37
Q6ZQW0	Indoleamine 2,3-dioxygenase 2 (EC 1.13.11.-)	IDO2 INDOL1	37
Q8BH82	N-acyl-phosphatidylethanolamine-hydrolyzing phospholipase D (EC 3.1.4.54)	Napepld Mbldc1	37
Q96UX5	Heat shock protein 78, mitochondrial	HSP78 CAALFM_C203390CA	37
Q9UJZ1	Stomatin-like protein 2, mitochondrial	STOML2 SLP2 HSPC108	37

CHAPTER 7



Supplementary Figure S7.1 | Volcano plot (A) and hierarchical cluster analysis (B) of the expression profiles of differentially expressed genes between 25 °C and 37 °C. Genes and samples were hierarchically clustered using Pearson correlation.



Supplementary Figure S7.2 | One-DE gel of extracellular medium (A) and mycelium (B) of strain CBS339.90 grown at 25 °C and 37 °C for 4 days.

The following tables (S7.1, S7.2, S7.3, S7.4, S7.5, S7.6, and S7.7) are deposited in an excel file named “Supplementary Material Chapter 7”:

Supplementary Table S7.1 | Proteins identified in the secretome of CBS339.90 strain at 25 °C.

Supplementary Table S7.2 | Proteins identified in the cellular proteome of CBS339.90 strain at 25 °C.

Supplementary Table S7.3 | Proteins identified in the secretome of CBS339.90 strain at 37 °C.

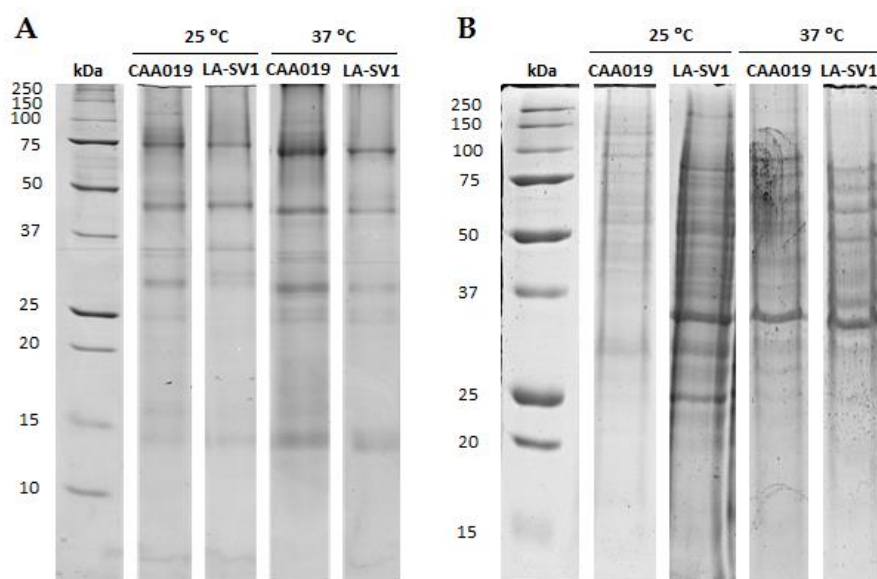
Supplementary Table S7.4 | Proteins identified in the cellular proteome of CBS339.90 strain at 37 °C.

Supplementary Table S7.5 | Up and down-regulated genes at 37 °C identified in CBS339.90 strain and correspondent GO biological process.

Supplementary Table S7.6 | Up and down-regulated proteins ($0.5 \geq FC \geq 2$) identified in the secretome of CBS339.90 strain and correspondent GO biological process.

Supplementary Table S7.7 | Up and down-regulated proteins ($0.5 \geq FC \geq 2$) identified in the cellular proteome of CBS339.90 strain and correspondent GO biological process.

CHAPTER 8



Supplementary Figure S8.1 | One-DE gel of extracellular medium (A) and mycelium (B) of strains CAA019 and LA-SV1 grown at 25 °C and 37 °C for 4 days.

The following tables (S8.1, S8.2, S8.3, S8.4, S8.5, S8.6, S8.7, S8.8, S8.9, S8.10, S8.11, S8.12) are deposited in an excel file named “Supplementary Material Chapter 8”:

Supplementary Table S8.1 | Proteins identified in the secretome of CAA019 strain at 25 °C.

Supplementary Table S8.2 | Proteins identified in the secretome of CAA019 strain at 37 °C.

Supplementary Table S8.3 | Proteins identified in the cellular proteome of CAA019 strain at 25 °C.

Supplementary Table S8.4 | Proteins identified in the cellular proteome of CAA019 strain at 37 °C.

Supplementary Table S8.5 | Proteins identified in the secretome of LA-SV1 strain at 25 °C.

Supplementary Table S8.6 | Proteins identified in the secretome of LA-SV1 strain at 37 °C.

Supplementary Table S8.7 | Proteins identified in the cellular proteome of LA-SV1 strain at 25 °C.

Supplementary Table S8.8 | Proteins identified in the cellular proteome of LA-SV1 strain at 37 °C.

Supplementary Table S8.9 | Up and down-regulated proteins ($0.5 \geq FC \geq 2$) identified in the secretome of CAA019 strain and correspondent GO biological process.

Supplementary Table S8.10 | Up and down-regulated proteins ($0.5 \geq FC \geq 2$) identified in the cellular proteome of CAA019 strain and correspondent GO biological process.

Supplementary Table S8.11 | Up and down-regulated proteins ($0.5 \geq FC \geq 2$) identified in the secretome of LA-SV1 strain and correspondent GO biological process.

Supplementary Table S8.12 | Up and down-regulated proteins ($0.5 \geq FC \geq 2$) identified in the cellular proteome of LA-SV1 strain and correspondent GO biological process.

Estes anexos só estão disponíveis para consulta através do CD-ROM.
Queira por favor dirigir-se ao balcão de atendimento da Biblioteca.

Serviços de Biblioteca, Informação Documental e Museologia
Universidade de Aveiro